Investigating the Expression and Function of IL-16 in the Central Nervous System under Normal and Inflammatory Conditions

Shehla Unaiza Hridi

A thesis submitted in fulfilment of the requirements for the degree of Doctor of Philosophy

November 2018

University of Strathclyde
Strathclyde Institute of Pharmacy and Biomedical Sciences
University of Strathclyde,
Glasgow, G4 0RE

Author’s Declaration

This thesis is the result of the author’s original research. It has been composed by the author and has not been previously submitted for examination which has led to the award of a degree.

Signed:

Date:

Abstract

Multiple Sclerosis (MS) is an inflammatory demyelinating disease of the central nervous system (CNS). MS pathophysiology is complex and $CD4^+$ T cells are one of the key mediators involved in the disease initiation and progression. Interestingly CD4 is also the receptor for interleukin-16 (IL-16), a pro-inflammatory cytokine. Previous research has shown that IL-16 is involved in the development of several autoimmune diseases such as rheumatoid arthritis (RA), systemic lupus erythematosus (SLE), Graves' disease (GD) and MS, but the exact role of IL-16 during MS initiation and progression remains unclear. Therefore, the aim of this study was to understand the role of IL-16 in CNS inflammation by: (i) examining the expression and distribution of IL-16 in the CNS and investigating whether expression levels correlate with the severity of neuroinflammation in experimental autoimmune encephalomyelitis (EAE), a murine model of MS; and (ii) by further determining the function of IL-16 in the CNS under normal physiological condition.

We immunised C57BL/6j mice with myelin oligodendrocyte glycoprotein (MOG_{35-55}) to induce EAE and utilised immunohistochemistry to study the expression of IL-16 and its receptor CD4 in the lymphoid and CNS tissues at different stages of EAE. While CD4 was expressed in lymphoid tissues of both EAE and control mice, CD4 expression in CNS tissues was only observed during EAE. For IL-16, its levels in the lymphoid organs and CNS tissues of EAE mice were significantly increased compared to tissues of naïve and PBS controls, as confirmed by the quantification of the percentage of $IL\text{-}16^+$ cells in tissues. Surprisingly, soluble IL-16 produced by splenocytes was similar between groups of naïve, and PBS or MOG_{35-55} immunised mice, and there was no difference with or without MOG_{35-55} stimulation in the culture. To identify the cell source of IL-16 in the lymphoid and CNS tissues we next utilised double immunofluorescence staining and our data showed co-localisation of IL-16 with some immune cells during EAE, with $CD11b^+$ cells (macrophages and microglia) expressing the highest percentage of IL-16 in both types of tissues. However, in CNS, IL-16 was also co-localised with CNS resident cells including neurons in both EAE and control mice and astrocytes only during EAE. However further study is required to fully understand the exact underlying action mechanisms of IL-16 in EAE.

Following that we investigated the role of IL-16 in CNS function by examining whether IL-16 modulates neuronal excitability and synaptic activity in mouse primary hippocampal cultures. We observed application of recombinant IL-16 (rIL-16) protein impaired sEPSC frequency and amplitude in a CD4-independent manner. We examined the mechanisms underlying these effects with rIL-16 reducing GluA1 S831 phosphorylation and inhibiting Na^+ channel function.

Taken together, our data suggest that IL-16 expression levels in both lymphoid organs and CNS tissues correlate with CNS inflammation, and $CD11b^+$ cells are the main source of IL-16 in both tissues during CNS inflammation in our EAE disease model. Under normal physiological condition, IL-16 reduces neuronal excitability and synaptic activity via multiple mechanisms and it is likely that its function is not solely dependent on the presence of CD4.Clearly IL-16 have a role both under normal and pathophysiological state but whether it is detrimental or beneficial is yet to be identified and requires further investigation to identify the exact role and potential of IL-16 in treatment of MS.

Publications

1. Shehla U Hridi, A. W. J. Franssen, Hui-Rong Jiang, Trevor J Bushell, Interleukin-16 inhibits sodium channel function and GluA1 phosphorylation via CD4- and CD9-independent mechanisms to reduce hippocampal neuronal excitability and synaptic activity. *Mol Cell Neurosci.* 2019; 95:71-78.

2. Mark Barbour, Rachel A Wood, Shehla U Hridi, Chelsey Wilson, Trevor J. Bushell and Hui-Rong Jiang, The therapeutic effect of anti-CD52 treatment in murine experimental autoimmune encephalomyelitis is associated with altered IL-33 and ST2 expression levels, *J Neuroimmunol*, 2018. 15; 318:87-96.

3. Peter W Tinning, Aimee J P M Franssen, Shehla U Hridi, Trevor J.Bushell and Gail McConnell, A 340/380 nm light emitting diode illuminator for Fura-2 AM ratiometric calcium imaging of live cells with better than 5 nM precision, *J Microsc*, 2018; 269(3):212-220.

Conferences

1. Hridi S, McCann L, McConnell G, Bushell T J, Jiang H R. Increased expression of IL-16 in the brain of experimental autoimmune encephalomyelitis. In BNA Festival of Neuroscience 2018. Birmingham UK.

2. Hridi S, McCann L, McConnell G, Bushell T J, Jiang H R. Increased expression of IL-16 in the brain of experimental autoimmune encephalomyelitis. In BNA Festival of Neuroscience 2017. Birmingham UK.

3. Hridi S, Bushell T J, Jiang H R. Expression of IL-16 in Central Nervous System during the Development of Experimental Autoimmune Encephalomyelitis. In Glasgow Neuroscience Day 2017.Glasgow UK.

4. Hridi S, Bushell T J, Jiang H R. Expression of IL-16 in Central Nervous System during the Development of Experimental Autoimmune Encephalomyelitis. In BSI/NVVI Congress December 2016. Liverpool UK

Acknowledgements

I express my sincere gratefulness and appreciation to my supervisor Dr.Hui-Rong Jiang, for her invaluable guidance and encouragement, constant advice, supervision and unfailing help throughout my PhD. Also, my heartfelt gratitude goes to my co-supervisor Dr. Trevor Bushell, for his insightful comments and advice, but also for the hard question which incented me to widen my knowledge. Their guidance helped me in all the time of research and writing of this thesis. I could not have imagined having a better supervisors and mentor for my PhD study.

I have been fortunate to work with some fantastic people in Jiang's lab and I take great delight in acknowledging Dr. Mark Barbour for his continuous help in the lab, and for his valuable inputs and suggestions throughout my PhD. I'd also like to thank Chelsey for being an amazing colleague, for listening to me and being so supportive and motivating during my tough times and for all the fun we have had in the last four years. Aimee, for helping me during my time in Bushell's lab. My thanks also extend to all the 5th floor colleagues for their constant help and advice, specially Kerrie and Chelsey. I would also thank Carol and Lee for their help in BPU.

My deepest gratitude goes to my parents, family and father and mother in-laws for their relentless support, words of encouragement and prayers. In addition, I would also thank my uncle Salamat, aunty Sajeda, aunty Sultana and family friend Lincon for their support during my PhD. I would like to convey my heartfelt thanks to my husband Sifat, for his never-ending sacrifices, for putting up with all my stressing and moaning during my PhD and for always supporting and encouraging me throughout the tough years. Without him by my side, I would never have made it this far.

Lastly, but above all, I would like to thank Almighty Allah for giving me the strength and blessings to complete this thesis.

Abbreviations

AMPARs	α-amino-3-hydroxy-5-methyl-4-isoxazolepropionic acid receptors
AP	Action Potential
APC	Antigen presenting cell
APC	Allophycocyanin
ATP	Adenosine triphosphate
BBB	Blood brain barrier
BB	Blocking buffer
BSA	Bovine serum albumin
Ca^{2+}	Calcium ion
CAMK-II	Calmodulin-dependent protein kinase II
CD	Cluster of differentiation
CFA	Complete Freund's adjuvant
CNP	2',3'-cyclic nucleotide 3'phosphodiesterase
CNS	Central nervous system
CO_2	Carbon dioxide
CR	Complement Receptor
CSF	Cerebrospinal fluid
CT	C-terminal
CTLs	Cytotoxic T lymphocytes
CpG	Cytosine Phosphate Guanine
dH_2O	Distilled water
DAPI	4',6-diamidino-2-phenylindole
DC	Dendritic cell
DIV	Days *in vitro*
DMTs	Disease-modifying therapies
DNA	Deoxyribonucleic acid
DPX	Distyrene, plasticizer, xylene
DTT	Dithiothreitol
EAE	Experimental autoimmune encephalomyelitis
EDTA	Ethylene diaminetetra acetic acid
ELISA	Enzyme-linked immunosorbent assay
FACS	Fluorescence-activated cell sorting

FITC	Fluorescein isothiocyanate
FCS	Fetal calf serum
FGF	Fibroblast growth factor
FoxP3	Forkhead box P3
GA	Glatiramer acetate
GD	Graves' disease
GAPDH	Glyceraldehyde 3-phosphate dehydrogenase
GluR	Glutamate Receptor
GluA	Glutamate receptor, ionotropic, AMPA
GluK	Glutamate receptor, ionotropic, Kainate
GM	Grey matter
GM-CSF	Granulocyte-macrophage colony-stimulating factor
GPCRs	G-protein-coupled receptors
H^+	Hydrogen
HBSS	HEPES-based salt solution
H&E	Haematoxylin and Eosin
HCO_3^-	Bicarbonate
HCM	Hippocampal conditioned medium
HRP	Horseradish peroxidase
IHC	Immunohistochemistry
i.p	Intraperitoneal
iTreg	Inducible Treg
IFNs	Interferons
IFN-α	Interferon Alpha
IFN- β	Interferon Beta
IFN- β1	Type 1 beta interferon
IFN- β1b	Type 1b beta interferon
IFN-γ	Interferon gamma
Ig	Immunoglobulin
IHC	Immunohistochemistry
IL	Interleukin
K^+	Potassium ion
KARs	Kainate receptors
LC	Liquid chromatography

LTD	Long-term depression
LTP	Long-term potentiation
LNs	Lymph nodes
LPS	Lipopolysaccharide
MBP	Myelin basic protein
mGluR	Metabotropic glutamate receptor
mRNA	Messenger RNA
MHC	Major Histocompatibility complex
MOG	Myelin oligodendrocyte glycoprotein
MS	Multiple sclerosis
NaCl	Sodium chloride
NIL-16	Neuronal Interleukin -16
Na^+	Sodium ion
NK	Natural killer
NKT	Natural killer T cells
NMDARs	N-methyl-D-aspartate receptors
NO	Nitric oxide
OCT	Optimal cutting temperature
OPC	Oligodendrocyte precursor cell
PAMPs	Pathogen associated molecular pattern
PBS	Phosphate buffered saline
PBS-T	Phosphate buffered saline-Tween 20
PE	Phycoerythrin
Percp 710	Peridinin chlorophyll protein omplex 710
PerCPCy5.5	Peridinin chlorophyll protein complex cyanine 5.5
Pen/Strep	Penecillin Streptomycin
PKA	Protein kinase A
PKC	Protein kinase C
PNS	Peripheral nervous system
PLL	Poly-L-lysine
PLP	Proteolipid protein
Poly (I:C)	Polyinosinic: polycytidylic acid
PPMS	Primary progressive MS
PRMS	Progressive relapsing MS

PRR	Pattern recognition receptors
PTX	Pertussis toxin
qPCR	Quantitative polymerase chain reaction
rIL-16	Recombinant IL-16
RA	Rheumatoid Arthritis
RAGE	Receptors for advanced glycation end products
RANTES	Regulated on activation normal T cell
RBC	Red blood cell
RNS	Reactive nitrogen
ROI	Region of interest
ROS	Reactive oxygen species
RPM	Revolutions per minute
RRMS	Relapsing remitting MS
RT	Room temperature
sEPSCs	Spontaneous excitatory postsynaptic currents
S818	Serine 818
S831	Serine 831
S845	Serine 845
S880	Serine 880
s.c	Subcutaneous
SDS	Sodium dodecyl sulfate
SDS-PAGE	Sodium dodecyl sulfate polyacrylamide gel electrophoresis
SEM	Standard error of the mean
SLE	Systemic lupus erythematosus
SPMS	Secondary progressive MS
STWS	Scott’s tap water solution
T840	Threonine 840
T876	Tyrosine 876
TBS	Tris buffered saline
TBS-T	Tris buffered saline-Tween 20
TCR	T cell receptors
Tconv	Conventional T cells
TEMED	Tetramethylethylenediamine
Tfh	T follicular helper

TGF-β	Transforming growth factor beta
Th	T helper
TLRs	Toll like receptors
TMB	3,3',5,5'-Tetramethylbenzidine
TNF-α	Tumour necrosis factor Alpha
Treg	Regulatory T cell
TREM	Triggering receptor expressed on myeloid cells
TRITC	Tetramethylrhodamine
VLA	Very late antigen
WM	White matter

List of figures

List of Tables

1. General Introduction

1.1 Central nervous system (CNS)

The CNS is considered as one of the most complex organs in the body due to its physiological structure and functions (Gosselin and Rivest., 2007). Furthermore, it is considered as one of the most remarkably intricate machines in the whole universe with an ability to encounter, store, recollect and examine the most complicated information. The CNS has enormous potential to recondition itself according to surrounding environmental changes and experience (Weil *et al*., 2008), which has always encouraged significant research interest into CNS function under both physiological and pathophysiological conditions.

The CNS has the ability to influence the activity of all the parts of the body and also to receive and integrate information from the rest of the body and then react accordingly with the required response. The CNS includes two main components: the spinal cord (Figure 1.1) (cervical, thoracic, lumbar and sacral regions) and the brain (Figure 1.2) (cerebral hemispheres, midbrain, cerebellum, diencephalon, pons and medulla oblongata). The spinal cord is involved in controlling minor musculoskeletal reflexes without the brain being involved. It also receives and processes sensory information from the peripheral organs (e.g. skin, muscles and joints) and then transmits motor commands to those peripheral organs (Bican *et al*., 2013). The brainstem is the posterior part of the brain, which structurally continues to the spinal cord and plays a very important role in communication between the brain and the spinal cord. The brain is considered as the control centre which controls multiple functions such as information processing, perception, motor control, arousal, homeostasis, motivation, memory and learning. There are numerous resident cells and microvasculature within the CNS. The main cell types are neurons, microglia, astrocytes and oligodendrocytes (ODCs). Together these cells form a complicated cellular network (Figure 1.3) and each of these cells play critical role in maintaining regular CNS function. The brain is consist of a highly selective semipermeable membrane termed as blood brain barrier (BBB) that maintains a regulated interface between the peripheral circulation and the CNS. It is called

the BBB because of its unique property of tightly regulating the movement of ions, molecules, and cells between the blood and the brain. It is made up of cerebral microvascular endothelium and maintained by critical interaction with mural immune and glial cells and creates a tight junction that is essential for the health and function of the CNS.

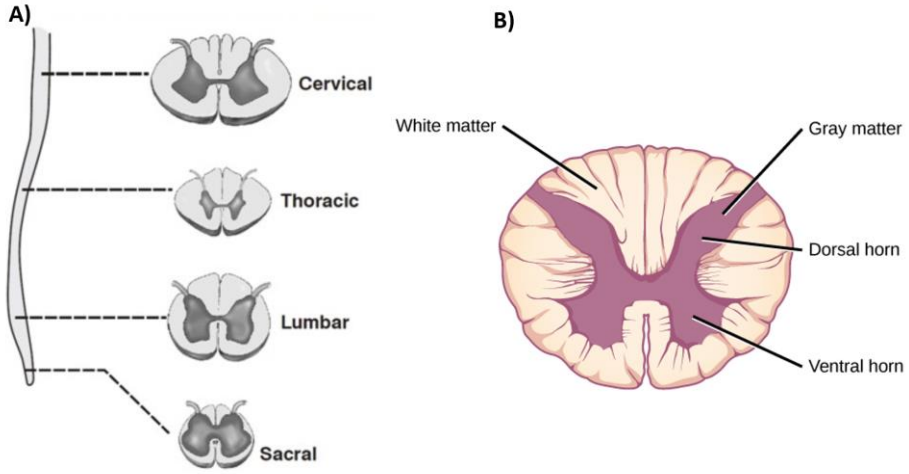

Figure 1.1: Diagram of the Spinal Cord A) *illustrates four different segments of the spinal cord, extending from the brainstem cervical, thoracic, lumber and sacral.* ***B)*** *illustrates a cross-section of spinal cord showing the gray matter (containing cell bodies and interneurons) and white matter (containing axons) (Lumen learning 2017).*

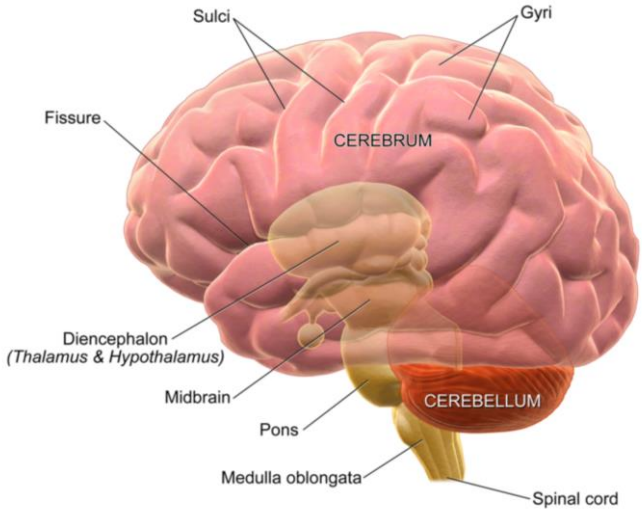

Figure 1.2: Diagram of the brain. *The diagram illustrates six different parts of the brain; spinal cord extending from the medulla oblongata in the brainstem, cerebellum is situated just behind the pons. Midbrain just above the pons, the diencephalon which lies just above the mid-brain is composed of two major parts: the thalamus and hypothalamus. The largest region of the brain is made up of cerebral hemispheres (Blausen gallery, 2014).*

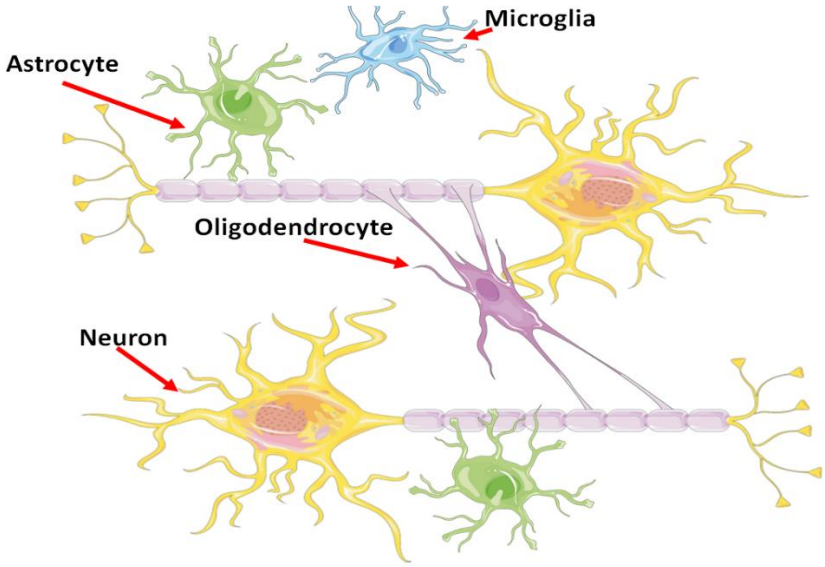

Figure 1.3: Schematic representation of different cell types in the central nervous system. *This diagram shows a schematic arrangement of neurons and the three types of supporting cells: astrocytes, microglia and oligodendrocytes in the CNS. Smart servier medical art 2005.*

1.1.1 Neurons

The neurons are the basic unit of the CNS but also the most important part of the system. There are approximately 10^{11} neurons in the human brain (Kandel., 2000) which are the only information processing structures of the CNS. Neurons process information received by a stimulus and transmit the information to other neurons (Fodstad, 2002). Various neurons share a similar simple basic structural composition. A neuron is made up of four different regions which includes the cell body, dendrites, the axon and axon (pre-synaptic) terminals (Figure 1.2) (Kandel, 2000). Each region is responsible for playing a specialised and important role during the processing and transmission of signals. The cell body known as soma contains the nucleus of the neuron and is involved in protein synthesis and metabolic processes. The dendrites and the axon arise from the cell body. Dendrites play a major role in receiving incoming signals from other nerve cells whereas the axon functions as the main conducting unit for carrying signals to other neurons (Kandel, 2000). The signals are called action potentials and together with glutamate, these are used to communicate signals from one neuron to another. Axons are fine projections

from the cell body of a neuron which extends to form numerous branches of axon terminals before forming synaptic connections to transfer signals to other neighbouring neurons (Kandel, 2000). The region between the axon terminals and dendrites, are known as synapses. These are the connections between a presynaptic terminal and a postsynaptic neuron allowing neurons to communicate by means of synaptic transmission, either chemically or electrically (López-Muñoz *et al*., 2006).

Many neurons have an insulated layer around their axons, which is known as myelin sheath. The myelin sheath is an extended and modified plasma membrane which wraps around the nerve axon in a spiral orientation (Raine., 1984). In the peripheral nervous system (PNS), myelin membranes originate from Schwann cells while in the CNS it originates from oligodendroglia cells (Morell and Quarles.,1999). 70-85% of the dry mass of myelin consists of lipid, which includes glycolipid (mainly galactocerebroside, GalC) and its sulphated analogue sulfatide, cholesterol and phospholipid (Swapna *et al*., 2006), while the water content is only 40%. The high lipid contents of the myelin components allow the myelin sheath to achieve its function. Myelin also has a low proportion of protein contents (15-30%), however the protein composition of myelin sheath varies between CNS and PNS. In the CNS, 60-80% of the protein content is proteolipid protein (PLP) and myelin basic protein (MBP) and myelin oligodendrocyte glycoprotein (MOG), myelin-associated glycoprotein and 2',3'-cyclic nucleotide 3'phosphodiesterase (CNP) constitute the remaining protein content (Quarles *et al*., 2006).

Each myelin producing cell wraps one segment of an axon, leaving regular intervals or gaps between each segment of the axons, which are known as Nodes of Ranvier (Caldwell *et al*., 2000). These gaps contain Na^+/K^+ ATPases, Na^+/Ca^{2+} exchanges and voltage gated Na^+ channels that generate action potentials along the axons (Caldwell *et al*., 2000; Craner *et al*., 2004). The main function of myelin sheaths is to insulate the axons and propagate rapid signal transduction and increasing action potential speed (Hartline and Colman., 2007). The myelin sheath increases the membrane resistance and enhances axonal depolarisation between action potentials and the Nodes of Ranvier are responsible for rapid propagation of impulse, as it allows the action potential

to jump from one node to the next along the axons via Na^+ channels with very little energy expended (Caldwell *et al*., 2000; Arancibia-Carcamo & Attwell., 2014). A myelin sheath is also involved in maintenance and survival of axons and the regulation of axonal maturation as demonstrated during the demyelinating disease multiple sclerosis (MS) (Duncan *et al*., 2011). When axons become demyelinated, the conduction of electrical impulses is reduced, and this prevents neurons from communicating efficiently with one another. Eventually, this can result in motor and sensory deficits ultimately leading to blindness and paralysis as observed in CNS diseases like MS (Lucchinetti *et al*., 2000).

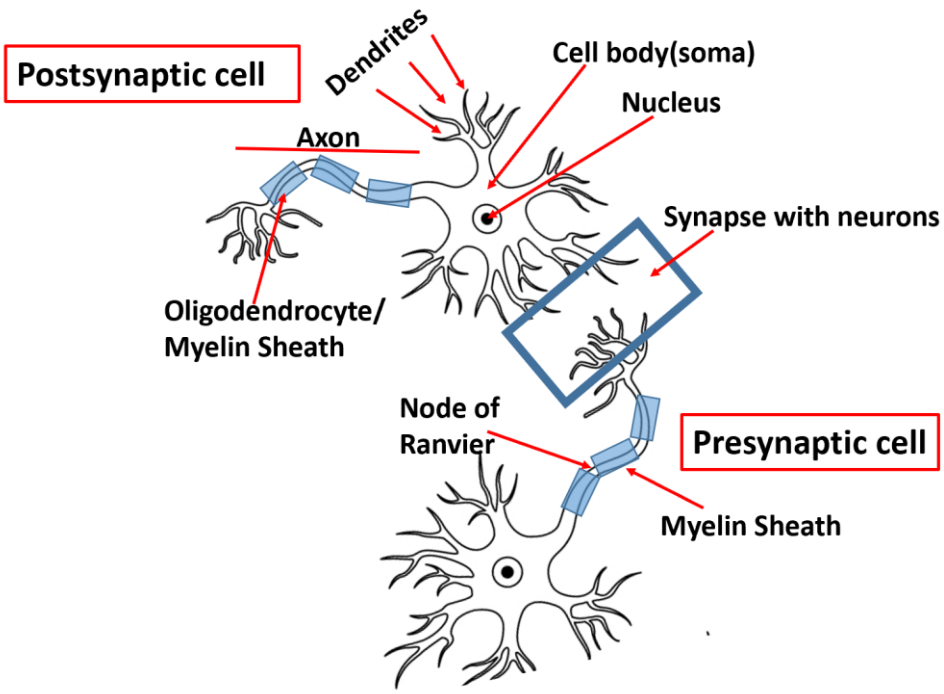

Figure 1.4: Schematic representation of typical neuron structure and its interaction with another neuron. *A typical neuron consists a cell body (soma), dendrites and an axon. The soma contains the cellular organelles such as the nucleus, mitochondria etc. Dendrites are the thin extensions that arise from the cell body and forms many branches. An axon is a cellular extension arising from the cell body. Neurons receive signals via the dendrites which are passed from the previous neuron across the synaptic cleft and the axon. The neuron is myelinated by oligodendrocytes in the CNS and Schwann cells in the PNS. Nerves are myelinated in section creating regular intervals between the myelin sheath, called the Nodes of Ranvier. RBPAonline.com 2018.*

1.1.2 Glial cells

Glial cells are the most abundant cells of the CNS. These cells are known to be associated with wide range of diverse functions, with some providing structural and nutritional support to the surrounding neurons and some insulating the axons and helping to speed up the signal transmission process of the neurons (Wang *et al.*, 2006; Allaman *et al.*, 2011). In recent years, glial cells were also identified participating in the development, function, and disease of the CNS (Parpura *et al*., 2012). There are two major classes of glial cells in the nervous system: macroglia and microglia. Macroglia are further divided into two different subtypes: OPCs the cells that produce myelin and astrocytes which are involved in many vital functions of the CNS. By contrast, microglia functions as the innate immune system of the CNS and they are the resident immune cells of the brain.

1.1.2.1 Oligodendrocytes (ODCs)

ODC are glial cells which originate from ectodermal cells (Shin *et al*., 2012) and are responsible for insulation of the axons by forming myelin sheaths around the axons (Kandel, 2000). In the CNS, differentiation of oligodendrocyte progenitor cells (OPCs) gives rise to myelin producing (ODCs) which are distributed throughout the CNS within the white and grey matter (Miller., 1996). OPC migration is directed by regulatory signals including growth factors such as platelet derived growth factor (PDGF) (Spassky *et al*., 2001), fibroblast growth factor (FGF), hepatocyte growth factor (Ohya *et al*., 2007; Yan & Rivkees., 2002) and chemotropic molecules (Jarjour *et al*., 2003). Major myelin component formation begins as the OPC enters the terminal differentiation stages and switches to a pre-myelinating ODCs (Kukley *et al*., 2010). While the ODCs primarily involved in myelination, they are also proposed to be involved in axonal growth and maintenance, support axonal metabolism, and contribute to neuronal survival (Bankston *et al*., 2013; Funfschilling *et al*., 2012). Oligodendrocytes have very complex and unique differentiation and metabolism process which makes it vulnerable to disease. Oligodendrocytes consume large quantity of oxygen and ATP which causes the production of

toxic by-products like hydrogen peroxide. Such by products if not metabolised properly can lead ODS apoptosis and CNS degradation (Mouzannar *et al*., 2001). Oligodendrocyte plays critical role in MS disease pathogenesis, death of oligodendrocytes are the major aspects of MS pathogenesis resulting in a loss of myelin that ensheaths axons and eventually reducing electrical impulse conduction and preventing neurons to communicate effectively among them (Brandl & Lassmann., 2010). Furthermore, remyelination by OPCs can occur in the lesion of MS (Reynolds *et al*., 2002) and insufficient OPC migration into demyelinated regions of CNS causes poor remyelination in MS patients (Boyd and Zhang, 2013).

1.1.2.2 Astrocytes

Astrocytes constitute a majority of the cell population of the brain and they are the most abundant form of macroglial cell in the CNS. No region of the brain is without astrocytes and they spread throughout the CNS contiguously and in a well-structured manner and are linked together through gap junctions (Sofroniew and Vinters, 2010). They are also involved in the formation of the endothelial cell lining of the blood vessels and the BBB (Bernacki *et al*., 2008). Even though astrocytes display Na^+ and K^+ voltage-gated ion channels, astrocytes do not have any electrical excitability, they maintain a relatively stable membrane potential (Orkand *et al*., 1966). However, it is now known that astrocytes are excitable cells in relation to levels of intracellular calcium (Araque and Navarette, 2010; Parpura and Verkhratsky, 2012). The processes from astrocytes envelop about four neuronal bodies on average and more than a hundred dendrites (Halassa *et al*., 2007), with numerous studies indicating that astrocytes signalling can affect hundreds of neurons. Astrocytes are involved in providing nutrients to the cells when the extracellular levels of growth factor or nutrients (glucose and lactose) are low in the synaptic cleft (Kintner *et al*., 2004). It also plays a vital role in maintaining the ionic concentration in the extracellular spaces between the neurons, and maintains extracellular osmolality, pH and buffers excess K^+ ions and neurotransmitters released from the synaptic cleft (Kofuji and Newman., 2004). Excess K^+ may lead to hyperpolarization of the neuron and alter the CNS homeostasis and compromise CNS

function, the gap junctions present between astrocytes and oligodendrocytes help in K^+ buffering (Orthmann-Murphy *et al*., 2008) and maintain K^+ homeostasis in the CNS (Ostby *et al*., 2009). Accumulation of excess glutamate at the synaptic cleft leads to neurotoxicity, and astrocytes are also found to be involved in taking up excess glutamate from the synaptic cleft to protect the neurons from the glutamate toxicity (Danbolt, 2001). Astrocytes also exhibit anti-oxidative property by acting as carbon dioxide (CO_2) sink through converting CO_2 to H^+ and HCO_3^- with the help of carbonic anhydrase expressed in astrocytes which eventually restore a proper pH (Belanger and Magistretti., 2009).

Astrocytes also play an important role in regulating the neuronal functions by integration of neuronal firing and synaptic connections via their cytoplasmic calcium waves (Santello and Volterra., 2009; Mónica and James., 2014). The cytoplasmic calcium level increases within the astrocytes in response to the neuronal activity (Wang *et al.*, 2006; Winship *et al.*, 2007). The calcium waves can travel from the site of generation and it can propagate in the neighbouring cells as well as the extracellular environment (Sanderson *et al.*, 1994). These calcium waves are also found to release various gliotransmitters (glutamate, adenosine triphosphate; ATP and D-serine) that are involved in modulating synaptic transmission between the neurons (Halassa *et al.*, 2007; Savtchouk and Volterra., 2018). Additionally, the glutamate released by astrocytes is suggested to be directly involved in altering both excitatory and inhibitory neuronal activity and synaptic plasticity (Gan *et al*., 2011).

Studies on CNS diseases suggest that the abnormal function of the astrocytes contributes to the development of various neurodegenerative diseases including MS (Allaman *et al*., 2011; Nair *et al.*, 2008). Under such conditions, astrocytes become activated through altered gene expression, hypertrophy and proliferation and release various cytokines, chemokines, reactive oxygen species and growth factors (Farina *et al*., 2007; Rothhammer & Quintana., 2015). Such pathological conditions in the CNS ultimately compromise the intrinsic anti-oxidative property as well as glutamate clearance property of astrocytes, eventually leading to neuronal death (Allaman *et al*., 2011). Astrocytes also

respond to severe CNS insult by a process known as astrogliosis. It is predicted that mediators of astrogliosis could be produced by a variety of CNS cells such as neurons, microglia, ODCs or pericytes. Such regulators include cytokines (IL-6, LIF, CNTF, TNF-α, IFN-γ, IL-1 and IL-10), lipopolysaccharide (LPS) and other Toll-like receptors (TLRs) ligands; glutamate and noradrenalin (neurotransmitters); Adenosine triphosphate (ATP), Reactive oxygen species (ROS), hypoxia, glucose deficiency, β-amyloid, $NH4^+$ and cell proliferation regulators such as endothelin-1 (Acosta *et al*., 2006; Akaoka *et al*., 2001; Andreiuolo *et al*., 2009; Araque *et al*., 1999). Astrogliosis leads to cellular and morphological changes and often results in scar formation (Fitch & Silver., 2008). However, the changes caused by astrogliosis vary depending on the severity of the CNS insult or injury (Bushong *et al*., 2002; Sofroniew., 2009). Mild to moderate astrogliosis is usually associated with mild infection or non-penetrating trauma with limited tissue remodelling and following the resolution of the damage the astrocytes often return back to its normal appearance similar to healthy state (Bushong *et al*., 2002; Sofroniew., 2009). However, severe astrogliosis is associated with CNS focal lesions and severe infections, which occurs during MS in response to neuroinflammation. During severe CNS insult and astrogliosis there is significant increase in Glial fibrillary acidic protein (GFAP) expression by astrocytes together with increased cellular hypertrophy and extensive proliferation (Sofroniew., 2009; Sofroniew., 2010).

1.1.2.3 Microglia

Microglia represent 5-20% of the total glial population in the CNS, depending on the CNS regions. Unlike macroglia or neurons, microglia within the CNS are derived from the mesoderm which migrates into the CNS during embryogenesis where they undergo maturation (Derecki *et al*., 2013). They can be found anywhere in the CNS, but they reside mostly in the grey matter and white matter, the choroid plexus, ventricles, perivascular spaces and meninges (Ransohoff and Cardona., 2010). Microglial cells in the CNS are able to sense and respond to any injury or CNS insult and they are able to remove debris from the site of injury (Kreutzberg, 1996). Among glial cells, the microglia cells are the major phagocytic cells (Rivest, 2009), which can sense and

modulate neuronal activities and help cleaning apoptotic neuronal cells (Tambuyzer *et al*., 2009). Microglia have a small cell body with numerous fine projections (Hanisch and Kettenmann., 2007). Under normal physiological conditions, microglia are in a resting state, but their extended processes are constantly monitoring the surrounding environment and communicating with neurons, astrocytes and blood vessels and responding to normal physiological responses and abnormal changes in their microenvironment to maintain the homeostasis of the CNS (Nimmerjahn *et al*., 2005; Dibaj *et al*., 2011). Microglia are extremely sensitive to slight changes in their microenvironment including any differences in ion homeostasis.

Microglia are considered as a part of the innate immune system of the CNS, and the CNS resident macrophages/phagocytes (Streit *et al*., 1999). Microglia cells often act as efficient antigen presenting cells (APCs) in the CNS (Ransohoff and Cardona., 2010). Under normal conditions, microglia cells express very low levels of a set of cell surface proteins known as the major histocompatibility complex (MHC) I and II, which are essential for the acquired immune system to recognize foreign molecules and determines histocompatibility. Upon activation, these molecules are up-regulated together with co-stimulatory molecules such as CD40, CD80 (B7-1), CD86 (B7-2), and leukocyte function-associated antigen-1 (LFA-1, CD11a/CD18 integrin) that eventually enable them to act as APCs and activate T cells, and causes cytokine and chemokine release and promote inflammation (Wlodarczyk *et al*., 2014). After the elimination of the pathogen and post-inflammation, microglia play a role in promoting repair and remapping when required through anti-inflammatory secretion and neuronal tissue regrowth (Welser-Alves *et al*., 2011). In the CNS, in response to the stimulation of cell membrane receptors and potassium channels, microglia release neurotrophic factors (Hu *et al*., 2015), which promotes neuronal growth and differentiation, and also regulates synaptic plasticity by modifying and eliminating synaptic structures (Hansson and Rönnbäck, 2003). Microglial cells also play a critical role in synaptic development and maintenance of neuronal interactions through activation of complement system (Zabel and Kirsch, 2013).

During CNS injury, microglia are often activated before any other glial cells in the CNS (Nimmerjahn *et al*., 2005). The activated microglia form amoeboid structures with ramified phenotypes (Kreutzberg, 1996), and release different inflammatory mediators including cytokines, ROS, nitric oxide (NO), neurotoxic secretary products and free radical species which lead to damage of the healthy neurons (Heneka and O'Banion, 2007).

Similar to macrophages (discussed later in the chapter), activation of microglia can be broadly characterised into two phenotypes based on their immune responses, which are termed as classical or alternative (Michelucci *et al.*, 2009). Activated microglia cells can either be classically activated M1 or alternatively activated M2 microglia cells. M1 microglia cells are usually associated with a reaction against viruses and bacteria that are activated by LPS and IFN-γ, TLR ligand, TNF-α and cell surface markers CD86 and CD68 and are able to produce pro-inflammatory cytokines such as IL-1, IL-6, IL-23 and TNF-α (Michelucci *et al.*, 2009). In contrast, M2 microglia is usually activated by IL-13 and IL-4 and which produces arginase and IL-10 and is associated with anti-inflammatory responses and helps in regeneration of tissues (Michelucci *et al.*, 2009). A transition from M1 microglia to M2 can allow any damage to be efficiently repaired.

Due to the diverse roles that microglia cells play, it is not surprising that they have been found to be involved in various neurodegenerative diseases including MS (Napoli and Neumann, 2009). Furthermore an *in vivo* model for microglial inactivation has also demonstrated to delay onset disease in an animal model of MS and reduce disease clinical symptoms suggesting the critical role of microglia in development of MS (Heppner *et al*., 2005). Microglia cells contribute to EAE development by acting as APCs to activate autoreactive T cells and secrete a number of cytokines including IL-6, IL-23, IL-1β and TGF-β which are all required for the differentiation of Th17 cells, a major inflammatory player in the initiation and development of MS and EAE (Goldmann and Prinz, 2013).

1.2 Communication between neurons

1.2.1 Neuronal Signalling

Neurons have unique ability to support the general functions in the CNS. The neurons communicate within the cell through intracellular signalling and through intercellular signalling they can communicate between cells. For rapid communication at a long distance, neurons send out electrical signals known as action potentials along the axons using a mechanism known as conduction. Conduction is a process by which cell body of a neuron communicates with its own terminal via axon. The communications between neurons are then achieved at the synapse by a process known as neurotransmission (Kandel *et al*., 2000; Gosselin & Rivest., 2007).

1.2.2 Conduction of the action potential down the axon

When a neuron is stimulated an electrical signal known as action potential (AP) moves along the axon which results from flow of ions along the neuronal cell membrane and enables faster movement of the signal along the neuron (Kandel., 2000). Generally, neurons maintain a balance of ions inside the cell which differs from the balance outside the cell. This uneven distribution of ions creates an electrical potential across the cell membrane which is known as the resting membrane potential and also described as the steady state of cells. This is a dynamic process that is balanced by ion leakage and ion pumping. In the cell membrane, there is sodium-potassium pump which maintains the electrochemical gradient through active transport to expel 3 Na^+ ions for every 2 K^+ ions entering the cell. The average resting membrane potential for most neurons is between –65 mV to -70mV. The cell membrane of a resting cell is more negative inside than outside, in other words the cell is polarised. Any stimulus from the surrounding environment or from the neighbouring neuron alters the permeability of the membrane causing the voltage gated Na^+ channel to open and allow Na^+ ions to move into the cell. Because the concentration of Na^+ is higher outside the cell than inside the cell, ions rushes into the cell driven by the concentration gradient. And as Na^+ is a positively charged ion, it changes the relative voltage immediately inside the cell relative to immediately

outside. The influx of Na^+ ions entering the cell causes the membrane potential to become less negative and increases the voltage within the cell, this condition is termed as depolarisation which allows the AP to pass down the axon into the axon terminal (Fields and Stevens-Graham., 2002; Platkiewicz & Brette., 2010). When the depolarization reaches a certain point to initiate an AP, this is known as a threshold potential (-50 to -55mV). Na^+ ion continue to enter the cell even after the membrane potential becomes zero.

Once the membrane potential reaches the maximum depolarised potential (+30 mV) the voltage gated Na^+ ion channel begins to close, and Na^+ ion entry into the cell decreases, however the K^+ channel opens and as a consequence, K^+ ions diffuse out of the cell. As K^+ ions leave the cell, the membrane potential begins to move back toward its resting voltage. This is called repolarization. Repolarization returns the membrane potential to -70mV, but during this stage K^+ channels are slightly delayed in closing, accounting for short overshoot which is known as hyperpolarization. During hyperpolarization the membrane potential is slightly more negative than the resting potential. As the voltage gated K^+ ion closes, the active transport of Na^+/K^+ ion re-establishes the resting membrane potential when the concentrations of K^+ ion outside and inside the cells are equal (Figure 1.3) (Fields & Stevens-Graham, 2002).

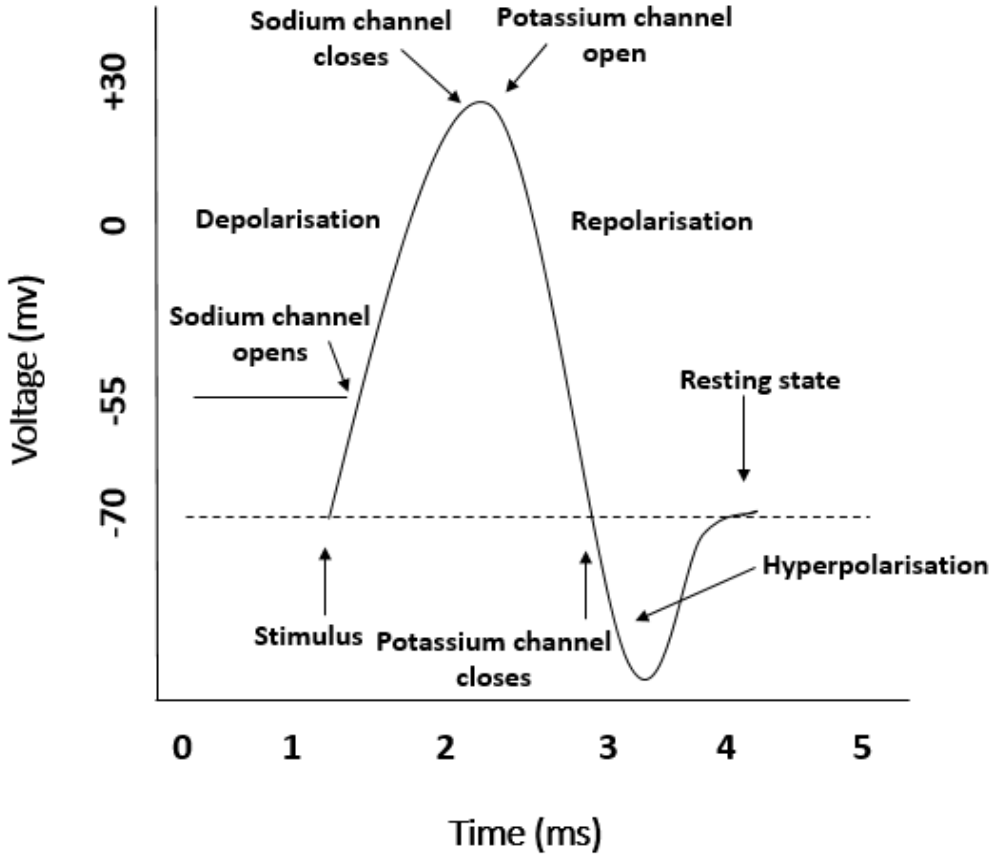

Figure 1.5: Schematic representation of the different stages of firing of an action potential. *Initially, the activation gates on the Na^+ and K^+ channels are closed, and the membrane's resting potential is maintained (-70mV). A stimulus opens the activation gates on some Na^+ channels. Na^+ influx through those channels depolarizes the membrane. If the depolarization reaches the threshold (-55mV) it triggers action potentials. Depolarization passes the threshold and more voltage-gated sodium channels open, causing a rapid entry of Na^+, while the K^+ channels activation gates remain closed. The inactivation gates on most Na^+ channels close blocking Na^+ influx. The activation gates on most K^+ channels open permitting K^+ efflux which again makes the inside of the cell negative and repolarize the membrane (+30mV). Both gates of Na^+ channels are closed, but activation gates on some K^+ channels are still open, causing additional K^+ to flow into the extracellular fluid, and the neuron hyperpolarizes (-75mV). Voltage-gated potassium channels close eventually, and the cell returns back to resting ion permeability allowing the membrane to return to the resting state.*

1.2.3 Synaptic transmission

The ability of the neurons to communicate with each other by moving chemical or electrical signals across a synapse is termed as synaptic transmission. Neurons convey their information using an electrical signal; the dendrites receive the signal and the information is then passed along the axon until it reaches axon terminal and the synapses (Kandel *et al*., 2000).

Chemical synaptic transmission is a process where a neuron converts its electrical signal into a chemical signal allowing the electrical signal to be passed onto the next neuron (Kandel *et al*., 2000). When the AP signal arrives at the axon terminal, local depolarization causes calcium channels to open (Fields & Stevens-Graham, 2002). As Ca^{2+} enters the presynaptic terminal, its concentration increases inside the terminal in comparison to outside, Ca^{2+} initiates the vesicles to fuse with the presynaptic membrane and then releases the neurotransmitter into the synaptic cleft via exocytosis. The synaptic cleft is a space between both neurons that prevents them directly transmitting AP and synapses are intercellular junctions between excitable cells. Once released, the neurotransmitter diffuses through the synaptic cleft and binds to appropriate receptors on postsynaptic membranes causing either the opening or closing of ion channels based on the nature of the neurotransmitter and the receptor it interacts with (Belousov *et al*., 2001; Hyzinski-García *et al*., 2009). Depending on the type of neurotransmitter released such as glutamate, the signals can be excitatory, which leads to the transmission of the AP, or inhibitory with the main inhibitory neurotransmitter being gamma-amino butyric acid (GABA) which prevents further action potential generation (Kandel *et al*., 2000). When the ionotropic glutamate receptors are activated, Na^{+} /K^{+} ions enter the neuron and depolarise the cell, which initiates another AP to relay information in the postsynaptic region (Figure 1.4) (Rasband & Shrager., 2000).

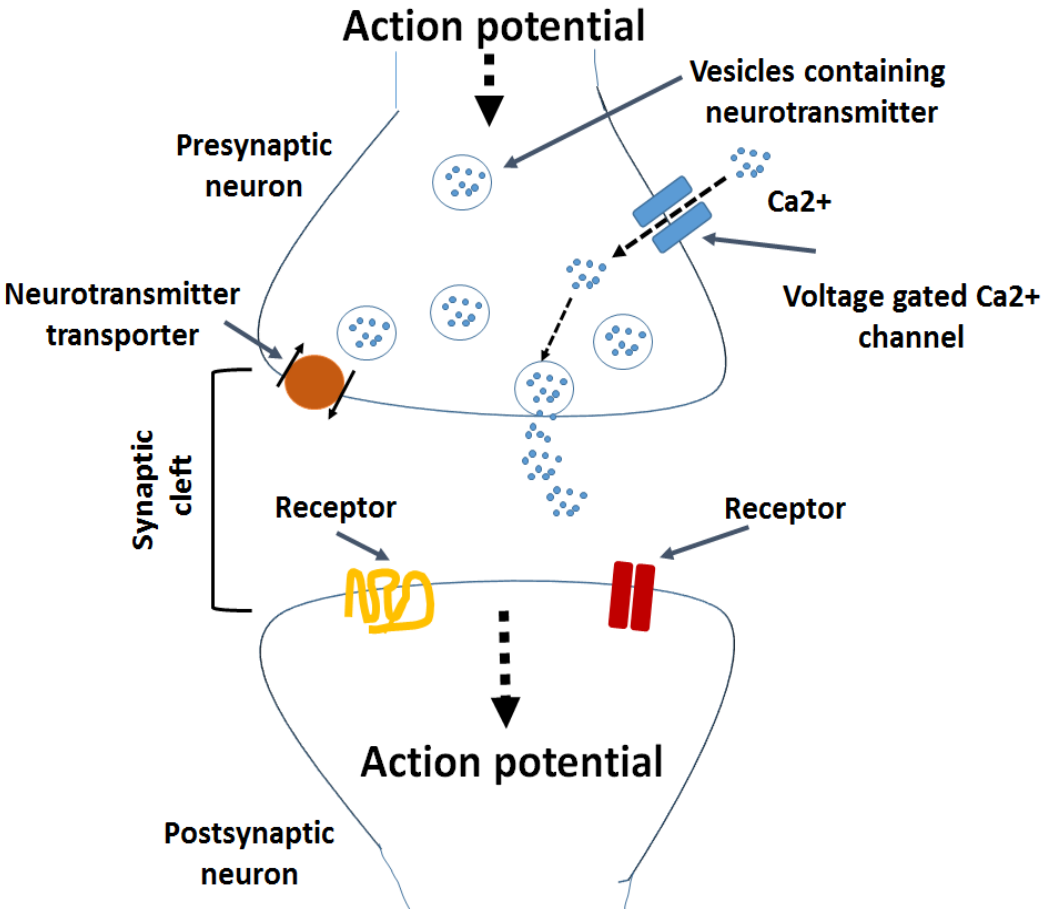

Figure 1.6: Signal transmission at a chemical synapse: *Action potential depolarizes the presynaptic axon terminal that causes voltage-gated Ca^{2+} channels to open resulting in an influx of Ca^{2+}. As the Ca^{2+} enters the presynaptic terminal it triggers exocytosis of synaptic vesicles, as a result neurotransmitter are released and diffuse across the synaptic cleft, before binding to neurotransmitter receptors in the postsynaptic neurons. This binding causes a postsynaptic potential, which once it reaches the threshold level initiates an action potential in the postsynaptic neuron.*

1.2.4 Glutamate receptors

Glutamate is the principal excitatory neurotransmitter in the CNS that exerts its function through the glutamate receptors found in the CNS (Meldrum, 2017). Glutamate receptor present on the postsynaptic neuron are subdivided into two categories: those that act as ion channels are known as ionotropic receptors and those when activated are linked to intracellular second messengers known as metabotropic receptors. Ionotropic receptors consist of N-me-

thyl-D-aspartate receptors (NMDARs), α-amino-3-hydroxy-5-methyl-4-isoxazolepropionic acid receptors (AMPARs) and kainate receptors (KARs) (Marmiroli and Cavaletti, 2012).

1.2.4.1 NMDA receptors

NMDARs are classically found on the postsynaptic neuron, however increasing evidence suggests the existence of presynaptic NMDARs (Tzingounis and Nicoll., 2004; Zorumski and Izumi., 2012). NMDARs have the highest affinity for glutamate. They form heteromeric assemblies composed from GluN1, GluN2A, GluN2B, GluN2C, GluN2D, GluN3A and GluN3B subunits. NMDARs have distinct features including being ligand-gated and voltage dependent however, for its activation, it requires both glutamate and either glycine or D-serine as a co-agonist (Tong *et al*., 2008), and when activated it allows positively charged ions to flow through the cell membrane. Depolarisation of the neuron is an essential factor for activation of NMDARs, as under resting conditions, a magnesium ion is bound extracellularly in the ion channel preventing the activation of the receptor (Ascher *et al*., 1988; Nikolaev *et al*., 2012). This furthermore prevents any unwanted ions passing through into the neuron, however depolarisation results in magnesium removal. This removal allows Ca^{2+}, Na^{+} and K^{+} ions to pass through the NMDAR leading to depolarisation of postsynaptic neurons (Wang *et al*., 2011).

1.2.4.2 AMPA receptors

AMPARs are localised postsynaptically and consist of four subunits known as GluA1-4, which can assemble into either homomeric or heteromeric assemblies (Boulter *et al*., 1990). AMPARs are activated by glutamate binding but they have lower affinity to glutamate in comparison to NMDAR but higher than kainate receptors. Unlike NMDARs, the majority of AMPARs are impermeable to calcium due to the presence of the GluA2 subunit (Jonas, 2000; Mayer, 2006) however AMPARs are required for the initial excitatory signal when glu-

tamate is released (Mayer, 2006). AMPARs are the main contributors to excitatory synaptic transmission, mediating the fast and rapid excitation of many synapses. When glutamate binds, it activates the receptor and activation opens the pore of the channel, permitting the inward flow of sodium and potassium, resulting in the depolarization of the neuronal membrane (Sprengel., 2006; Platt., 2007) and allowing action potentials to carry on from neuron to neuron (Sprengel., 2006). Depolarisation of the neuron under high frequency of electrical signal results in the release of the magnesium ion bound to NMDARs and allows calcium influx through them. Allowing AMPARs to play a role in glutamate mediated synaptic transmission. Furthermore, increased or decreased AMPAR expression at the postsynaptic membrane can regulate synaptic plasticity through long-term potentiation and long-term depression respectively, (Lüscher *et al*., 1999; Emond *et al*., 2010).

1.2.4.3 Kainate receptors

Kainate receptors (KARs) are a third subtype of ionotropic glutamate receptor; it has the weakest affinity for glutamate in comparison to NMDARs and AMPARs. It is composed of GluK1–5 subunit and functional receptors form homomers but have the capability to make heteromers. Heteromers can be assembled if GluK4 or GluK5 is expressed with the other subunits, however they do not form functional channels if they are expressed on their own (Kew and Kemp, 2005). KARs performs different roles from the other two ionotropic receptors (Copits & Swanson, 2013). However, it shares many characteristics with AMPARs (Pinheiro and Muller, 2008). Like NMDARs, they are also localised presynaptically as well as postsynaptically (Chittajallu *et al*., 1999). Studies have shown that KARs have different roles in synaptic transmission including carrying part of current charge in the postsynaptic region, while in the presynaptic region, it has been proposed to regulate transmitter release at both excitatory and inhibitory synapse (Lerma, 2006).

1.2.4.4 Metabotropic receptors

Metabotropic glutamate receptors are G-protein-coupled receptors (GPCRs) that are found both presynaptically and postsynaptically in neurons and activate a cascade of events leading to protein modification and are involved in the perception of pain, learning and memory (Nicoletti *et al*., 2011). Metabotropic receptors are classified into three groups based on sequence similarities, pharmacological properties and intracellular signal transduction mechanism and consist of eight different subtypes: mGluR1– 8 (Pitsikas *et al*., 2014) which have roles in anxiety, learning and memory and their activation can either be excitatory or inhibitory. Group 1 (mGlu1 and mGlu5) are coupled to Gq/G11 whereas, group 2 (mGlu2 and mGlu3) and group 3 (mGlu4, mGlu7 and mGlu8) are classically coupled to Gi/Go (Simonyi *et al.,* 2010; Pitsikas, 2014).They are involved in modulating CNS function by controlling neuronal excitability and causing changes in synaptic excitability through release or inhibition of neurotransmitter and also proposed to be involved in certain forms of long term depression (Grueter and Winder, 2009).

1.3 Immune system

The immune-system is a complex but organized system which protects the body by responding to any invasion of foreign particles or micro-organisms (Abbas *et al*., 2010). The immune system is divided into two different subdivisions: innate immune system and adaptive immune system (Figure 1.5). These two immune systems interact with each other through direct cell contact such as dendritic cells (DCs) activating T cells, or through indirect interaction through chemical mediators such as cytokines, chemokines and antibodies (Heeg *et al*., 2007).

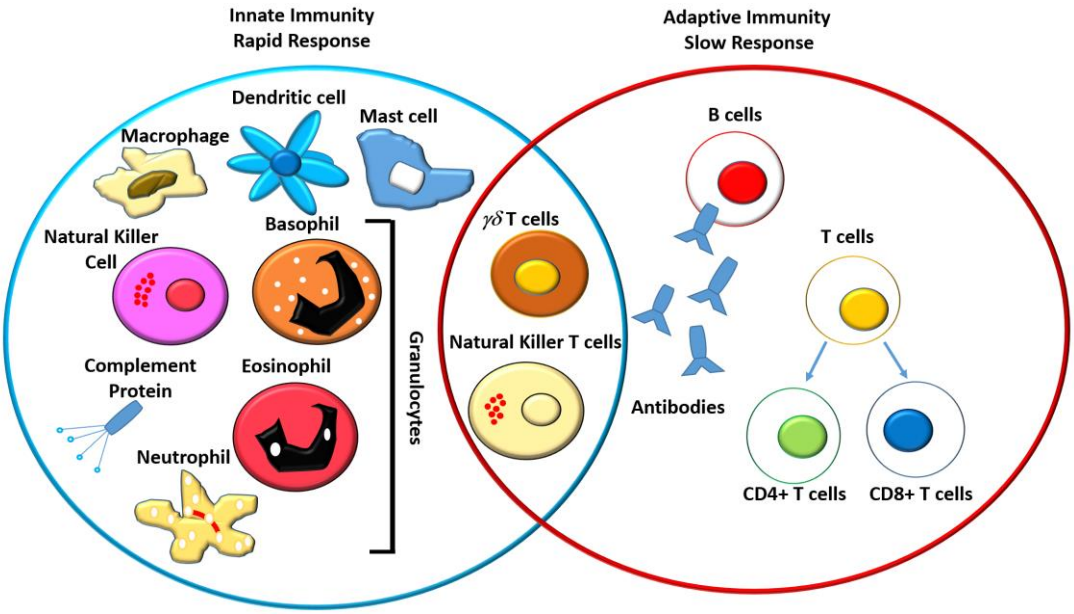

Figure 1.7: Immune cells in the innate and adaptive immune system. *The adaptive and innate immune systems are inter-connected, for example dendritic cells which belongs to the innate immune system is also an important adaptive immune system cell activator. The adaptive immune system consists of antibodies, B cells, and CD4⁺ and CD8⁺ T cells, and these enable a highly specific response against a particular target. Natural killer T cells and γδ T cells are cytotoxic lymphocytes that overlap both innate and adaptive immunity. When the innate immune system fails to defence the invasion by pathogens it initiates the adaptive immune response to defence and at times they often work together to fight against any pathogenic invasion. Schematic adapted from Dranoff., 2004.*

1.3.1 Innate immune system

The innate immune system acts as the initial line of defence against the invading pathogens and helps in controlling infection, delivering protective response against pathogens within minutes to hours. The innate immune system is consisting of a number of soluble factors and proteins as well as a diverse set of cells, including granulocytes, macrophages, DCs and natural killer (NK) cells. It also alerts adaptive immune responses to the presence of pathogens by presenting antigens (Fearon and Locksley., 1996). Innate immune cells such as DCs, macrophages and neutrophils can engulf pathogens, maintain immune homeostasis but can also play a detrimental role during autoimmunity and other inflammatory diseases. Other myeloid-derived cells such as mast cells, eosinophil and basophils are also involved in initiating the inflammatory response to alert the adaptive immune system (Kaufmann and Steward., 2005).

TLRs are mostly expressed in DCs and macrophage and play a very significant role in innate immune system for fighting off pathogens (Rodrigues *et al*., 2006; Arika *et al*., 2012). In response to infection, TLRs recognize the unique chemical structure (lipids, carbohydrates, nucleic acids) of the pathogen referred as pathogen associated molecular pattern (PAMPs) which is differentiable from the host cell molecules (Rodrigues *et al*., 2006; Arika *et al*., 2012). There are specific TLRs for PAMPs, and recognition of the different pathogen component leads to activation of specific signalling pathways, which helps in clearance of the infectious agents (Arika *et al*., 2012; Gazzineli *et al*., 2006). TLR mediated recognition at the site of infection induces DC maturation and migration to the draining lymph nodes where they activate antigen specific T cells, thus directing the innate system to the adaptive immune system (Arika *et al*., 2012).

1.3.1.1 Dendritic cells

DCs are innate immune cells that are derived from hematopoietic bone marrow progenitor cells and recognised as the professional APC in the immune system. Like macrophages and neutrophils, DCs can degrade any pathogens, however their main function is to process antigenic materials and present it on the surface of specific T cells. Immature DCs process foreign antigens into small peptides, which are then displayed on their cell surface in combination with major histocompatibility complex molecules (MHC) which allows presentation to, and activation of, T cells. Before migrating to the draining lymph nodes, mature DCs up-regulates adhesion to intracellular adhesion molecule-1 (ICAM-1) and expression of co-stimulatory molecules (CD80, CD86 and CD40) that required for T cell proliferation and activation (McCarthy *et al*., 1997). In the LNs they present the antigenic peptides to naïve T lymphocytes, inducing T cell proliferation and polarisation into antigen specific effector or regulatory cells. The activated T lymphocytes subsequently modulate immune responses through production of a collection of immunomodulatory cytokines such as IL-17, IFN-γ, IL-4, IL-5, IL-10 and others (Banchereau and Steinman., 1998). Therefore, they are considered to be an essential link between the

innate and adaptive immune responses, and therefore play pivotal roles in many immune mediated diseases.

1.3.1.2 Macrophages

Macrophages are a type of white blood cells and one of the key cells involved in immune response. Tissue resident macrophages are present in most of the tissues of our body and are derived from yolk sac erythro-myeloid progenitors in the embryo, whereas the circulating macrophages are derived from bone marrow myeloid progenitor cells. During an infection or tissue damage, monocytes are rapidly recruited from the circulation to the tissue, where they differentiate into macrophages. Function of macrophages mainly involves phagocytosis of any pathogens and apoptotic cells and presentation of antigen to T cells via MHC molecules. Furthermore besides its critical role in innate immunity macrophages also help initiate adaptive immunity. As discussed earlier in this chapter microglial cells are known as the CNS resident macrophages and are the immunocompetent cell of the CNS (Kreutzberg., 1996; Streit *et al*., 1999). Their main functions are similar to that of macrophages, which involves phagocytosis of cellular debris and pathogenic material and antigen presentation via MHC molecules. As mentioned earlier in this chapter, both activated macrophages and microglia can be divided into two subtypes, classical activated macrophages (M1) and alternatively activated macrophages (M2). M1 macrophages are pro-inflammatory cytokine (TNF-α, IFN-γ , IL-12, IL-6, iNOS, NO and proteases) releasing cells which, promotes T helper responses, and contribute in amplification of inflammation.

1.3.1.3 NK cells

NK cells are innate lymphoid cells which, plays a crucial role in the innate immune response. The key function of NK cells includes perforin and granzyme-mediated apoptosis of infected cells and production of IFN-γ, IL-17, and TNF-α cytokines.

1.3.2 Adaptive immune system

The adaptive immune system is the second branch of the immune system which acts as the second line of defence towards foreign particles when the innate immune system fails to control it. It is also known as acquired/specific immune response due to its capability of specifically recognising certain parts of a pathogen known as the antigen. The adaptive immune response is mediated by T lymphocytes and B lymphocytes, which amplifies the innate response and functions in shaping of the immune response whether it be an antibody mediated response due to a greater preference for B lymphocytes or cell mediated due to T lymphocyte preference, is dependent on the innate response. In addition, this will also lead to immunological memory development, therefore if the same pathogen becomes a threat in the future, a known response to eliminate the threat will be produced (Wager *et al*., 2011; Casadevall and Pirofski., 2012). The adaptive immune system is shaped through life by the pathogens our body encounter and provides long lasting immune response. However, these responses cannot recognise and act against pathogens without a specific mechanism enabling them to do so.

1.3.2.1 T cells

T cells are classified as lymphocytes, which are an essential part of the adaptive immune response. Lymphoid progenitor cells that are derived from the bone marrow migrates to the thymus; thymocyes at their earliest stage do not express CD4 or CD8 and so, they are classified as double-negative ($CD4^-CD8^-$) cells. However, as the cells progress to develop, they become double-positive thymocytes ($CD4^+CD8^+$) before undergoing positive and negative selection and finally becoming mature to single-positive ($CD4^+CD8^-$ or $CD4^-CD8^+$) thymocytes. Thymocytes expressing T cell receptors (TCRs) specific for MHC-class-I differentiate into $CD8^+$ T cells, whereas those expressing TCRs specific for MHC-class-II ligands mature into $CD4^+$ T cells. T cells are primarily involved in cellular immune processes through production of cytotoxic proteins, including perforin and granzymes and numerous inflammatory mediators like cytokines. Some of these cytokines are usually lymphocyte growth factors, and

some functions as pro-inflammatory or anti-inflammatory molecules, while other cytokines polarize the immune response to antigen (Dinarello., 2007). However, the secretion of cytokines depends on many factors including the T cell subset (CD4 or CD8), the antigens encountered and the milieu of these cells. T cells recognise any antigen in two steps which includes capturing or processing of antigen by APCs followed by antigen presentation to naïve T cells. APCs capture antigens by receptor-mediated endocytosis, phagocytosis and pinocytosis, and form short peptide fragments by degrading these internalized proteins through proteolysis (Blum *et al*., 2013). The peptide-binding region of MHC molecule loads the small peptide fragments and forms a peptide-MHC (pMHC) complex, which are then presented on the surface of APCs, where they can be taken by naïve T cells via their TCR. Once the T cells are activated within the peripheral lymphoid tissues (spleen and lymph nodes), they re-enter the cell cycle and start to proliferate rapidly to differentiate into its effector T cells, which are able to produce molecules that are required for their specific helper or cytotoxic functions (Murphy., 2011).

Naïve $CD4^+$ T cells get activated following the presentation of fragment of peptide antigen loaded onto MHC-II molecules on the surface of APCs, (Figure 1.6) along with costimulatory signals via CD28-CD80/CD86 interactions (Sela-Culang *et al*., 2013).

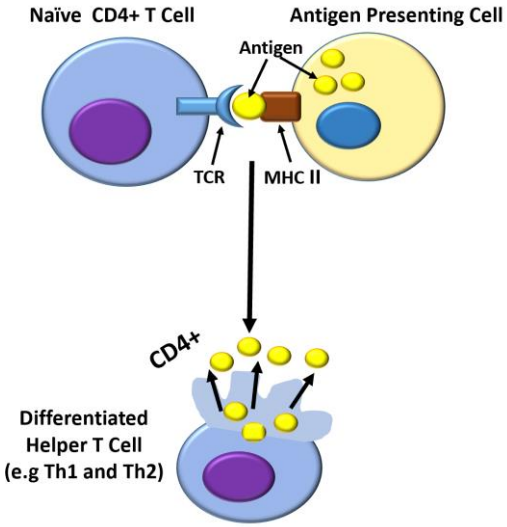

Figure 1.8: Activation of naïve $CD4^+$ T cells*. Naïve $CD4^+$ T cell get activated by antigen presenting cells presenting the antigen by the MHC-II.*

Activated CD4$^+$ T cells then differentiate into different subsets of T helper (Th) cells: Th1, Th2, Th17, induced regulatory T cells (iTreg cells) and Th22 cells or T follicular helper (Tfh) cells which all have unique differentiation profiles, phenotypes and effector functions (Figure 1.7) (Zhu and Paul., 2008). Some of these helper cells are involved in assisting antibody production by B cells, enhancement and maintenance of cytolytic functions of cytotoxic T cells, regulation of macrophage activation and suppression of immune responses to prevent autoimmunity (Zhu *et al*., 2010). Th1 and Th2 are the two main subsets of T helper cells. Th1 cells secrete IL-2 and IFN-γ in response to intracellular bacteria and viruses and are primarily involved in the activation of macrophages (Biedermann *et al*., 2004). Whereas Th2 cells secrete IL-4, IL-5 and IL-13 in response to allergens or helminth antigens and plays vital role in assisting the production of antibodies by B cells (Carli *et al*., 2009). In addition to the traditional Th1 and Th2 subsets, Th17 is another subset of pro-inflammatory Th cell defined by their production of IL-17, IL-17F, IL-21, and IL-22. Th17 cells and the cytokines produced by these cells mediate host defensive mechanisms to various infections, including extracellular bacterial infections, they ae also involved in the pathogenesis of many autoimmune diseases (Ouyang *et al*., 2008).

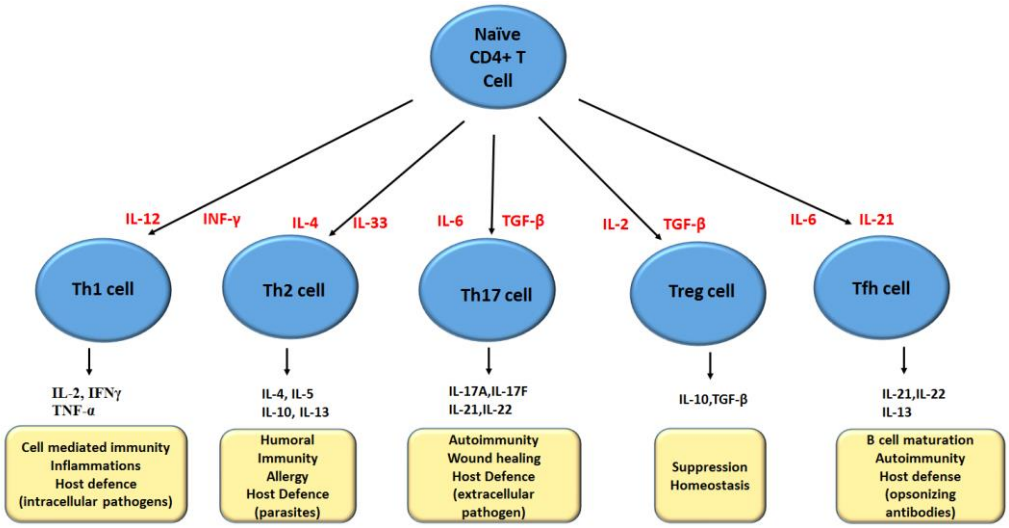

Figure 1.9: CD4$^+$T cell differentiation. *The activated CD4+T cells differentiate into different T helper cell subsets depending on the cytokines present within the local environment. The main subtypes of CD4$^+$T cells are Th1, Th2, Th17, Treg and Tfh cells, all of which have unique differentiation profiles, phenotypes and effector functions.*

Regulatory T cells also known as Treg cells is another important subset of $CD4^+$ T cells which function to maintain self-tolerance and immune homeostasis. Treg cells utilise factor forkhead box P3 (FOXP3) and produces inhibitory cytokines such as TGF-β and IL-10 (Sakaguchi *et al*., 2009). Treg cells can be classified as either natural or inducible. Natural Treg cells are a small subpopulation of CD4 cells, which can be distinguished by the expression of IL-2 receptor (CD25) and the transcription FoxP3 within the thymus (Costantino *et al*., 2008). Whereas inducible Treg cells (iTreg) are differentiated from naïve conventional T cells (Tconv) within the periphery by an antigen in the presence of anti-inflammatory cytokines IL-10, TGF-β and retinoic acid (RA) (Chen *et al*., 2003; Costantino *et al*., 2008). T regulatory 1 (Tr1), Th3 and subsets of $CD8^+$ T cells belong to the iTreg cell group (Chen *et al*., 2003; Costantino *et al*., 2008) and plays key role in tolerance to self and non-self-antigens (Sakaguchi., 2004). These Tregs has been identified in healthy individuals however failures of the thymic and peripheral tolerance mechanisms have shown to contribute in development of autoimmune diseases.

The naïve $CD8^+$ T cells are involved in providing resistance toward various pathogen invasions (Harty *et al*., 2000). $CD8^+$ T cells predominantly recognize peptides processed from endogenously synthesized antigens and presented by MHC class I molecules (Figure 1.8) (Haring *et al*., 2006; Strioga *et al*., 2011) and $CD8^+$ T cells can be activated by MHC I molecules found on almost all nucleated cells (Lehner & Cresswell., 2004). Activated $CD8^+$ T cells differentiate into $CD8^+$ cytotoxic T cells (CTLs) which secrete either Th1-like IL-2 and IFN-γ or Th2-like IL-4, IL-5, IL-6, and IL-10 cytokines. Both $CD8^+$ CTL types kills cancer cells or damaged and infected cells (Sad *et al*. 1995). Unlike $CD4^+$ T cells, $CD8^+$ T cells are able to induce death directly by the release of cytotoxic molecules such as granzymes and perforin (Brehm *et al*. 2005). These cytotoxins are responsible for targeted cell destruction, once they are released from the granules they can trigger apoptosis in any cells by penetrating the lipid bilayer. Just like cytokines, cytotoxins can act locally or at a distance, and sometimes target bystander cells (Fleischer, 1986).

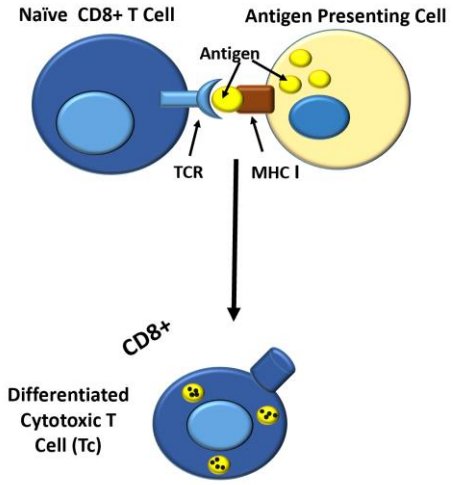

Figure 1.10: Activation of naïve CD8⁺ T cells*. Naïve CD8⁺ T cells get activated when the antigen presenting cells present the antigen by the MHC I.*

1.3.2.2 B cells

B cells are key lymphocytes involved in the humoral immunity of the adaptive immune system. Development of B cell occurs within the bone marrow and peripheral lymphoid tissues (spleen). Upon activation, following an immune response and stimulation by foreign antigens and with the help of activated T helper cells (Mauri & Bosma., 2012) naïve B cell cells differentiate into plasma B cells or memory B cells. Plasma cells secrete specific antibodies towards the antigen (Liu *et al*., 2010), whereas memory B cell forms the memory of the specific antigen, so the next infection caused by the same antigen can be resolved quickly. Antibodies secreted by plasma cells are the secreted form of B cell receptor (BCR) which binds pathogen or their toxic products in the extracellular spaces of the body and plays crucial role in neutralizing and opsonizing a pathogen by making it more susceptible to the action of phagocytes, and activating complements (Mauri & Bosma., 2012).

1.4 Communication between CNS and immune system

For a long time, the CNS have been regarded as being immune privileged due to the fact that the persistence of the allograft of brain tissue was better than any other peripheral organs and the neuronal function of the CNS was solely dependent on its tightly regulated microenvironment (Hawkins and Davis.,

2005). To maintain the homeostasis within the CNS, the BBB plays a critical role (Weiss *et al*., 2009). The BBB is a specialised structure that exists between the blood vessels and the brain parenchyma and plays a critical role to maintain the proper function within the CNS, by protecting and maintaining the balance of the CNS from fluctuations of nutrients, hormones, metabolites and blood constituents including endogenous and exogenous compounds (Hawkins and Davis., 2005; Weiss *et al*., 2009). The BBB consists of a very highly restricted receptor system that only allows regulated movement of oxygen and carbon dioxide, nutrients such as glucose into the CNS and toxic substances and metabolite out of the CNS (Persidsky *et al*., 2006; Weiss *et al*., 2009; Banks & Erickson., 2010). Most importantly BBB prevents the entry of pathogens that have the ability to cause damage by destroying the vulnerable tissue of the brain (Ballabh *et al*., 2004). BBB thus serves as a first line of defence against the infiltration of immune cells and micro-organisms (Abbott *et al*., 2010).

The BBB is formed of several different types of cells including the endothelial cells, and pericytes and astrocytes, (Persidsky *et al*., 2006; Abbot et., 2006). In BBB, a single layer of endothelial cells attached together forms a tight junction which are 50-100 times tighter than those in the peripheral endothelium (Abbott., 2002; McCaffrey *et al*., 2007). In comparison to any other endothelial cells in the body, the endothelial cells of the BBB have very distinctive physiological properties (Weiss *et al*., 2009) which lack perforation (Reese & Kanovsky., 1967), but have restricted and controlled permeability. These endothelial cells have a highly reduced incidence of paracellular and transcellular permeability (Fenstermacher *et al*., 1988) and contain a large number of mitochondria, associated with a strong metabolic activity (Oldendorf *et al*., 1977). The presence of pericytes in BBB also enables the BBB to form tight junctions (Armulik *et al*., 2010). The basement membrane of the BBB is embedded with contractile connective tissue cells called pericytes, which develop around capillary walls and share the basal membrane with brain capillary endothelial cells (Hurtado-Alvarado *et al*, 2013). Absence of pericytes has shown to form weak BBB with increased permeability (Bergers & Song., 2005).

Several studies have also reported the presence of astrocytes in the basement membrane of BBB, where they extend their long processes whose end feet wraps around the endothelial and the cerebral micro-vessel walls, surrounding majority of the capillaries formed by the endothelial cells (Abbott *et al*., 2006). Astrocytes release a number of soluble factors such as basic fibroblast growth factor, angiotensin, angiopoietin I and glial-derived neurotrophic factor which help in the maintenance of BBB integrity (Larochelle *et al*., 2011). Astrocytes have also demonstrated to have critical influence on the BBB by enhancing endothelial cell tight junctions and reducing gap junctions through astrocyte-endothelial interactions (Tao-Cheng *et al*., 1987). Together these cells with their distinctive characteristics control the passage of different molecules in and out of the CNS. However, the properties of the BBB may vary according to the need of the CNS, and they can adjust their functions especially during disease condition (Banks., 2009).

However, the concept of the CNS as an immunologically and pharmacologically privileged site has changed over recent years. New research evidence suggests that there is a vast network of communication between the CNS and the immune system (Gosselin & Rivest., 2007). It is now well established that the immune cells and molecules are present in the CNS and when required they provide defence support to the CNS through immune response (Engelhardt and Coisne., 2011; Ransohoff and Brown., 2012). BBB dysfunction or breakdown occurs in numerous neurological diseases and conditions such as brain trauma, stroke and oedema, following the dysfunction or breakdown of the BBB, entry of harmful and toxic components together with immune cells to the CNS occur which later contribute to disease pathology. It is favourable to have minimum damage to the CNS due to an effective immune response, however the activation of the immune response may also damage healthy host cells and tissues causing impairment in CNS function, thus induce transient or enduring behavioural changes in the host and lead to the progression of neurodegenerative diseases (Amor *et al*., 2010; Chaplin., 2010). The pathology of inflammatory neurodegenerative disease like MS has been demonstrated to be influenced by the entry of immune cells of BBB which leads to the autoimmune destruction of the myelin sheath. These studies suggest that the CNS is not immune privileged as previously reported, and there is a well-maintained

communication between the CNS and the immune system which however is tightly regulated by the BBB (Weiss *et al*., 2009).

1.5 Multiple sclerosis

MS is an autoimmune, chronic neuroinflammatory demyelinating disease of the CNS, caused by damage to myelin sheaths and neurons following traumatic, anoxic, infectious, and immunological events (Skundric *et al* 2006; McFarland and Martin, 2007; van Horssen *et al*., 2011). Often chronic persistence and/or reoccurrence of inflammation in the CNS causes chronic progressive and/or relapsing demyelination and damage to axons and ODCs, which ultimately leads to clinical symptoms such as paralysis and disability (Skundric *et al.,* 2006). MS is characterized by the heterogeneous clinical symptoms with complex pathology and pathogenesis.

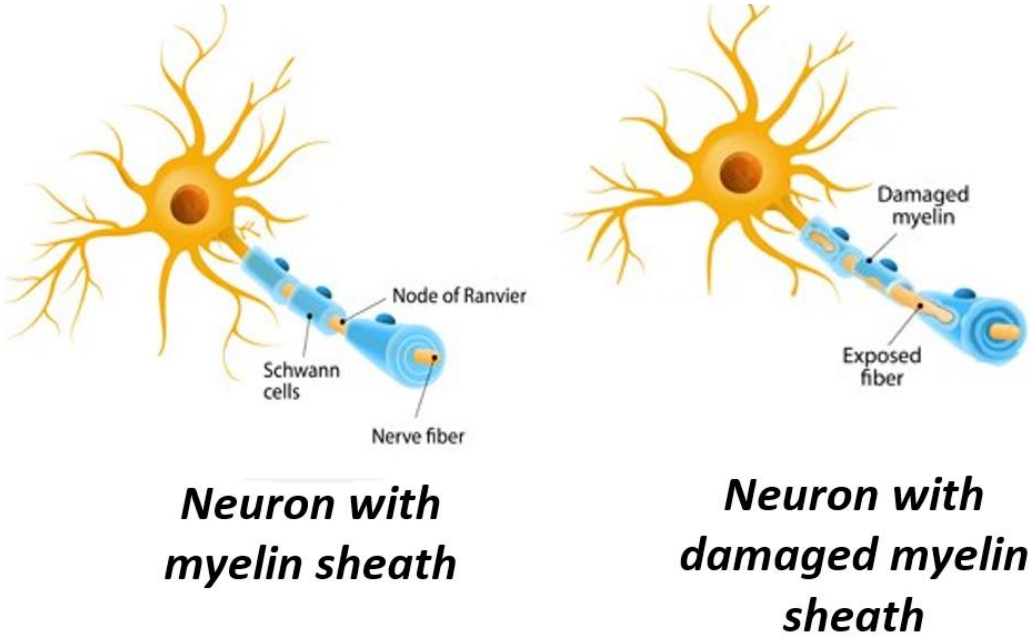

Figure 1.11: Diagram of healthy axons and demyelinated axons. *Axon of a healthy neuron is usually insulated with layer of fatty material termed myelin, which enable the neurons to quickly conduct impulses between the brain and different parts of the body. During MS, immune cells from the body's own immune system attack and destroy the myelin sheath, leaving the nerve cell fibres unprotected which causes disruption in transmission of nerve impulses and triggers many of the symptoms of MS.*

Several pathophysiological processes such as inflammation, demyelination and axonal damage mediate the disease manifestation of MS. Pathological studies suggest four different patterns in demyelination in the MS lesion based on: myelin protein loss (pattern I); geography and extension of plaques (pat-

tern II); patterns of oligodendrocyte destruction (pattern III); and immunopathological evidence of complement activation (pattern IV) (Lucchinetti *et al*., 2000). Pattern I and II demonstrate close similarities to T-cell–mediated and T-cell plus antibody–mediated autoimmune encephalomyelitis, respectively. Patterns III and IV are highly reminiscent of a primary oligodendrocyte dystrophy, reminiscent of virus- or toxin-induced demyelination rather than autoimmunity (Lucchinetti *et al*., 2000). Although MS is considered a white matter disease, grey matter is also affected (Lucchinetti *et al*., 2000; Lassmann *et al*., 2001; Lassmann *et al*., 2007). The complex immunopathology of MS is distinguished by activation of microglia and infiltration of peripheral immune cells (macrophages and lymphocytes) into the brain and spinal cord (Hickey *et al*., 1991).

1.5.1 MS incidence and prevalence

In developed countries, MS is a common CNS disease leading to neurological disability in young adults (Zipp *et al*., 2006). MS is a disease of all ages but mostly affects people aged between 20-40 (Tienari., 1994), with peak age of disease onset at 30 years of age (Compston *et al*., 2006).

2.5 million of world's population suffers from MS (Thompson *et al*., 2006), with global prevalence rate unevenly distributed. MS prevalence is lower in the populations living in close proximity of the equator but is elevated with latitude in both the northern and southern hemispheres. The disease is common among the populations of northern European descent, especially in Scandinavia, the British Isles, the northern tier of the United States and southern Canada (Compston., 1997). In Asia and South America the prevalence rate is less than 5 cases per 1000,000 varying to 11 and 74 cases per 100,000 in Australia. Whereas the prevalence rates range between 100 to 200 cases per 100,000 in Scotland and North America (Milo and Kahana., 2009). Women are affected by MS more commonly than men, in a ratio as high as 3.2:1 (Orton *et al*., 2006).

In 2010 it was estimated that 126 669 people were living with MS in the UK (203.4 per 100, 000 population) and that 6003 new cases were diagnosed that

year (9.64 per 100, 000/year) (Mackenzie *et al*., 2013). The MS prevalence in England and Wales is between 100-140 per 100,000, about 170 in Northern Ireland and the highest prevalence rate of 190 in Scotland (Rosati., 2001; Multiple Sclerosis Trust., 2009), with Scotland having the highest incidence and prevalence rates in the UK. A study of north east Scotland found prevalence of MS to be 229 in Aberdeen, 295 in Shetland and as high as 402 in Orkney (Visser *et al*.,2013).

1.5.2 MS aetiology

Despite immense scientific efforts, the aetiology of MS is still largely unknown. Research suggests that there are several risk factors for MS disease including genetic predisposition and environmental factors (Munger *et al*., 2006; Handel *et al*., 2011) as well as viral/microbial infections (Sundström *et al*., 2004; Thacker *et al*., 2006). It is accepted that interaction between susceptibility genes and environmental triggers results in MS (Compston and Coles 2008; Ramagopalan *et al*., 2010). Genetic epidemiology studies indicate genetics may explain up to 30% of the risk of MS (Dyment *et al.,* 2004), Several genes including HLA-DRB1, IL-2Rα, IL-7R and tyrosine kinase 2 (TYK2) (Hafler *et al*., 2007; Ban *et al*., 2009) have been suggested to be associated with MS susceptibility, with HLA-DRB1 being one of the major genes associated with MS risk (Jersild *et al.,* 1973; Francis *et al*., 1991; Oksenberg *et al*., 2004). HLA-DRB1 in particular is not specific to MS and is linked to increased risk of developing other autoimmune conditions including rheumatoid arthritis and type 1 diabetes (Kerlan-Candon et al., 2008; Erlich et al.,2008). Furthermore, genome-wide association studies have identified novel loci with links to disease susceptibility (Patsopoulos et al., 2011; Gourraud et al., 2012), including classes of genes which function as part of the immune system, in particular those associated with T cell activation and proliferation (Sawcer et al., 2011). However, these risk factors on their own are not enough to cause MS they can convey susceptibility to the disease which can be triggered by an environmental factor or viral infection (Pohl et al., 2009; Fga et al 2002; Ascherio et al., 2007). However, any links between MS and viral or environmental factors remain inconclusive.

Geoepidemilogical and immigration studies have proposed environmental factors as one of the vital and highly important risk factors for MS (Ebers 2008; Kahana *et al*., 2009). Two environmental factors that are likely to be involved in MS pathology are certain infectious agents like Epstein-Barr virus and insufficient sunlight exposure (insufficient vitamin D and UV radiation) (Ebers 2008; Kahana *et al*., 2009). Along with these two factors, smoking has been also identified as a risk factor for developing secondary progressive MS (SPMS) (Healy *et al.,* 2009). However, it is not clear and is still under investigation that how these factors contribute to the initiation and development of MS.

1.5.3 Clinical subtype and symptoms of MS

MS is mediated by inflammatory lymphocytes which transmigrate into the CNS and cause tissue damage and neurological impairment. Many studies have demonstrated the presence of multiple leukocytes (lymphocytes, macrophages, and DCs) in the MS lesion suggesting their contribution to the formation of the CNS lesion (Skundric *et al*., 2006; McFarland and Martin 2007; Peterson and Fujinami, 2007, Skundric *et al*., 2015). Based on the extent of gradual decrease in inflammation over time, MS lesions are typically classified as acute, subacute and chronic (Newcombe *et al*., 1993). The loss or inhibition of motor neurons and demyelination of nerve fibres results in impaired APs, thus gives rise to a wide variety of symptoms associated with MS. And the location of the lesions within the CNS determines the nature of the symptoms. Numbness of the face and body are often one of the first symptoms of MS. However, in some patient's vision problems such as blurred or double vision or vision loss can also be the first symptom, which are caused by inflammation and lesions of the optic nerve. Almost 80% of the MS patients suffer from fatigues, however other symptoms include bladder dysfunction, stiff muscles and painful muscle spasms. Some MS patients can also suffer from speech problems, have difficulty with balance and feel dizzy most of the time. Furthermore, some patients can have problems with memory, concentration, information processing and reasoning. Many patients suffer from emotional

changes, including depression, stress, anxiety and mood swings (Michalski *et al*., 2010; Kister *et al*., 2013).

MS has very heterogeneous clinical presentations and has been classified as four clinical subtypes on the basis of both the initial and the current clinical disease course (Noseworthy *et al*., 2000): relapsing-remitting MS (RRMS), secondary progressive MS (SPMS), primary progressive MS (PPMS) and progressive relapsing MS (PRMS). RRMS is characterised by clinical symptoms or relapses followed by improvement. During this disease course patients experience episodes of neurological disability and recovery that can last for many years (Noseworthy *et al*., 2000). 80-85% of the MS patients have RRMS, which is most typical in young patients. RRMS usually begins with a clinically isolated syndrome (Miller *et al*., 2005) with unilateral optic neuritis, a brainstem syndrome or partial myelitis. Clinical symptoms and episodic inflammation develop gradually over several days and peaks after 1-2 weeks, followed by gradual and subsequent improvement over several weeks or months. After 10 to 25 years of RRMS, the majority of these patients (90%) will enter a secondary progressive disease course with or without attacks, called SPMS. It is characterized by a steady decline in neurological function (Noseworthy *et al*., 2000). A minority of patients (10-15%) have PPMS from onset. If any patient following the initial onset of MS exhibits steady neurological function decline without relapses and increase in symptom severity, they are described as having PPMS. This subtype is mostly a non-inflammatory subtype (Lublin and Reingold, 1996; Compston and Coles, 2002). PRMS is an uncommon subtype of MS, which affects around 5% of the patients. It is characterised by a progressive decline of neurological function with more severe attacks.

1.5.4 Drugs and treatment for MS

Over the past 20 years many drugs have been identified as disease-modifying therapies (DMT) for MS, which mainly target the inflammatory component of the disease. Several follow-up studies have evaluated the efficacy of DMTs and have shown that these treatments are only partially effective in halting the disease process, decrease the relapse rate and reduce the number of MRI

lesions in patients with RRMS (The IFN- β Multiple Sclerosis Study Group., 1993; Johnson *et al*., 1995; Jacobs *et al*., 1996; PRISMS Study Group, 1998). There is no treatment currently available to prevent or cure MS.

There are several DMTs which are shown to improve outcome by delaying disease progression significantly (Freedman., 2011). IFNs are cytokines that are normally released from lymphocytes in response to pathogens. Beta-interferon (IFN-β) is used as the first line of therapy with several drugs on the market. There are four IFN-β drugs that are approved as a treatment for MS, Avonex and Rebif (IFN-β1a) and Betaseron and Extavia (IFN-β1b); (Loma and Heyman., 2011). The mechanism of IFN-β's action on MS disease is not fully understood but it has been demonstrated to block IFN-γ mediated disintegration of endothelial tight junctions (Minagar *et al*., 2003) and to reduce BBB permeability to inflammatory cells *in vitro* (Kraus *et al*., 2004; Markowitz, 2007). Based on the observation from other studies IFN-β is believed to inhibit T-cell proliferation and increase the release of IL-10, reduce T-cell migration from the periphery to the CNS, and alter the T cell cytokine secretion profile toward anti-inflammatory responses (Markowitz, 2007). MRI data of MS patients with RRMS have demonstrated that treatment with IFN-β reduced disease severity and episode duration by reducing the size of the lesions in the CNS (Gupta *et al*., 2005).

Glatiramer acetate (GA) also belongs to the first line of therapy for MS. GA, a synthetic polypeptide with 40-100 amino acids, is composed of random sequences of four amino acids (tyrosine, glutamate, alanine, and lysine), which are common in myelin basic protein (MBP). GA is an immune modulator which is believed to shift the immune responses from Th1 to Th2 type, thus shifting of proinflammatory responses towards anti-inflammatory responses (Farina *et al*., 2005; Johnson, 2010).

Other drugs available for MS treatment in the market include Alematzumab, Daclizumab and Rituximab, which are monoclonal antibodies targeting $CD52^+$ lymphocytes, $CD25^+$ NK and T cells and $CD20^+$ B cells, respectively (Buttmann and Rieckmann, 2008; Barten *et al*., 2010; Nicholas *et al*., 2011). Fingolimod (Gilenya) is another immunomodulating drug approved for treating MS. It blocks sphingosine-1-phosphates receptor in T cells that results in

an inhibition of T-cell migration from lymphoid tissue into the peripheral circulation and CNS (Nicholas *et al*., 2011). Mitoxantrone (Novantrone) is an immunosuppressive cytotoxic agent that inhibits B-cell, T-cell, and macrophage proliferation and impairs antigen presentation and production of proinflammatory cytokines (Nicholas *et al*., 2011; Loma and Heyman, 2011). Natalizumab is a monoclonal antibody of vascularate cell adhesion molecule 1. It works by blocking very late antigen (VLA) -4 on the surface of the lymphocytes and eventually blocks the transmigration of inflammatory lymphocytes to the CNS via BBB (Steinman, 2005). Natalizumab being one of the most popular drugs for MS has recently shown to develop progressive multifocal leukoencephalopathy in patients following treatment with this drug and therefore led to its reduced use currently (Loma and Heyman, 2011).

In recent years, apart from the conventional treatments a new form of treatment known as the autologous haematopoietic stem cell transplantation (AHSCT) has shown promises to ameliorate and terminate MS disease activity (Burman, J. et al., 2017; Muraro, P.A. et al., 2017; MStrust., 2019). AHSCT uses high doses of chemotherapy to wipe out the existing erroneous immune system in the MS patient's body, and then rebuilt the immune system using the transplanted stem cells collected from patients' blood before the chemotherapy to stop the immune system to attack the myelin and causes inflammation in the brain and spinal cord (Burman, J. et al., 2017; Muraro, P.A. et al., 2017; MStrust., 2019).

Despite the presence of the above treatments, there are limitations of the current available drugs with side effects and many non-responding patients. Even though AHSCT has shown success in treating MS, it is a highly costly treatment and has several risks and side effects, which includes being immunocompromised and susceptible to infection immediately after the conditioning chemotherapy and until the immune system has been rebuilt by the stem cells following the transplantation stage (Broder, M.S. et al., 2017). There are chances of developing other autoimmune conditions such as autoimmune thyroiditis and other chemotherapy related side effects such as fatigue, weakness and a temporary loss of appetite, increased risk of bleeding and bruising and worsening of the MS symptoms (Burman, J. et al., 2017; Muraro, P.A. et al.,

2017; MStrust., 2019). Use of high dose of chemotherapy can cause longer term side effects such as lowered fertility, or early menopause. Furthermore, there is also a risk of dying due to the procedure. Thus, further studies are required to identify new therapeutic targets and treatments for better cure of MS patients. In addition, most of the DMTs, including IFN- β -1b and GA (Baren *et al*., 2010), are effective only on RRMS but not on PPMS. Combination therapy strategies have also been suggested to target a range of disease mechanisms because of the complex and heterogeneous nature of MS pathogenesis. Unfortunately, the large, randomised, controlled trials based on previous promising preliminary studies have shown negative or conflicting results. Thus, further studies are required to understand better of MS pathogenesis and to identify new therapeutic targets and treatments for patients.

1.6 Animal models of MS disease

EAE is the most commonly used animal model for the inflammatory demyelinating disease of the CNS like MS because of its immunopathological resemblance, EAE is characterized by mononuclear cell infiltration into the CNS and demyelination observed in MS (Lindsey, 2005; Comabella and Khoury, 2011).

Over the past 50 years, an immense amount of research has been carried out to establish and develop an animal model of MS disease in an effort to study and understand the pathogenesis of encephalomyelitis. Patients, when given a repeated injection of Pasteur's vaccine (consisting of a suspension of dried spinal cord collected from rabbit with rabies), displayed encephalomyelitis that was different from that of rabies. Following that, encephalomyelitis had been demonstrated when rabbits and monkeys were administered with series of injections of neural tissues which indicated the encephalomyelitis resulted from the unintentional induction of an autoimmune response against neural antigens (Koristchoner *et al*.,1925; Rivers *et al*., 1933; Rivers *et al*., 1935).

Induction of EAE became easier and more trustworthy when complete Freund's adjuvant (CFA) was introduced. CFA is an emulsion of mineral oil containing dried mycobacteria such as *mycobacterium tuberculosis* (M. tuberculosis) and was first developed in 1940's by Jules Freund (Derelanko and Auletta., 2014). Injecting antigen in CFA induces a strong activation of local cells, and therefore a vigorous and prolonged immune response against the antigen (Freund and McDermott 1942; Freund, 1947; Freund, 1956). In 1946, Kabat *et al* reported the induction of EAE in 3 out of 4 monkeys using three weekly injections of rabbit brain emulsion in CFA. Following that, success of EAE induction using CFA was reported in rabbits, monkeys, and guinea pigs (Kabat *et al*., 1947; Morgan *et al*.,1947; Morisson *et al*.,1947; Freund et al.,1947) and in many other species like dogs, cats, rats, sheep, goats, pigs, chickens, and pigeons (Lindsey *et al*., 2005). However, there was a failure in the initial attempt of inducing EAE in mice until later in 1949 when Olitsky and Yager successfully induced EAE in mice. Many of the mice developed the neurologic symptoms after 3-5 injection of brain tissue in CFA around 3 weeks after the first injection. In 1955, Pertussis vaccine injected separately in addition to the CFA was demonstrated to induce higher incidence of EAE (Lee *et*

al., 1955), and purified pertussis toxin is now routinely used in addition to CFA (William., 2005).

1.6.1 Mouse strain and CNS antigen in EAE induction

In recent years, murine EAE is often induced by a combination of subcutaneous injection of an emulsion of myelin protein in CFA, which provides a depot for sustained release of self-antigen, together with an intraperitoneal injection of pertussis toxin, which helps in disrupting BBB (Hofstetter *et al*., 2002; Linthicum *et al*., 1982). The immunisation thus enabling the infiltration of immune cells into the CNS, imitating the primary wave of the RRMS in humans.

EAE is induced by autoimmune response against specific CNS antigens such as myelin proteins. Most commonly used are MBP and (PLP), and MOG. Immunization with PLP, MBP, or peptides corresponding to the immunodominant epitopes of MBP (MBP_{84-104}), MOG (MOG_{92-106}), or PLP ($PLP_{139-151}$ and $PLP_{178-191}$) induces EAE in SJL mice strains (Miller *et al*., 2007). Similarly, immunization with the peptide corresponding to the immunodominant epitope of MOG (MOG_{35-55}) induces EAE in C57BL/6 mice (Miller *et al*., 2007).

There is a wide variation in its susceptibility to EAE among the different strains of the mice. In addition, different mouse models exhibit different disease phenotype such as relapsing-remitting, acute and chronic EAE. Relapsing EAE is normally seen in the SJL or F_1 hybrid of SJL mouse immunised with MBP/PLP, which allows assessment of the pathogenesis and immunoregulation of T cell–mediated demyelination as well as the efficacy of various immunoregulatory therapy strategies in a relapsing autoimmune disease setting (McRae *et al*., 1992). EAE in C57BL/6 mice immunised with MOG/PLP displays a chronic-progressive clinical course (Tompkins *et al*., 2002), while in other mouse strains such as $H\text{-}2^u$ (PL/J and B10.PL), immunised with MBP/PLP, the disease is normally acute and self-limiting, and is not characterized by clinical relapses (Miller *et al*., 2007).

Active induction of EAE by immunization with myelin antigens emulsified in CFA has both induction and effector phases occurring in the same animal. In

mice, peripheral immunization with myelin antigens leads to the breakdown of peripheral tolerance and allows the activation of myelin antigen-specific T cells in the secondary lymphoid organs. This is followed by myelin specific T cell proliferation and effector cell differentiation enabling emergence from the secondary lymphoid organs. The integrin expressed by the effector T cells allow them to cross the BBB and the CNS resident antigen presenting cells presenting the myelin antigens cause the reactivation of the effector T cells (Kawakami *et al*., 2004). Once the effector T cells are reactivated, they produce pro-inflammatory cytokines like IFN-γ, IL-17, granulocyte-macrophage colony-stimulating factor (GM-CSF), and TNF-α, that causes damage to the nerve tissues. Furthermore, pathogenic T cells produce chemokines that recruit non-specific cellular effectors like γδ T cells, monocytes, macrophages, and neutrophils into the CNS (Lees *et al*., 2008; Kroenke *et al*., 2008). Thus, the activation of these inflammatory cells and the damage they mediate are critical for the damage of the myelin-sheathed axonal tracts and the formation of CNS lesions.

In addition to active induction of EAE, it can also be induced using passive induction by adoptive transfer of pre-activated myelin-specific T cells into naïve mice (Stinissen *et al*., 1998). In this type of induction, activation of autoreactive cells specific for the CNS are induced in one group of animals and then the activated autoreactive cells are transferred to a second group of naïve animals (Lavi and Constantinescu., 2005). In passive EAE, the effector phase is directly introduced by the adoptive transfer of activated myelin-specific Th1 or Th17 cells collected from already immunized mice into naïve mice (Cross *et al*., 1990; Raine *et al*., 1984; Zamvil *et al*., 1985). Thus, passive induced EAE is considered to be an important tool contributing in the characterization of the function of T effector cells in developing EAE.

Even though the clinical features of passive and active induction of EAE are similar, more reagents are required for passive induction in comparison to the active induction. However, there are many advantages of using passive induction over active induction including: 1. The time point of introduction of encephalitogenic T cells to the recipient mice is the same as the day of adoptive transfer. 2. No antigen depot is present *in vivo* to lead continuous de novo activation

of naïve T cells. 3. *In vivo* encephalitogenic T cells can be easily tracked. 4. A good tool to study the infiltration of antigen specific T cells in the CNS.

While there is a wide range of EAE models which are key to our understanding of the heterogeneous clinical symptoms in different patients, it is very important to consider the advantages and disadvantages of the active and passive EAE induction methods and choose the right mice strain for different purposed studies. In the SJL/J mouse, both active induction and adoptive transfer of disease typically take a relapsing–remitting form which is very useful in studying immunoregulation and epitope spreading, while EAE in C57BL/6 mouse displays chronic–progressive disease following active or passive EAE induction which is a very popular model for studying MS due to the availability of transgenic and knockouts on the H-2^b background (Derik *et al*., 2012).

1.7 Current understanding of the role of immune cells and molecules in MS and EAE development

In the CNS, acute inflammatory response occurs when there is an acute injury or infection (Carlson *et al*., 1998) while chronic inflammatory response is a characteristic of autoimmune like MS and neurodegenerative diseases like Alzheimer's (Heneka and O'Banion., 2007). MS is a chronic immune-mediated demyelinating disease which inflicts varying degrees of disability depending on the CNS damage inflicted (sensorimotor, cerebellar, visual, cognitive and neuropsychiatric) (Lim and Constantinescu., 2010). The main pathophysiological features of MS include increased BBB permeability, infiltration and accumulation of inflammatory molecules and cells in the CNS, axonal and myelin sheath damage, loss of oligodendrocytes, and formation of lesion in the CNS.

Based on current findings it is believed that autoimmune-driven processes are involved in initiating MS and myelin specific $CD4^+$ Th1 and Th17 cells act as driving force in the autoimmune processes, but also other cell types like $CD8^+$ T cells, B cells, macrophages and NK cells contribute to the pathogenesis of MS (Sospedra and Martin., 2005; Kasper and Shoemaker., 2010), such as myelin stripping, degeneration of axonal cytoskeleton, and/or damage to oligodendrocytes in MS lesions (Hickey *et al*., 1991). As apoptosis is involved in the regulation and elimination of auto-reactive T and B cells and macrophages from the circulation and prevents their migration into the CNS, irregular regulation of apoptosis and other immune function can lead to CNS inflammation and related tissue damage (Zipp, 2000; Pender., 2007). MS lesion are mostly found in the white mater, in close proximity to the ventricle of the cerebellum, brain stem, spinal cord and optic nerve (Compston and Coles., 2008). However, this lesion often disperses to other areas of the white matter as well as grey matter but in a lesser extent (Geurts *et al*., 2005). During the early stage of the disease remyelination of the axons occur, as the oligodendrocytes form new myelin sheaths on demyelinating axons and enable them to keep functioning. However, with progression of the disease the number of oligodendrocytes decreases due to immune mediated apoptosis and remyelination fails as the extent of myelin damage becomes severe.

Over the years, extensive research has been carried out both *in vitro* and *in vivo* in order to understand the complex events entailed in MS pathogenesis. The exact cause of MS is still unclear however what we do understand about MS is that the immune system plays a big role in the disease. Our current understanding of the immunopathology of MS is that the inflammation associated to MS is a consequence of an increased BBB permeability which allows autoreactive myelin-specific T cells to enter the CNS. EAE pathophysiology is similar to that of MS, except the initiating antigen. In MS/EAE the CNS antigens get released into the periphery via the cervical lymph nodes where they are activated. These antigens are then presented to T cells by APCs such as DC within the periphery and initiate the activation and expansion of T cells (Wucherpfennig & Strominger., 1995; Furtado *et al*., 2008). DCs contributes to EAE pathogenesis by producing and releasing inflammatory mediators such as TNF-α, IL-6 and IL-1β, which can contribute to inflammation and axonal damage, and IL-12 and IL-23 which promote Th1 and Th17 differentiation respectively (Bailey-Bucktrout *et al*., 2007). Both healthy subjects and MS patients contain auto reactive T cells but compared to the healthy subjects the T cells are more activated and have a memory phenotype in MS (Diaz-Villoslada *et al.*, 1999). The activated T cells in MS migrate towards the BBB and interact with BBB via adhesion molecules to enter the CNS (Furtado *et al*., 2008; Piccio et al. 2002). After entering CNS, the T cells are restimulated by local and infiltrating APCs (microglia/astrocytes/B cells/DCs) (Steinman, 1999). These activated inflammatory T cells then initiate damage of myelin and ODC lysis by secreting immune molecules such as IFN-γ and IL-17, and by activating resident CNS cells to release cytotoxic molecules like ROS and reactive nitrogen species (RNS) (Lorenz *et al*., 2003). All these processes lead to further demyelination and damage of the axons, the hallmark of MS and EAE. Interestingly partial or full remyelination, mainly mediated by ODCs entering the demyelinated area, occurs simultaneously as demyelination is ongoing and involves many of the same types of immune and CNS cells and molecules (Rodriguez., 2007) (Figure 1.10).

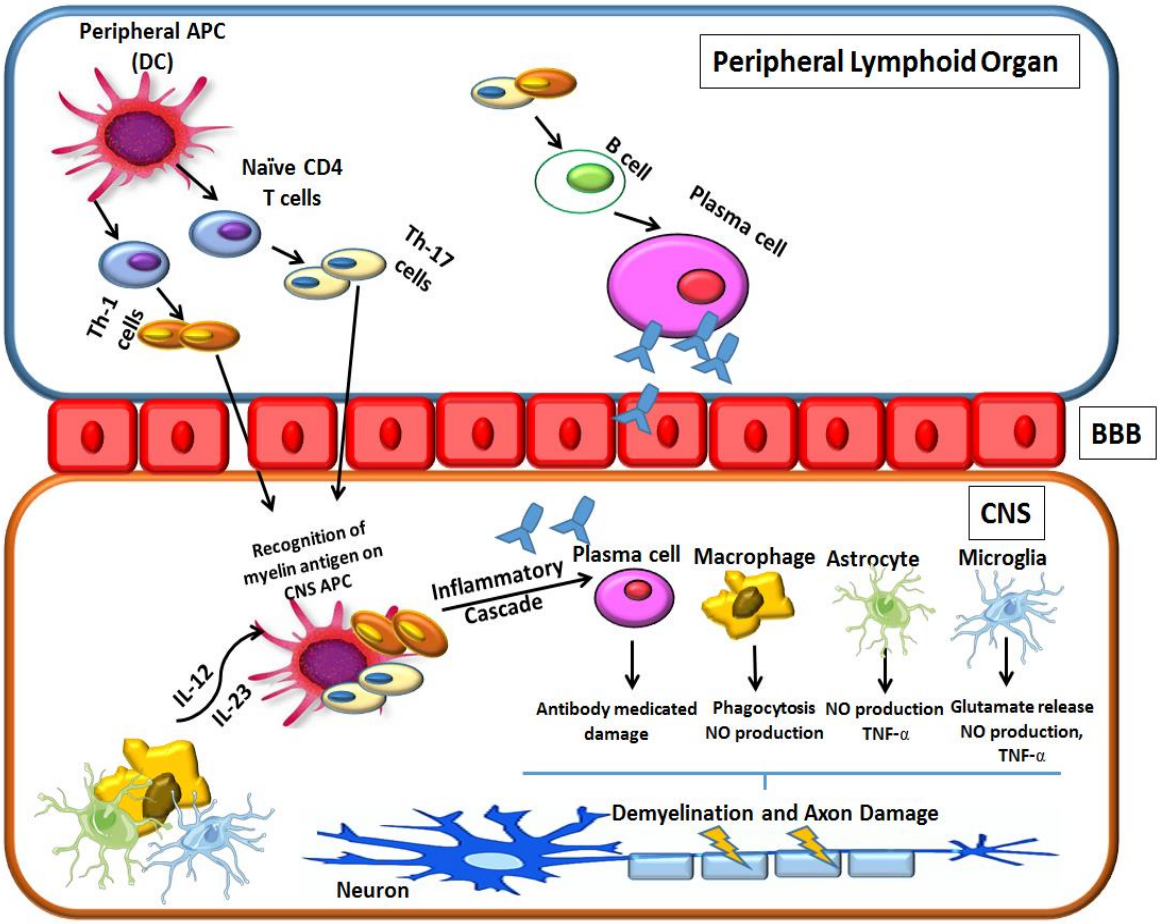

Figure 1.12: Immunopathogenesis of MS or EAE. *Naïve CD4⁺ T cells are activated in the peripheral lymphoid organ by APCs such as DCs, activated T cells then cross the damaged BBB and enter the CNS. Following the entry CD4⁺T cells are then reactivated by infiltrating and CNS APCs. Reactivated, CD4⁺ T cells release pro-inflammatory mediators which amplify local inflammation by activating resident microglia and astrocytes as well as further recruiting other immune cells such as B cells, DCs, and macrophages from periphery. In summary these inflammatory cascades eventually lead to the process involved in myelin and axonal damage*.

1.7.1 Dendritic Cells (DCs) in MS

Many studies have demonstrated the role of DCs, in the pathogenesis of MS. Recent data suggests DCs are abundantly present within the brain lesions of MS patients and regions of CNS inflammation during EAE development, particularly in the meninges and perivascular infiltrate, appearing just before disease onset (Huang *et al*., 1999; Suter *et al*., 2000; Bailey *et al*., 2007). During MS/EAE DCs display an altered phenotype and/or function by production and release of pro-inflammatory cytokines such as IL-6, TNF-α, IFN-γ, IL-1β (Huang *et al*., 1999) IL-12 and IL-23 (Vaknin-Dembinsky *et al*., 2008) which

promote Th1 and Th17 differentiation respectively (Huang *et al*., 1999; Bailey *et al*., 2007).

EAE induction in naïve C57BL/6j mice was also achieved by an adoptive transfer of DCs with MOG_{35-55} peptide with or without PTX and CFA injection (Weir *et al*., 2002), which confirms DCs are the main APCs involved in the initiation of EAE through activation of myelin-specific T cells. Once the auto reactive $CD4^+$ T cells are activated by APCs they migrate into the CNS where they undergo reactivation to exert its functions that induce disease pathogenesis. Another important side of DC functioning is that, it contributes to MS/EAE pathogenesis through secreting a glycoprotein known as osteopontin, which is involved in chemotaxis, activation and differentiation of immune cells (Hur *et al*., 2007). Isolated DCs from MS patients and inflammatory plaques of EAE models have shown to express osteopontin in an increased level (Hur *et al*., 2007) which has been linked to T cells differentiation specially towards Th17 phenotype (Murugaiyan *et al*., 2008). Thus, DCs being the primary APCs directing T-cell differentiation and functions, are considered extremely important in directing the immune pathology characteristic of MS.

1.7.2 Macrophages/Microglia in MS

Macrophage accumulation and microglial activation is one of the key features seen in MS/EAE inflammation. Both macrophage and microglia are known for their function to promote antigen presentation and reactivation of encephalitogenic T cells. Macrophages are involved in the development of MS/EAE; however, there are reports of both detrimental and protective effects. Inhibition of inflammatory responses in macrophages by administration of an anti-inflammatory drug semapimod in EAE mice has demonstrated to supress the production of inflammatory cytokines such as TNF-α, IL-6, IL-1β and NO and decreases the EAE severity, indicating the crucial contribution of macrophages to the pathogenic response of EAE (Martiney *et al*., 1998). Recent studies have suggested different roles for different phenotype of macrophages during the development of MS and EAE. A correlation between M1 cells with EAE clinical severity was observed, with the highest accumulation of M1 cells observed during the peak clinical severity. In contrast, alternatively activated M2

macrophages function as anti-inflammatory cells to supress EAE severity (Vaknin *et al*., 2011).

Accumulation of microglia has been observed within the demyelinated regions in a cuprizone induced demyelinating model (Remington *et al*., 2007), suggesting an important role of microglia cells in CNS demyelination. Microglial cells have been often found to be activated even before the onset of MS/EAE symptoms and cellular infiltration into the brain. During the disease they are regarded as an effective APCs which can potentiate the demyelination process by presenting myelin antigens to the infiltrating lymphocytes. During MS/EAE, microglial cells get activated immediately and act as the major source of pro-inflammatory cytokines and chemokines including TNF-α, IL-6 and IL-23p19 which directly causes tissue damage or recruitment of more leukocytes (Aloisi., 2001). In response to IL-23 or IL-1β, microglia also act as a source of IL-17, contributing to the inflammation (Kawanokuchi *et al*., 2008).

During MS/EAE, besides their detrimental functions, macrophages/microglia can also help in recovery by removing tissue debris via phagocytosis of degraded myelin products within active inflammatory lesions (Shechter *et al*., 2009). This is an essential step in EAE recovery as myelin debris can inhibit axonal regeneration and oligodendrocyte precursor cell differentiation, preventing remyelination (Kotter *et al*., 2006).

1.7.3 T cells in MS

$CD4^+$ T cells are regarded as the main effector cells in the development of MS and EAE. However, $CD4^+$ T cells can be neuroprotective or pathogenic depending on the cells they interact with and the microenvironment (Peterson and Fujinami., 2007) they are in. For a long time, MS/EAE was considered a Th1-cell mediated disease with IFN-γ the main mediators of the inflammation causing MS/EAE lesions (Compston and Cole., 2008), as adoptive transfer of myelin-specific $CD4^+$ Th1 cells into naïve mice were sufficient to induce EAE, whereas Th2 cells were not (Merrill *et al*., 1992). Abundant IFN- γ was also detected in MS/EAE lesions (Lees and Cross., 2007) and treatment of MS patients with IFN-γ also displayed more severe disease (Panitch *et al*., 1987).

Surprisingly IFN-γ KO mice developed more severe EAE with higher mortality rate when compared with the WT controls (Ferber *et al*., 1996). This established, Th1 cells are unlikely to be solely responsible for the inflammation and demyelination observed in MS/EAE development and that other mechanisms are also involved. Further research demonstrated the involvement of numerous other cell types and subsets, with Th17 cells playing a vital role in MS and EAE pathogenesis (McFarland and Martin., 2007). Th17 cells secrete the pro-inflammatory cytokines IL-17, IL-6 and are regulated by IL-23 (Langrish *et al*., 2005, Steinman., 2007). Differentiation of Th1 cells requires IL-12, a study induced EAE in p35 and p40 deficient mice (the two protein subunits that compose IL-12) and found IL-12p40 deficient mice were resistant to EAE (Segal *et al*., 1998) however IL-12p35 deficient mice developed the disease (Becher *et al*., 2002). The IL-12p40 chain is also a component of IL-23 along with the IL-23p19 subunit and deletion of IL-12p19 developed resistance to EAE, determining the importance of IL-23 in development of EAE. In addition, IL-23 has been demonstrated to be essential for the development and expansion of Th17 cells. EAE induction by adoptive transfer of Th17 cells (Jäger *et al*., 2009) further confirmed Th17 cells as the key mediators of EAE pathogenesis along with Th1 cells.

In addition to Th cells, Treg cells have been also linked to MS pathology as they have demonstrated to supress the effector functions of myelin-specific $CD4^+$ and $CD8^+$ T cells and thus play a protective role in MS/EAE (Kohm *et al*., 2002; McGeachy *et al*., 2005). In healthy individuals Treg cells control the auto-reactive T cells while in MS patient's dysfunction in the regulatory capacities of the Treg cells suppress the activation of such cells (Viglietta *et al*., 2004). Adoptive transfer of either purified Tregs, or Tregs isolated from EAE mice have shown to reduce the EAE severity and decreased CNS infiltration, associated to IL-10 production (Kohm *et al*., 2002; McGeachy *et al*., 2005). In addition, increased susceptibility of EAE has been demonstrated when Treg cells were depleted using an anti-CD25 monoclonal antibody (Reddy *et al*., 2005) confirming the importance of Treg cells in ameliorating disease severity and contributing to recovery.

Initially $CD4^+$ T cells were thought to be the only responsible T cell for the pathogenesis of MS and EAE; however, several studies demonstrated the higher prevalence of $CD8^+$ T cells compared to $CD4^+$ T cells within MS/EAE lesions near the demyelinated axons (Lassmann *et al*., 2007; Deb *et al*., 2010). It is now evident from different studies that $CD8^+$ T cell can induce EAE in C57BL/6 mice and potentially involved in EAE development (Sun *et al*., 2001; Goverman., 2011). Van Oosten and colleague (1997) further demonstrated the failure of a clinical trial to reduce MS through depletion of $CD4^+$ T cells using a monoclonal anti-CD4 antibody. The study demonstrated no change in lesion development and or relapse rate. However, depletion of both CD4 and $CD8^+$ T cells using anti-CD52 monoclonal antibody reduced further development of lesion and reduced the relapse rate (Coles *et al*., 1999) demonstrating the involvement of $CD8^+$ T cells in MS/EAE pathogenesis. However, the exact mechanism of $CD8^+$ T cells in MS /EAE pathogenesis is still unclear. It is known that once activated, $CD8^+$ T cells can produce inflammatory mediators such as IFN-γ, IL-17 and TNF-α which would contribute to the inflammatory response. During MS/EAE contribution of $CD8^+$ T cells in tissue damage by directly targeting oligodendrocytes, astrocytes and axons/neurons has been demonstrated in several studies (Mars *et al*., 2011). Under inflammatory conditions CNS resident cells, including astrocytes and microglia can express MHC-I molecules within MS lesions (Höftberger *et al*., 2004) and thus can provide the means for $CD8^+$ T cell expansion and activation, along with peripheral APCs which have migrated into the CNS. Furthermore, $CD8^+$ T cells can induce demyelination via MHC I molecules present on neurons and ODCs via Fas-FasL signalling and perforin (Kivisäkk *et al*., 1999). Perforin secreted by the cytotoxic T cells causes the generation of holes in the membranes of cells, resulting in cellular lysis, and is often the cause of ODC death (Kivisäkk *et al*., 1999), cytoplasmic vacuolation, and the breakdown of the nuclear envelope. Moreover, perforin mRNA is expressed in the cerebrospinal fluid (CSF) cells and blood mononuclear cells of MS patients (Kivisäkk *et al*., 1999; Matusevicius *et al*., 1998).

1.7.4 B cells, NK and NKT cells in MS

Although T cell, DCs, macrophages are important for MS, the importance of other immune cells such as B cells, NK and NKT cells should not be overlooked (Piccio *et al*., 2002; Nowak *et al*., 2009; Sayed *et al*., 2010). The presence of immunoglobulin in the CSF of MS patients and elevated levels immunoglobulin and B cells in MS lesions clearly suggests the involvement of B cells in MS pathology (Cepok *et al*., 2005; Morris-Downes *et al*., 2002). Under normal physiological condition B cells are unable to cross the BBB, however they can enter the CNS during an inflammatory response to enhance the inflammation in the CNS (Knopf *et al*., 1998).

During MS/EAE B cells act as APCs for auto-reactive T cells, by co-stimulating and recruiting T cells and by the production of myelin-specific antibodies that results in myelin destruction (Jagessar *et al*., 2012). Autoantibodies produced by B cells plays important role in CNS demyelination, and an extensive antibody and complement deposition has been observed in pattern II lesions in 50% of the patients (Lucchinetti *et al*., 2000). Autoantibodies to MOG and other myelin proteins (PLP and MBP) are also involved in demyelination through fixation and activation of the complement cascade (Piddlesden *et al*., 1991). Furthermore, B cells can produce cytokines such as IL-6, which in combination with TGF-β can facilitate the generation of pathogenic Th17 cells and the production of pro-inflammatory cytokines (Bettelli *et al*., 2008). In addition, B cells can also promote a Th1 response by enhancing IFN-γ production (Menard *et al*., 2007), all together this suggests an involvement of B cells in MS/EAE pathogenesis. However, a beneficial property of B cells in EAE recovery has been also demonstrated in a different study. It has shown that in absence of B cells, EAE mice did not demonstrate to recover but rather displayed higher clinical severity due to lack of IL-10 producing B cells, which are fundamental for EAE remission (Matsushita *et al*., 2008). Furthermore IL-10 derived from B cells has shown to down-regulate Th1 responses and ameliorate EAE pathogenesis (Fillatreau *et al*., 2002). Taken together these studies suggest contrasting functions of B cells during MS/EAE likely due to the presence of unique B cell subsets or the stage of disease pathogenesis.

In EAE, both NK/NKT cells has been regarded to have protective roles. A drug Linomide which enhances NK cells activities have shown to limit EAE development (Karussis *et al*., 1993) while another study has shown that addition of anti-NK cell antibodies worsens disease severity (Matsumoto *et al*., 1998). Both studies suggest an involvement of NK cells in suppressing EAE. Unlike conventional T cells, NKT cells recognize antigen presented via CD1d on the surface of APCs, and activated cells can produce IFN-γ, IL-2, IL-4 and IL-17 and directly kill infected cells. Furthermore, adoptive transfer of spleen cells derived NKT cells to C57BL/6 TCR knockout mice showed to induce recovery from passive EAE (Fritz *et al*., 2011), which strongly suggests a protective role NKT cells.

1.8 IL-16 cytokine

Many immune cytokines play important roles in the pathogenesis and regulation of various immune mediated disease including MS. Thus, understanding the exact role of these immune molecules in MS development, are key to develop therapeutic strategies for MS patients. IL-16 is one of these cytokines which play an important role in regulation of autoimmune inflammation (Skundric *et al*., 2005, Skundric *et al*., 2006).

In 1982, IL-16 was first identified as a lymphocyte chemoattractant factor secreted by lymphocytes (Cruikshank and Cruickshank, 1982; Cruikshank *et al*., 2000). IL-16 is located on chromosome 7 in mice and chromosome 15 in humans and is highly conserved. Murine IL-16 protein exerts the same biological activity as human IL-16 on human T cells (Cruikshank *et al*., 2000). In human, IL-16 is generated as a precursor protein known as pro-IL-16, which is constitutively produced by unstimulated peripheral T lymphocytes, it is made up of 631-amino acid precursor, with a molecular mass between 68-80kDa. This pro-IL-16 is then enzymatically cleaved by active caspase 3, releasing the bioactive form of IL-16, which consists of a 121 amino acid peptide with a molecular mass of 17kDa (Zhang *et al*., 1998; Wu *et al*., 1999 Cruikshank *et al*., 2000). Bioactivity of IL-16 only occurs after auto-aggregation of IL-16 in di-

mers/tetramers (Cruikshank *et al*., 2000) and a bioactive IL-16 is the only cytokine that contains PDZ domains, which allow for protein-protein interactions (Wilson *et al*., 2003). These PDZ domains are located in the C-terminal region of the protein. Both $CD8^+$ and $CD4^+$ cells have been reported to produce IL-16 (Berman *et al*., 1985) but we now know that IL-16 is also produced by other immune cells including B cells and monocytes (Kaser *et al*., 2000; Elssner *et al*., 2004). IL-16 can be released upon stimulation of cells**,** however the release mechanism is unclear and not completely understood (Laberge *et al*., 1995; Cruikshank *et al*., 2000;). Activation and release of IL-16 is regulated mostly among T cell subsets and the mechanism behind its secretion varies between different cell types. The resting $CD8^+$ cells contain active caspase-3, which cleaves pro-IL-16, resulting in a pool of preformed, bioactive IL-16. In contrast, resting $CD4^+$ cells only contain pro-caspase-3 and therefore only have pro-IL-16 (Cruikshank *et al*., 2000; Laberge *et al*., 1996). TCR mediated or cytokine induced activation of $CD4^+$ cells leads to enzymatic cleavage of pro-caspase-3 into active caspase-3 resulting in release of bioactive mIL-16 (Wilson *et al*., 2004, Skundric *et al*., 2006, Skundric *et al*., 2005; Wu *et al*., 1999).

IL-16 protein exhibits selective and potent chemoattractant activity only in $CD4^+$ cells, particularly Th1 subset cells (Lynch *et al*., 2003). In addition to its chemotactic function, IL-16 also exerts proinflammatory and immunomodulatory properties that include chemoattraction and activation of T cells (Cruikshank *et al*., 2000). Significant increase in the number of $CD4^+$ cells in pleural effusion were observed after 12 hours of an intrapleural injection of recombinant human IL-16 protein, which reached to its peak after 24 hours of the injection (Quin *et al*., 2005). Bioactive IL-16 protein also functions as a growth factor. Marked increase in $CD4^+$ cell proliferation was observed when they were cultivated with both IL-16 and IL-2 *in vitro*. However, adding only IL-2 did not alter the proliferation (Parada *et al*., 1998).

Expression of the CD4 receptor on cell surface is required for IL-16 bioactivities (Cruikshank *et al*., 2000). However recently, IL-16 demonstrated to induce migration in human lung epithelial cells (A549) via the CD9 receptor (Blake *et al*., 2018). Not much researches have been done on association of IL-16 with CD9 receptor, but it has been studied and established that any cell that have

CD4 receptor will respond to IL-16 protein. However, cross-linking of the CD4 receptors is thought to be necessary, since only the multimeric forms (dimers and tetramers) of IL-16 induce bioactivity, not the monomer (Cruikshank *et al*., 2000). CD4 is described as a protein which is predominantly expressed in T cells and involved in recognising antigen in the context of MHC class II (Panes, 1989). CD4 molecule is also expressed by some mononuclear cells (e.g. monocytes and macrophage) involved in regulation of innate and adoptive immune responses (Skundric *et al*., 2015). The activation of the CD4 receptor by IL-16 results in phosphorylation of STAT 6, a protein in the cytoplasm, which then translocates into the nucleus and exerts its effects by activating or repressing target genes (Liu *et al*., 2007). In addition to its effect on T cells, IL-16 is known to induce intracellular calcium rises, auto-phosphorylation of $p56^{lck}$, IL-2Rα expression and cytokine production (Skundric *et al*., 2015).

Furthermore IL-16 has been also identified to have dual effect on inflammation. Some studies designate IL-16 as a pro-inflammatory cytokine, which attracts $CD4^+$ cells (Center *et al*., 1996; Nicoll *et al*., 1999). When rhIL-16 was cultivated *in vitro* with human monocytes the secretion of the pro-inflammatory cytokines IL-1β and TNF-α was observed (Mathy *et al*., 2000*).* However, other studies have indicated an anti-inflammatory function of IL-16 as the treatment with rhIL-16 in a mouse model of human synovial tissue from subjects with rheumatoid arthritis (RA), resulted in a decrease in mRNA expression IL-1β and TNF-α (Klimiuk *et al*., 1999). In addition, in mouse models of encephalomyelitis and renal ischemia-reperfusion injury, anti-IL-16 treatment blocked the influx of $CD4^+$ cells and improved the severity of the disease (Skundric *et al*., 2005; Wang, *et al*., 2008).

Interestingly, in addition to its role in inflammation, a neuronal form of IL-16 known as neuronal IL-16 precursor (NIL-16) have been identified and characterised (Kurschner & Yuzaki., 1999). NIL-16 is a larger splice variant of the immune cell-derived IL-16 precursor protein, pro-IL-16, with two extra PDZ domains in the N-terminal region (Kurschner & Yuzaki., 1999). They are selectively expressed in post-mitotic neurons of the hippocampus and cerebellum (Fenster *et al*., 2007), which are cleaved by caspase-3 similar to pro-IL-16 in immune cells and results in the release of mature IL-16 (Kurschner & Yuzaki.,

1999). Furthermore, NIL-16 induces the upregulation of the transcription factor c-fos, (Kurschner and Yuzaki, 1999; Fenster *et al*., 2010), enhances neurite outgrowth (Fenster *et al*., 2010) and interacts with neurotransmitter receptors and several ion channel proteins (Kurschner & Yuzaki., 1999; Fenster *et al*., 2007).

1.8.1 Role of IL-16 in immune-mediated diseases

Recent research suggests that IL-16 plays an important role in the development of many autoimmune diseases including RA, systemic lupus erythematosus (SLE), Graves' disease (GD) and MS.

SLE, commonly known as lupus, is an autoimmune connective tissue disease which affects almost any organ of the body. Patients with lupus have a hyperactive immune system that generates auto-antibodies that attack tissue throughout the body including kidney, brain, heart, lungs as well as blood, skin and joints. This disease is characterised by periods of illness or periods of wellness or remission (Lee *et al*., 1998). Research has indicated high levels of IL-16 in the blood plasma of patients with SLE compared to healthy patients and the level of IL-16 has been correlated with the severity of the disease (Lard *et al*., 2002). However, the exact function of IL-16 in SLE is currently not known.

RA is a chronic systemic inflammatory disease which primarily affects the synovial membranes and articular structures of the joints causing severe pain and resulting in swollen and deformed joints (Fraz *et al*., 1998). A massive influx of immune cells into the synovial area of joints of RA patients indicated the involvement of chemotactic signal in local recruitment of these inflammatory immune cells. Studies of RA patients demonstrated a high level of IL-16 in the synovial fluid compared with osteoarthritis, non-rheumatoid arthritis, and other healthy controls (Fraz *et al*., 1998). Furthermore, the studies demonstrated production of IL-16 by synovial fibroblast cells and the associated chemoattraction of $CD4^+$ cells into the synovial tissue in RA patients but not in healthy

controls or patient with non-inflammatory or non-autoimmune disease like osteoarthritis (Blaschke *et al*., 2001). This research finding indicates a pathogenic role for IL-16 in RA disease.

GD is an autoimmune disease that affects the thyroid and the production of autoantibodies, thus resulting in hyperthyroidism. It causes thyroid induced ophthalmopathy and dermopathy (Pritchard *et al*., 2002). Increased production of regulated on activation normal T cell (RANTES) and IL-16 has been demonstrated in the fibroblast of GD patients (Pritchard *et al*., 2002), suggesting a possible involvement of IL-16 in GD.

1.8.2 Role of IL-16 in MS

As previously discussed, MS is a neurodegenerative autoimmune disease which has been shown to be modulated by $CD4^+$ and $CD8^+$ T cells as well as macrophages/microglia (Bever *et al*., 2003; Mereli *et al*., 1991). $CD4^+$ T cells are considered to have crucial role in the pathogenesis of MS/EAE, as myelin-specific autoimmune T cells can initiate inflammation, and cause damage to oligodendrocyte and axons leading demyelination. Interestingly in MS/EAE lesions, major cellular sources of intrathecally produced IL-16 include $CD4^+$ and $CD8^+$ T cells, B cells and activated resident microglia (Skundric *et al*., 2005a; Skundric *et al*., 2005b; Skundric *et al*., 2006).

In the CNS of RRMS patients, both pro- and secreted IL-16 has been found to be in elevated within the MS lesion in comparison to the controls (Skundric *et al*., 2006). Increased level of IL-16 has been correlated to the elevated levels of T-bet^+ and active-caspase-3^+ infiltrating cells observed in the MS lesion (Skundric *et al*., 2006). IL-16 immunoreactivity has been observed in $CD4^+$ Th1 cells, $CD8^+$ T cell, B cells and occasionally in microglia (Skundric *et al*., 2006). Furthermore, IL-16 has been found to be secreted by $CD8^+$ CTLs collected from MS patients when stimulated with the appropriate peptide such as PLP (Biddison *et al*., 1997). *In vitro* studies have also demonstrated a regulatory role for IL-16 in EAE through chemoattaraction of myelin-specific $CD4^+$ T cells, (Biddison *et al*., 1998). Furthermore, a correlation between increased

production of secreted IL-16 and $CD4^+$ Th1 cell mediated neuroinflammation, and phosphorylation of axonal cytoskeleton has been observed within the MS lesion (Skundric *et al*., 2005; Skundric *et al.*, 2006). In addition, current research evidence suggests IL-16 contributes to ongoing neuroinflammation by regulating the migration of CD4 expressing T cells regardless of their activation state and chemoattracting additional waves of $CD4^+$ T cells, which is of critical importance for immune modulation and potential therapy of MS (Biddison *et al*., 1998; Skundric *et al*., 2006).

During EAE, co-immuno-precipitation of IL-16 with CD4 was observed in the CNS of relapsing EAE mice (Skundric *et al*., 2005a), and elevated levels of IL-16 in the CNS of EAE mice were correlated with the levels of infiltrated $CD4^+$ T cells (Skundric *et al*., 2005b). In addition, increased IL-16 levels along with an increased active-caspase-3 and $CD4^+$ levels were correlated with stages of clinically active disease (Skundric *et al*., 2005b). Subsequently, production of bioactive IL-16 has been also observed when T cells isolated from EAE immunised mice has been restimulated or polyclonally activated with PHA/$MOG_{35-55.}$ (Skundric *et al*., 2005b). Further research have also demonstrated that in mice with relapsing EAE, $CD4^+$ T cells produce pro- and bioactive IL-16 and subsequently release it locally, which then binds to CD4 receptor and selectively chemoattracts $CD4^+$ T cells and regulates $CD4^+$ cell migration regardless of their activation state (Skundric *et al*., 2005b). However, during the remission stage of the disease IL-16 levels were significantly reduced in the EAE mice which was consistent with the clearance of infiltrating cells from the CNS (Skundric *et al*., 1993). Skundric *et al*., (2005a) further demonstrated that treatment with anti-IL-16 ameliorates RREAE disease as well as diminishing the infiltration of $CD4^+$ T cells in CNS, the result of which is reduced levels of demyelination and ultimately the sparing of axons. These findings from both MS and EAE studies clearly suggest a role for IL-16 in MS pathogenesis through $CD4^+$ Th1 cell mediated neuroinflammation.

1.9 Research Hypothesis and Aims

Current research findings suggest a crucial role of IL-16 produced by infiltrating $CD4^+$ T cells in CNS neuroinflammation and the development of MS/EAE relapses (Skundric *et al*., 2005). Despite different studies providing an understanding of the possible role of IL-16 in mediating immune responses, little is known about the exact role and underlying mechanisms of IL-16 function in CNS compartment. Based on the previous studies we now clearly understand that IL-16 has some role in inflammatory CNS diseases like MS, however whether this role is beneficial or detrimental yet to be fully investigated. Furthermore, a recent observation by Shrestha *et al*., in 2014 has demonstrated that immune cell-derived IL-16 is neuroprotective against kainate- and oxygen-glucose deprivation (OGD)-induced excitotoxicity in organotypic slice cultures (Shrestha *et al*., 2014). Thus, we hypothesise that IL-16 may have a protective role during MS/EAE and carried out this study as an approach to fully understand the pattern of IL-16 regulation and its functions both under inflammatory and normal conditions is essential.

The primary aims of this study therefore are:

- To establish EAE as a research model for MS disease for this study, and to characterise the changes of immune responses associated with EAE onset and progression.
- To determine the expression of IL-16 and its receptor CD4 in spleen, lymph node and CNS tissues of EAE and control mice over the course of the disease, and to investigate whether the expression level of IL-16 correlates with neuroinflammation in the CNS of EAE mice.
- To determine the cellular localisation of IL-16 within the spleen/lymph node of naïve, PBS and MOG_{35-55} immunised mice.
- To determine the cellular localisation of IL-16 within the spinal cord and brain of naïve, PBS and MOG_{35-55} immunised mice.
- To assess the expression and cellular localisation of IL-16 in primary hippocampal cultures.
- To determine the effect of rIL-16 on hippocampal neuronal excitability and synaptic activity.

2 Materials and Methods

2.1 Lab chemicals and consumables

Table 2.1: List of lab chemicals, consumables and their suppliers

Product	Supplier
Eppendorf Micro Amp Fast Optical 96-Well reaction plates Optical adhesive cover	Applied Biosystems (UK)
BD FACS Canto system BD FACS Diva Software Fixation and Permeabilization Solution Kit with BD Golgi Stop *Mycobacterium tuberculosis* TMB substrate solution	BD Bioscience (UK)
Epoch plate reader	BioTek (USA)
Avidin-HRP Cell stimulation cocktail plus protein transport inhibitor	eBioscience (UK)
Acetone Haematoxylin Phosphatase inhibitor cocktail 100x rIL-16	Fisher Scientific (UK)
KS 250 basic IKA shaker T25 basic IKA homogeniser	Labortechnik (Germany)
B-27 serum replacement cDNA reverse transcription Kit Foetal Bovine Serum (FBS) High Capacity cDNA Reverse Transcription Kit L-glutamine Neurobasal-A medium Penicillin streptomycin RNAlater SYBR Select Master Mix TRIzol reagent	Life Technologies/Invitrogen (UK)
$CD4^+$ T cell Isolation Kit (mouse) CD11b Microbeads Kit (mouse/human) LS Column MACS MultiStand	MACS Miltenyi Biotec (UK)
Histoclear Hydromount	National Diagnostics (USA)

Bovine albumin serum (BSA) Complete Freunds Adjuvant (CFA) Concanavalin A (conA) Eosin Y D-glucose DPX mounting medium Ethylene glycol tetra acetic acid (EGTA) Ethylene-di-amine tetra-acetic acid (EDTA) Ethanol Guanosine-5'-triphosphate (GTP) HEPES Gill 2 haematoxylin Magnesium adenosine Triphosphate (MgATP) Methanol Normal serum Paraformaldehyde (PFA) Papain Phosphatase inhibitor cocktail 2 Phosphatase inhibitor cocktail 3 Poly-L-lysine Potassium methyl sulphate (KMeSO3) Protease inhibitor RBC lysis buffer qPCR primers Sodium chloride (NaCl) Sodium hydroxide (NaOH) Triton X-100 solution Tris buffered saline (TBS) Trypan blue Tween-20 Hyderogen chloride (HCl)	Sigma-Aldrich (UK)
CL2 Centrifuge Cryostat	Thermo Scientific (UK)
Pertusis Toxin	Tocris Bioscience (UK)
Avidin/Biotin Kit HRP Substrates: Peroxidase Substrate, ImmPACT AMEC Red ImmEdge TM PEN Microscope glass slides, M.O.M Immunodetection Kit Vectashield mounting medium with DAPI	Vector Lab (UK)
OCT mounting medium Slide cover slip/cover glass	VWR (UK)

2.2 Experimental animals

C57BL/6J wild type mice were bred in-house at the University of Strathclyde animal unit (Biological Procedure Unit), originally obtained from Charles River UK. The mice were housed in cages with access to water and standard diet ad libitum under standard laboratory conditions (temperature 21 ^{o}C, humidity 45-65%) with a 12-hour light starting at 7am -12 hours' dark cycle starting from 7pm. All animal care and experimental procedures were conducted in accordance with the UK Home Office guidelines Animals Act 1986 (Scientific Procedures) and were conducted under a Project License to Dr Hui-Rong Jiang (PPL70/8520 ''Pathophysiology of autoimmune diseases'').

2.3 Induction and clinical observation of EAE

To induce EAE, 6-8 weeks old female C57BL/6J mice were immunized subcutaneously on day 0 with 100µg of MOG_{35-55} in 50 µl of PBS emulsified with 50 µl of CFA (4.4-5.5mg/ml *Mycobacterium tuberculosis)*. The injection site was shaved and sprayed with 70% ethanol prior to immunisation and each mouse received two injections with 50µl on each side of the lower back. PBS control mice received 50µl of PBS emulsified in 50 µl of CFA without MOG peptide. In addition, 100ng pertussis toxin (PTX) in 100µl PBS was administered intraperitoneally on Day 0 and Day 2. Naïve control mice received no injections. Weights and the clinical symptoms were monitored and recorded daily after immunisation. Clinical symptoms were scored appropriate to the 0-4 scale shown in Table 2.2 (Jiang et al., 2012).

Table 2.2: Clinical score and signs during EAE

Clinical Score	**Clinical Sign**
Grade 0	Normal gait, tail moves and can be raised
Grade 1	Loss of tail tone, normal gait
Grade 2	Hind limb weakness
Grade 3	Hind limb paralysis
Grade 4	Hind limb paralysis & forelimb

2.4 Immunohistochemistry (IHC)

2.4.1 Tissue preparation for IHC

Naïve, PBS and MOG_{35-55} immunised mice were sacrificed via asphyxiation in a CO_2 chamber at day 12 (EAE onset), 16 (EAE peak) and 26 (EAE resolution) post immunisation. Following the perfusion with PBS; spleen and inguinal lymph nodes were removed from using a tweezer. To collect the brain, the head was removed using scissors making sure not to damage the cortical region of the spinal cord below. An incision was made in the skin near the brain stem and the skin was pulled back exposing the skull. The occipital region of the skull was cut and using curved tweezers the skull was removed in sections by positioning the tweezers underneath the skull, not touching the brain and lifting upwards. Once the skull had been carefully removed, the brain was then detached from the optic nerve and surrounding nerve fibres by carefully positioning scissors underneath the brain. The brain was removed from the skull cavity by inserting curved tweezers underneath the brain and gently lifting it out. Spinal cords were removed by hydrostatic pressure using a 19G needle and PBS. After collection all the organs were placed in Optimal Cutting Temperature compound (OCT) mounting medium and frozen on dry ice for before being cut into 7 µM thick sections on a Shandon cryotome (Thermo Scientific) for immunohistochemistry.

2.4.2 Tissue sectioning for IHC

Spleen, lymph node, spinal cord or brain were harvested from naïve, PBS and MOG35-55 immunised mice at different time points post immunisation. The tissues were then cut into 7µM thick sections using cryostat (Thermo Scientific; UK) and collected on properly labelled glass slides. Once air dried, slides were stored at -20°C until required for the immunohistochemical staining.

2.4.3 Solutions used for IHC

Phosphate buffered saline (PBS): 10x PBS was prepared dissolving 80g NaCl, 2g KCl, 14.4g Na_2HPO4, 2.4g KH_2PO4 in 1000ml dH_2O: pH 7.4; 1x PBS was prepared using 100 ml of 10 times PBS in 900ml of dH_2O.

Tris buffered saline (TBS): 10x TBS was prepared dissolving 24g Tris base, 88g NaCl in 1000ml dH_2O; pH 7.4; 1x TBS was prepared using 100 ml of 10 times TBS in 900ml of dH_2O.

Immunohistochemistry (IHC) fixative solution: 75% acetone and 25% absolute ethanol kept at -20^oC.

IHC blocking buffer (BB): 5% foetal bovine serum v/v (FBS, 2.5ml) and 1% Bovine serum albumin w/v (BSA, 5mg) in 50 ml of PBS.

Tris buffered saline-Tween (TBS-T): 1x TBS + 0.05% Tween 20 (500µl).

Scott's tap water substitute (STWS): 2g $NaHCO_3$, 20g $MgSO_4$ in 1000ml dH_2O.

2.4.4 Haematoxylin and eosin (H&E) staining

Tissue sections were first fixed in ice cold IHC fixative solution for 10 minutes before being rehydrated in TBS for a further 10 minutes. Tissues were then stained in Gill 2 haematoxylin for 10 minutes and then washed under running water for 5 minutes. Tissue sections were further differentiated with 2 dips in 0.1% Hydrochloric acid in 70% ethanol and then washed under running water for 3 minutes. This was followed by blueing in STWS for 3 minutes followed by another 5 minutes wash before being incubated in Eosin Y solution for 6 minutes. Then the tissue sections were washed in running water and were periodically checked under a microscope until desired staining was obtained. Tissue was then dehydrated through dipping in 70% and 95% ethanol followed

by 5 minutes in 100% ethanol. The slides were then cleared in histoclear for 5 minutes and mounted with Histomount.

2.4.5. Immunoenzyme staining

Tissue sections were stained with different cell-surface marker antibodies listed in Table 2.5. Frozen slides were first left on bench for 10 minutes to allow the tissues to come up to RT prior to the fixation in ice cold fixative for 10 minutes. After fixation, the tissues were allowed to air dry at RT for another 20-30 minutes before being rehydrated in TBS for 25 minutes. After the rehydration step, the tissues were blocked with IHC BB for 45-60 minutes. Tissues were then washed and incubated with Avidin solution for 15 minutes followed by a brief wash in TBS and further incubation with a Biotin solution for 15 minutes. After another brief rinsing of the slides in TBS, the tissues were then directly incubated with appropriately pre-diluted specific primary antibodies in BB. The slides were placed in a moisture chamber and incubated overnight at 4° C. Next day the slides were allowed to equilibrate to RT for 30minutes before being washed (3 x 5minutes) in TBS-T. During this time the slides were placed on the shaker at 100 rpm speed (IKA KS 250 basic; Labortechnik) to ensure appropriate flow of TBS-T. After washing, the tissues were then incubated with relevant biotin secondary antibodies (Table 2.6) for 30-45 minutes at RT. The tissues were then carefully washed in TBS-T and incubated at RT with horseradish peroxidase for 30 minutes. This is followed by another washing step before incubation with AMEC ImmPACT Red Peroxidase System at RT for about 1-2 minutes. Tissues were then briefly washed in TBS and counterstained with haematoxylin for 15-30 seconds before being washed again and mounted with hydromount medium. The stained slides were viewed using a bright field microscopy (Nikon Eclipse 50). Images of three different magnifications (x10, x20, and x40) were taken using a digital camera (Nikon Digital Sight DS-U3) connected with a computer containing NIS Element F 3.2 imaging software.

2.4.6 Immunofluorescence staining

Frozen slides were first left on bench for 10 minutes to allow the tissues to come up to RT prior to the fixation in ice cold fixative for 10 minutes. After fixation, the tissues were allowed to air dry at RT for another 20-30 minutes before being rehydrated in TBS for 25 minutes. Following rehydration, the tissues were blocked with IHC BB for 45-60 minutes. Tissues were then washed and incubated with Avidin solution for 15 minutes followed by a brief wash in TBS and further incubation with a Biotin solution for 15 minutes. After another brief rinsing of the slides in TBS, the tissues were then directly incubated with appropriately pre-diluted primary antibodies (listed in Table 2.3) of interest in IHC BB. The slides were placed in a moisture chamber and incubated overnight in 4° C cold room. The following day, slides were washed with TBS-T (3 x 10 minutes). The tissues were then incubated for 1 hour with relevant fluorescent secondary antibodies (listed in Table 2.4) specific for the primary antibodies added. Tissues were washed in TBS-T (3 x 10 minutes) and mounted with Vectashield including DAPI and sealed with clear nail varnish. Images of the tissue sections were obtained using an epifluorescent microscope (Nikon Eclipse TE2000-S) connected to NIS-Elements image software.

Table 2.3: Primary antibodies used in immunohistochemistry

Antibody	**Host species**	**Supplier**	**Cat. No.**	**Immunogen/cells**
IL-16	Rabbit	Fisher	PA5-20670	IL-16
MAP-2	Chicken	Millipore	AB5543	Neuron dendrites
NeuN	Mouse	Millipore	MAB377	Neuron cell body
GFAP	Mouse	Cell signalling	36708	Astrocyte
CD45	Rat	eBioscience	14-0451-85	Immune cells
CD4	Rat	eBioscience	14-0042-85	CD4 T Cells
CD8	Rat	BD	550281	CD8 T Cells
F4/80	Rat	eBioscience	14-4801-85	Macrophages
CD11b	Rat	eBioscience	14-0112-85	Pan Macrophages

Table 2.4: Secondary antibodies used during immunohistochemistry

Antibody	Host species	Conjugate	Supplier	Cat. No.
Anti-Rat	Mouse	Biotin	eBioscience	13-4813-85
Anti-Rab-bit	Goat	Biotin	BD	550338
Anti-Rat	Goat	Alex-Fluor 488	Thermo Fisher	A-11006
Anti-Rat	Chicken	Alex-Fluor 555	Thermo Fisher	A-21434
Anti-Rab-bit	Donkey	Alexa-Fluor 488	Thermo Fisher	A-21206
Anti-Mouse	Donkey	Alex-Fluor 555	Thermo Fisher	A-31570

Table 2.5: Isotype control antibodies used in immunohistochemistry

Species	Isotype	Supplier
Rat	IgG2	Vector
Rabbit	IgG	Vector
Mouse	IgG1	eBioscience
Goat	IgG	R&D

2.4.7 Immunoenzyme stained section quantification:

Spleen/lymph node and spinal cord: Tissue sections from spleen/lymph node (Figure 2.1 A) and spinal cord (Figure 2.1 B) were stained for specific cell markers and counterstained with haematoxylin and bright field images of right half of each tissue sections were taken at x10 magnification. Scale of images was set using ImageJ to the scale bar applied by Nikon NIS-Elements imaging software and the images were analysed using ImageJ software. 10 regions of interest (ROI) each with a dimension of 243 µm x247 µm was assigned consistently tissue sections of the spleen/lymph node and spinal cord to cover the whole image of tissue.

For spinal cord sections, 6 ROIs were assigned in the white matter region which includes the lesion or an equivalent area, and 4 ROIs in the grey matter. All cells expressing the desired marker (red) associated to haematoxylin nuclei (blue) were counted in each ROI and the cell counts were expressed as a

percentage out of the total number of cells stained with haematoxylin nuclei (blue) present in the field of view of the total ROI assigned in the tissues (Figure 2.1 A&B). Each cell markers were assessed in tissues collected from either 3 or 5 mice per group and were quantified using the described method to represent the data as an average of the total number of mice assessed, with n representing the number of animals.

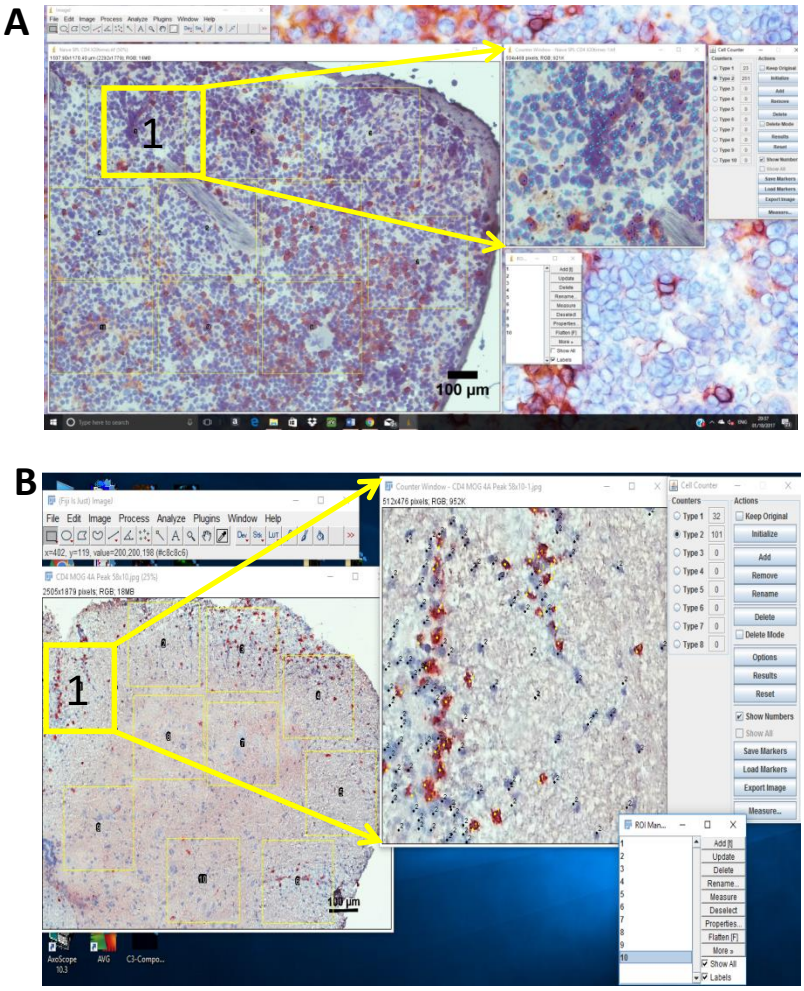

Figure 2.1: Quantification of CD4⁺ cells in spleen/lymph node and spinal cord tissue using ImageJ. *Representative image showing the quantification of CD4⁺ cells in the EAE* ***(A)*** *spleen and* ***(B)*** *spinal cord tissue section.*

Brain: Brain tissue sections were stained for the specific cell markers and counterstained with haematoxylin. Bright field images of brain cerebellum and hippocampus were taken. To quantify the percentage $CD4^+/CD45^+$ cells out of total cells in each region, images of two different areas of cerebellar white

matter and two different areas of the hippocampal dentate gyrus (where the most immune cell infiltrations were seen) were taken at x20 magnification. To quantify the percentage of IL-16^{+} cells, images of cerebellar white matter, granular layer and molecular layer (Figure 2.2A) and hippocampal C1, C2, C3 and two areas of Dentate Gyrus (Figure 2.2B) were taken at x20 magnification. Scales of images were set using ImageJ to the scale bar applied by Nikon NIS-Elements imaging software and the images were analysed using ImageJ software. 3 ROIs, each with a dimension of 250 µm x 230 µm, were assigned in each image (Figure 2.4). All cells expressing the desired marker (red) associated to haematoxylin nuclei (blue) were counted in each ROI and the cell counts were expressed as a percentage out of the total number of cells stained with haematoxylin nuclei (blue) present in the field of view of the 3 ROIs (Figure 2.3). Each cell markers were assessed in tissues collected from either 3 or 5 mice per group and were quantified using the above described method to present the data as an average of the total number of mice assessed, with n representing the number of animals.

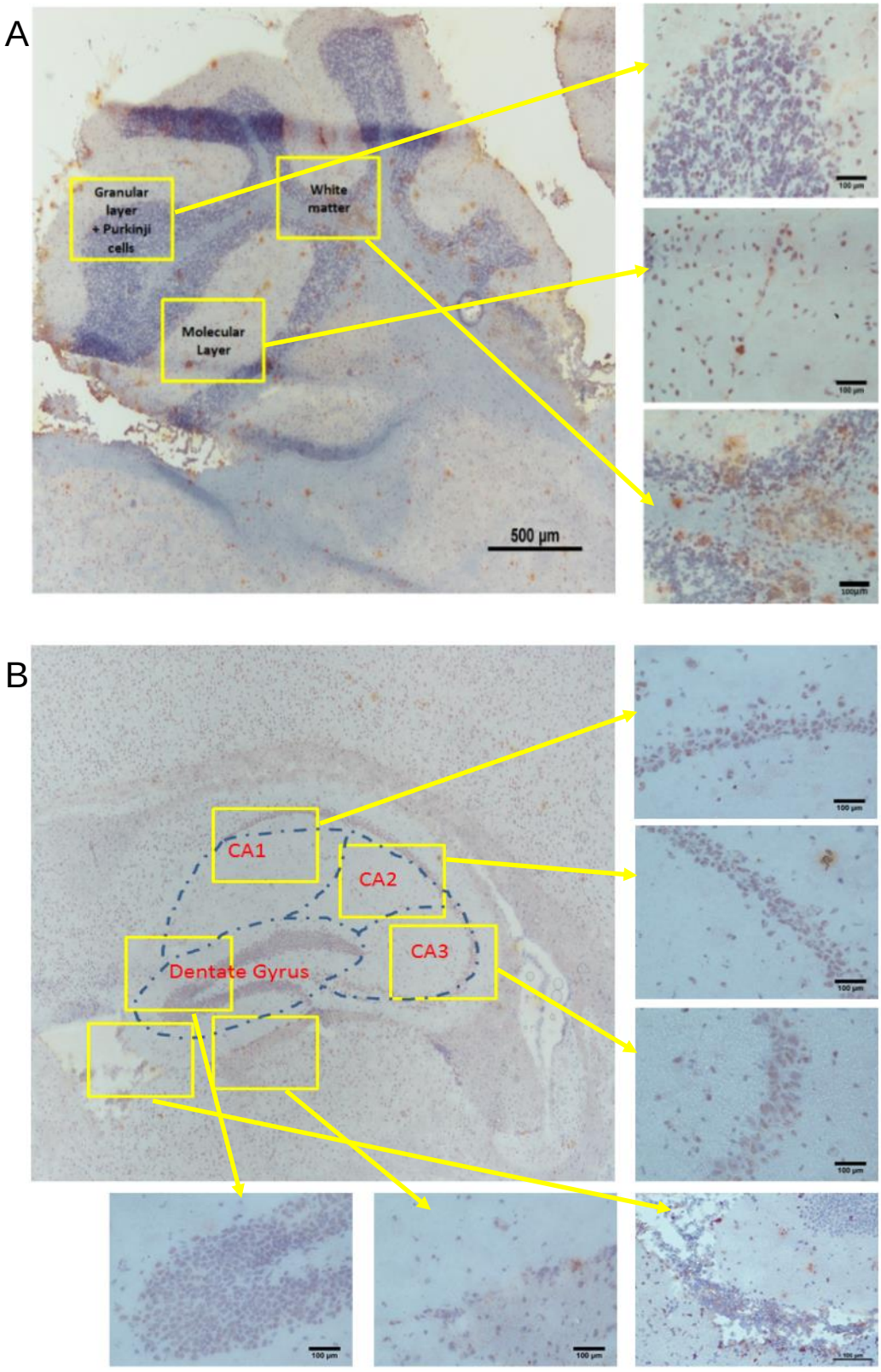

Figure 2.2: *Images showing the brain regions* ***A)*** *cerebellum (white matter, molecular layer, and granular layer + purkinje cells) and* ***B)*** *hippocampus (CA1, CA2, CA3 and 2 parts of dentate gyrus) were quantified for IL-16 positive cells.*

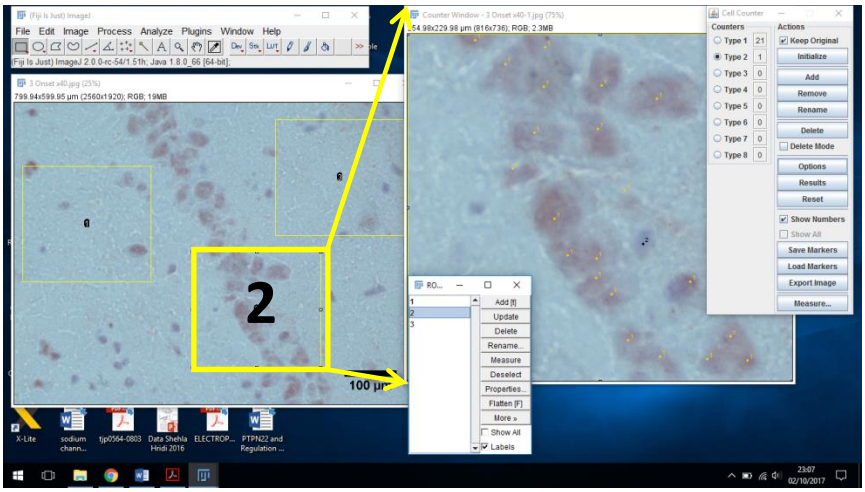

Figure 2.3: Quantification of IL-16 positive cells in brain tissue using ImageJ. *Representative image showing the quantification of IL-16^{+} cells in hippocampal CA2 region of EAE brain tissue section.*

2.4.8 Immunofluorescence stained section quantification

Spleen/lymph node and spinal cord: Tissue sections from spleen/lymph node (Figure 2.4 A) and spinal cord (Figure 2.4 B) were stained for specific cell surface markers (CD45/CD4/CD11b/F4/80) along with IL-16, and then mounted with Vectashield with DAPI. To quantify the percentage CD45^{+} cells co-expressing IL-16, epifluorescence images of right half of spleen/lymph node tissue sections were taken at x20 magnification and spinal cord tissue sections were taken at x10 magnification. Scales of images were set using ImageJ to the scale bar applied by Nikon NIS-Elements imaging software and the images were analysed using ImageJ software. 3 ROIs each with a dimension of 290 µm x 306 µm were assigned on spleen/lymph node tissue sections, and 10 ROIs (6 in white matter and 4 in grey matter) were assigned on spinal cord tissue section. All cells expressing both CD45 (red) and IL-16 (green) associated to DAPI (blue) were counted in each ROI and similarly cells expressing CD45 (red) associated to DAPI (blue) was also counted in each ROI using ImageJ cell counter tool (Figure 2.4 A&B). The co-localised cell counts were expressed as a percentage out of the total number of cells expressing CD45 (red) associated to DAPI (blue) in the field of view of the total ROI assigned in the tissues (Figure 2.4 A&B). Each cell markers were assessed in tissues collected from either 3 or 5 mice per group and were quantified using

the described method to present the data as an average of the total number of mice assessed, with n representing the number of animals.

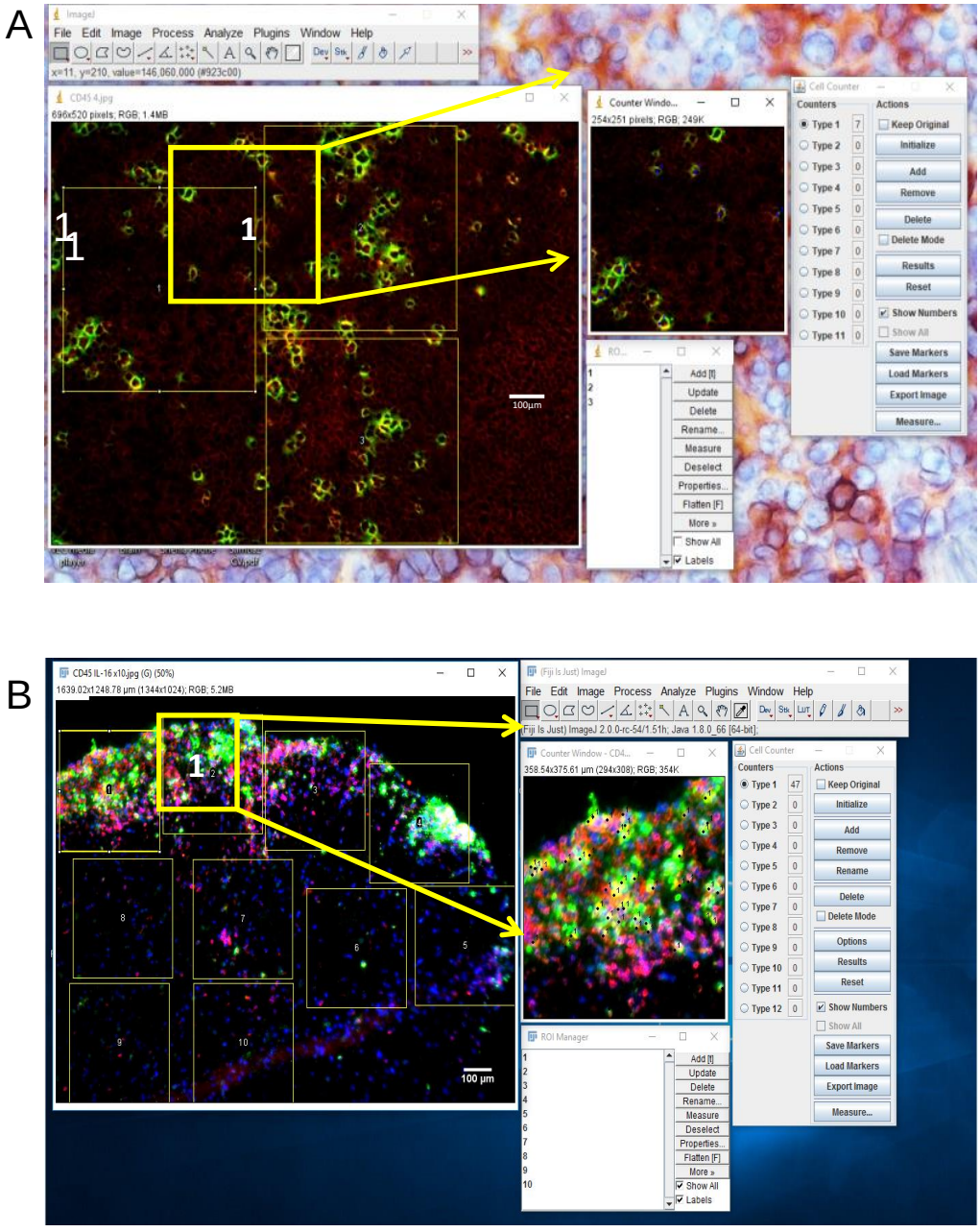

Figure 2.4: Quantification of IL-16 expression by CD45⁺ cells using ImageJ. *Representative image showing the quantification of IL-16 co-localised with CD45⁺ cells in the EAE* ***(A)*** *spleen and* ***(B)*** *spinal cord tissue sections.*

Brain: Brain tissue sections (Figure 2.5 A) were stained for specific cell surface markers (CD45/CD4/CD11b/F4/80) along with IL-16, and then mounted

with Vectashield with DAPI. To quantify the percentage $CD45^{+}$ cells co-expressing IL-16, the tissue sections were imaged using Meso Lens microscope which allowed us to obtain subcellular details from wide-field epifluorescence images at x4 magnification. Scales of images were set using ImageJ and also were analysed using ImageJ software. 1 ROI with a dimension of 3280 µm x 3104 µm was assigned on hippocampus and cerebellum of the brain tissue sections and cells expressing both CD45 (red) and IL-16 (green) associated to DAPI (blue) and cells expressing CD45 (red) associated to DAPI (blue) were counted in each ROI using ImageJ cell counter tool (Figure 2.5 A&B). The co-localised cell counts were expressed as a percentage out of the total number of cells expressing CD45 (red) associated to DAPI (blue) in the field of view of the ROI for the hippocampus and the cerebellum of the brain tissue sections respectively (Figure 2.6 A&B). Each cell markers were assessed in tissues collected from either 3 or 5 mice per group and were quantified using the described method to represent the data as an average of the total number of mice assessed, with n representing the number of animals.

A

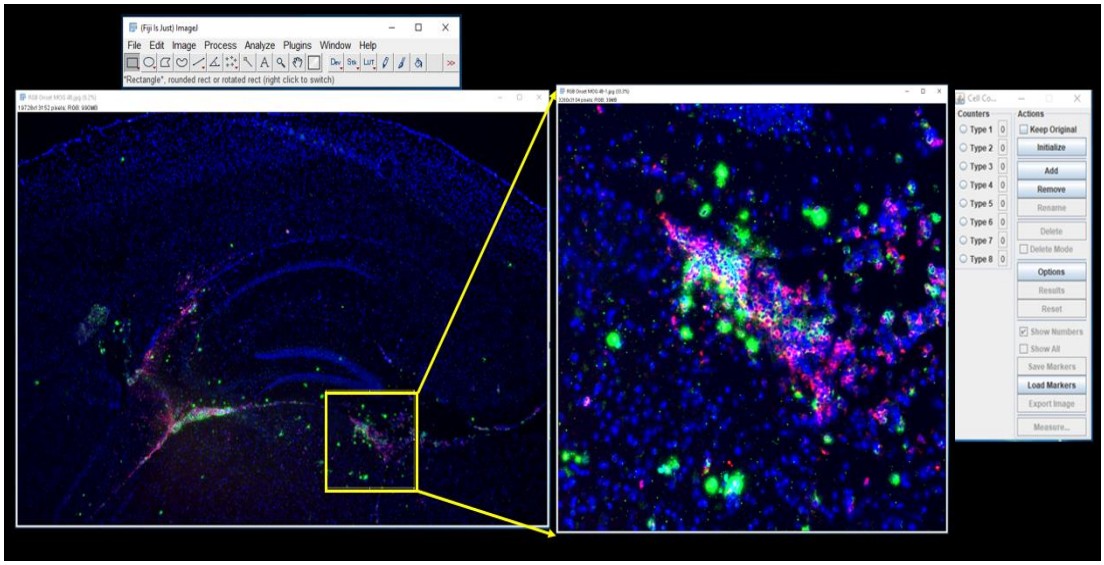

B

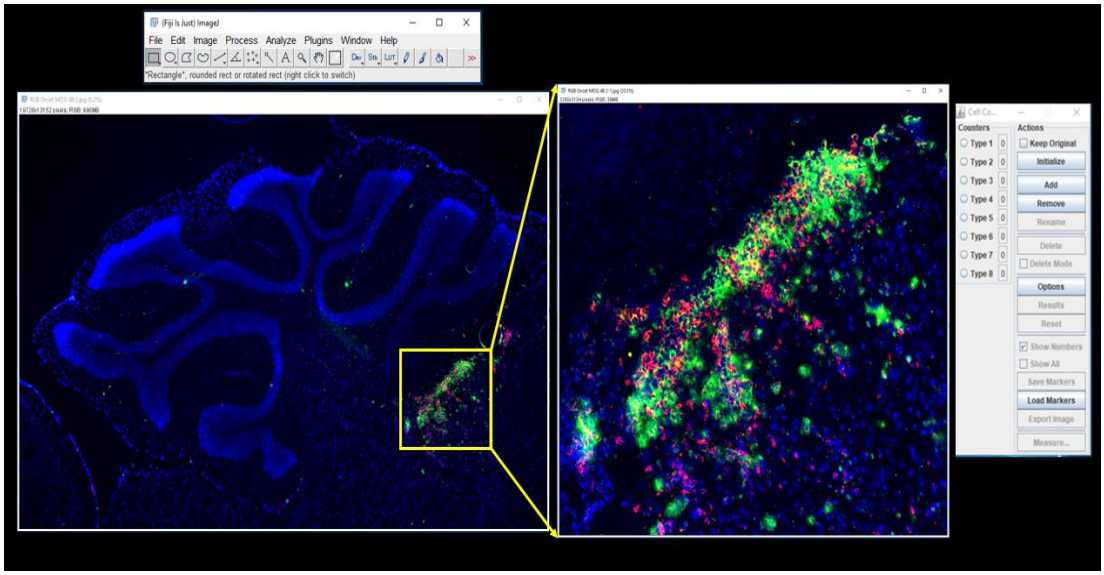

Figure 2.5: Quantification of IL-16 expression by CD45^{+} cells in brain tissue section using ImageJ. *Representative image showing the quantification of IL-16 co-localised with CD45^{+} cells in the* ***(A)*** *Hippocampus and* ***(B)*** *Cerebellum of EAE brain tissue section.*

2.5 Serum Isolation

Mice were sacrificed at EAE onset, peak and resolution stages of the disease. Immediately after sacrificing the mice, blood was collected from each mouse and placed on ice. Whole blood samples were centrifuged for 15 minutes at 4°C at 13000 rpm. Serum was carefully removed and placed in fresh tube for ELISA assay.

2.6 Cell preparation from whole blood

Blood collected from each mouse was transferred to eppendorf tubes containing 0.5 ml PBS containing EDTA (5mM) and placed on ice before transferring to a 15ml tube. 10ml of 1x red blood cell (RBC) lysis buffer prepared in distilled water was then added to each sample and incubated for 10 minutes with occasional shaking. The lysis buffer reaction was stopped by adding 20ml of PBS to each sample. Cells were then centrifuged at 1400 RPM at 4°C for 5 minutes. The supernatant was discarded, and the pellet was re-suspended in appropriate buffer and counted for FACS staining and analysis.

2.7 Cell preparation from spleen and inguinal lymph node

Mice were sacrificed at three time points during the course of the disease (onset, peak and resolution) and spleens and inguinal lymph nodes were harvested and placed in sterile PBS for cell culture. Next tissues were disrupted using the back of a syringe plunger to form a cell suspension. The suspension was then filtered through sterile nitrex nylon mesh (Cadisch precision meshes). Suspension was spun at 1400 RPM at 4°C for 5 minutes and the spleen pellet was resuspended in 5ml RBC lysis buffer for 5 minutes. Spleen/lymph node suspension was then re-filtered, spun and resuspended in complete RPMI media (RPMI-1640 (Lonza; UK) with 10% FCS (Biosera Gold; UK), 100mg/ml streptomycin, 100 U/ml penicillin and 2mM L-glutamine). Cells were counted and re-suspended to an appropriate concentration for culture.

2.8 Spleen and inguinal lymph node stimulation

Cell suspensions from spleens and lymph nodes were cultured in 24 well tissue culture plates at $2x10^6$ cells/well. Cells were cultured with media alone, media with 50 µg/ml MOG_{35-55} or media with 50 µg/ml conA and incubated at 37°C in a cell incubator with 5% CO_2 for 24 and 72 hrs. Supernatants were collected for assessment of different cytokines using ELISA.

2.9 Brain and Spinal cord lysate preparation

Cerebellum, cerebrum with the brain stem and spinal cord were collected in individual bijous containing 1x protease and phosphatase inhibitor cocktail prepared in PBS solution. The tissue samples were then homogenised, and the homogenates were transferred to 1.5 ml eppendorf tubes. Samples were then centrifuged at 13000 rpm for 15 minutes and the supernatant from each sample was collected in 1.5ml fresh eppendorf tubes, which were used on the same day for ELISA.

2.10 CD11b isolation

To isolate CD11b cells, blood samples, spleens and CNS (spinal cord and brain) tissues harvested from EAE peak mice were pooled and processed as described in sections 2.8 and 2.9 respectively. Cells were counted and resuspended in cell isolation buffer (1x PBS with 0.5% BSA and 2 mM EDTA) to get appropriate final concentration. Cell suspension was then briefly centrifuged at 336 RPM for 10 minutes. As described by the manufacturer, supernatant was then completely pipetted off before re-suspending the cell pellet in buffer (90µl of buffer per 10^7 total cells) and then mixed and incubated with (10µl per 10^7 total cells) CD11b microbeads for 15 minutes at 4°C. After the incubation, cells were then washed once by adding buffer (1-2ml of buffer per 10^7 total cells) and centrifuged at 300xg for 10 minutes. Supernatant was then completely pipetted off and cells were resuspended in buffer (10^8 total cells in 500 µl of buffer). To perform cell separation, LS column was placed in the magnetic field of the MACS Separator. The column was prepared by rinsing with 3ml of buffer before adding the prepared cell suspension. The CD11b negative unlabelled cells passing through the column were collected in a suitable tube and the wash steps were performed three times with 3ml of buffer each time. To collect the CD11b positive micro-bead attached cells, column was removed from the MACS separator and placed on top of a collection tube, 5ml of buffer was then added to the top of the column, and cells were then washed off the column with pressure using a plunger. Isolated cells were then incubated with

media alone or with LPS for 24 hours, and supernatants were collected for assessment of IL-16 levels using ELISA.

2.11 Enzyme Linked Immunosorbent Assay (ELISA)

ELISA was used to examine the level of soluble protein levels in the samples using paired antibodies together with recombinant protein as the standard. High binding 96 well plates (Greiner Bio-One) were coated with 50µl specific capture antibodies (using concentrations as mentioned on the certificate of analysis; Table 2.6) diluted in PBS and incubated overnight at 4°C (IL-16 incubated overnight at RT). The plates were then aspirated and washed 3 times with ELISA wash buffer (1x PBS with 0.05% Tween-20) before incubation with assay diluent (1x PBS with 10% Foetal calf serum) for 1 hour at RT. The plates were then again aspirated and washed 3 times before adding 50µl of recombinant standards (diluted in assay diluent) and the samples (lymphocyte cell culture supernatant, blood serum or CNS lysate) in each well, and incubated at RT for 2 hours. The plates were aspirated and washed and then the matching detection antibodies were added for 1 hour at RT (2 hours for IL-16) followed by another wash step. Following that, avidin-HRP was added to each well and incubated for 30 minutes at RT, which is followed by a final wash step. TMB substrate solution was then added to each well until a definitive blue colour had developed and stop solution (1M sulphuric acid) was added to stop any further reaction. The plate was read at 450 nm in Epoch plate reader using the Gen5 1.10 software.

Table 2.6: Antibodies used in ELISA

Antibody	Supplier	Cat No.
IL-6 capture	eBioscience	14-7061
IL-6 detection	eBioscience	13-7062
IL-6 recombinant	eBioscience	14-8061
IL-10 capture	eBioscience	14-7101
IL-10 detection	eBioscience	13-7102
IL-10 recombinant	eBioscience	14-8101
IL-16 capture	R&D	DY1727
IL-16 detection	R&D	DY1727
IL-16 recombinant	R&D	DY1727
IL-17A capture	eBioscience	14-7175
IL-17A detection	eBioscience	13-7177
IL-17A recombinant	eBioscience	14-8171
IFN-γ capture	eBioscience	14-7313-68B
IFN-γ detection	eBioscience	13-7312-68C
IFN-γ recombinant	eBioscience	39-8311-60

2.12 Cell staining for fluorescence activated cell sorting (FACS) analysis

Whole blood from each mouse was collected and processed following the method mentioned in section 2.6 cells were counted and re-suspended in FACS buffer (1% BSA in PBS) to appropriate concentrations and then 0.5 x10^6 cells were transferred to each FACS tube. Cells were then washed adding FACS buffer followed by centrifugation at 1400 RPM at 4^{o}C for 5 minutes and the supernatant was discarded. Cells were then incubated with 100µl of α-mouse CD16/CD32 Fc antibody (eBioscience, UK) for 5 minutes at 4°C in the fridge to block non-specific Fc receptors. After the incubation the appropriate antibodies (Tables 2.7 and 2.8) diluted in 100µl FACS buffer were added to each tube and incubated in the dark at 4°C for 30 minutes. Cells were washed twice in 1ml FACS buffer and re-suspended in 0.5ml FACS buffer. Cells were analysed using BD FACS Canto system and BD FACS Diva software.

Single spleen cells were prepared following the method as mentioned on section 2.8, $2x10^6$ cells/well were cultured in 24 well plated. Cells were treated with cell stimulation cocktail (PMA and ionomycin) which contained protein transport inhibitors (Brefeldin A and Monensin) to stimulate the cells to produce cytokines and trap them inside the cells. After 18 hrs, $0.5 x10^6$ cells from each sample were collected and added to each FACS tube with 1ml FACS buffer. Samples were centrifuged at 1400 rpm for 5 minutes at 4°C and the supernatant was removed. Cells were then stained with specific cell surface marker antibodies listed in Table 2.7.

For staining of intracellular antigens, the Fixation and Permeabilization Solution Kit with BD Golgi Stop was used according to the manufacturers' instructions. Cells were first stained with surface marker antibodies and washed, followed by incubation in fixation/permeabilization solution for 20 minutes at 4 °C. Cells were then washed two times with BD Perm/Wash buffer to maintain cell permeabilization and then incubated with the appropriate intracellular antibodies for 30 minutes at 4°C in the dark. Following two more wash steps in BD perm/wash solution, cells were resuspended in staining buffer and analysed as above as mentioned in 2.2.11. Cells were analysed using BD FACS Canto system and BD FACS Diva software. To analyse the FACS data the graph's axis parameters were initially set to side scatter in the Y-axis and forward scatter in the X-axis. A polygonal lymphocyte gate was then drawn around the cells discarding the dead cells at the left corner of the graph. By double-clicking on the polygonal lymphocyte gate in the graph window a new graph was opened to displaying only the subset of cells that fall in the polygonal lymphocyte gate. Two-parameter density plots were then obtained from this gated lymphocyte, to display two measurement of fluorescence parameters, one on the x-axis and one on the y-axis depending on which cell types we have shown in Figure-2.6 , the lymphocytes determined by forward and side scatter were stained with CD4(Pe-Cy7) and CD25 (FITC) to identify the T cell and activated T cell populations. This data was then visualized with density plot where the graph was split into four quadrants allowing us to determine the cells single positive for each marker and both double negative and double positive. In this graph 13.8% of the lymphocyte's population is made up of $CD4^+$

T cells and 1.06% activated $CD4^+$ T cells. When the expression levels do not show distinct populations or are not mutually exclusive the appropriate controls were used to help us determine the positive and negative populations.

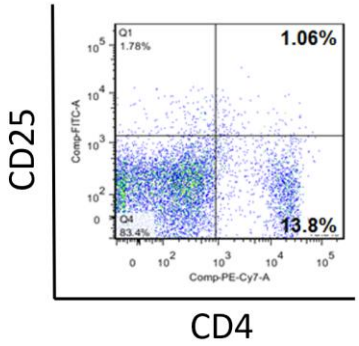

***Figure 2.6: Two-parameter (dual colour fluorescence) density plot**. Spleen cells collected from naïve was stained with CD4 and CD25. The lymphocytes were determined by the forward and side scatter profile and T cell and activated T cell percentages were determined using different gating methods.*

Table 2.7: Antibodies used in FACS analysis

Antibody	**Conjugate**	**Manufacturer**	**Cat No.**
IL-16	PE	Biolegend	519106
IL-17A	APC	eBioscience	17-7177-81
CD3	FITC	eBioscience	11-0032-82
CD4	FITC Percy5.5	eBioscience	53-0041-80 45-0042-82
CD8	Percy5.5	eBioscience	45-0081-82
CD11c	FITC	eBioscience	11-0114-82
CD19	APC	eBioscience	17-0193-83
CD25	488	eBioscience	53-0251-82
CD40	Percp 710	eBioscience	46-0401-80
CD45	PE	eBioscience	12-0451-82
B220	FITC	eBioscience	11-0452-82
F4/80	Percy5.5	eBioscience	45-4801-80
IFN-y	FITC	BD Pharma	554411
MHC-II	APC	eBioscience	17-5909-42

Table 2.8: Isotype control antibodies used in FACS

Species	Isotype	Conjugate	Manufacturer	Cat No.
Rat	IgG1	FITC	eBioscience	11-4301-81
Rat	IgG2a	PE Percp-cy5.5	eBioscience	12-4321-82 46-4321-82
Rat	IgG2b	PE	eBioscience	25-4031-81
Hamster	IgG	PE	eBioscience	12-4888-81

2.13 Primary hippocampal culture

2.13.1 Solutions used for primary hippocampal culture

Poly-L-lysine (PLL): 10x stock solution (0.1mg/ml) was prepared by dissolving 5mg of the PLL powder in 50 ml of water. 1ml of this solution is diluted in 9ml of water to give a final concentration of 0.01mg/ml and the solution was filter sterilized using Millex syringe-driven filter unit (0.22 µm).

H enzyme solution: 116 mM NaCl, 5.4 mM KCl, 26 mM $NaHCO_3$, 1.3 mM NaH2PO4, 2 mM MgSO4, 2mM CaCl2, 0.5 mM EDTA, 25 mM D-glucose; pH to 7.4. The solution was stored at -20 ^oC until required during culture.

Hippocampal culture media (prepared on the day of the culture): 97% Neurobasal A (48.5 ml) supplemented with 2% B27 supplement (1ml) and 1% L-glutamine (0.5 ml).

2.13.2 Preparations for primary hippocampal culture

Poly-L-lysine (0.01 mg/ml) coating of the autoclaved sterile coverslips or 6-well plate was achieved by applying 200µl to each coverslip and 1ml in each well of six well plate and air drying at RT for 1 hr followed by several washes in autoclaved water. Coverslips were then allowed to rest on a sterile paper towel and allowed to dry in the tissue culture cabinet prior to plating into sterile 33 mm petri dishes (2-3 coverslips per dish). To obtain the hippocampal conditioned medium (HCM) some petri dishes were plated with only one coverslip in each dish.

2.13.3 Method for primary hippocampal culture

To culture the hippocampal neurons, 1-2-day-old C57BL/6J mice pups of either sex were killed by cervical dislocation followed swiftly by decapitation in accordance with Schedule 1 procedures of the UK Home Office guidelines, Animals Act 1986 (Scientific Procedures). A size 11 scalpel blade was used to pierce the skin and the skull down in the middle. The skull was then removed using small curved tweezers and using a small spatula the brain was carefully lifted out of skull and placed onto sterile filter paper. The brain was then gently cut into two hemispheres using a scalpel. One half of the hemisphere was then flipped onto its side and the cortex removed to reveal the hippocampus. The upper and lower sections of the hippocampus are then removed using the scalpel and collected in a petridish containing H-enzyme solution. In the same way, the hippocampus is collected from the second hemisphere.

Following this, the tissue was suspended in a pre-warmed filter sterilized solution of papain (7.5 mg of papain in 5 ml H-enzyme solution) and incubated at 37°C for 20 minutes. Enzymatic digestion was brought to an end by transferral of the hippocampal tissue into filter sterilised 1% bovine albumin serum solution, (60 mg of BSA in 6ml of H-enzyme). The tissue was then triturated using a series of three flame polished sterile glass pasteur pipettes of decreasing tip diameter until no clumps of cells remained visible. A pellet of cells was recovered by centrifugation (2000 rpm, 2 minutes, RT) and the resulting pellet was re-suspended in 1ml of hippocampal culture medium. Clustered cells are then gently broken down using a pipette. Following suspension in media, 10µl of media from the top and bottom was taken in two eppendorf and mixed with 10µl of Trypan blue. The cells were then loaded onto a haemocytometer (Hawksley, UK), cell concentration was counted and subsequently diluted to a final density of 5.5×10^5 cells/ml.

Once the specific concentration was obtained, cells were plated onto sterilized Poly-L-lysine coated coverslips (100 µl per coverslip) or six well plate (1ml per well of 6-well plate). Cells were allowed to adhere to the coverslips or 6-well

plates at 37°C / 5% CO_2 for 1 hour, following which excess cells were removed by pipetting off any remaining media and then carefully adding 2ml of hippocampal culture media per petri dish. The cultures were incubated in hippocampal media at 37°C / 5% CO_2 for 11-15 days *in vitro* (DIV). All the steps for the preparation of the culture were carried out under sterile conditions inside the laminar flow hood (Walker Safety Cabinets LTD, UK). The cultures were regularly checked under bright field microscope to ensure they were growing properly without any occurrence of contamination or cell death. Medium collected from dishes that had one coverslip made up the HCM.

2.14 Immunocytochemistry in primary hippocampal cell cultures

Primary hippocampal cultures (11-15 DIV) were washed thrice with PBS and then fixed in ice-cold 4% paraformaldehyde for 10 mins. The cultures were then washed with PBS and treated with ice cold 100% methanol for 10 minutes prior to the permeabilization with 0.01% Triton-X (in PBS) for 10 minutes. Following this, the cultures were washed and then treated with blocking buffer solution (5% FCS in PBS) for 1 hour to block any non-specific binding sites.

Primary antibodies (Table 2.3) were prepared at the appropriate dilution in blocking buffer to identify particular cellular components. The antibody solution (100 µl) was applied directly to the coverslip and incubated overnight (16-20 hours) at 4º C in a moisture box. The following day the cultures were washed thrice with PBS and then directly incubated for 1 hour in a dark room with appropriate fluorescent secondary antibodies prepared in BB at optimal dilutions. Some coverslips were used as controls and were treated with secondary antibody alone (Table 2.4) to confirm that non-specific staining was not occurring. To remove the excess secondary antibodies, all coverslips were washed thrice with PBS and mounted onto microscope slides using 5µl of Vectashield mounting medium containing DAPI and allowed to set. Once set, the edges of the coverslips were sealed using black nail varnish and upon drying, the slides were wrapped with foil paper and stored at 4ºC until imaged.

The immunostaining was imaged using an OLYMPUS BX51W1 microscope with a Q-imaging digital camera and using Win Flour v3.4.4 imaging software (J Dempster, University of Strathclyde). Cells were imaged using a 40x water immersion lens with appropriate excitation filters used to visualize Alexa Flour 488 (A488) and Alexa Flour 555 (A555) signals respectively.

2.15 Whole cell patch clamping in primary hippocampal culture

2.15.1 Electrophysiology rig for patch clamping

The set-up for allowing whole cell patch clamp recording consists of a faraday cage preventing interference from external electrical noise. Inside the cage, a submerged recording chamber, an inverted microscope (Nikon Eclipes TS100, Japan) equipped with 40x objective lens and a manipulator (MP-225 Sutter instrument company, USA) were mounted on an anti-vibration table (Intacell Isolate System). A computer with the Clampex software to analyse the signals from the cells, a vacuum pump, the amplifier and the external solution collection reservoir all were placed outside the faraday cage, (Figure 2.7).

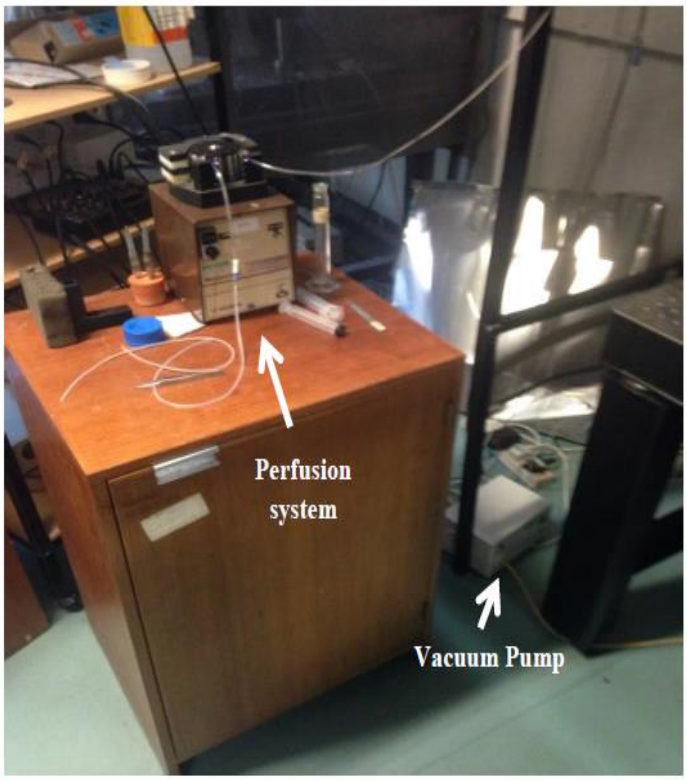

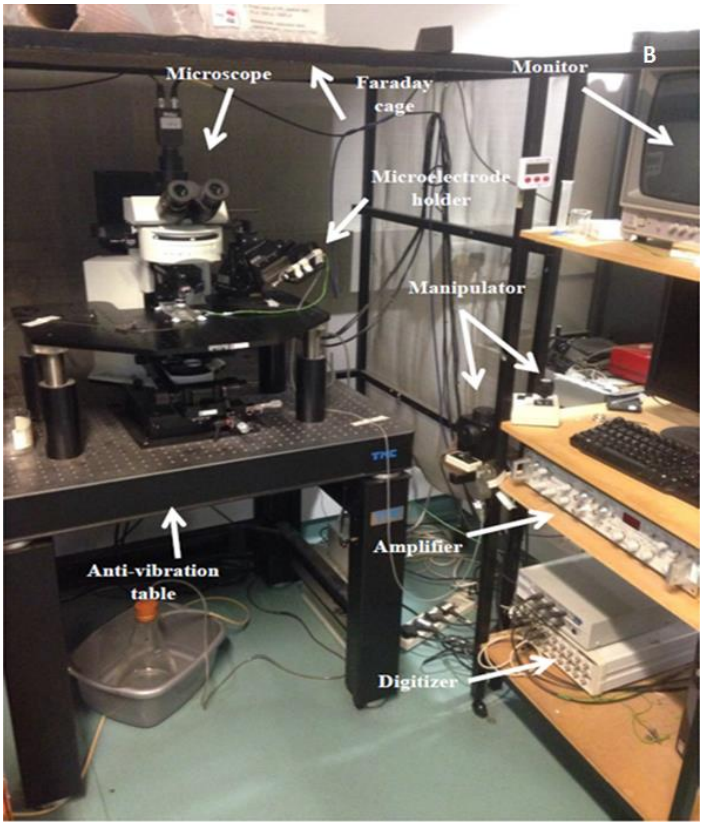

Figure 2.7: Images showing the set-up used in patch clamp electrophysiology. *It is consists of a fara-day cage, inside the cage, a submerged recording chamber, an inverted microscope equipped with 40x objective lens and a manipulator mounted on an anti-vibration table. A computer with the Clampex soft ware to analyse the signals from the cells, a vacuum pump, the amplifier and the external solution collection reservoir all were placed outside the faraday cage.*

2.15.2 Whole cell patch clamping

The coverslip with cultured cells was submerged in the chamber (Figure 2.8) which was continuously perfused with freshly prepared HEPES-based salt solution (HBSS) which contained (in mM): NaCl 140, KCl 5, $MgCl_2$ 2, CaCl2 2, HEPES 10, d-glucose 10, pH 7.4, 310 mOsm. Cells were visualised using bright field microscopy and healthy cells (smooth cell surface) were chosen for patch clamping. Borosilicate glass micropipettes (1.5 mm O.D x 0.86 mm I.D. Harvard Apparatus, 4-6 MΩ) were pulled with an electrode puller (DMZ-Universal, Germany) and filled with internal solution which contained (in mM) KMeSO4 130, KCl 20, Mg-ATP 4, Na-GTP 0.3, EGTA 0.3, HEPES 10, pH 7.2, 290 mOsm was placed in the head stage which is attached to the micromanipulator. With the help of the micromanipulator, the glass electrode was

moved into the external solution over the coverslip and then carefully moved towards the cell soma (Figure 2.10). Once the tip of glass micropipette touched the membrane, a slight negative pressure was applied to obtain a gigaohm seal. Once a gigaohm seal was obtained, careful and gentle suction was applied to rupture the membrane patch to obtain the whole cell configuration. Signals in the experiments were captured by an Axopatch 200B amplifier (Molecular Devices, USA), digitized at 10 kHz and filtered at 2 kHz. To analyse for Na^+ and K^+ currents, experiments were conducted in voltage clamp mode using Clampex software with 14 depolarization steps (-90mV to +40mV) every 10s from an initial holding potential of -70mV. Spontaneous excitatory postsynaptic currents (sEPSCs) were recorded over a 3-minute baseline period at a holding potential of -70mV. All neuronal recordings were obtained from cultures that had been treated in one of the three conditions outlined below.

- **rIL-16 treatment:** A petri dish containing a single hippocampal coverslip was treated with recombinant IL-16 (rIL-16, 300pg/ml) and then allowed to incubate for 1 hour in an incubator before carrying out electrophysiological recordings.
- **rIL-16 recovery:** A single coverslip was treated as outlined above and then transferred in a petri dish with HCM and left in an incubator for 3 hours and then used for recording.
- **rIL-16 control:** As an appropriate vehicle control for rIL-16 treatment, the hippocampal coverslips were treated with only water (300pg/ml) for 1 hour in an incubator before carrying out recording.

Sodium and potassium currents were analysed offline using Clampfit 10.3 software and MiniAnalysis software, for sEPSCs (Synaptosoft, USA) where n represents the number of cells recorded from a minimum of 5 separate cultures. All data are expressed as mean ± S.E.M.

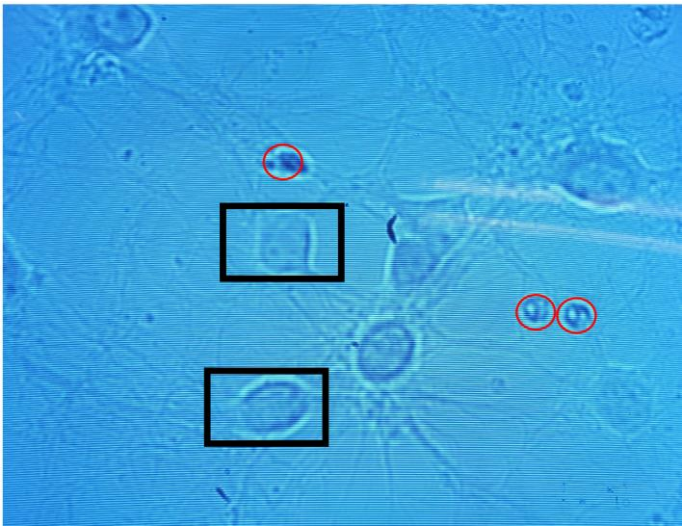

Figure 2.8: Image showing a coverslip with cultured cells submerged in the chamber for patch clamp electrophysiology. *The cells within the red circles are dead cells and the cells within the black border are healthy cells which were patched.*

2.16 Western blotting

2.16.1 Solutions used for western blot

Western blot transfer buffer: 10x stock transfer buffer was prepared by dissolving 480mM Tris base, 390mM Glycine and 0.06% (w/v) Sodium dodecyl sulphate (SDS) in dH_2O. 1x transfer buffer was prepared using 100 ml of 10x transfer buffer in 900ml of dH_2O.

Western blot wash buffer (PBST): 1x PBS+0.1 % Tween 20.

Western blot blocking buffer: 10 ml of PBST with 5% semi skimmed milk (0.5g).

Western blot secondary antibody diluent: 20 ml of PBST with 1% semi skimmed milk (0.2g).

Western blot resolving gel buffer: 2x buffer was made using 750mM Tris base, 4mM EDTA and 0.2% w/v SDS in dH_2O; pH 8.9.

Western blot stacking gel buffer: 2x buffer was made using 250mM Tris base ,4mM EDTA and 0.4% w/v SDS in dH_2O; pH 6.8.

Western blot running buffer: 10X buffer was made using 250mM Tris Base, 1,92M Glycine and 1% SDS in dH_2O

Western blot resolving gel 2x: 5ml of 2x resolving gel buffer, 4ml of 30% Acrylamide (Carl Roth GmbH and Co.) and 0.8 ml dH_2O was mixed well before adding 8µl Tetramethylethylenediamine (TEMED) and 200 µl of 10 % ammonium persulfate (APS; 0.1 g in 1 mL PBS).

Western blot stacking gel 2x: 3 ml of stacking gel buffer, 0.9 ml Acrylamide, and 1.95 ml dH_2O was mixed well before adding 7.5 µl TEMED and 150 µl 10 % APS.

Western blot SDS loading buffer: 4x buffer was made using 0.4% w/v bromophenol blue, 200mM Tris base, 40% glycerol and 8% w/v SDS in dH_2O. 1x buffer was prepared using 100 ml of 4x SDS loading buffer in 900ml of PBS and 25mM dDithiothreitol (DTT).

2.16.2 Sample preparation

Hippocampal cultures were grown in a 6-well plate as described earlier. At DIV13, 3 wells were treated with rIL-16 (300pg/ml, 1hr) with the other 3 wells treated with vehicle (1h) to act as a control followed by brief wash in ice-cold (x2) PBS. 500µl lysis buffer (50mM Tris, 150mM NaCl, 1mM EDTA, 1% Triton X-100, 0.5% sodium deoxycholate, 1:100 protease inhibitor and phosphatase inhibitor cocktail 2 & 3; pH 7.4) was then added to each well and cells were successively scraped from one well and then added to the next well until all cells were collected from all 3 wells and transferred to an eppendorf tube. Cell lysates were then centrifuged at 16,000 rpm at 4°C for 10 minutes and supernatant were transferred to fresh eppendorf and stored at -20°C for future use to quantify protein and carry out western blot.

2.16.3 Protein quantification

The total protein concentration was analysed using a Bradford protein assay using BSA as a protein standard to develop a standard curve with concentrations ranging from 0 - 20 µg/ml. Samples and the protein standard BSA were prepared in triplicate and then transferred to cuvettes and absorbance were read in spectrometer at 595 nm. A standard curve was plotted and used to calculate the amount of protein in 10 µl of each sample with 5 µg of total cellular protein used for each experiment. The samples were then made up in x4 loading buffer and then heated to 95ºC for 5 mins before storing them at -20ºC until used.

2.16.4 SDS-polyacrylamide gel electrophoresis

Glass plates were cleaned and assembled in the appropriate casting frames. Resolving gel (4.6 ml) were poured between assembled plates and allowed to set for 10 minutes. While waiting for the resolving gel to set, stacking gels were prepared. Once the resolving gel was set, the SDS was discarded and stacking gels were poured on top of the set resolving gel. A comb was then inserted, and everything was allowed to set for approximately 30 minutes before the comb was removed. The gel cassettes were then assembled in a Bio-Rad Mini-PROTEAN IITM 46 electrophoresis tank. Both inner and outer tanks were filled with running buffer. A molecular weight marker (15µl) was loaded into the first lane followed by samples (30 µl) into each lane using a Hamilton syringe. The gel electrophoresis was then run at 90 V for approximately 30 minutes followed by 150 V for 1 hour and 30 minutes or until the dye had run to the bottom of the gel.

2.16.5 Blotting to sample into nitrocellulose membrane

Once the gel had finished running, it was transferred to a nitrocellulose membrane. Nitrocellulose membrane was soaked in transfer buffer and the gels were arranged in a transfer cassette in following order: 1. sponge; 2. blotting paper; 3. nitrocellulose; 4. gel; 5. blotting paper; 6. sponge. The assembled

cassette was then placed in a Bio-Rad Mini Trans-Blot tank and filled with transfer buffer and run overnight at 120 mA.

2.16.6 Western blotting

Following the protein transfer to nitrocellulose, the membranes were then incubated in western blot blocking buffer for 1 hour on a shaker with 100 RPM to block non-specific binding. The membrane was then directly incubated overnight at 4° C with appropriately pre-diluted specific primary antibodies (Table 2.11) in PBS-T. Next day, the membranes were washed (4 x 5minutes) in PBS-T. During this time, the membranes were placed on the shaker at 100 rpm speed (IKA KS 250 basic; Labortechnik) to ensure appropriate flow of PBS-T. After washing, the membranes were then incubated with relevant fluorophore conjugated secondary antibodies (Table 2.12) prepared in diluent for 50 minutes at RT. The membranes were then carefully washed in PBS-T before scanning and capturing the images using Odyssey scanner (Licor; UK). The captured images were then normalised to Anti-β Actin and quantified using an Odyssey scanner (Licor; UK).

Table 2.9: Primary antibodies used in western blotting

Antibody	Host	Supplier	Cat. No.	Marker
Anti-Glutamate Receptor 1	Rabbit	Abcam	ab109450	Glutamate Receptor 1
Anti-Glutamate Receptor 1(Phospho S845)	Rabbit	Abcam	ab76321	Phospho S845
Anti-Sodium Channel Pan	Rabbit	Sigma	SAB4502713	Sodium channels
Anti-Phospho-Glutamate 1	Rabbit	Millipore	04-823	Phospho S845
Anti-β Actin	Mouse	Abcam	Ab8226	β-Actin

Table 2.10: Secondary antibodies used during western blotting

Antibody	Host	Conjugate	Supplier	Cat. No.
Anti-Rabbit	Donkey	IR Dye	LI-COR, UK	926-32213
Anti-Mouse	Donkey	IR Dye	LI-COR, UK	926-32212

2.17 Statistical analysis

All statistics were carried out using Graph Pad Prism software. All data are expressed as mean ± S.E.M in all experiments. EAE clinical data and percentage weight change was analysed using 2-way ANOVA with repeated measure with Bonferroni post-hoc test. Statistical analysis of all other data was performed using a 1-way ANOVA with Bonferroni post hoc. A p value < 0.05 was taken as indicative of statistical significance.

3. Analysing the expression of IL-16 in lymphoid organs and CNS

3.1 Introduction

MS is an autoimmune, demyelinating disease which affects over 2.5 million people worldwide (Christophi *et al*., 2009). EAE is the most commonly used animal model for studying MS because of its close immunopathological resemblance (Lindsey *et al*., 2005; Comabella and Khoury., 2011). In MS/EAE the inflammatory response is driven by myelin specific T cells crossing the BBB to the CNS. Following the entry, the T cells are reactivated by APCs to release pro-inflammatory mediators and cytokines which induce activation of resident microglia and astrocytes as well as other immune cells such as B cells, DCs and macrophages, which then produce more inflammatory cytokines and chemokines involved in myelin and axonal damage (Ransohoff *et al*., 1993; Sun *et al*., 1997 and Oh et a., 1999).

IL-16 is a cytokine which was initially identified as a lymphocyte chemoattractant factor in T cells (Cruikshank and Center., 1982; Cruikshank *et al*., 2000). IL-16 is predominantly produced by $CD4^+$ and $CD8^+$ cells, (Berman *et al*., 1985) as a precursor protein known as pro-IL-16, which gets enzymatically cleaved by caspase 3, releasing the bioactive form of IL-16 (Zhang *et al*., 1998). Other cells that can produce IL-16 include monocytes/macrophages, DCs, mast cells, fibroblasts and microglia (Skundric *et al*., 2015). IL-16 is also the ligand for the CD4 receptor and cell surface expression of CD4 is required to exert the bioactivities of IL-16 observed in immune cells (Skundric *et al*., 2015). Through interaction with CD4, IL-16 can chemoattract a variety of $CD4^+$ immune cells. In addition, IL-16 has been also designated as a pro-inflammatory cytokine that exhibits immunomodulatory properties, including the activation of T cells (Cruikshank *et al*., 2000) and macrophages.

Several studies have suggested that IL-16 plays an important role in the development of various autoimmune diseases including MS (Biddison *et al*.,

1997; Skundric *et al*., 2005; Skundric *et al*., 2015). With IL-16 found to be secreted from MS patient derived cytotoxic T lymphocytes (CTLs) when stimulated with the myelin specific antigen proteolipid protein (PLP), suggesting a role for IL-16 in MS disease (Biddison *et al*., 1997). Furthermore, anti-IL-16 antibody treatment also showed to ameliorate relapses in EAE mice and diminish the CNS infiltration by $CD4^+$ T cells. Importantly, a recent observation demonstrated that conditioned media from lymphocyte preparations containing IL-16 is neuroprotective against kainate-induced excitotoxicity and neuronal death, which further suggests that IL-16 may play a protective role in certain CNS diseases (Shrestha *et al*., 2014). However, the exact role of IL-16 in the CNS during MS/EAE initiation and progression is likely to be complex and requires further investigation.

The aims of this chapter therefore are:

1: To establish EAE as a research model for CNS neuroinflammatory disease such as MS for this study, and to characterise the immunological changes associated with EAE onset and progression.

2: To characterise the expression of IL-16 and its receptor CD4 in spleen, lymph node and CNS tissues of EAE and control mice over the course of the disease, and to determine whether the expression level of IL-16 correlates with neuroinflammation in the CNS of EAE mice.

3.2 Results

3.2.1 MOG_{35-55} induced EAE in C57BL/6J mice

EAE was induced in 7-8-week-old C57BL/6J female mice through s.c administration of MOG_{35-55} peptide emulsified in CFA on day 0, followed by i.p injection of PTX on day 0 and 2 (Figure 3.1). Naïve and PBS immunised mice were also included as controls to determine the symptoms observed in EAE mice were MOG_{35-55} specific.

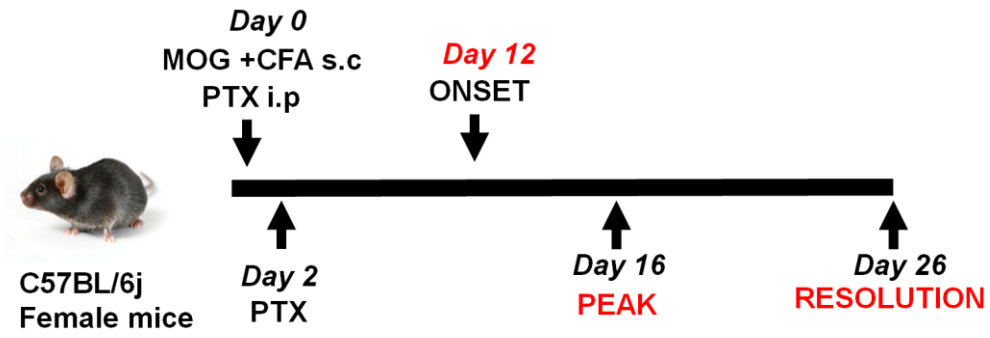

Figure 3.1: EAE induction and time course of disease development. *On day 0, 7-8 weeks old C57BL/6J female mice were injected with MOG_{35-55} peptide emulsified in CFA, followed by intraperitoneal (i.p) injection of PTX on day 0 and 2. Symptomatic onset of EAE began at day 12, progressed and reached the peak at day 16 before gradually recovered by from day 18 until day 26.*

Mice were monitored daily for clinical signs of EAE development and disease severity was scored daily post immunization using the previously described scoring system (Table 2.2). Early symptoms of EAE development include developing paralysis starting at the tail with normal mice being able to hold their tail up in the air (Figure 3.2 A), whereas in EAE mice the tail began to lose its strength and became limp (Figure 3.2 B; EAE score=1). As the disease progressed, the mice displayed hind limb weakness (Figure 3.2 C; EAE score =2) and eventually complete hind limb paralysis (Figure 3.2 D; EAE score =3).

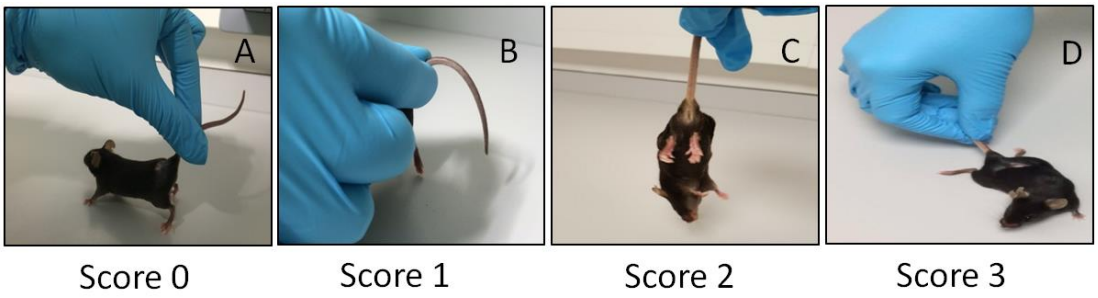

Figure 3.2: EAE clinical symptoms. *Clinical symptoms were evident as mice developed paralysis.* ***(A)*** *0: no sign of symptoms;* ***(B)*** *1: complete loss of tail tone;* ***(C)*** *2: hind limb weakness;* ***(D)*** *3: hind limb paralysis.*

Mice from naïve and PBS immunised groups, did not develop any EAE clinical signs, and therefore all mice within these groups maintained a clinical score of 0 over the full-time course (Figure 3.3). In contrast, mice immunized with MOG_{35-55} developed a monophasic disease course with EAE onset occurring around day 12 when the mice started to exhibit loss of tail tone (Figure 3.3 A). 35% of MOG_{35-55} immunised mice displayed clinical signs of EAE at day 12 post immunisation and the incidence increased to 100% by day 15 post immunisation (Figure 3.3 B). Disease severity reached its peak at day 16 when the mean clinical score of the group reached 2.1± 0.2. After day 16, mice began to gradually recover, with a steady decrease in clinical score. However full recovery was never achieved within the 26-day period and mice still displayed an average clinical score of 0.5 at day 26.

In addition, the weight of individual mice from each group was monitored throughout. Mice were weighed on day 0 and every 2 days after immunization and then twice a day from the onset of clinical symptoms. The relative percentage weight change calculation revealed naïve and PBS mice, which did not develop EAE, steadily gained weight over the course of time (Fig. 3.3 C) whereas the MOG_{35-55} immunised mice started to lose weight just before EAE onset around day 11. Between days 12-17 when the mice reached the maximum disease severity they were at their lightest weight. After this, as the mice reached their recovery stage they started regaining weight.

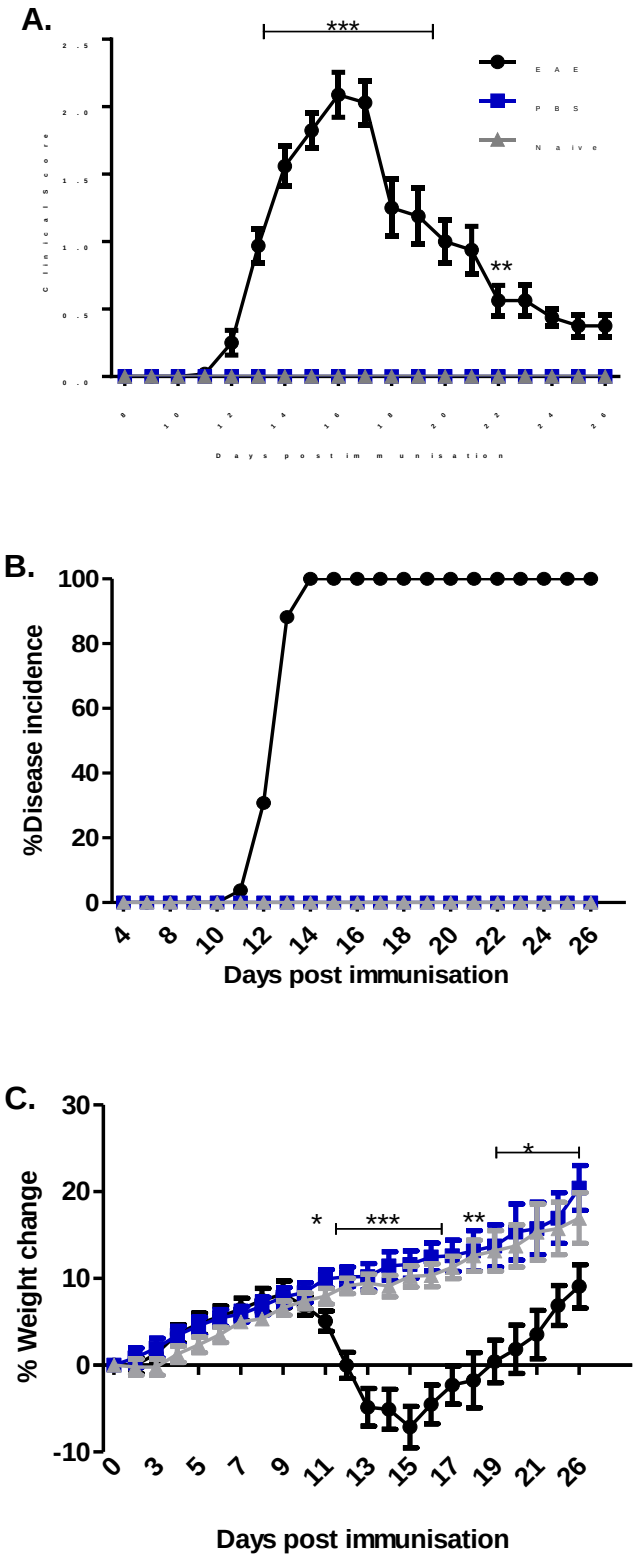

Figure 3.3: Monophasic disease course displayed by EAE mice. (A) *Mean EAE clinical score of mice as assessed using the scoring system described previously.* ***(B)*** *Percentage of disease incidence.* ***(C)*** *Percentage weight change of all animals in each group. Data represents mean ± S.E.M. Naïve, (n=11); EAE (n=15); PBS (n=11). Statistical significance was determined by two-way repeated measures ANOVA with Bonferroni post-hoc test. *P<0.05, **P <0.01 ***P<0.001 versus naïve and PBS control groups. n=number of animals.*

3.2.2 Cellular infiltration in CNS tissues of EAE mice

Histological analysis was used to investigate the extent of inflammation and the levels of cellular infiltration in the spinal cord and brain tissues over the course of EAE. H&E staining was carried out on these tissues harvested from naïve, PBS immunised mice at day 16 post immunisation (equivalent time to day 16; EAE peak of MOG_{35-55} immunised mice) and MOG_{35-55} immunised mice at day 12 (EAE onset), day 16 (EAE peak) and day 26 (EAE resolution) post immunisation.

No signs of cellular infiltration were observed in spinal cord tissues collected from naïve (Figure 3.4A) and PBS day 16 mice (Figure 3.4B). In MOG_{35-55} immunised mice, cellular infiltration was first observed in the inflammatory lesions of spinal cord tissues at day 12 of EAE (Figure 3.4C), predominantly within the WM. The inflammation was increased further at day 16 of EAE (Figure 3.4D). By the time EAE reached the day 26 (Figure 3.4F) there was cellular infiltration within the spinal cord.

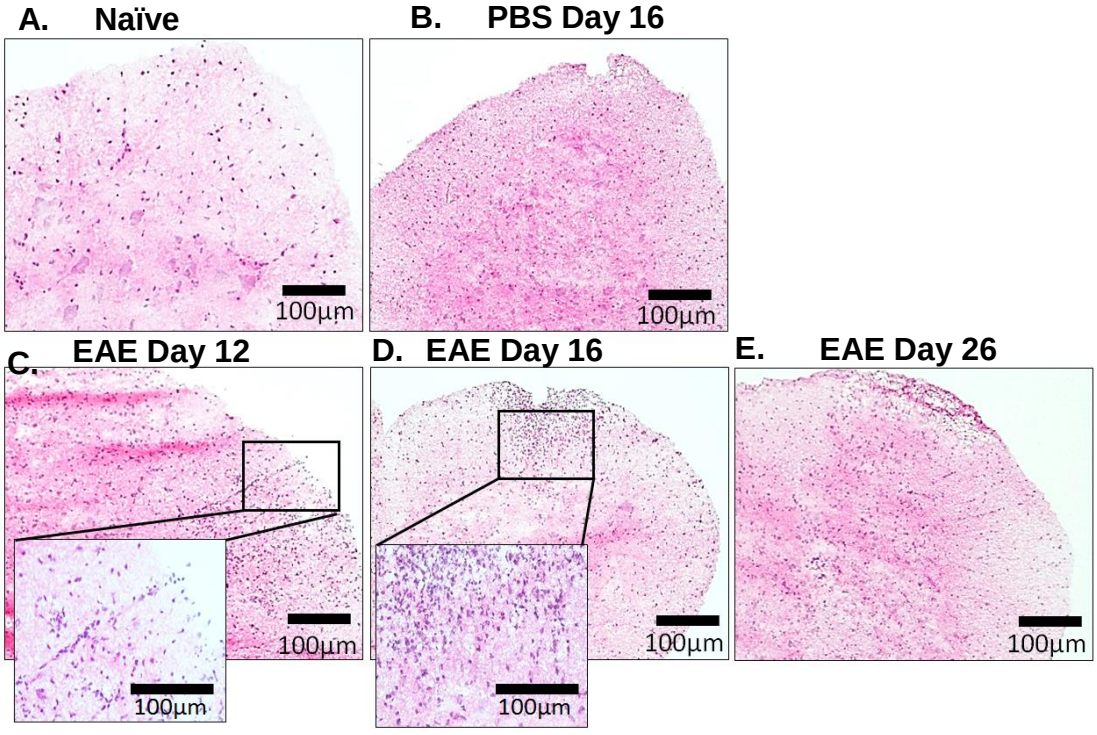

Figure 3.4: Cellular infiltration observed in the spinal cord of EAE mice. *Spinal cord sections were stained with H&E to show the extent of inflammation and cellular infiltration in* ***(A)*** *naïve mice,* ***(B)*** *PBS mice at day 16 post immunisation and* MOG_{35-55} *mice at* ***(C)*** *day 12,* ***(D)*** *day 16, and* ***(E)*** *day 26. n=3 for all groups. Primary images X10 magnification, scale bars = 100µm; Secondary images X20 magnification, scale bars = 100µm.*

As observed with spinal cord tissues, signs of cellular infiltration were also absent within the brain tissues of naïve (Figure 3.5A) and PBS day 16 mice (Figure 3.5B). The brain tissues collected from MOG_{35-55} immunised mice (Figure 3.5 C-D) demonstrated similar levels of cellular infiltration as seen in the spinal cord of the mice. Cell infiltration was observed mostly within the cerebellum of day 16 EAE mice, particularly in WM.

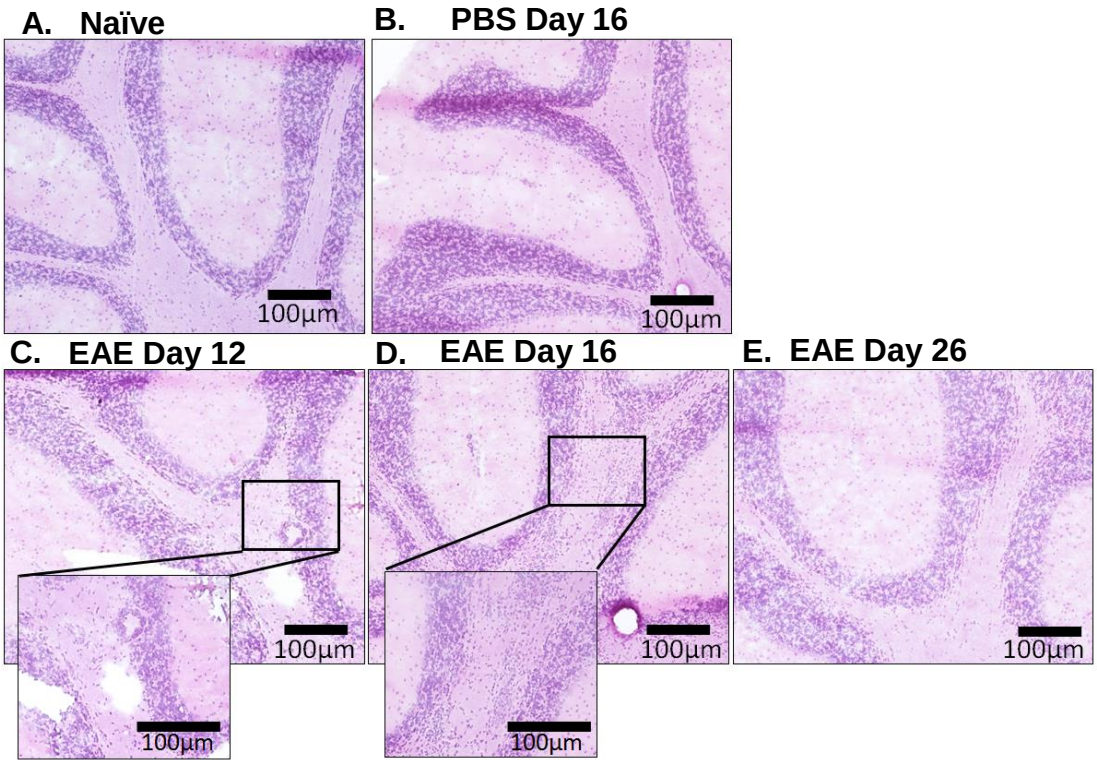

Figure 3.5: Cellular infiltration observed in the brain of EAE mice. *Brain sections were stained with H&E to show the extent of inflammation and cellular infiltration in* ***(A)*** *naïve,* ***(B)*** *PBS mice at day 16 post immunisation and* MOG_{35-55} *immunised mice at* ***(C)*** *day 12,* ***(D)*** *day 16, and* ***(E)*** *day 26 post immunisation. n=3 for all groups. Primary images X10 magnification, scale bars = 100µm; Secondary images X20 magnification, scale bars = 100µm.*

3.2.3 Immune cell infiltration in the CNS of EAE mice

To further examine the extent of inflammation and immune cell infiltration in the CNS over the course of EAE, tissue sections were stained with anti-CD45 (a marker for immune cells) using IHC. CD45 is known to be expressed on almost all hematopoietic cells and is positive for microglial cells in the CNS. However, the CD45 antibody used in our lab has always showed to have specificity for only hematopoietic cell and was never tested positive for microglia cells in the CNS of naïve and PBS mice, thus we commonly use this as a marker for infiltrating immune cell to check the extent of inflammation in the CNS of EAE mice. As expected, no evidence of $CD45^+$ cells and inflammation were observed in the CNS of naïve (Figure 3.6B; 3.7B; 3.8B) and PBS day 16 mice (Figure 3.6C; 3.7C; 3.8C). An isotype control was also included to determine the specificity of the CD45 antibody and that also produced a negative result (Figure 3.6A; 3.7A; 3.8A).

In the spinal cord of MOG_{35-55} immunised mice, expression of CD45 was evident at day 12 of EAE predominantly within the WM as clusters of cells forming the inflammatory lesions, which further increased when the clinical symptoms reached its peak at day 16 (Figure 3.6E). As the disease started to resolve, the expression of CD45 was decreased at day 26 (Figure 3.6F). We next quantified the number of $CD45^+$ cells in relation to total cell number within the comparable ROI in the spinal cord tissue sections at different EAE time points (Figure 3.6G). The data revealed $CD45^+$ cells accounted for 59 ± 2% of total cells in spinal cord of EAE mice at day 12, which increased to 67± 2% at day 16 during the EAE peak stage and then reduced to 22 ± 1% at EAE resolution at day 26, with both EAE day 12 and day 16 significantly higher than EAE day 26.

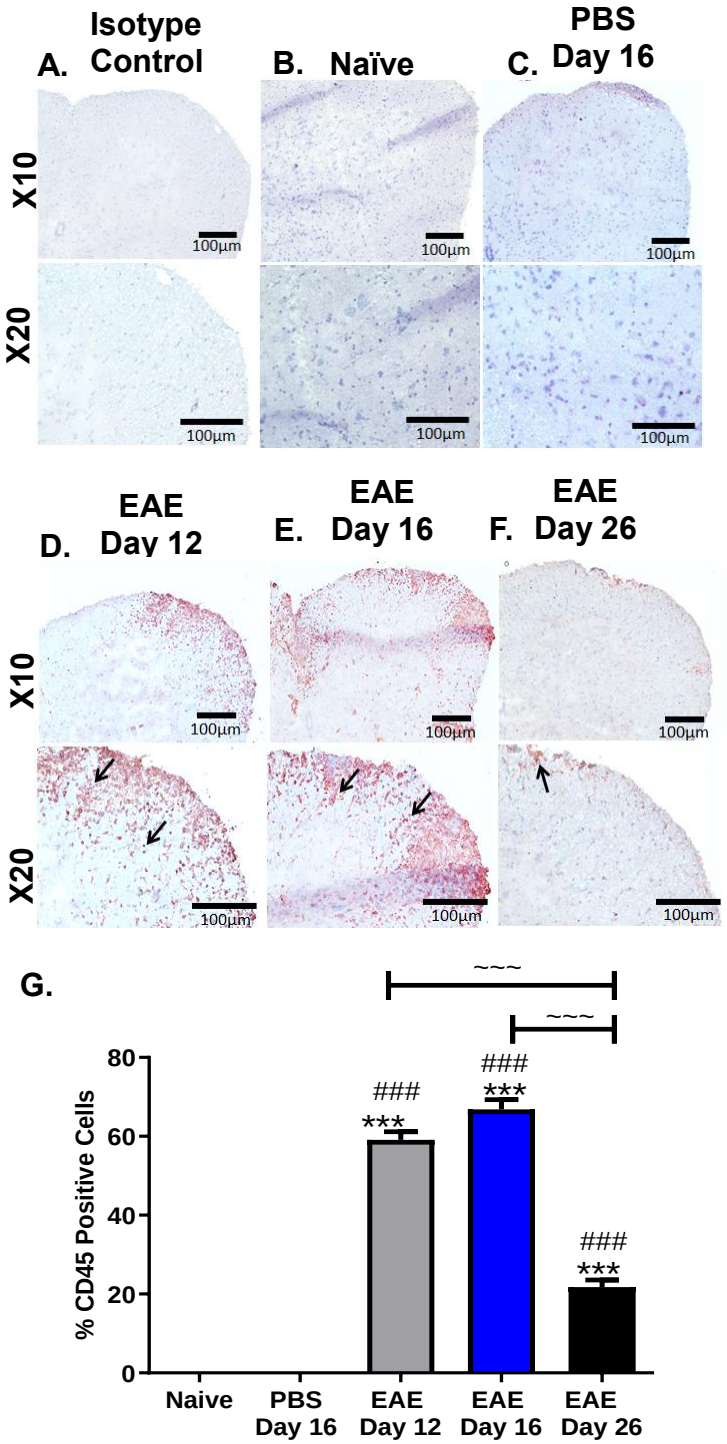

Figure 3.6: Immune cell infiltration in the spinal cord of EAE mice. *Spinal cords harvested from* ***(B)*** *naïve, and* ***(C)*** *PBS, or* ***(A, D-F)*** *MOG_{35-55} immunised mice were stained with isotype control or anti-CD45 (Amec Red) and counterstained with haematoxylin (blue). Arrows indicate infiltration of immune cells. Data are representative of each group. n=3 for all groups. Images X20 magnification, scale bars = 100µm.* ***(G)*** *Percentage of infiltrating CD45 positive cells in spinal cord tissues of control and different stages of EAE mice has been quantified using the cell counter tool of Image J software and result expressed as mean ± S.E.M. Statistical significance was determined by one-way ANOVA with Bonferroni post-hoc. Significance determined by post hoc test. ***P<0.001 versus naïve, $^{###}$P<0.001 versus PBS day 16, $^{~~~}$P<0.001 versus EAE day 26.*

Following the examination of CD45 expression on spinal cord sections, sagitally processed brain sections were next checked for CD45 expression. As observed with the spinal cord tissue, no signs of $CD45^+$ cells or inflammation were present within the brain regions of naïve and PBS day 16 mice (Figure 3.7B & C and 3.8B & C). In EAE mice, CD45 expression was assessed mainly within two regions of brain: the hippocampus (Figure 3.7) and the cerebellum (Figure 3.8). In the hippocampus, $CD45^+$ cells were observed in all stages of EAE mice (Figure 3.7D, E &F). Quantification of the number of $CD45^+$ cells in relation to total cell number within the comparable ROI in the hippocampus of EAE mice (Figure 3.7G) revealed that $CD45^+$ cells accounted for 44 ± 2% of total cells at day 12 post immunisation, which was increased to 61 ± 1 % at day 16, before falling back to 16 ± 1% at day 26. The quantification also confirmed that both EAE day 12 and day 16 had significantly higher percentage of $CD45^+$ in comparison to EAE day 26. In the cerebellum of EAE mice (Figure 3.8G) quantification of the number of $CD45^+$ cells in relation to total cell number within the comparable ROI in the cerebellum at different EAE time points demonstrated, $CD45^+$ cells accounted for 58 ± 2% of total cells at day 12 which increased to 66 ± 2 % at EAE day 16 before dropping back to 23 ± 3% at day 26.The quantification also revealed both EAE day 12 and day 16 had significantly higher percentage of $CD45^+$ in comparison to EAE day 26.

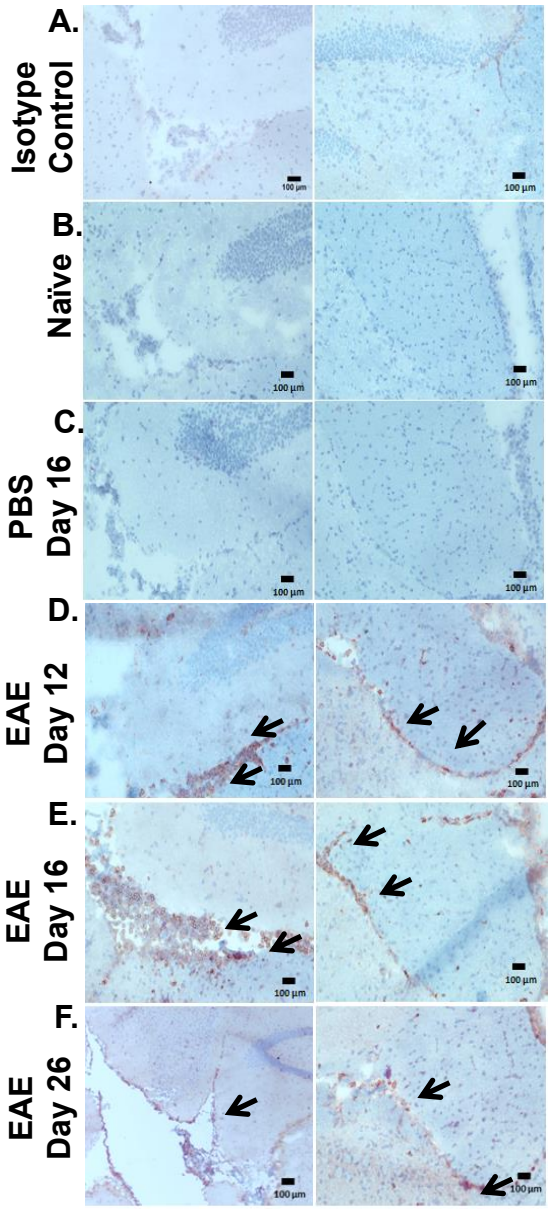
A.
Isotype Control
B.
Naïve
C.
PBS Day 16
D.
EAE Day 12
E.
EAE Day 16
F.
EAE Day 26
100 µm

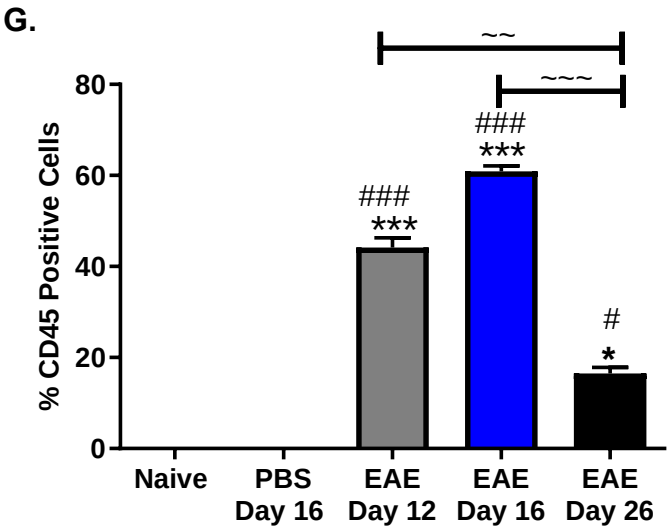

Figure 3.7: Immune cell infiltration in the hippocampus of EAE mice*. Brains harvested from* ***(B)*** *naïve, and* ***(C)*** *PBS, or* ***(A, D-F)*** *MOG_{35-55} immunised mice were stained with isotype control or anti-CD45 (Amec Red) and counterstained with haematoxylin (blue). Arrows indicate infiltration of immune cells. Data are representative of each group. n=3 for all groups. Images X20 magnification, scale bars = 100µm.* ***(G)*** *Percentage of infiltrating CD45 positive cell at each stage of EAE has been quantified using the cell counter tool of Image J software and result expressed as mean ± S.E.M. Significance determined by one-way ANOVA with Bonferroni post hoc test. *P<0.05, ***P<0.001 versus naïve, $^{\#}$P<0.05, $^{\#\#\#}$P<0.001 versus PBS day 16, $^{\sim\sim}$P<0.01, $^{\sim\sim\sim}$P<0.001 versus EAE day 26.*

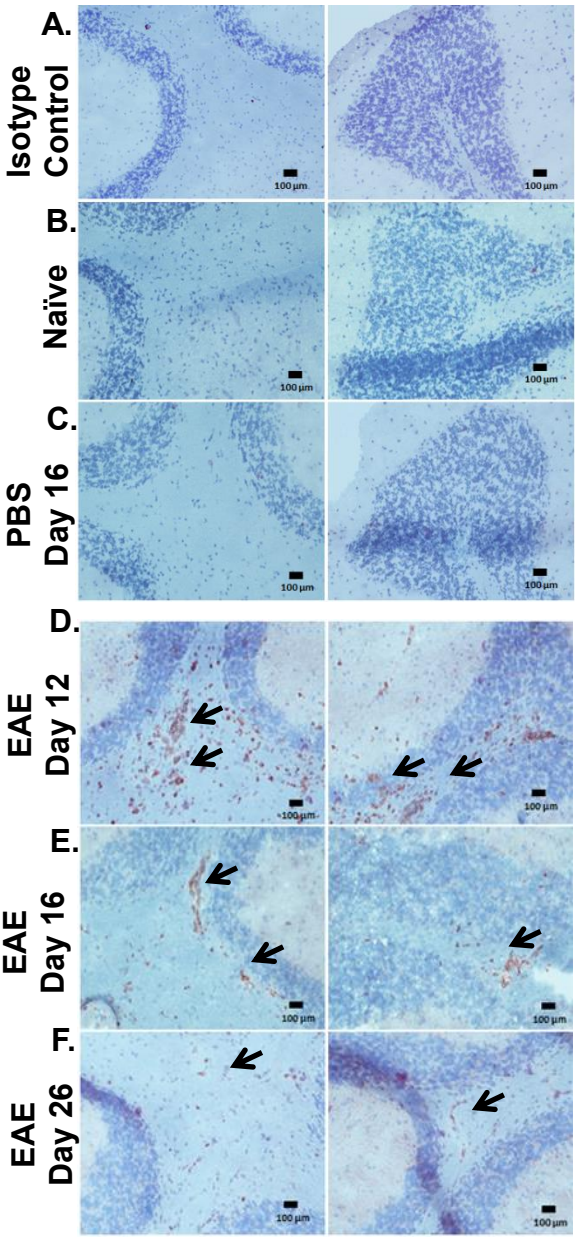
A.
Isotype Control
B.
Naïve
C.
PBS Day 16
D.
EAE Day 12
E.
EAE Day 16
F.
EAE Day 26
100 µm

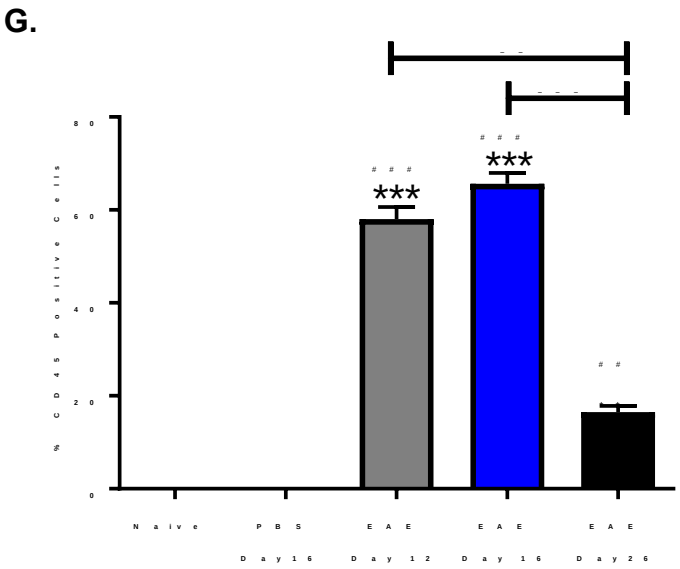

Figure 3.8: Immune cell infiltration in the cerebellum of EAE mice. *Brains harvested from* ***(B)*** *naïve, and* ***(C)*** *PBS, or* ***(A, D-E)*** *MOG_{35-55} immunised mice were stained with isotype control or anti-CD45 (Amec Red) and counterstained with haematoxylin (blue). Arrows indicate infiltration of immune cells. Data are representative of each group. n=3 for all groups. Images X20 magnification, scale bars = 100µm.* ***(G)*** *Percentage of infiltrating CD45 positive cell at each stage of EAE has been quantified using the cell counter tool of Image J software and result expressed as mean ± S.E.M. Significance determined by one-way ANOVA with Bonferroni post hoc test. **P <0.01, ***P<0.001 versus naïve, $^{\#\#}$P <0.01, $^{\#\#\#}$P<0.001 versus PBS day 16, $^{\sim\sim}$P<0.01, $^{\sim\sim\sim}$P<0.001 versus EAE day 26.*

3.2.4 Identification of immune cell phenotype in the peripheral lymphoid organs of EAE and control mice

To investigate the correlated systemic inflammatory response in EAE mice, splenocytes were collected from the naïve, and PBS or MOG_{35-55} immunised mice at day 16 post immunisation and analysed using FACS.

First, we examined the $CD4^+$ and $CD8^+$ T cells (Figure 3.9A and B) and our data showed that the percentages of $CD4^+$ and $CD8^+$ T cells out of total splenocyte population in naïve, PBS and EAE mice were similar. However, the percentage of $CD4^+$ T cells co-expressing CD25, a marker for activated T cells, was significantly elevated in the spleen of both PBS (1.30 ± 0.02%) and EAE (1.24 ± 0.05%) mice compared to the naïve control (0.90 ± 0.04%) (Figure 3.9A). Similarly, significantly increased levels of $CD8^+CD25^+$ cells were also observed in EAE mice (2.13 ± 0.11%) in comparison to naïve control mice (1.39 ± 0.06%) but no difference was observed between the PBS (2.50 ± 0.65%) and EAE mice or PBS and naïve mice (Figure 3.9B).

B cells were also examined and no difference in the percentage of B cells were identified, as cells expressing both CD19 (B lymphocyte antigen) and B220 (antigen which is expressed on B lymphocytes throughout their development), in naïve (44.7 ± 1.05% of total cells), PBS day 16 (37.37 ± 2.28% of total cells) or EAE day 16 (36.46 ± 1.95% of total cells) mice groups (Figure 3.9E).

Following this, the percentage of DCs and their activation status were also evaluated (Figure 3.9C). $CD11c^+$ cells were significantly elevated in EAE mice (1.27 ± 0.05%) in comparison to naïve (0.79 ± 0.03%) and PBS (0.90 ± 0.10%) controls. However, the percentage of $CD11c^+$ cells also expressing CD40 (a co-stimulatory molecule found on APCs required for their activation) was found to be significantly elevated in EAE mice (1.96 ± 0.12%) in contrast to the naïve controls (1.37 ± 0.08%) (Figure 3.9C). However, no difference was observed between the EAE and the PBS (1.98 ± 0.32%) mice. $CD11c^+$MHC-II^+ cells were also examined; the percentage of these cells were significantly increased in both EAE (3.43 ± 0.18%) and PBS (3.28 ± 0.30%) mice in comparison to the naïve controls (2.41 ± 0.16%). Interestingly, the percentage of MHC-II^+ DCs remained similar in all three groups (Figure 3.9D).

Thus, the data above suggested an active immune response in the periphery of both PBS and EAE mice compared to the naïve controls, this was also indicated by the

increased size of the inguinal lymph nodes, which is the closest lymph node for drainage of immunisation from the injection site at the lower back of the PBS and EAE mice (Figure 3.8F).

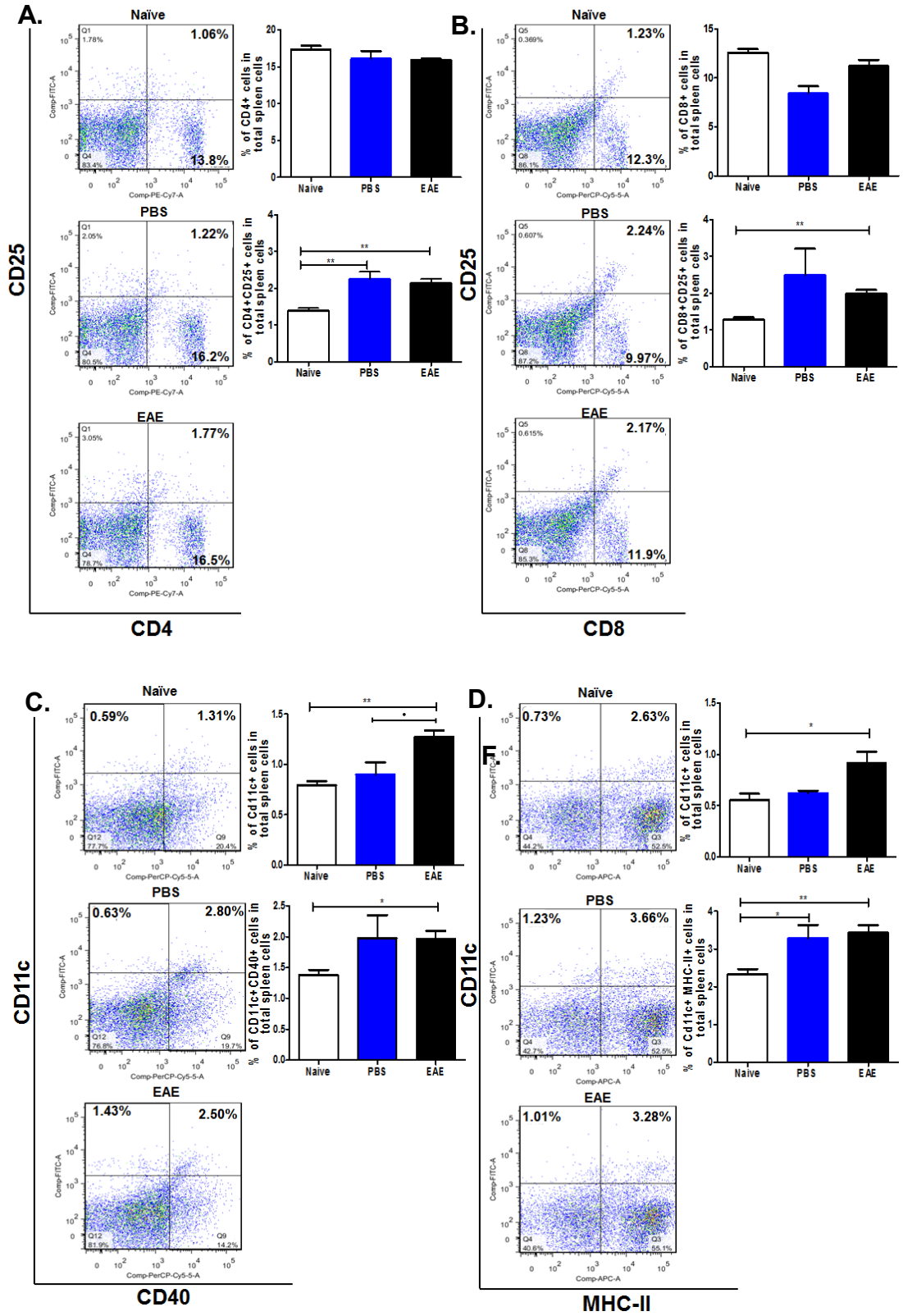

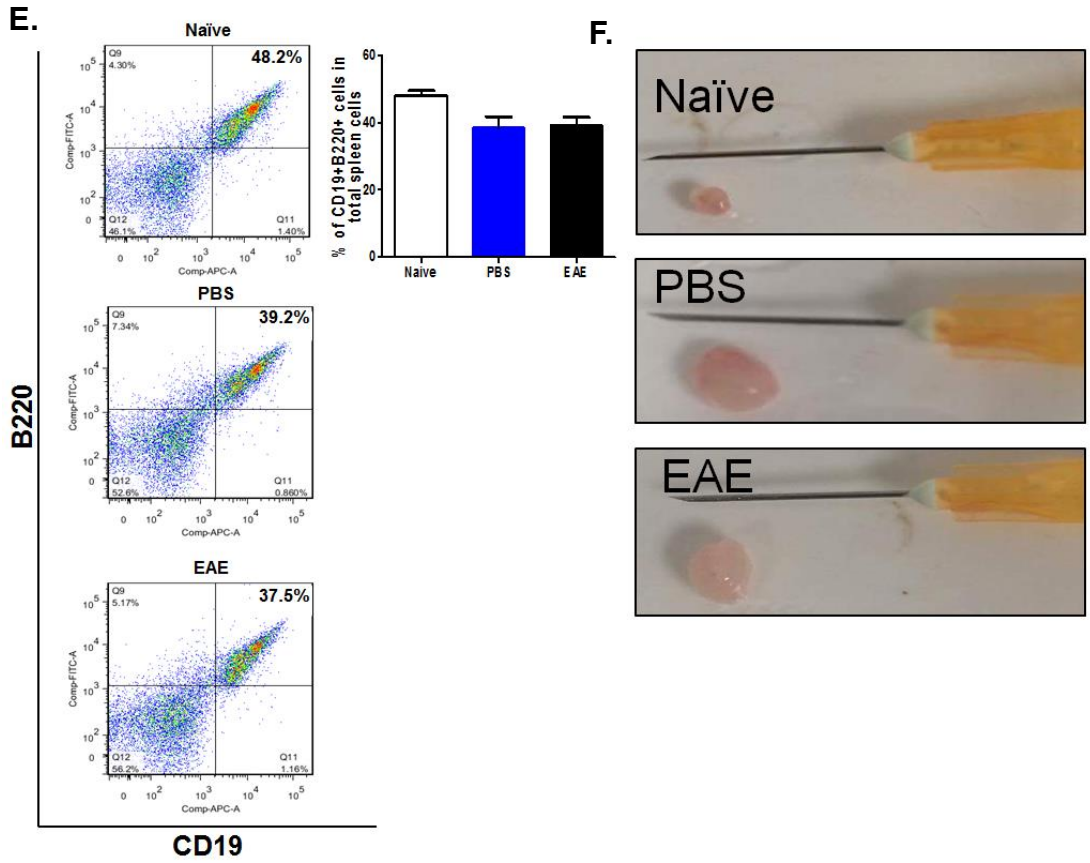

Figure 3.9: Phenotype of immune cells in the spleen of naïve, PBS and EAE mice. *Spleen cells collected from naïve, and PBS or MOG_{35-55} immunised mice at day 16 post immunisation was stained for FACS analysis of* ***(A)****CD4 and CD25,* ***(B)*** *CD8 and CD25,* ***(C)*** *CD11c and CD40 or* ***(D)*** *CD11c and MHC-II,* ***(E)*** *B220 and CD19.* ***(F)*** *Representative images of inguinal lymph nodes from naïve, PBS peak and EAE peak mice. Data are representative of each group, naïve n=4, PBS n=4 and EAE n=6. Result presented as mean ± S.E.M. Statistical significance was determined by one-way ANOVA with Bonferroni post hoc test *P<0.05, **P <0.01 versus naïve and PBS day 16. n=number of animals.*

3.2.5 Antigen-specific cytokine production by EAE splenocytes

After showing the activation of immune cells in the spleen of both PBS and MOG_{35-55} immunised mice, we then examined the MOG_{35-55} specific cytokine production from splenocytes obtained from naïve and PBS or MOG_{35-55} immunised mice at day 12, day 16 and day 26 post immunisation. Splenocytes from all groups of mice were cultured for 72 hrs with media alone or media supplemented with MOG_{35-55} (50µg/ml) and the supernatants were analysed by ELISA for expression of cytokines including IFN-γ, IL-17, IL-6 and IL-10, which are known to be important in EAE pathogenesis. Spleen cells from naïve and PBS mice when treated with either media alone or media supplemented with MOG_{35-55} showed no or very low levels of any of the examined cytokines at any time points. Spleen cells from EAE mice, when treated with media alone showed no production of any of the examined cytokines except IFN-γ at day 12. However, the levels of all the cytokines were significantly increased in the supernatant of cells stimulated with MOG_{35-55}.

Spleen cells from EAE mice cultured with media alone produced 549 ± 245 pg/ml of IFN-γ at day 12 post immunisation (Figure 3.10A). Upon MOG_{35-55} stimulation spleen cells in the culture, showed increased IFN-γ production, with 1479 ± 24 pg/ml at day 12 post immunisation, which reduced to 659 ± 43 pg/ml and 419 ± 116 pg/ml. at day 16 and day 26 (Figure 3.10A). Spleen cells from onset EAE mice at day 12 post immunisation produced 386 ± 39 pg/ml of IL-17 when re-stimulated with $MOG_{35-55,}$ which significantly increased to 584 ± 39 pg/ml as mice exhibited peak clinical symptoms at day 16 before decreasing to 284 ± 28 pg/ml during the resolution stage of EAE at day 26 (Figure 3.10B). Similarly, IL-6 production was only detected in EAE spleen culture following MOG_{35-55} stimulation, with 248 ± 19 pg/ml of IL-6 at day 12 which was significantly increased to 395 ± 42 pg/ml at day 16 before dramatically decreasing to 115 ± 25 pg/ml at day 26 (Figure 3.10C).

While highest levels of antigen specific IFN-γ, IL-17 and IL-6 production was observed in splenocytes from onset and peak EAE mice, IL-10 production by MOG_{35-55} stimulated splenocytes were lowest at 1147 ± 39 pg/ml during the onset of EAE, but the level gradually increased to 1427 ± 37pg/ml during EAE peak at day 16 before reaching the significantly highest level of 2191 ± 208pg/ml at day 26 during the EAE resolution stage (Figure 3.10D).

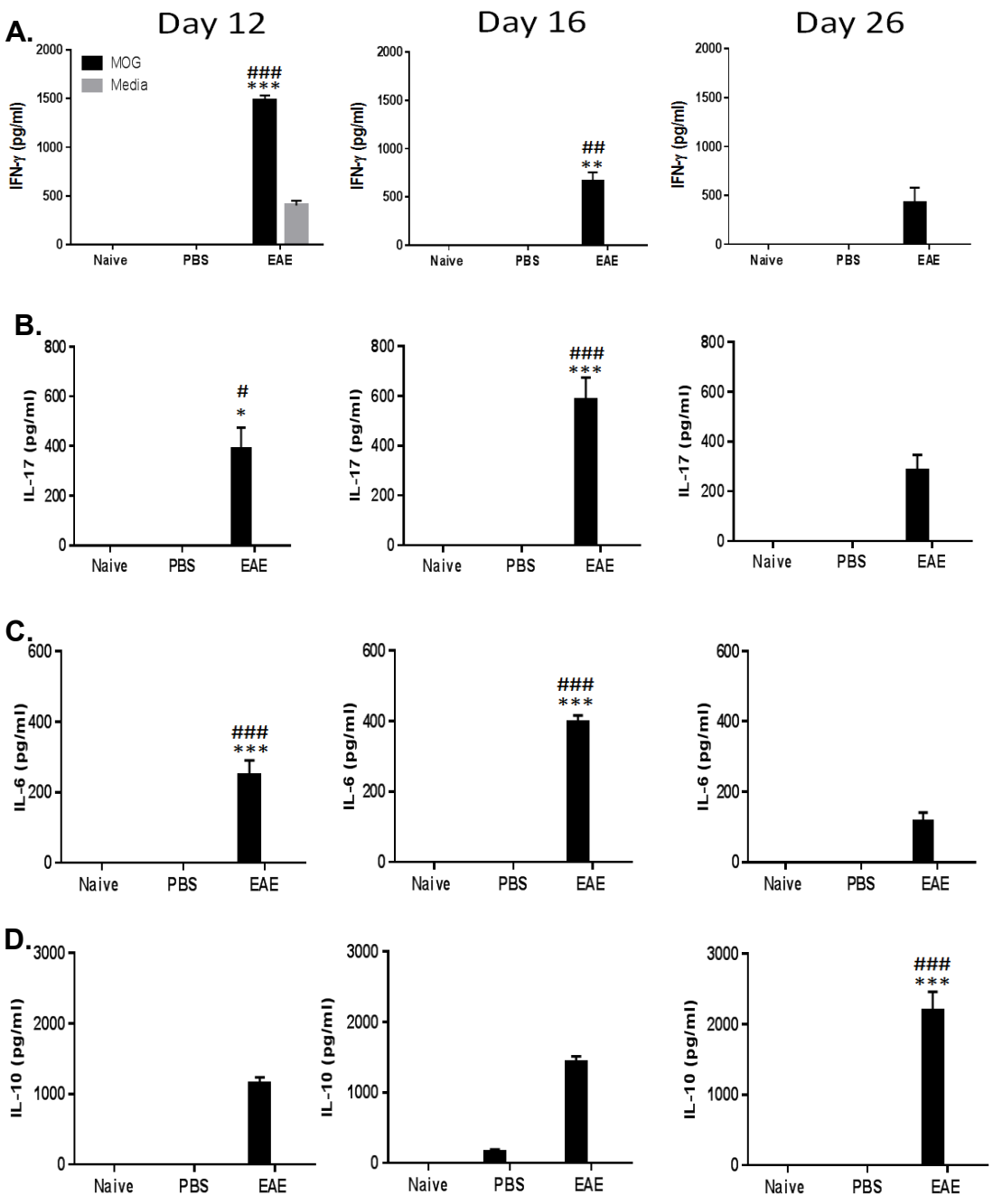

Figure 3.10: MOG_{35-55} induced cytokine production by EAE spleen cells. *Spleen cell suspensions prepared from naïve, and PBS or MOG_{35-55} immunised mice were incubated either with RPMI alone or RMPI containing MOG_{35-55} (50 µg/ml). Supernatants were collected after 72 hours and were checked for **(A)** IFN-γ, **(B)** IL-17, **(C)** IL-6 and **(D)** IL-10 levels by ELISA. Naïve=3, PBS n=4, EAE n=5. Result illustrated as mean ± S.E.M. Statistical significance was determined by two-way repeated measures ANOVA with Bonferroni post-hoc test *P<0.05, **P <0.01 ***P<0.001 versus EAE peak; #P<0.05, ##P <0.01, ###P<0.001 versus EAE resolution. n=number of animals.*

3.2.6 IL-16 production by spleen/lymph node cells

We have established that spleen cells from EAE mice produce high levels of antigen specific IFN-γ, IL-17, IL-6 and IL-10, confirming the dynamic immune responses during EAE development. Next, we focused on investigating the production of IL-16 by spleen and inguinal lymph node cells from naïve, PBS and MOG_{35-55} immunised mice. Since we did not know how long the cells needed to be re-challenged with MOG_{35-55} to produce the detectable levels of IL-16, all cells were cultured for 24 and 72 hrs with media alone or media supplemented with MOG_{33-55} (50µg/ml).

Our data showed that spleen cells from naïve, PBS and MOG_{35-55} immunised mice demonstrated consistent high levels of IL-16 in all three groups and throughout EAE disease course with or without MOG_{35-55} in the culture (Figure 3.11 and 3.12). Cells were also stimulated with conA as a positive control to ensure cells were functional and cytokine production could be determined, again the data showed no significant difference in IL-16 production in comparison to MOG_{35-55} treated or untreated cells. Splenocytes re-challenged to MOG_{35-55} for 72 hrs (Figure 3.11B) demonstrated slightly higher levels of IL-16 in comparison to the 24 hrs re-stimulation (Figure 3.11A); however, there wasn't a significant difference.

After 24 hours in culture, splenocytes from naïve mice and PBS immunised mice at day 16 post immunisation when cultured with media alone produced 426 ± 43 pg/ml and 552 ± 64 pg/ml of IL-16 (Figure 3.11A) and produced 221 ± 41 pg/ml and 306 ± 33 pg/ml of IL-16 respectively upon MOG_{35-55} re-challenge. Spleen cells from EAE mice cultured with media alone produced 363 ± 45 pg/ml of IL-16 at day 12, and 500 ± 24 pg/ml at day 16 which reduced to 138 ± 24 pg/ml at day 26. Upon MOG_{35-55} stimulation, the levels of IL-16 produced by splenocytes were 294 ± 59 pg/ml, 271 ± 28 pg/ml and 110 ± 28 pg/ml respectively at day 12, day 16 and day 26 of EAE disease course. After 72 hours in culture, spleen cells from naïve and PBS day 16 mice produced 227 ± 30 pg/ml and 346 ± 25 pg/ml of IL-16 respectively when re-stimulated with MOG_{35-55} and 196 ± 48 pg/ml, 350 ± 34 pg/ml without any treatment (Figure 3.11B). Splenocytes from EAE mice cultured with media alone produced 741 ± 43 pg/ml of IL-16 at day 12, which decreased to 378 ± 44 pg/ml at day 16

before reaching 308 ± 67 pg/ml at day 26. Upon MOG_{35-55} re-challenge the levels of IL-16 produced by splenocytes were 599 ± 21 pg/ml at day 12 and further reduced to 329 ± 51 pg/ml at day 16 before reaching 196 ± 50 pg/ml at day 26.

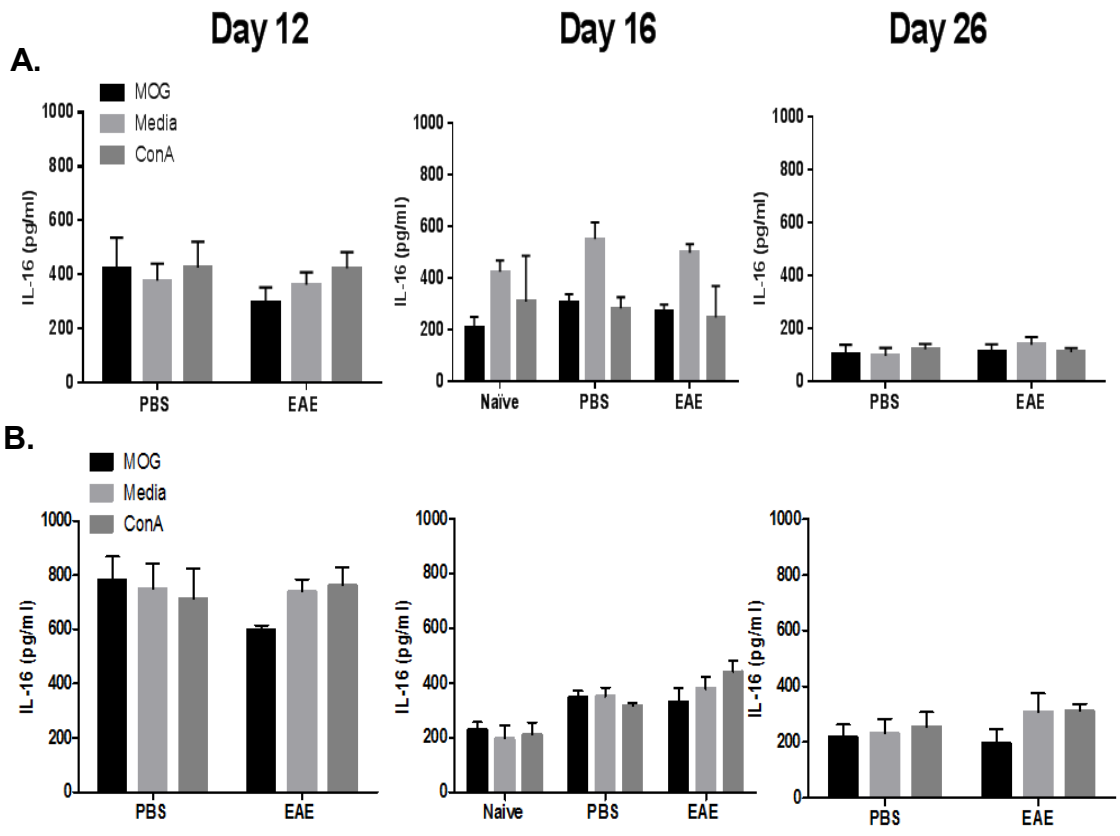

Figure 3.11: IL-16 production by spleen cells of naïve, PBS and EAE mice. *Spleen cell suspensions prepared from naïve, PBS and MOG_{35-55} immunised mice were incubated either with RPMI alone or RPMI containing MOG_{35-55} (50 µg/ml). Supernatants were collected after* ***(A)*** *24 and* ***(B)*** *72 hours of culture and used to detect IL-16 production by ELISA. Naïve=3, PBS n=4, EAE onset/peak/resolution, n=6 in each stage. Results illustrated as mean ± S.E.M. Statistical significance was determined by one-way ANOVA with Bonferroni post hoc test.*

Lymph node cells from naïve, PBS and MOG_{35-55} immunised mice were also cultured for 24 and 72 hrs with or without MOG_{35-55} stimulation and supernatants were harvested for IL-16 level analysis. At day 26 no IL-16 was detected in lymph node cells obtained from PBS or EAE mice culture in media alone or even after MOG_{35-55} re-challenge, and therefore data were not included in the figure. After 24 hrs culture with media alone, lymphocytes from EAE mice produced 306 ± 92 pg/ml of IL-16 at day 12 which further decreased to 134 ± 22 pg/ml at day 16 and eventually produced undetectable level of IL-16 at day 26. Upon MOG_{35-55} stimulation, the level of IL-16 produced by lymphocytes was 150 ± 13 pg/ml and 93 ± 42 pg/ml at day 12 and day 16 respectively.

Lymphocytes collected from naïve and PBS day 16 showed 71 ± 30 and 109 ± 16 pg/ml IL-16 productions respectively when re-challenged with MOG_{35-55} for 24 hours, whereas cells with media alone produced 46 ± 16 pg/ml and 195 ± 52 pg/ml of IL-16 respectively (Figure 3.12A). The data thus demonstrated similar findings from the spleen cells that IL-16 was constitutively produced by lymph node cells, and there was no significant difference between any of the groups.

After 72 hours in culture, naïve lymphocytes demonstrated 222 ± 28 pg/ml of IL-16 productions when stimulated with MOG_{35-55} but 159 ± 20 pg/ml of IL-16 with media only. Cells from PBS immunised mice at day 16 post immunisation produced 341 ± 28 pg/ml of IL-16 when cultured with media alone which was decreased to 296 ± 23 pg/ml with MOG_{35-55} stimulation. In EAE mice, lymphocytes cultured with media alone produced 308 ± 166 pg/ml of IL-16 at day 12 and at day 16. After re-stimulation with MOG_{35-55}, 256 ± 170 pg/ml and 322 ± 78 pg/ml of IL-16 were observed at day 12 and at day 16 respectively.

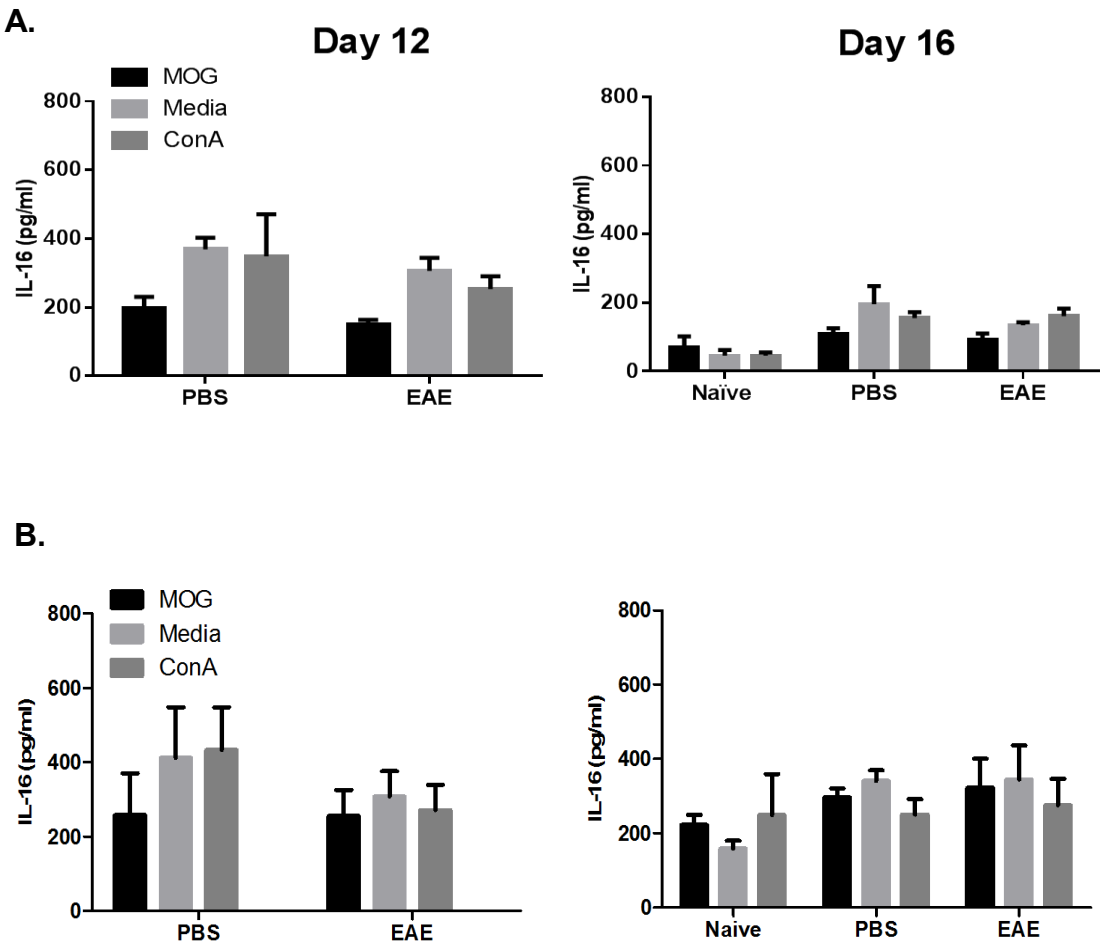

Figure 3.12: IL-16 production by lymph node cells of naïve, PBS and EAE mice. *Lymph node cell suspensions prepared from naïve, PBS and MOG_{35-55} immunised mice were incubated either with RPMI alone or RMPI containing MOG_{35-55}(50 µg/ml). Supernatant were checked for IL-16 production after* ***(A)*** *24 and* ***(B)*** *72hours by ELISA. All samples are analysed in triplicate; Naïve=3, PBS n=4, EAE n=6. Result illustrated as mean ± S.E.M. Statistical significance was determined by one-way ANOVA with Bonferroni post hoc test.*

3.2.7 Expression of IL-16 in spleen and lymph node tissues of EAE and control mice

We have shown that spleen and lymph node cells spontaneously produced considerate level of IL-16 under normal and inflammatory condition and MOG_{35-55} stimulation in culture had no effect on this production. We next carried out immunohistochemical staining to examine the expression and distribution of IL-16 in spleen (Figure 3.13) and lymph node (Figure 3.14) tissue under normal and inflammatory condition and to investigate whether expression levels correlate with inflammation. Expression levels in EAE mice at day 12, 16 and 26 were compared with control tissues of naïve and PBS mice at day 16 post immunisation. As previously we did not observe any difference in CNS infiltration or MS/EAE specific peripheral cytokine production in PBS mice at day 12, 16 and 26 post immunisations, so we decided to only assess PBS mice at day16 post immunisation. We chose day 16 post immunisation as at this time point EAE mice demonstrated the highest CNS infiltration and production of MS/EAE specific peripheral cytokine.

While isotype control antibody had no positive staining (Figure 3.13A), IL-16 expression was observed in the tissues harvested from naïve, PBS and EAE mice at all stages (Figure 3.13B-F). We next quantified the percentage of IL-16^+ cells out of the total cells within the comparable ROI in the tissue sections. In the spleen of PBS (15 ± 2%), EAE day 12 (15 ± 1%) and EAE day 16 (19 ± 1%) mice the percentage of IL-16^+ cells were significantly higher compared to that of the naïve (7 ± 0.3%) tissues. However, there were no differences between the percentages of IL-16^+ cells expressed in PBS and MOG_{35-55} immunised mice at any time point and also no difference in EAE mice between day 12, day 16 or day 26 (14 ± 0.1%) as confirmed by quantitative analysis using the Image J (Figure 3.13G).

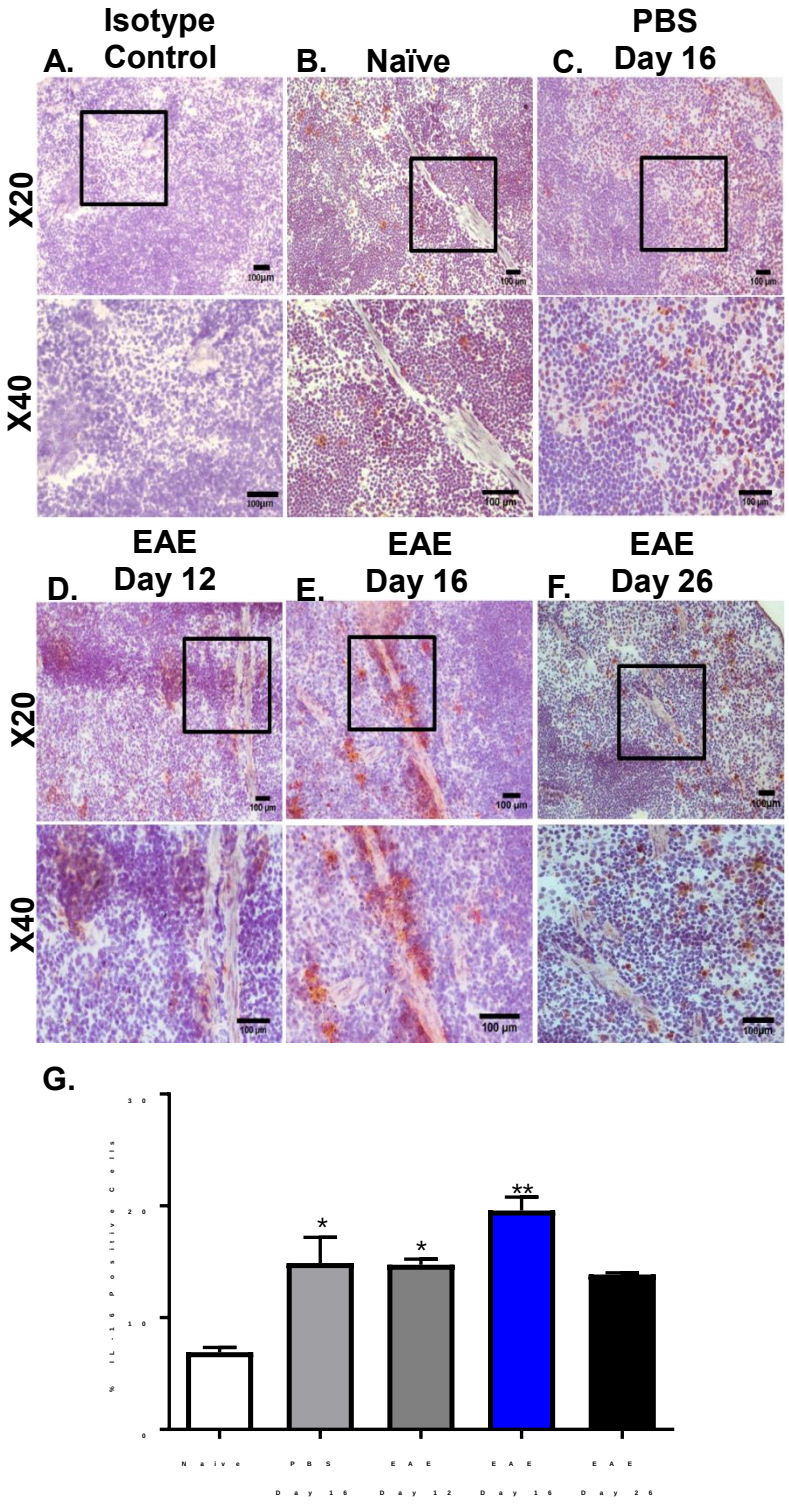

Figure 3.13: IL-16 expression in spleen tissues of naïve, PBS and EAE mice*. Spleens harvested from* ***(A and B)*** *naïve,* ***(C)*** *PBS and* ***(D-F)*** *MOG_{35-55} immunised mice were stained with isotype control or anti-IL-16 (Red) and counterstained with haematoxylin (blue). Data are representative of each group. n=3 for all groups. Primary images X20 magnification, scale bars = 100µm; Secondary images X40 magnification, scale bars = 100µm.* ***(G)*** *Percentage IL-16 positive cells out of the total cells in the ROI in each group and at each stage of EAE has been quantified as previously described using the cell counter tool of Image J software and result expressed as mean ± S.E.M. Statistical significance was determined by one-way ANOVA with Bonferroni post hoc test *P<0.05, **P <0.01 versus naïve****.***

In lymph node tissues, IL-16 expression was also observed in naïve, PBS and EAE mice at all stages (Figure 3.14B-F). Analysis of percentage IL-16$^+$ cells within the comparable ROI revealed that lymph node tissues from EAE day 16 mice accounted for 25 ± 2% of IL-16$^+$ cells of the total cells which was significantly higher than the naïve lymph node tissues which was 15 ± 2%. However, there were no differences in percentage of IL-16$^+$ cells in tissues between naïve and PBS (17± 2%), or between any of the PBS, EAE day 12 (20 ± 1%), day 16 or day 26 mice (16 ± 1%) (Figure 3.14 G).

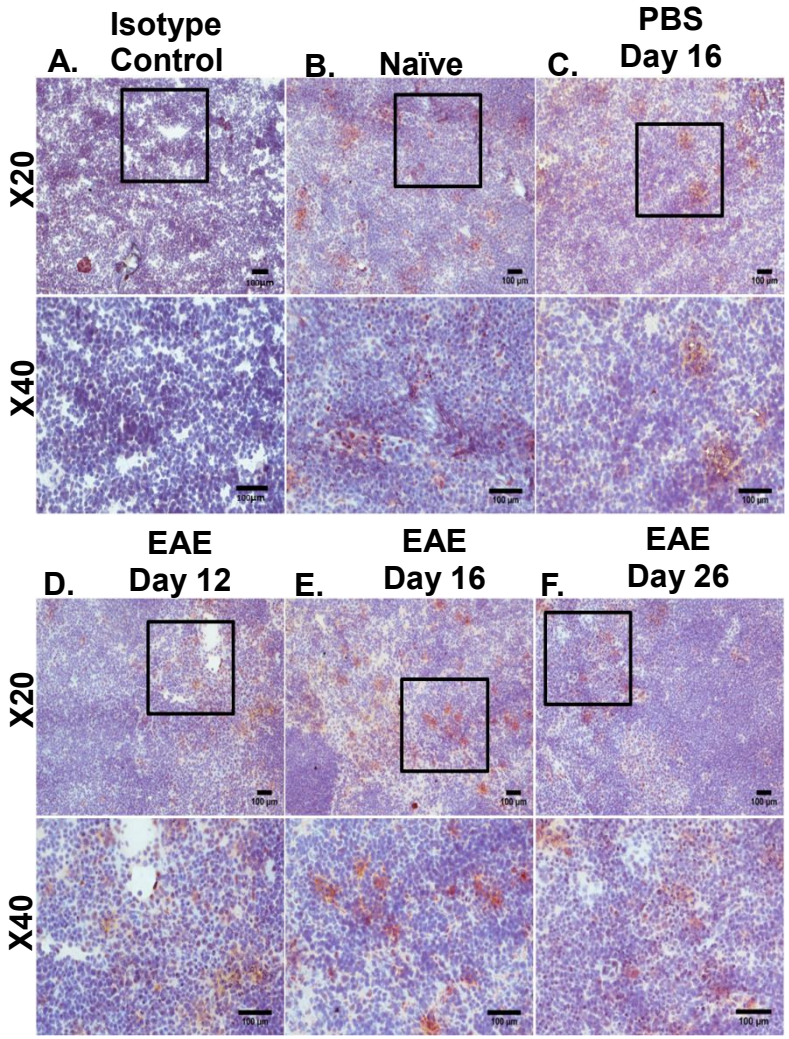

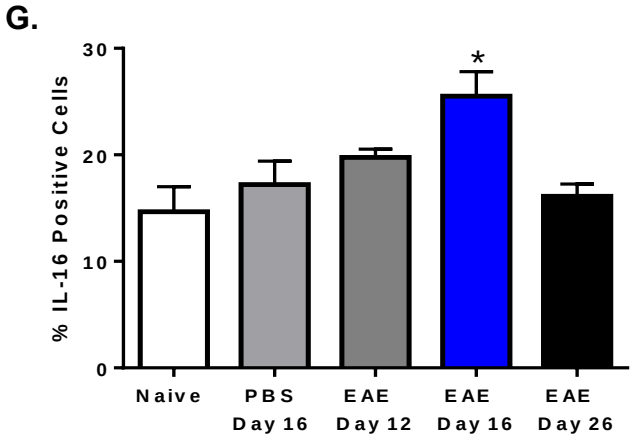

Figure 3.14: IL-16 expression in lymph node tissues of naïve PBS and EAE mice. *Lymph nodes were harvested from* ***(A and B)*** *naïve* ***(C)*** *PBS and* ***(D-F)*** *MOG_{35-55} immunised mice and were stained with isotype control or anti-IL-16 (Red) and counterstained with haematoxylin (blue). Data are representative of each group. n=3 for all groups. Primary images X20 magnification, scale bars = 100µm; Secondary images X40 magnification, scale bars = 100µm.* ***(G)*** *Percentage IL-16 positive cells out of the total cells in the ROI in each group and at each stage of EAE has been quantified as previously described using the cell counter tool of Image J software and result expressed as mean ± S.E.M. Statistical significance was determined by one-way ANOVA with Bonferroni post hoc test. Statistical significance was determined by one-way ANOVA with Bonferroni post hoc test. *P<0.05 versus naïve.*

3.2.8 Expression of CD4 in spleen and lymph node tissues of EAE and control mice

Since IL-16 is a ligand for the CD4 receptor, we next examined the expression and distribution of $CD4^+$ cells in the spleen (Figure 3.15) and lymph node (Figure 3.16) tissues under normal and inflammatory conditions.

As expected no positive expression was observed in the spleen and lymph node tissues with isotype control antibody (Figure 3.15), CD4 expression was observed in the spleen and lymph node tissues from naïve, PBS and EAE mice at different time point of the disease (Figure 3.15B-F). We next analysed the percentage $CD4^+$ cells out of the total cells within the comparable ROI in tissue sections. Percentage $CD4^+$ cells within the comparable ROI of spleen tissues from PBS day 16 (20 ± 1%), EAE day 12 (19 ± 0.5%) and EAE day 16 (24 ± 0.4%) mice were significantly higher in comparison to the naïve (12 ± 0.3%) spleen tissues. No differences in percentage $CD4^+$ cell was observed in the tissues from PBS day 16 or EAE day 12, EAE day 16 or EAE day 26 mice. However, percentage of $CD4^+$ cells in tissues from EAE day 26 (13 ± 0.3%) mice returned to the similar level as observed in naïve control (Figure 3.15G).

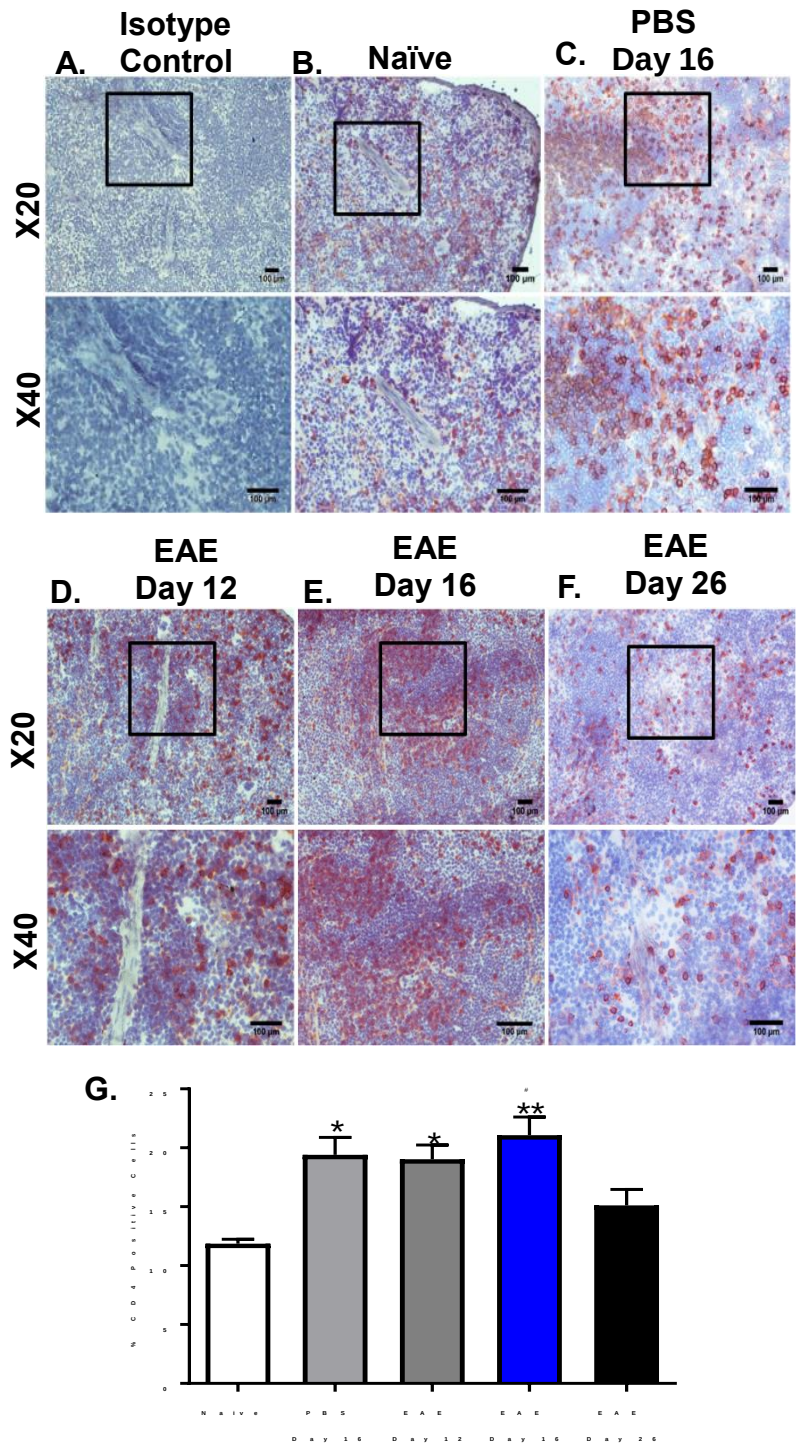

Figure 3.15: CD4 expression in spleen tissues of naïve, PBS and EAE mice*. Spleens harvested from* ***(A and B)*** *naïve* ***(C)*** *PBS and* ***(D-F)*** *MOG_{35-55} immunised mice and were stained with isotype control or anti-CD4 (Red) and counterstained with haematoxylin (blue). Data are representative of each group. n=3 for all groups. Primary images X20 magnification, scale bars = 100µm; Secondary images X40 magnification, scale bars = 100µm.* ***(G)*** *Percentage CD4 positive cells out of the total cells in the ROI in each group and at each stage of EAE has been quantified as previously described using the cell counter tool of Image J software and result expressed as mean ± S.E.M. Statistical significance was determined by one-way ANOVA with Bonferroni post hoc test Statistical significance was determined by one-way ANOVA with Bonferroni post hoc test *P<0.05, **P <0.01 versus Naïve, #P<0.05 versus PBS day 16.*

In lymph node tissues quantification of $CD4^+$ cells showed that EAE day 12 (25 ± 2%) and EAE day 16 (25 ± 3%) mice had significantly higher percentage of $CD4^+$ cells within the comparable ROI in comparison to the tissues collected from naïve (13 ± 1.3%) mice. Lymph nodes from EAE day 26 (24 ± 2%) mice did not show any statistical difference in percentage $CD4^+$ cells in comparison to the naïve and PBS day 16 (15 ± 0.5%) controls.

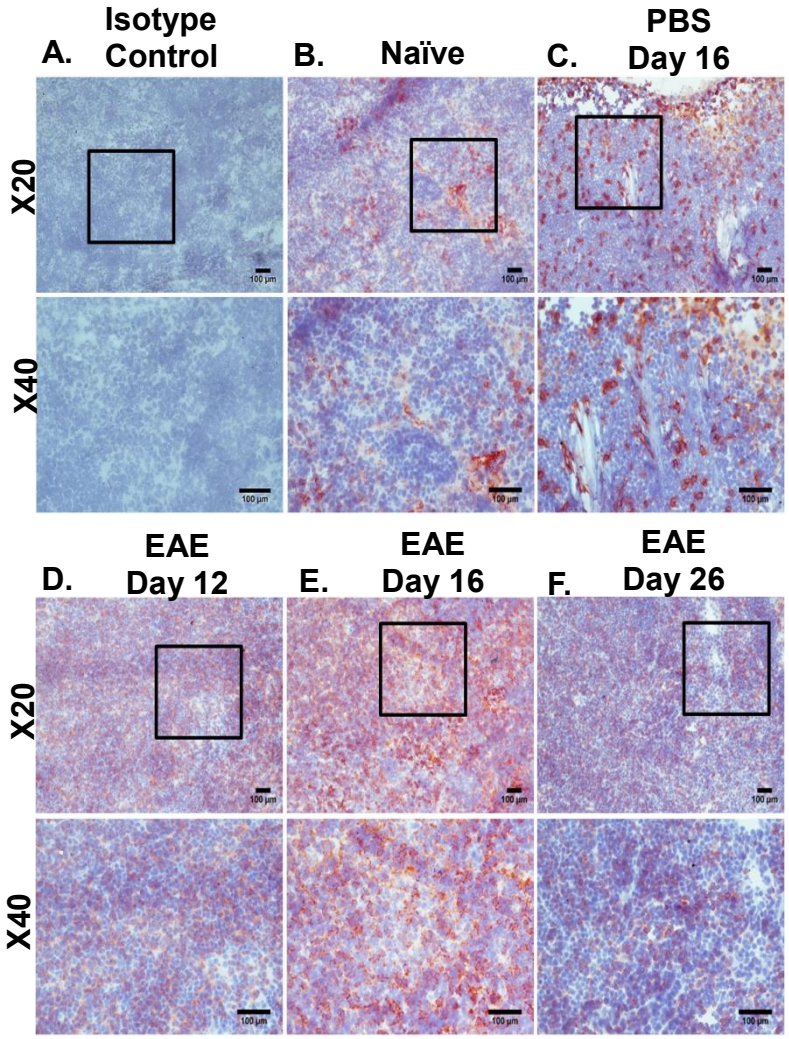

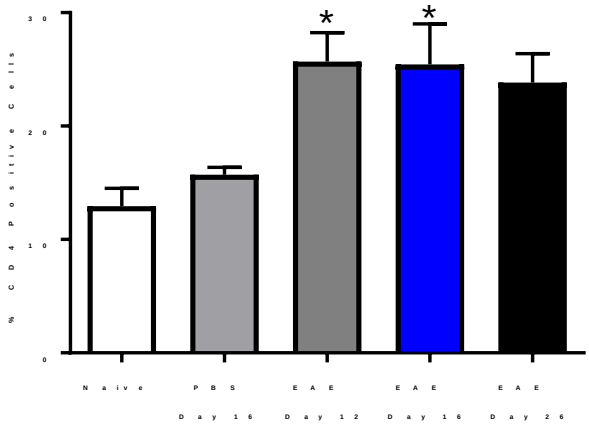

Figure 3.16: CD4 expression in lymph node tissues of naïve, PBS and EAE mice*. Lymph node harvested from* ***(A and B)*** *naïve* ***(C)*** *PBS and* ***(D-F)*** *MOG_{35-55} immunised mice and were stained with isotype control or anti-CD4 (Red) and counterstained with haematoxylin (blue). Data are representative of each group. n=3 for all groups. Primary images X20 magnification, scale bars = 100µm; Secondary images X40 magnification, scale bars = 100µm.* ***(G)*** *Percentage CD4 positive cells out of the total cells in the ROI in each group and at each stage of EAE has been quantified as previously described using the cell counter tool of Image J software and result expressed as mean ± S.E.M. Statistical significance was determined by one-way ANOVA with Bonferroni post hoc test Statistical significance was determined by One-way ANOVA with Bonferroni post hoc test. *P<0.05 versus naïve.*

3.2.9 Serum level of IL-16 in EAE and control mice

After evaluating the expression and production of IL-16 by spleen and lymph node cells we next collected blood from naïve mice, PBS mice at day 16 post immunisation and EAE mice at day 12, day 16 and day 26 post immunisation stages and prepared serum samples to determine the level of IL-16 using ELISA.

PBS control group didn't show any significant difference in IL-16 levels in comparison to the naïve controls (Figure 3.17). However, the levels of IL-16 at EAE day 12 (560 ± 105 pg/ml) and EAE day 16 (410 ± 62 pg/ml) were significantly higher compared to that of the naïve (137 ± 18 pg/ml) and PBS day 16 (177 ± 10 pg/ml) control groups as well as EAE day 26 (232 ± 15 pg/ml). However, EAE day 26 had reduced IL-16 levels in comparison to EAE day 12 and day 16 but was not significantly different from naïve and PBS day 16 groups.

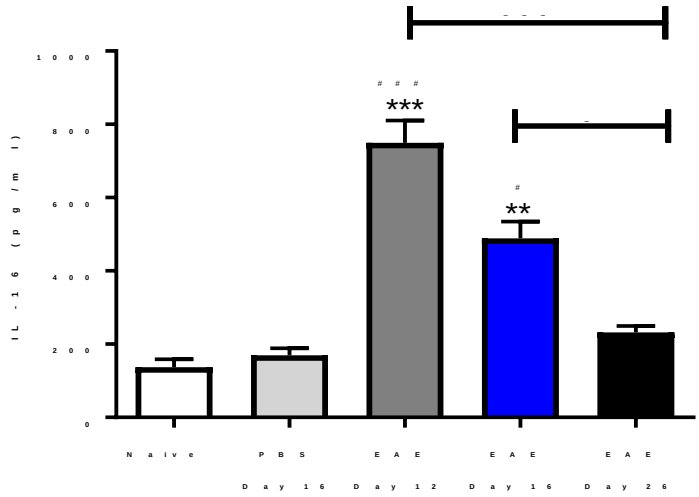

Figure 3.17: Increased serum level of IL-16 in EAE mice. *Blood collected from the naïve mice, PBS and MOG_{35-55} immunised mice were processed to obtain serum to determine the level of IL-16 using ELISA. All samples were analysed in triplicate; naïve n=3, PBS n=3, EAE n=5. Result illustrated as mean ± S.E.M. Statistical significance was determined by one-way ANOVA with Bonferroni post hoc test. **P <0.01 ***P<0.001 versus naïve, $^{\#}$P<0.05, $^{\#\#\#}$P <0.001 versus PBS day 16, $^{\sim}$P<0.05, $^{\sim\sim\sim}$P<0.001 versus EAE day 26.*

3.2.10 Spinal cord and brain homogenate level of IL-16 in EAE and control mice

Next, we examined the protein levels of IL-16 in CNS tissues. Spinal cords and brains (separated into cerebellum and cerebrum) were harvested from naïve mice, PBS immunised mice at day 16 post immunisation and MOG_{35-55} immunised mice at day 12, day 16 and day 26 post immunisation and tissues were homogenised to obtain the supernatants as described in Materials and Methods to determine the levels of IL-16 using ELISA.

Spinal cord of MOG_{35-55} immunised mice showed significantly elevated levels of IL-16 at day 12 (1881± 79 pg/ml) and day 16 (1873 ± 313 pg/ml) compared to the naïve (76 ± 11 pg/ml) and PBS (59 ± 8 pg/ml) controls, but the level was reduced at the day 26 (313 ± 21 pg/ml) EAE mice and demonstrated no significant difference in comparison to the control groups, however, both EAE day 12 and day 16 had significantly higher levels of IL-16 in comparison to day 26 (Figure 3.18 A).

IL-16 was also detected in the homogenised brain tissues of naïve (cerebellum 482 ± 61pg/ml; cerebrum 360± 22 pg/ml) and PBS day 16 mice (cerebellum 445 ± 28 pg/ml; cerebrum 428 ± 36 pg/ml). However the levels were significantly higher in brain tissues of EAE day 12 (cerebellum 1579 ± 107 pg/ml; cerebrum 1378 ± 53 pg/ml), and day 16 (cerebellum 2421 ± 89 pg/ml; cerebrum 1906 ± 88 pg/ml) mice and the level was reduced in tissues of at day 26 (cerebellum 652 ± 75; cerebrum 530 ± 8) EAE mice and showed no significant difference in comparison to the control groups. However, EAE day 26 was significantly lower than the EAE day 12 and EAE day 16 (Figure 3.18B and C).

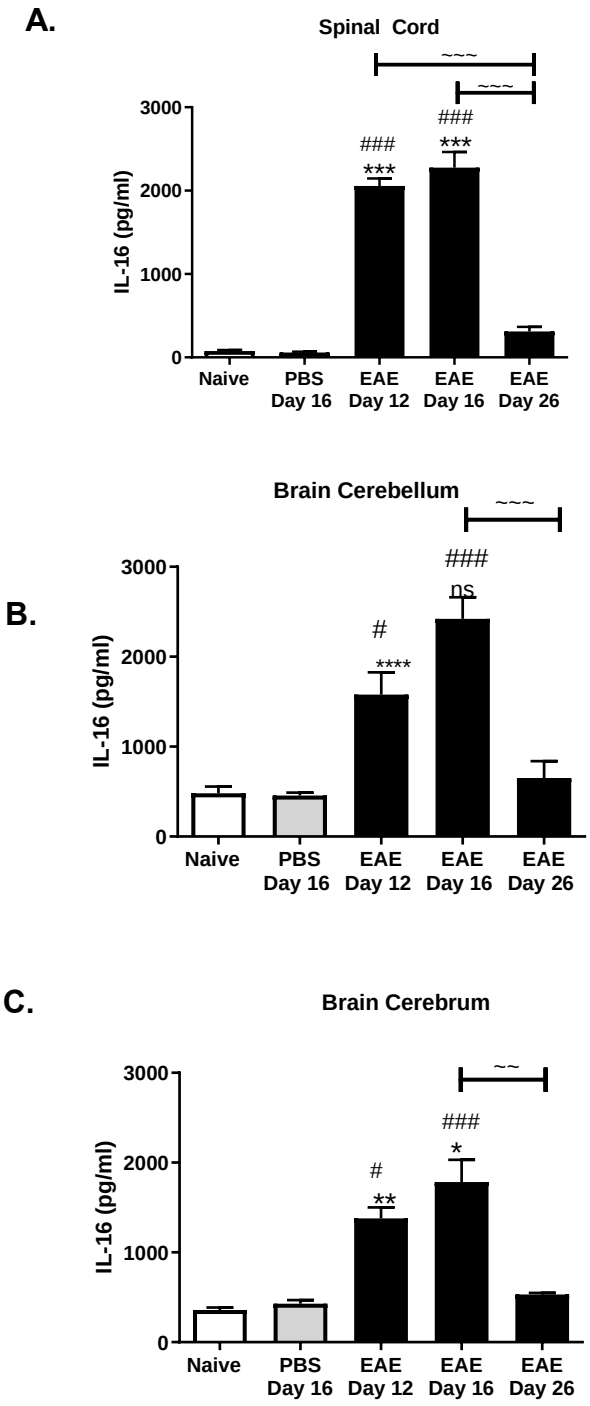

Figure 3.18 IL-16 level in CNS correlates with EAE progression. *Supernatants from homogenised* ***(A)*** *spinal cord,* ***(B)*** *brain cerebellum and* ***(C)*** *cerebrum were collected and prepared to check for IL-16 levels using ELISA. All samples were analysed in triplicate in ELISA; naïve n=3, PBS n=3, EAE n=5 in each time points. Result illustrated as mean ± S.E.M. Statistical significance was determined by one-way ANOVA with Bonferroni post hoc test *P<0.05, **P <0.01 versus naïve, #P<0.05, ###P<0.001 versus PBS day 16, ~~P <0.01, ~~~P<0.001 versus EAE day 26.*

3.2.11 IL-16 expression in the spinal cord tissues of EAE and control mice

Our data showed increased level of IL-16 in the CNS tissues of EAE mice, so, next we examined the localisation of IL-16 expression in CNS tissue.

Expression of IL-16 in murine spinal cord tissues were compared between naïve mice, PBS immunised mice at day 16 post immunisation and MOG_{35-55} immunised mice at day 12, 16 and 26 post immunisations. While tissues stained with isotype control antibody had no positive staining (Figure 3.19A), IL-16 expression was observed in the spinal cord tissues of all EAE and control mice (Figure 3.19 B-F). However, the levels of IL-16 expression were very different in tissues of EAE mice compared to that of the naïve and PBS day 16 controls. IL-16 was observed to be expressed in the GM of naïve, PBS day 16 and EAE spinal cord tissues at all clinical stages; however, during EAE day 12 and EAE day 16, IL-16 expression was also observed within the WM of the spinal cord, in close proximity to the infiltrating lesions (Figure 3.19D-F).

We next analysed, the percentage of IL-16^+ cells of the total cells within the comparable ROI in spinal cord tissue sections. The total percentage of IL-16^+ cells present in the spinal cord section were further divided to display the percentage IL-16^+ cells in the areas of GM, WM and lesion. The percentage IL-16^+ cells within GM showed no significant difference between the naïve (22 ± 2%), PBS day 16 (23 ± 2%) controls and EAE day 12 (21± 1%), day 16 (26 ± 1.5%) and day 26 (17± 1%). However a significant increase in the percentage of IL-16^+ cells was observed within the WM and the lesion (or equivalent area in control tissues) at in EAE day 12 (WM 17 ± 1%; lesion 22 ± 1%) and EAE day 16 mice (WM 18 ± 1%; lesion 25 ± 1.37%) compared to the naïve and PBS day 16 controls as well as EAE day 26 mice which demonstrate little IL-16 expression.

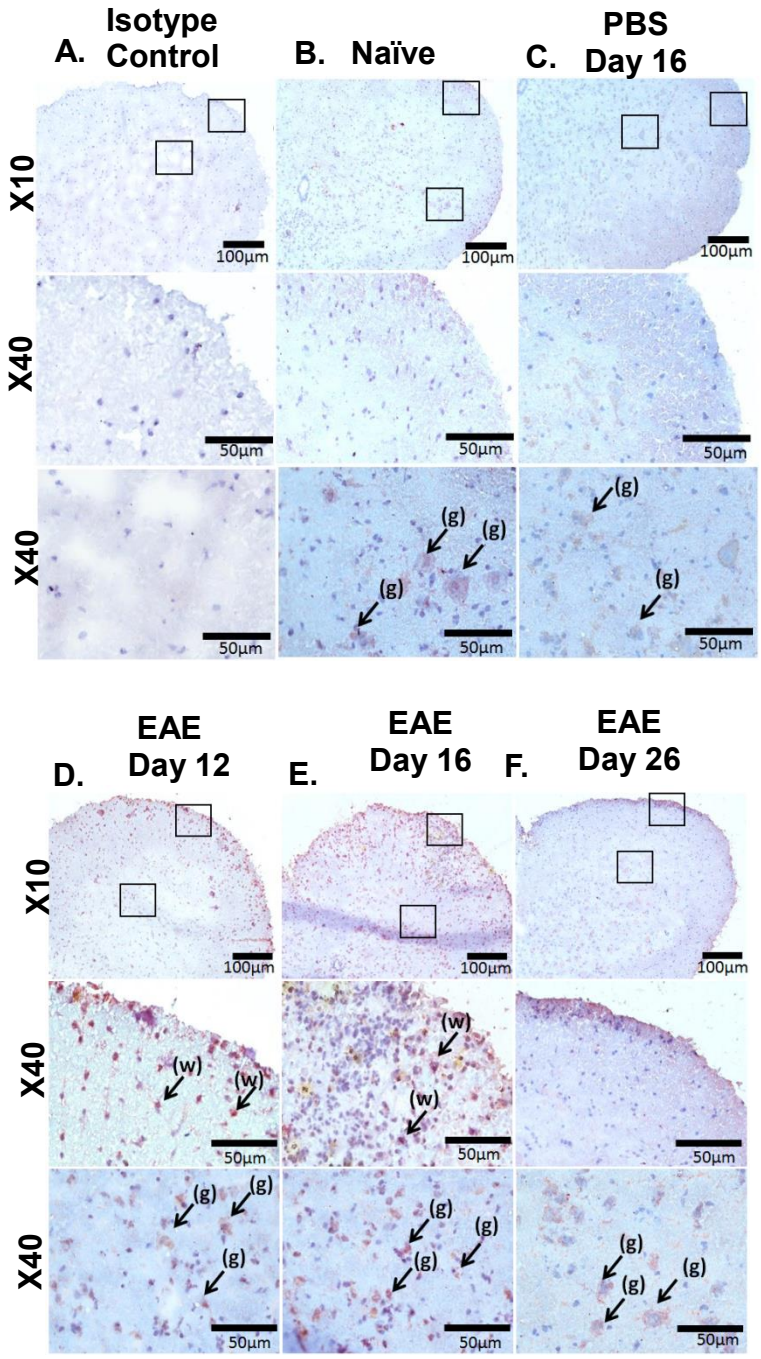
A. Isotype Control
B. Naïve
C. PBS Day 16
D. EAE Day 12
E. EAE Day 16
F. EAE Day 26
X10
X40
X40
100µm
50µm
(g)
(w)

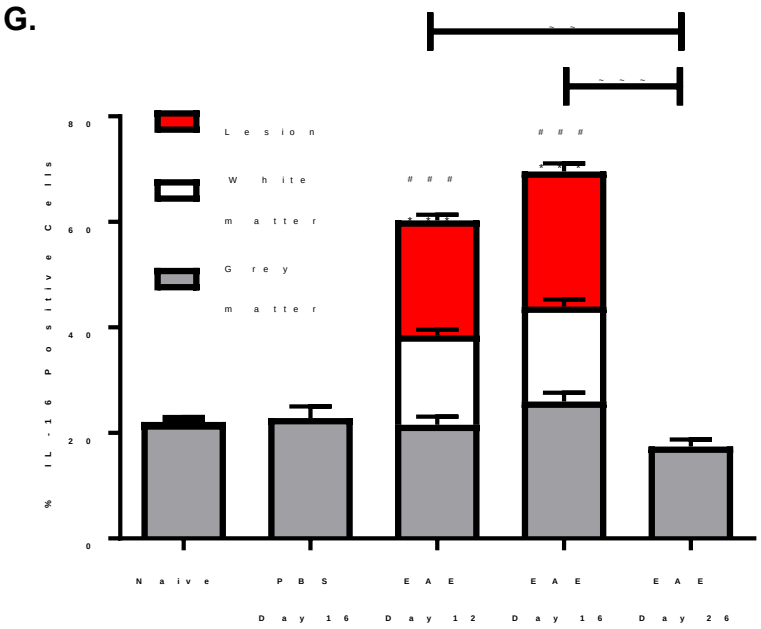

Figure 3.19: IL-16 expression in the spinal cord of EAE mice. *Spinal cords were harvested from* ***(A and B)*** *naïve and* ***(C)*** *PBS or* ***(D-F)*** *MOG_{35-55} immunised mice and stained with isotype control or anti-IL-16 (Amec Red) and counterstained with haematoxylin (blue). White matter* ***(w)*** *and grey matter* ***(g)*** *are indicated with arrows. Data are representative of each group. n=5 for all groups. Primary images X10 magnification, scale bars = 100µm; Secondary and tertiary images X40 magnification, scale bars = 50µm.* ***(G)*** *Percentage IL-16 positive cells in each group and at each stage of EAE has been quantified as previously described using the cell counter tool of Image J software and result expressed as mean ± S.E.M. Statistical significance was determined by one-way ANOVA with Bonferroni post hoc test. ***P<0.001 versus naïve, $^{###}$P<0.001 versus PBS day16, $^{~~}$P <0.01, $^{~~~}$P<0.001 versus EAE day 26.*

3.2.12 CD4 expression in the spinal cord tissues of EAE mice

Following the investigation of IL-16 expression in spinal cord tissues, we next studied the expression of its receptor CD4 in murine spinal cord tissues and compared the percentage of $CD4^+$ cells between naïve mice, PBS immunised mice at day 16 post immunisation and MOG_{35-55} immunised mice at day 12, day 16 and day 26 post immunisation. As expected tissues stained with isotype control antibody had no positive staining. $CD4^+$ cells were expressed in EAE spinal cord tissue during all three time points but were absent in the naïve and PBS day 16 controls (Figure 3.20). At EAE day 12, $CD4^+$ cells were observed within close proximity of the inflammatory lesions in the WM of the spinal cord and this pattern indicated the infiltration of $CD4^+$ cells during the onset of EAE at day 12. However, as the disease severity reached its peak at day 16, the expression of the $CD4^+$ cells increased and was observed within both WM and GM of the spinal cord. However, as EAE reached resolution at day 26, the $CD4^+$ cells were present in small clusters only within the WM of the spinal cord. In agreement with these observations, analysis of percentage $CD4^+$ cells out of the total cells within the comparable ROI in spinal cord tissue sections demonstrated dramatic increase within the tissues of EAE day 16 mice (27 ± 2%) in comparison to the EAE day 12 (21 ± 1%) and EAE day 26 mice (4 ± 2%) (Figure 3.20G), with both EAE day 12 and day 16 significantly higher than EAE day 26 mice.

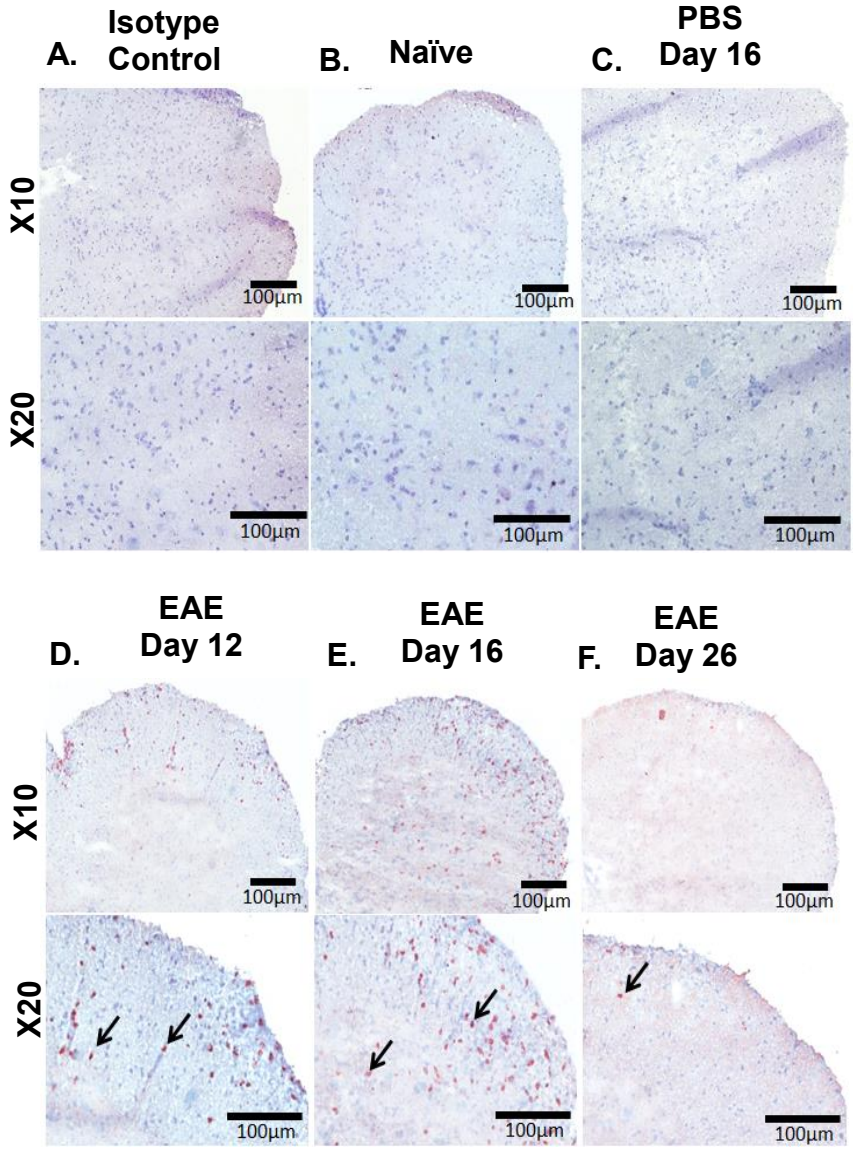
A. Isotype Control
B. Naïve
C. PBS Day 16
X10
X20
100µm
D. EAE Day 12
E. EAE Day 16
F. EAE Day 26
X10
X20
100µm

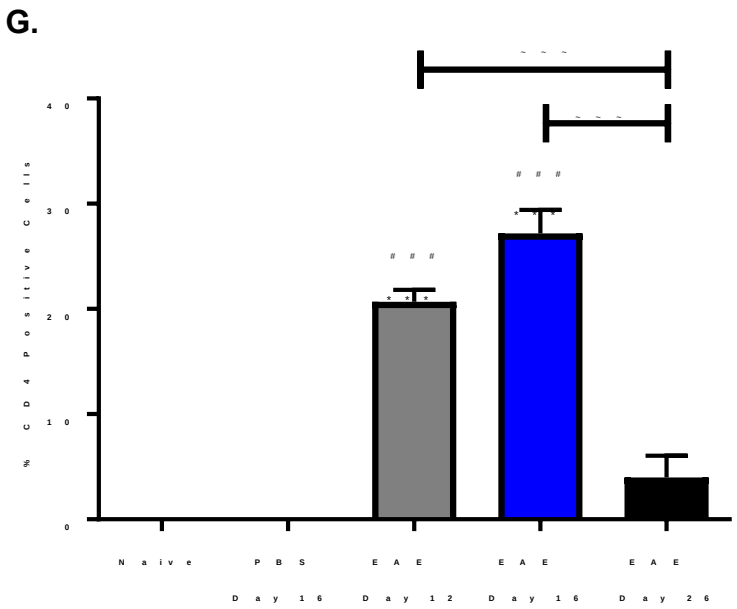

Figure 3.20: CD4 expression in spinal cord during EAE progression. *Spinal cords were harvested from* ***(A and B)*** *naïve and* ***(C)*** *PBS or* ***(D-F)*** *MOG_{35-55} immunised mice and stained with isotype control or anti-CD4 (Amec Red) and counterstained with haematoxylin (blue). Data are representative of each group. n=5 for all groups. Primary images X10 magnification, scale bars = 100µm; Secondary and tertiary images X20 magnification, scale bars = 50µm.* ***(G)*** *Percentage CD4 positive cells in each group and at each stage of EAE has been quantified as previously described using the cell counter tool of Image J software and result expressed as mean ± S.E.M. Significance determined by one-way ANOVA with Bonferroni post hoc test ***P<0.001 versus naïve, ###P<0.001 versus PBS day 16, ~~~P<0.001 versus EAE day 26.*

3.2.13 IL-16 expression in the brain tissues of EAE and control mice.

After examining the expression of IL-16 in spinal cord tissues, we next utilised IHC to determine IL-16 expression in sagittal sections of brain tissues. IL-16 expression was specifically assessed within the hippocampus (Figure 3.21) and the cerebellum (Figure 3.22) as the immune cell infiltration was particularly evident in these brain regions.

In the hippocampus, IL-16 was found to be expressed in the CA1-CA3 and dentate gyrus regions of the hippocampus in all groups of mice. However, quantification revealed an increased percentage of IL-16$^+$ cells within the hippocampus (including both CA1-CA3 and dentate gyrus) of EAE day 12 (66 ± 1%), and EAE day 16 (68 ± 2%) mice in comparison to naïve (60 ± 1%) and PBS day 16 (60 ± 1%) controls (Figure 3.21G).

No obvious cellular infiltration was observed in the CA1-CA3 regions in all group, and region-specific quantification showed no significant difference in the percentage of IL-16$^+$ cells in CA1, CA2 and CA3 regions between any of the groups. The quantification data revealed IL-16$^+$ cells accounted for 12 ± 1%, 11 ± 1% and 9 ± 1% of total cells in the CA1, CA2 and CA3 region of hippocampus respectively in naïve mice, which was similar in the PBS day 16 mice where IL-16$^+$ cells accounted for 12 ± 1%, 11± 1%, and 10 ± 1% of total cells in the CA1, CA2 and CA3 region of hippocampus respectively. MOG$_{35-55}$ immunised mice at day 12 (CA1-12 ± 1%, CA2-11 ± 1%, CA3 -11 ± 1%), day 16 (CA1-13 ± 1%, CA2-13 ± 1%, CA3 -11 ± 1%) and day 26 (CA1-12 ± 1%, CA2-11 ± 1%, CA3 -11 ± 1%) also had similar percentage of IL-16$^+$ cells (Figure 3.21 H, I and J). However, in the areas close to the dentate gyrus, cellular infiltration and lesions were observed and when quantified, significantly increased IL-16$^+$ cell were observed in EAE day 12 (27 ± 1%) and EAE day 16 (29 ± 2%) mice in comparison to naïve (22 ± 1%) and PBS day 16 (22 ± 1%) mice, but the level returned to levels similar to control during EAE resolution stage at day 26 (22 ± 1%) (Figure 3.21K). While quantifying the percentage of IL-16$^+$ cells in the hippocampus, the lesions found in the surrounding areas of the dentate gyrus were quantified separately, this data revealed that hippocampus without the lesion expresses the same percentage of IL-16$^+$ cells in

all three mice groups however the level in lesions or equivalent areas was increased by 5 ± 1% and 7 ± 1% in tissues of EAE day 12 and day 16 respectively, making them significantly higher than naïve and PBS controls, as well as EAE day 26 which did not demonstrate any lesion. This data further suggests the increased IL-16 expression observed within the EAE day 12 and day 16 group was likely due to the contribution of the infiltrating immune cells and the lesions found in the dentate gyrus.

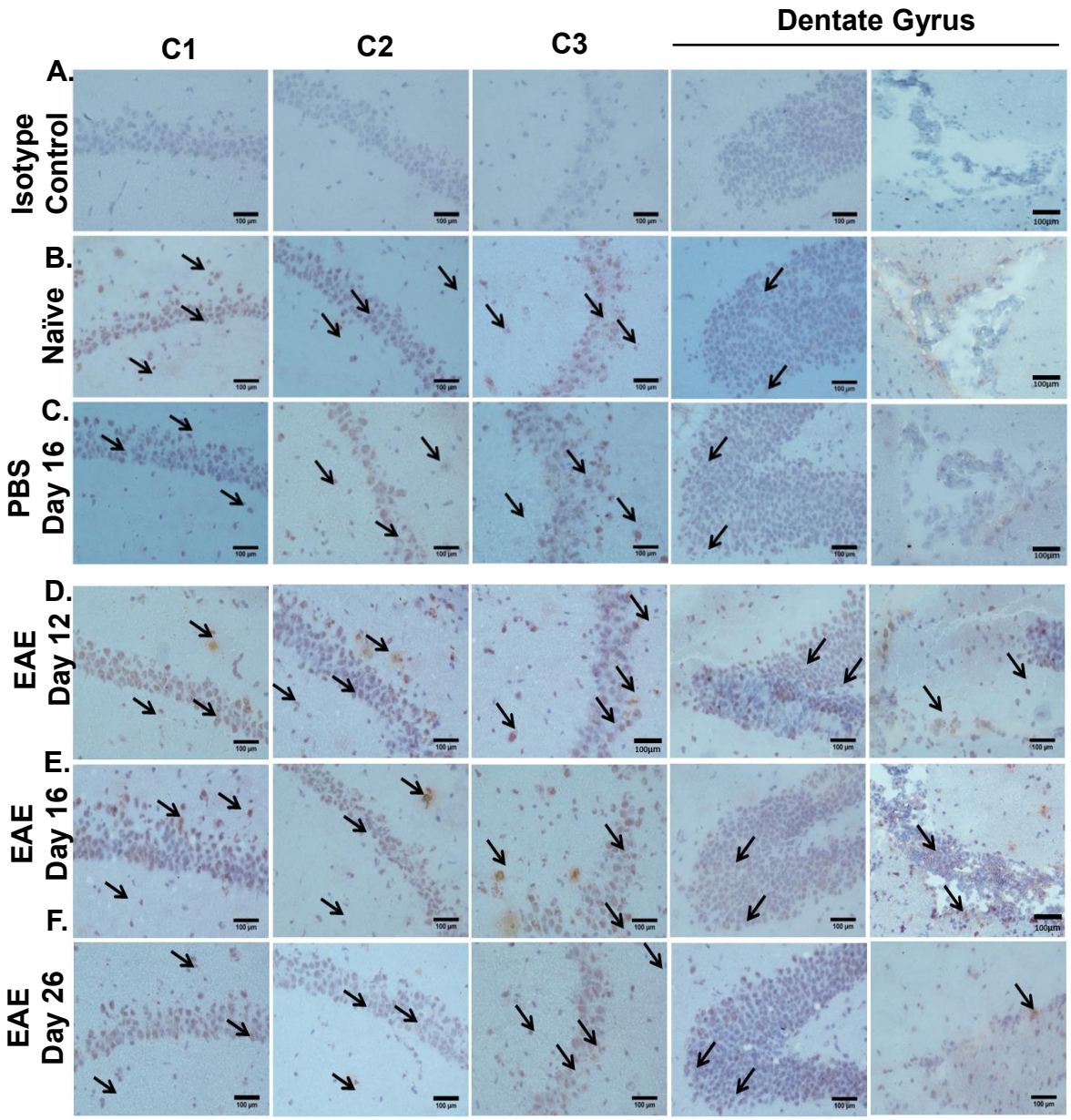
C1
C2
C3
Dentate Gyrus
A.
Isotype Control
B.
Naïve
C.
PBS Day 16
D.
EAE Day 12
E.
EAE Day 16
F.
EAE Day 26

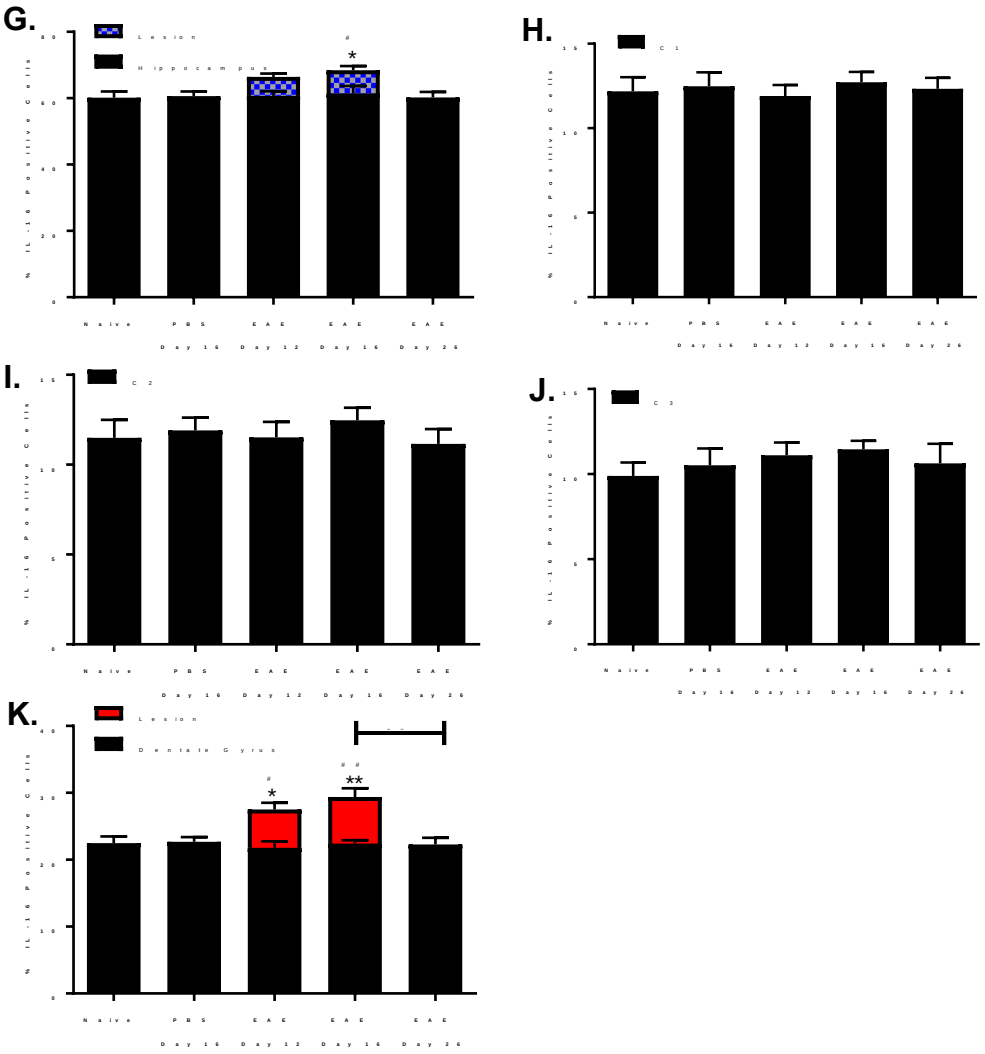

Figure 3.21: Increased expression of IL-16 in the hippocampus of EAE mice*. Brains were harvested from **(A and B)** naïve **(C)** PBS and **(D-F)** MOG_{35-55} immunised mice and stained with isotype control or anti-CD4 (Amec Red) and counterstained with haematoxylin (blue) to examine the expression and level of IL-16. Data are representative of each group. n=5 for all group. Images X20 magnification, scale bars = 50µm. **(G)** The total percentage positive cell in the hippocampus **(H)** C1, **(I)** C2, **(J)** C3 and **(K)** dentate gyrus in each group and at each stage of EAE has been quantified as previously described using the cell counter tool of Image J software and result expressed as mean ± S.E.M. Statistical significance was determined by one-way ANOVA with Bonferroni post hoc test *P<0.05, **P<0.01 versus naïve, $^{\#}$P<0.05, $^{\#\#}$P <0.01versus PBS day 16, $^{\sim\sim}$P<0.01 versus EAE day 26.*

In the cerebellum, IL-16 expression was observed in all the groups, however increased expression of IL-16 in areas in close proximity to the inflammatory lesion. Quantification of percentage IL-16$^+$ cells of the total cells within the comparable ROI in the cerebellum (Figure 3.22G) demonstrated significantly elevated expression in EAE day 12 (51 ± 1%) and EAE day 16 (53 ± 4%) mice in comparison to the naïve (33 ± 2%) and PBS day 16 (33 ± 2%) controls. However, in tissues of EAE day 26 mice, the percentage of IL-16$^+$ cells (39 ± 2%) returned to levels similar to that seen in control groups and was significantly lower than EAE day 12 and EAE day 16 mice

We further analysed the percentage IL-16$^+$ cells, based on different layers of the cerebellum, with these being the WM, granule cells + purkinje cells in the granular layer (GL) and molecular layer (ML). The data indicated significantly higher percentage of IL-16$^+$ cells in the WM (Figure 3.22H), GL (Figure 3.22I) and ML (Figure 3.22J) of EAE day 12 (WM 12 ± 5%; GL 27± 1%; ML 12 ± 1%) and EAE day 16 (WM 16 ± 7%; GL 29 ± 1% ML 13 ± 1%) mice compared to the naïve (WM 5 ± 2%; GL 22 ± 1%; ML 7± 1%) and PBS day 16 (WM 6 ± 2%; GL 22 ± 1% ML 6 ± 1%) controls. However, this up-regulation was reduced to levels similar to that of control groups at day 26 during EAE resolution stage (WM 6 ± 3%; GL 22 ± 1%; ML 9 ± 1%). And the WM of EAE day 12 and day 16 had significantly higher percentage of IL-16$^+$ cells in comparison to EAE day 26 mice.

While quantifying the percentage of IL-16$^+$ cells in WM and ML, lesions found in those regions were quantified separately, our data revealed that in the EAE mice, cerebellum without the lesion had similar percentage of IL-16$^+$ cells as observed in the cerebellum of naïve and PBS mice (Figure 3.22H and J) however during EAE day 12 and EAE day 16, percentage of IL-16$^+$ cells were increased by 10 ± 1% and 13 ± 1% respectively (Figure 3.22G), making the total percentage of IL-16$^+$ cells in the cerebellum of EAE day 12 and day 16 mice significantly higher than naïve, PBS as well as EAE day 26 mice. Suggesting the increased IL-16 expression observed within the cerebellum of EAE group was thus likely due to the inflammatory lesions found in molecular and the granular layers of the cerebellum.

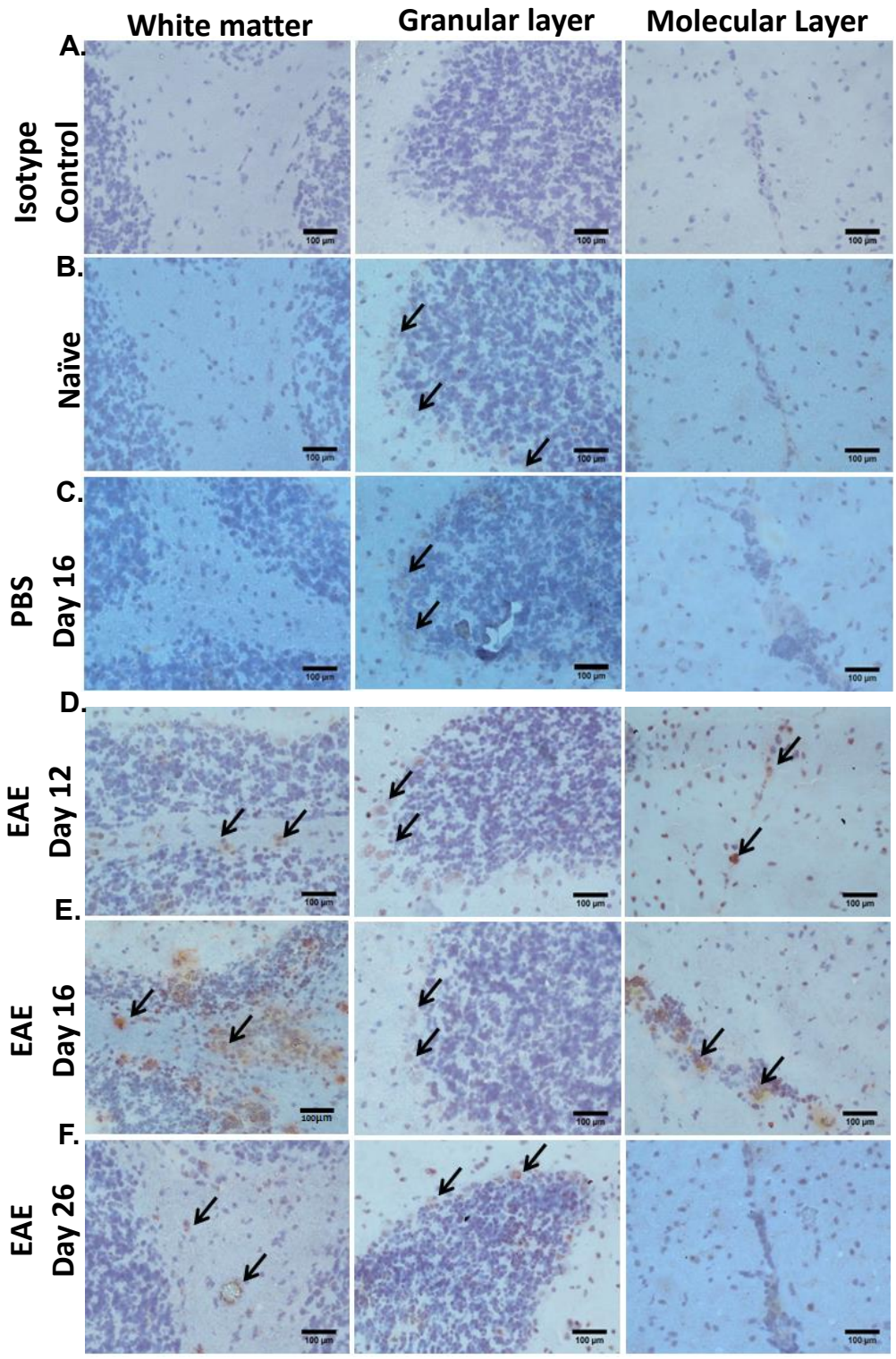
White matter
Granular layer
Molecular Layer
A.
Isotype Control
B.
Naïve
C.
PBS Day 16
D.
EAE Day 12
E.
EAE Day 16
F.
EAE Day 26
100 µm

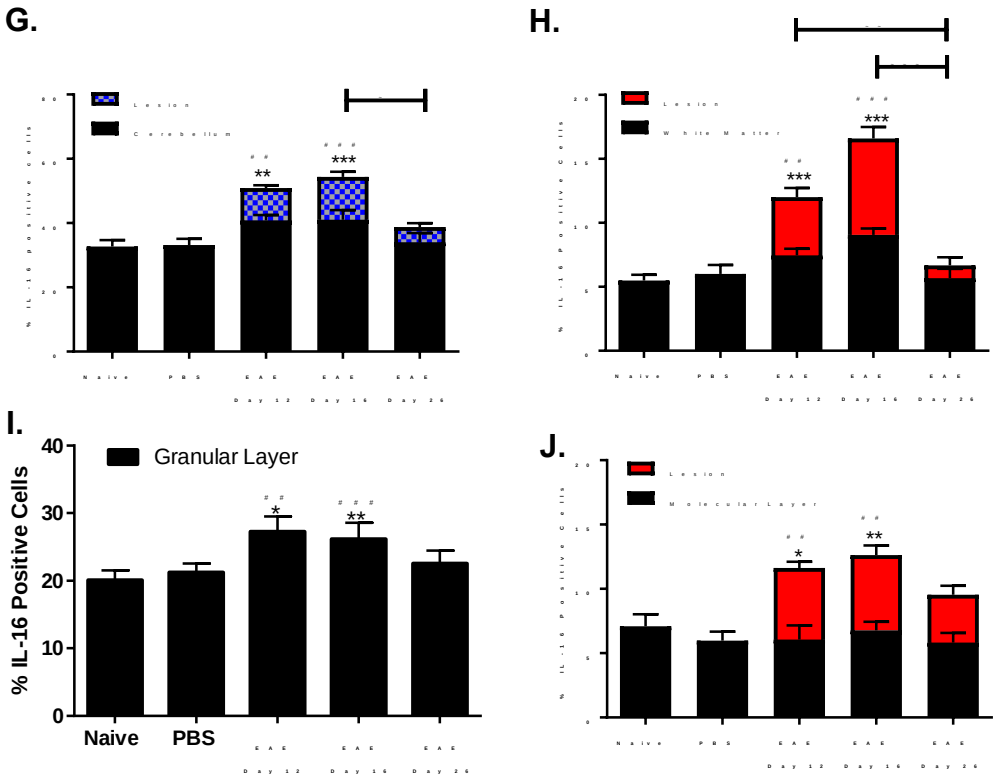

Figure 3.22: Increased expression of IL-16 in the cerebellum of EAE mice. *Brains were harvested from **(A and B)** naïve **(C)** PBS and **(D-F)** MOG_{35-55} immunised mice and stained with isotype control or anti-IL-16 (Amec Red) and counterstained with haematoxylin (blue) to examine the expression and level of IL-16. Data are representative of each group. n=5 for all group. Images X20 magnification, scale bars = 100µm. **(G)** The total percentage positive cell in the cerebellum **(H)** white matter **(I)** granular layer with granular cells and purkinje cells in each group **(J)** molecular layer and at each stage of EAE has been quantified as previously described using the cell counter tool of Image J software and result expressed as mean ± S.E.M. Statistical significance was determined by one-way ANOVA with Bonferroni post hoc test *P<0.05, **P <0.01 ***P<0.001 versus naïve, $^{\#\#}$P <0.01, $^{\#\#\#}$P<0.001 versus PBS day 16, $^{\sim}$P<0.05, $^{\sim\sim}$P<0.01 and $^{\sim\sim\sim}$P<0.001 versus EAE day 26.*

3.2.14 CD4 expression in the brain tissues of EAE mice

After examining the level of expression of IL-16, we also evaluated the extent of CD4 expression within the hippocampus (Figure 2.24) and cerebellum (Figure 2.25) of naïve mice, PBS immunised mice at day 16 post immunisation and MOG_{35-55} immunised mice at day 12, day 16 and day 26 post immunisation. As seen with the spinal cord sections, both the hippocampus and the cerebellum of the brain also demonstrated the similar pattern of CD4 expression in the EAE mice. The expression of $CD4^+$ cell was absent in the naïve and PBS day 16 controls; however, the level of expression was increased in the tissues of EAE mice. Most of the $CD4^+$ cells were observed within the close proximity of the inflammatory lesions in hippocampus and cerebellum. In the hippocampus of EAE mice $CD4^+$ cells were observed near the surrounding areas of dentate gyrus. When the percentage $CD4^+$ cells out of the total cells within the comparable ROI in the hippocampus of all mice groups were quantified 13 ± 1% was observed in tissues of EAE day 12 mice, this increased to 16 ± 1% in EAE day 16 mice and then significantly dropped to 6 ± 1% in the EAE day 26 mice (Figure 2.24G).

Within the cerebellum IL-16 expression demonstrated the same trend as seen in the hippocampus. Quantification of the percentage $CD4^+$ cells out of the total cells within the comparable ROI in the cerebellum revealed $CD4^+$ cells accounted for 21 ± 1% of total cells in EAE day 12 mice which increased to 29 ± 1% in EAE day 16 mice and as the disease started to recover the level significantly dropped to 9 ± 0.5% in EAE day 26 mice (Figure 2.25G).

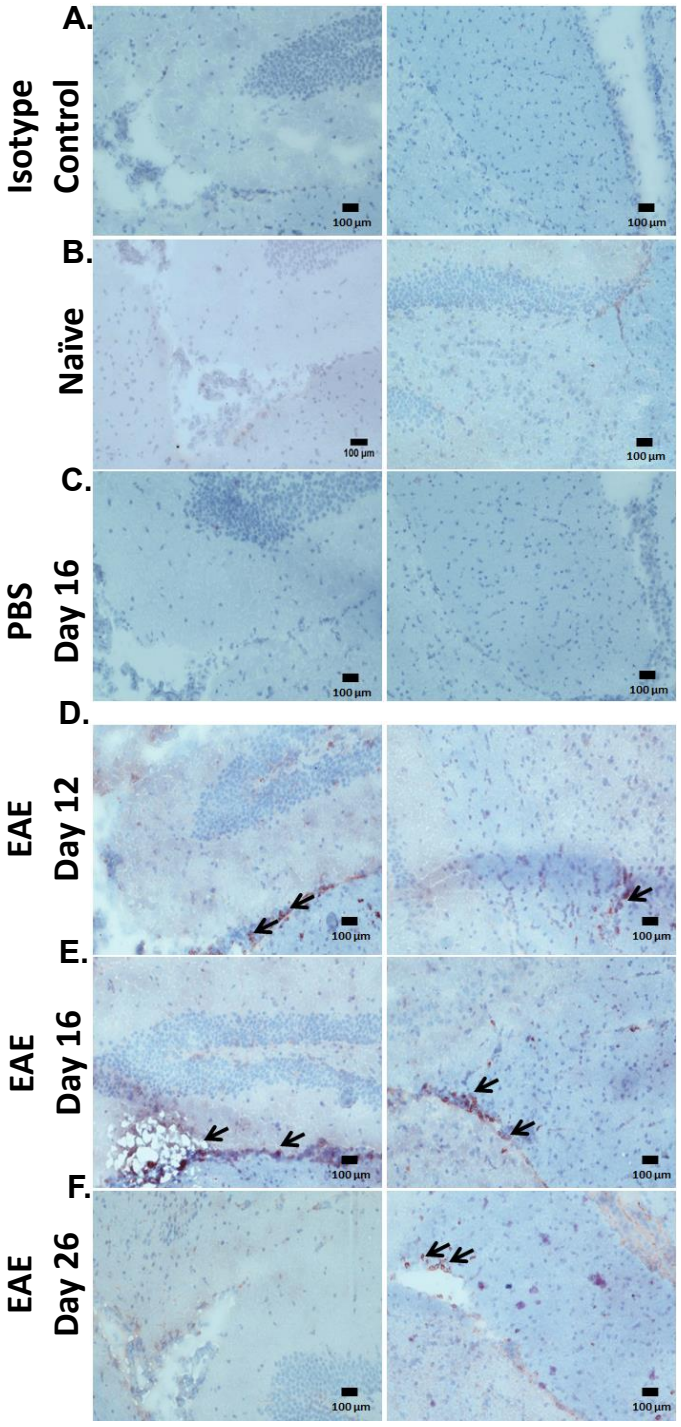
A.
Isotype Control
B.
Naïve
C.
PBS Day 16
D.
EAE Day 12
E.
EAE Day 16
F.
EAE Day 26
100 µm

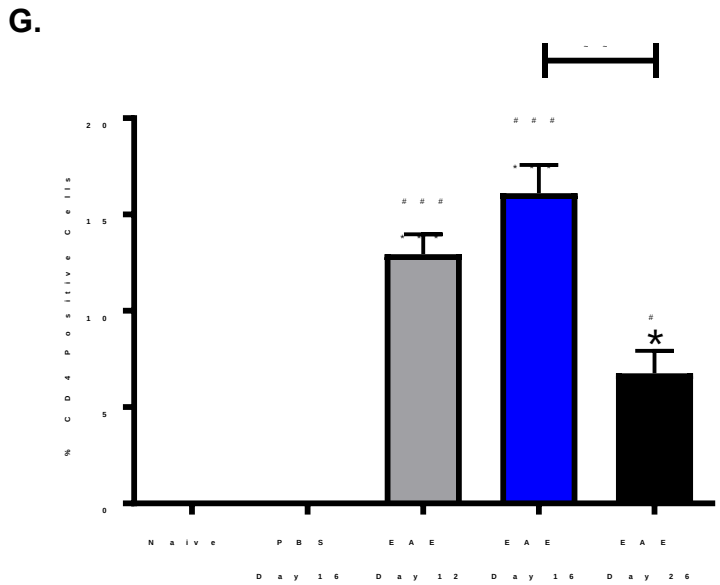

Figure 3.23: Expression of CD4 in hippocampus during EAE progression. *Brains were harvested from **(A and B)** naïve, and **(C)** PBS or **(D-F)** MOG_{35-55} immunised mice and stained with isotype control or anti-IL-16 (Amec Red) and counterstained with haematoxylin (blue).CD4 expressions are indicated with arrows and data are representative of each group. n=5 for all groups. Images are in X20 magnification, scale bars = 100µm. **(G)** Percentage of IL-16 positive cells in each group and at each stage of EAE has been quantified as previously described using the cell counter tool of Image J software and result expressed as mean ± S.E.M. Statistical significance was determined by One-way ANOVA with Bonferroni post hoc test. *P<0.05, ***P<0.001 versus naïve, $^{\#}$P<0.05, $^{\#\#\#}$P<0.001 versus and PBS day 16, $^{\sim\sim}$P<0.01 versus EAE day 26.*

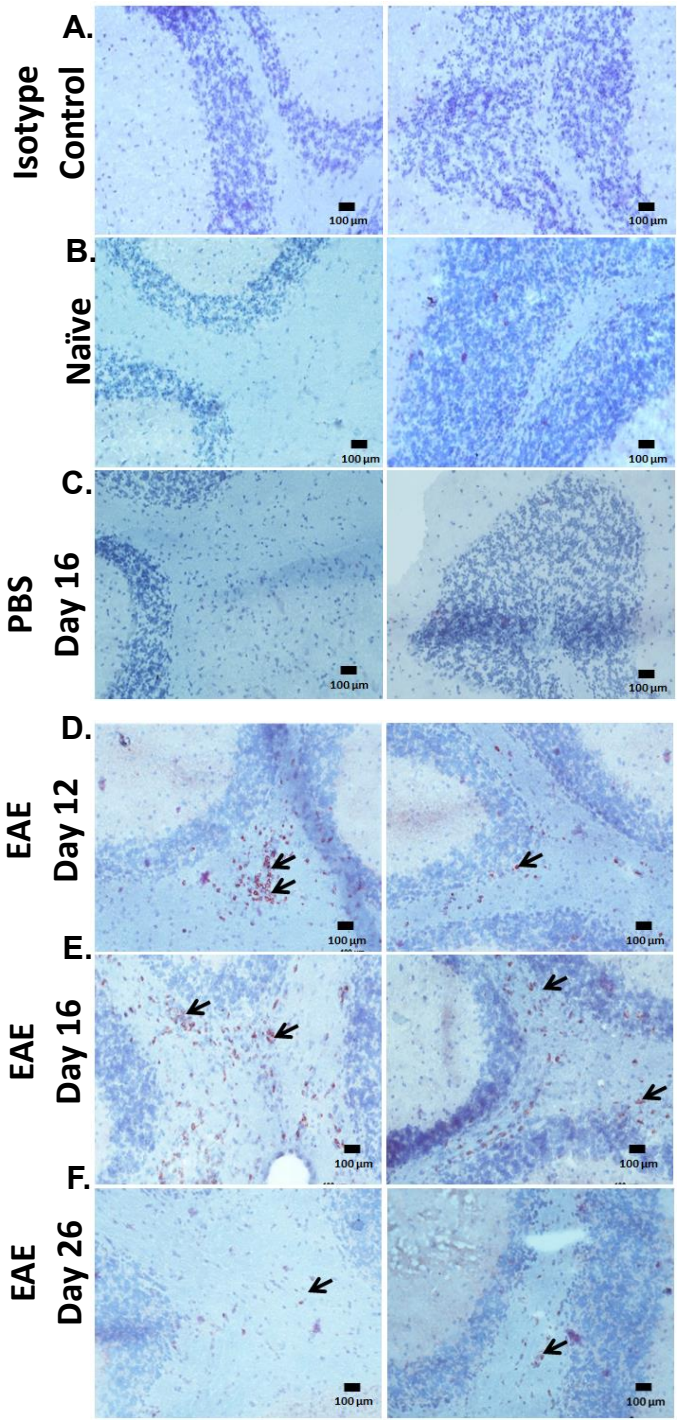
A.
Isotype Control
B.
Naïve
C.
PBS Day 16
D.
EAE Day 12
E.
EAE Day 16
F.
EAE Day 26
100 µm

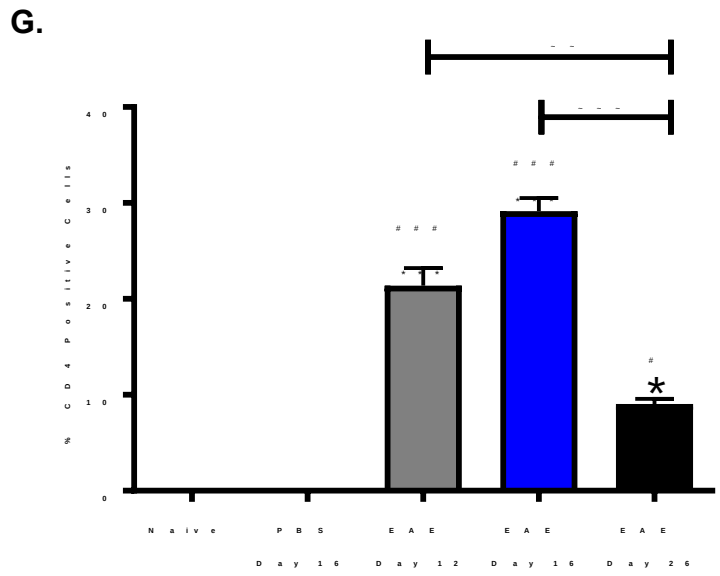

Figure 3.24: Expression of CD4 in cerebellum during EAE progression*. Brains were harvested from* ***(A and B)*** *naïve, and* ***(C)*** *PBS or* ***(D-F)*** *MOG_{35-55} immunised mice and stained with isotype control or anti-CD4 (Amec Red) and counterstained with haematoxylin (blue) to examine the expression and level of CD4.* CD4 expressions *are indicated with arrows and data are representative of each group. n=5 for all groups. Images are in X20 magnification, scale bars = 100µm.* ***(G)*** *Percentage IL-16 positive cells in each group and at each stage of EAE has been quantified as previously described using the cell counter tool of Image J software and result expressed as mean ± S.E.M. Statistical significance was determined by One-way ANOVA with Bonferroni post hoc test *P<0.05, **P <0.01 ***P<0.001 versus Naïve, $^{\#}$P<0.05 $^{\#\#\#}$P<0.001 versus and PBS day 16, ˜˜P<0.01, ˜˜P<0.001versus EAE day 26.*

3.3 Discussion

EAE is the most commonly used animal model for studying MS because of its close immunopathological resemblance to MS (Lindsey, 2005; Comabella and Khoury, 2011). In this study we have used the MOG_{35-55} induced EAE model, to investigate the potential role of IL-16 in CNS inflammation by studying the expression and distribution of IL-16 and its receptor CD4, within the CNS and lymphoid organs of EAE and control mice.

In accordance to the previous studies, C57BL/6J mice when immunised with MOG_{35-55} + CFA and PTX developed an acute monophasic EAE (Almolda *et al*., 2011; Farias *et al*., 2012 and Jiang *et al*., 2012). The onset of clinical signs of EAE such as limp tail and gaited walk was first observed at day 12. By day 16 EAE severity reached a peak with 100% of MOG_{35-55} immunised mice exhibiting partial and complete paralysis of hind limbs before reaching a recovery phase. Whereas, the naïve control group which did not receive any injection and the PBS control group which received PBS instead of MOG_{35-55} did not develop any clinical signs of EAE (Figure 3.3).

During the early stage of EAE, the peripheral inflammation triggers the migration of circulating leukocytes across the BBB and blood-cerebrospinal fluid barriers (BCSFB- which is formed by the epithelium of the choroid plexuses) to gain access to the CNS.In CNS cerebrospinal fluid (CSF) is a predominant route of T-cell trafficking. Vessels running in subarachnoid spaces of the lower part of the spinal cord are the initial site of T-cell entry into the CSF during EAE (Bartholomäus et al., 2009). CSF also plays a critical role in the distribution of immune cells within the forebrain and midbrain during EAE (Schmitt et al., 2012), with periventricular and superficial white matter structures being the primary targets of early T-cell infiltration (Brown et al., 2007). In the brain, leukocytes initially infiltrate distinctive extra ventricular CSF-filled compartments of the forebrain and midbrain such as the velum interpositum and ambient cisterns, and certain basal cisterns. Leukocytes further infiltrates periventricular and pericisternal parenchymal areas, along perivascular spaces or following a downward CSF-to-tissue gradient. With H&E staining (Figure 3.4, 3.5) and CD45 IHC (Figure 3.6, 3.7, 3.8) on CNS tissues we have further confirmed the presence of infiltrating immune cells within the CNS during EAE, exhibiting a

positive correlation between the severity of clinical symptoms and cellular infiltration in the CNS. On other hand control mice either from naïve group or PBS immunised group on other hand were unable to exhibit any signs of CNS inflammation either clinically or histologically. Quantification of $CD45^+$ cell number in the CNS further confirmed that the CNS tissues from mice with severe clinical symptoms had higher $CD45^+$ infiltrating cells, with highest percentage of $CD45^+$ cells observed at the EAE peak tissues which gradually decreased as the disease started to recover.

Several studies have demonstrated how infection in the periphery can contribute to the development of CNS disease. It has been discussed in multiple studies that during MS, systemic infection can cause relapses of the disease and the cytokines released during systemic inflammation can directly or indirectly contribute to CNS inflammation (Matsumura & Yamagata 1996; Perry *et al*., 2004; Moreno *et al*., 2011; Takahashi *et al*., 2013). The PBS immunised control group used in our study showed systemic inflammation was induced in these mice with the presence of a similar general systemic response between MOG_{35-55} and PBS immunised mice. In comparison to naïve controls, both PBS and MOG_{35-55} immunised mice, not only showed enlarged inguinal lymph nodes (Figure 3.9F), but also demonstrated an increased activation of $CD4^+$ and $CD8^+$ T cells with comparable percentage of $CD4^+CD25^+$ and $CD8^+CD25^+$ (Figure 3.9 A, B). In addition, significantly higher percentages of DCs were also observed in MOG_{35-55} immunised mice in comparison to naïve and PBS controls. However, the percentage $CD11c^+$ cells co-expressing CD40 (a co-stimulatory molecule found on APCs required for their activation) was found to be significantly higher in MOG_{35-55} immunised mice in contrast to the naïve control (Figure 3.9C). And percentage $CD11c^+MHC\text{-}II^+$ were also elevated in both PBS and MOG_{35-55} immunised mice in comparison to the naïve control (Figure 3.9D). In contrast to $CD4/CD8^+$ cells and DCs, percentage of $CD19^+$ B cells remained unchanged in all three mice groups with $CD19^+$ B cells co-expressing B220 (a molecule that regulates B-cell antigen receptor signalling) also showing no difference in any of the mice groups (Figure 3.9E), suggesting B cells are less likely involved in the immune responses activated by CFA and PTX. Interestingly despite the presence of an active immune response in the

periphery, PBS group did not demonstrate any CNS inflammation either clinically (Figure 3.3A) or histologically (Figure 3.4B, 3.5B). Therefore, our data suggest peripheral infection may contribute to MS/EAE severity after disease onset, but general activation of systemic immune response is not enough to initiate CNS inflammation. PBS immunised mice, which did not develop any clinical signs of EAE, further confirmed the effectiveness and specificity of CNS auto antigen MOG_{35-55} in inducing EAE.

To confirm the EAE cytokine profile, spleens from naïve, and PBS or MOG_{35-55} immunised mice were harvested at day 12, 16 and 26 post immunisations, and cells were re-stimulated with MOG_{35-55} *in vitro* to examine the level of production of IFN-γ, IL-17, IL-6 and IL-10 (Figure 3.10). Only splenocytes from mice originally immunised with MOG_{35-55}, but not naïve or PBS immunised mice, secreted increased level of IFN-γ, IL-17, IL-6 and IL-10 when re-challenged with MOG_{35-55} *in vitro* for 72 hours. The cells treated with medium alone showed little or no IFN-γ, IL-17, IL-6 and IL-10 production from either EAE or the control groups. This outcome further verifies the specificity of MOG_{35-55} in initiating the autoimmune response specific to CNS and also confirms the absence of MOG_{35-55} specific autoreactive T cells within the control groups. The data suggest that the spleen cells from MOG_{35-55} immunised mice have been primed *in vivo* allowing them to recognise the MOG antigen *in vitro* and to produce pro-inflammatory cytokines important in the immunopathogenesis of MS/ EAE (Zorzella-Pezavento *et al*., 2013, Barbour *et al*., 2018). Our data demonstrates increased levels of IFN-γ, IL-17 and IL-6 (Figure 3.10A-C) at EAE onset which further increases as it reaches the peak of the disease before decreasing at the resolution stage. Both IFN-γ and IL-17 have also shown to play an important role in EAE induction as adoptive transferring of myelin-specific Th1 and Th17 cells was able to induce EAE in naïve mice (Merrill *et al*., 1992; Jäger *et al*., 2009). Hence our data agrees with these previous reports that Th1 and Th17 cells play important roles in MS/EAE is development through production of pro-inflammatory cytokines like IFN-γ and IL-17.

Multiple studies have also demonstrated an elevated level of IL-6 within the serum and brain sample from MS patients or EAE animals (Gijbels *et al*., 1990; Maimone *et al*., 1997; Giralt *et al*., 2013). Furthermore, animals deficient with

IL-6 cytokine, e.g. IL-6 gene deficient mice have shown full resistance to EAE, demonstrating its importance in the development of the disease (Samoilova *et al*., 1998). Our study demonstrates an increased production of IL-6 from splenocytes of EAE mice after the MOG_{35-55} re-challenge, thus agreeing with previous studies that IL-6 is important in MS/EAE development. IL-6 is required for the differentiation of Th17 cells, the increased production of both IL-6 and IL-17 by splenocytes of EAE onset and peak mice but not the EAE resolution mice, may further suggest IL-6 mediates EAE development possibly through its role in the differentiation of Th17 cells (Serada *et al*., 2008).

A significant role of IL-10 in MS/EAE remitting phase was evident when IL-10 deficient mice displayed an inability to recover from EAE (Kennedy *et al*., 1992; Cao *et al*., 1999). MS patients suffering from acute relapses demonstrated lower levels of IL-10 mRNA in peripheral blood mononuclear cells while patients with stable disease were shown to have increased IL-10 mRNA (van Boxel-Dezaire *et al.*, 1999). In contrast to IFN-γ, IL-17 and IL-6, we found the levels of antigen specific IL-10 production by splenocytes to be at the lowest at disease onset stage, which increased at day 16 during EAE peak stage but was highest at the resolution stage (Figure 3.10D), which is consistent with the immunoregulatory nature of this cytokine in MS/EAE development.

While the roles of IFN-γ, IL-17, IL-6 and IL-10 in the pathogenesis of MS/EAE are well documented, less is known about IL-16. Several studies suggest an involvement of IL-16 in MS/EAE development and understanding its role may provide new insights into the immunopathogenesis of MS/EAE. Elevated levels of IL-16 expression observed within the peripheral lymphoid organs of severe relapse remitting and low-relapsing EAE model have been linked to the pro-inflammatory function of IL-16, suggesting an important role of IL-16 in MS/EAE regulation and disease progression (Skundric *et al*., 2005). Isolated T cells from spleen and inguinal lymph node of MOG_{35-55} immunised mice have also shown to produce elevated levels of IL-16 upon *in-vitro* re-stimulation with MOG_{35-55} antigen, similarly polyclonally activated naïve splenocytes demonstrated same levels of IL-16 expression in comparison to the control T cell isolated from spleen of non-immunised mice (Skundric *et al*., 2005). Our data demonstrated a production of IL-16 by cells from lymphoid organs from naïve,

PBS or MOG_{35-55} immunised mice, when they were cultured for 24 and 72 hours either with media alone or media supplemented with MOG_{35-55} (Figure 3.11 and 3.12). Surprisingly, none of the groups showed any significant difference with each other even after the MOG_{35-55} antigen re-challenge. It is well studied that spleen and lymph nodes are highly vascular in nature, and they have different compartments which contain distinct regions for immune cells. Leukocytes in the lymphoid organs include different subsets of T and B cells, DCs and macrophages. IL-16 is synthesised by a wide range of immune (T cells, eosinophils, and dendritic cells) and some non-immune cells (fibroblasts, epithelia) in the lymphoid organ and it is released when the cells are stimulated with mitogens, antigens or vasoactive amine (histamine or serotonin) (Cruikshank *et al*., 1994; Baier *et al*., 1997*)*. IL-16 production by the total spleen or lymph node cell population remains unchanged upon in-vitro MOG_{35-55} re-challenge is possibly because the culture contains varieties of immune and non-immune cells which are not specific to MS/EAE but are capable of producing IL-16. This may suggest a functional difference between IL-16 and the other established MS/EAE associated cytokine.

There are not many studies that have shown the expression and distribution of IL-16 in lymphoid organ during MS or any other inflammatory disease but few studies demonstrated that IL-16 is expressed within the peripheral human lymphoid tissues (Chupp et., al 1998; Schwab *et al*., 2001), with lymph nodes expressing majority of the IL-16 in the mantle zone corresponding to the T cells zone, with few cells expressing IL-16 within the follicles in the germinal centre (B cells zone) (Chupp et., al 1998; Schwab *et al*., 2001). Schwab *et al* (2001) also indicated the mRNA expression of IL-16 in spleen tissues (Schwab *et al*., 2001). Since we couldn't determine any differences in levels of production of IL-16 between the lymphoid cells obtained from EAE and the control mice groups we thought it was important to check the distribution and pattern of IL-16 and its receptor expression in the lymphoid organs of naïve, PBS and MOG_{35-55} immunised mice, any changes in distribution and pattern in the three different mice groups may give an insight to its role in MS/EAE. We utilised immunohistochemistry on spleen and lymph node tissue to assess the distribution of IL-16 expression and quantified the percentage of $IL\text{-}16^{+}$ cells using the Image J cell counting tool. In agreement with previous findings we have

also observed expression of IL-16 in all three mice with IL-16 expressed mostly within the red and white pulp of the spleen (Figure 3.13) and within the paracortex and follicle of the lymph node (Figure 3.14) in a clustered form. In addition, distinct expression of IL-16 was also observed within close proximity to the blood vessels in the EAE spleen (Figure 3.13B). When IL-16$^+$ cells were quantified, we observed significantly increased percentage of IL-16$^+$ cells out of the total cells within the tissues collected from the PBS day 16, EAE day 12 and EAE day 16 stage mice in comparison to the naïve control. However, in lymph node tissues a significantly higher percentage of IL-16$^+$ cells were only observed in the tissues of EAE day 16 stage mice in comparison to the naïve controls.

While our data demonstrated comparable levels of IL-16 production by splenocytes in all three mice groups which remained unaltered upon MOG_{35-55} rechallenge. However, IHC staining demonstrated the presence of increased percentage of IL-16$^+$ cells out of total cells in the spleen (PBS day 16, EAE day 12 and 16) and lymph node (EAE day 16) of PBS and MOG_{35-55} immunised mice in comparison to the naïve control (Figure 3.14). Our current understanding is that, while the antigen specific T cells might upregulate its expression of IL-16 after immunisation (Skundric *et al*., 2005) as also shown by IHC in our study, its contribution to the overall production of IL-16 by the whole splenocytes remained undetectable in culture. However, further investigation is required to understand the exact mechanisms contributing in this difference.

As CD4 is the proposed receptor for IL-16, we next assessed the CD4 expression in spleen and lymph node tissues, to check whether the expression level of CD4 correlates with IL-16 expression during EAE. CD4, the receptor for IL-16, is also a marker for T helper cells and an important component of the T cell receptor complex that identifies antigen bound to MHC class II molecules (Janeway., 1991; Koretzky., 2010). Many studies on EAE have already provided convincing evidences on the relation of EAE development with MHC class II allele expression and suggested a pathogenic as well as protective role of CD4$^+$ T cells in MS (Sonobe *et al*., 2007; Fletcher *et al*., 2010). Consistent with the previous studies demonstrating that T cells were restricted to the white pulp of the spleen (Mebius and Kraal, 2005), we too observed CD4

to be expressed within the white pulp of the spleen in all three mice groups, with PBS and EAE day 12 groups demonstrating significantly higher percentage of $CD4^+$ cells in comparison to naïve controls (Figure 3.15), and the level was further increased in EAE day 16 mice tissues. In comparison to naïve mice, the percentage of $CD4^+$ cells in lymph nodes was only observed to be increased in tissues of EAE day 12 and day 16 mice but not PBS day 16 mice or EAE mice during the resolution stage at day 26. The expression pattern and region of distribution observed in all three groups were consistent with what has been reported by others that $CD4^+$ T cells were primarily restricted within the paracortex of lymph node (Figure 3.16). This data further explained that increased expression of $CD4^+$ cells in lymphoid organs correlated with increased IL-16 expression in the lymphoid tissues from PBS and MOG_{35-55} immunised mice. The increased expression of IL-16 and CD4 in the spleen but not the lymph node tissues of PBS immunised mice may suggest a more robust general activation of the immune system in the spleen than the local lymph nodes.

MS/EAE pathogenesis has been shown to correlate with increased serum levels of pro-inflammatory cytokines and often the presence of cytokines in blood serum has been used as biomarker for the disease. Previously the serum level of IL-16 was observed to be highly elevated in MS patients during the remission phase of the disease (Farrokhi *et al*., 2017), in agreement with previous findings we have also observed elevated levels of IL-16 in the serum of MOG_{35-55} immunised mice (Figure 3.17). However, the level of IL-16 was increased at EAE day 12 which gradually reduced at EAE day 16, to a level which was still significantly higher than the naïve and PBS day 16 controls. The up-regulation was decreased at EAE resolution stage and reached the same level as naïve and PBS day 16 controls. This data suggests a correlation of serum IL-16 to the EAE pathogenesis as its level was elevated during the severe disease stages and reduced as the disease started to recover.

To understand the function of IL-16 in CNS inflammatory diseases, it was important to first investigate the expression of IL-16 in spinal cord and the brain. There is evidence of extensive production of both pro-IL-16 and active IL-16 in MS lesion and in the normal appearing grey and white matter of spinal cord

of MS patients (Skundric *et al*., 2006; Skundric *et al*., 2015). Using western blot analysis, both pro and secreted IL-16 have been found to be markedly increased in the spinal cord of MS patients compared with healthy controls (Skundric *et al*., 2006). To assess the protein level of IL-16 in the CNS, we utilised ELISA on supernatants collected from CNS homogenates. And as an approach to look into the regional expression of IL-16 and to further understand its pattern of expression within the CNS tissues we have also carried out immunohistochemical staining. IL-16 was detected in spinal cord homogenates of all three mice groups; however, the level was elevated in spinal cord at EAE day 12 which increased at EAE day 16 before reaching the same level as the controls at resolution stage at day 26 (Figure 3.18A).

This trend was further confirmed using IHC which showed clear expression of IL-16 within the spinal cord tissues (Figure 3.19). The expression pattern of IL-16 within the GM of naïve PBS and EAE mice was similar but during EAE day 12 and day 16, distinctive expression of IL-16 was observed in the WM suggesting an increase in expression of IL-16 with the severity of EAE. Quantification of IL-16^{+} cells revealed a significantly higher percentage of IL-16^{+} cells within the spinal cord of MOG_{35-55} immunised mice at EAE day 12 and day 16 time points, in comparison to the naïve and PBS day 16 controls. And there was no significant difference between naïve and PBS day 16 mice. When the quantification was carried out by regions (GM, WM and lesion) of spinal cord tissue sections, the expression of IL-16 within the GM showed similar level of expression among all three groups. However, when the cells expressing IL-16 in the WM was quantified, an increased percentage of IL-16^{+} cells were primarily found within the inflammatory lesion or equivalent area indicating a direct link between IL-16^{+} cells and cellular infiltration into the CNS. Naïve and PBS controls and EAE day 26 did not demonstrate any lesion or expression of IL-16 within the WM (Figure 3.19G).

When we analysed the protein level of IL-16 within the brain using ELISA, it was detected in naïve, PBS and MOG_{35-55} immunised groups. Since each brain regions are associated with specific functions and often involved in complex roles, we focused particularly on cerebellum and hippocampus, regions

closely associated to MS/EAE. Several reports revealed MS associated damages in cerebellum, and structural and functional alteration of hippocampus (Roosendaal *et al*., 2010; Tornes el al., 2014; Weier *et al*., 2015). Because of the difficulty in isolating hippocampus for preparing tissue homogenates for ELISA assay, cerebellum and rest of the brain were harvested and prepared. Both naïve and PBS control mice tissues demonstrated similar level of IL-16. However elevated level of IL-16 was apparent in MOG_{35-55} immunised mice at day 12 during EAE onset, which then increased at day 16 during peak stage before further reduction at resolution stage (Figure 3.18 B, C). We also analysed *in situ* expression of IL-16 within the brain tissues, it was found to be expressed in different regions of brain tissues in all three mice groups.

Consistent with the ELISA data, increased percentage of IL-16^+ cells were observed within the cerebellum and the hippocampus of MOG_{35-55} immunised mice. Within the hippocampus of all three mice groups, IL-16 was found in CA1, CA2, and CA3 region, predominantly within the pyramidal layers. In addition, IL-16 was also seen to be expressed in the granule cells of the dentate gyrus (Figure 3.21). However, during EAE an increased expression of IL-16 was observed in the surrounding area of dentate gyrus, where the cellular infiltration and the lesions were observed. Within the cerebellum in all three mice groups IL-16 was dispersed throughout the molecular layer and in the granule cells within the granular layer as well as on the purkinje cells near the granule cells, however during EAE IL-16 expression was predominantly found in the WM of the cerebellum where the cellular infiltration and the lesions were observed (Figure 3.22). The data are supported by previous studies which demonstrated the association of IL-16 with patients following focal cerebral infarctions, IL-16 was found to be expressed in brains by infiltrating immune cells including neutrophils, $CD8^+$ T cells and activated $CD68^+$ microglia/macrophages that have accumulated in lesion sites (Schwab *et al*., 2001). Similar to the spinal cord data, the IHC quantification of IL-16^+ cells in brain tissue also revealed an increased IL-16^+ cell percentage in proximity to the inflammatory lesions. However immune infiltration into the brain was less than that observed in the spinal cord and the change of the expression of IL-16 within the brain lesion were also less in comparison to what have been observed in the spinal cord, this suggests alterations in IL-16 expression in the CNS during EAE are

likely to be originated from the immune cell infiltration. Thus, our results of increased expression of IL-16 in CNS tissues of EAE mice at day 12 after immunisation correlates to the clinical and pathological changes during the development of EAE.

We have shown that IL-16 is expressed within the CNS tissues, and the level was significantly increased during the development of EAE. To understand the specific function of IL-16 in neuroinflammation, we also investigated the expression of its receptor CD4 as it is required to exert its function. It is well established that $CD4^+$ T cells are elevated in the CNS of EAE mice (Sonobe *et al*., 2007; Hoglund *et al*., 2014). Our data agreed with previous studies, while the expression of CD4 was found to be absent in naïve and PBS day 16 spinal cord tissues, increased expression was demonstrated in EAE mice tissues. $CD4^+$ cells were first observed in the spinal cord tissues at EAE day 12, and the quantification of the percentage of $CD4^+$ cells demonstrated an increase during the peak of EAE severity at day 16, which later reduced at the resolution stage of EAE at day 26 (Figure 3.20). Similar to the spinal cord, CD4 expression was evident only in the brain sections of MOG_{35-55} immunised mice and the percentage was increased in tissues of EAE peak mice (Figure 3.23 and 3.24). The findings were consistent with the clinical and pathological changes observed during EAE development and confirms our current understanding of the role of $CD4^+$ immune cells in CNS inflammation.

In conclusion, the up-regulation of IL-16 and its receptor observed in the lymphoid organs, and particularly in the CNS tissues of EAE mice in comparison to the naïve and PBS day 16 controls suggest that IL-16 may play a critical role in the development of CNS inflammatory diseases. The positive correlation of IL-16 expression with CD4 receptor in all the tissues of EAE mice indicates an important role of IL-16/CD4 signalling pathway during the neuroinflammation. However, the presence of IL-16 in the CNS tissues of naïve and PBS control groups while its receptor CD4 was absent indicates an alternate function of this cytokine under normal physiological state. Therefore, further study is required to look at the expression of IL-16 by CNS resident cells as well as infiltrating immune cells, which will help us to understand the function of IL-16 cytokine in the CNS under normal and neuroinflammatory conditions.

4.Identifying the types of cells expressing IL-16 in lymphoid and CNS

4.1 Introduction

MS/EAE pathology is characterised by demyelination in the WM and GM of the brain and spinal cord which is known as the lesions and indicates loss of myelin sheaths and ODCs. During the disease, inflammation is present at all stages but pronounced at the peak stage of the disease. The immune system plays a crucial role in the disease pathogenesis, with formation of early lesion by invading peripheral immune cells and leakage of the blood–brain barrier. Even though the exact aetiology is not clear, it is understood that during systemic infection in the periphery naïve T cells get activated by APCs, such as DCs, the activated T cells then differentiate to adopt Th1 or Th17 profile, characterised by the production of IFN-γ and IL-17 respectively (Zamvil & Steinman., 2003; Constantinescu *et al*., 2011; Cheng *et al*., 2017). Once the autoreactive T cells cross the BBB and enter the CNS they are re-stimulated with myelin antigens presented by the local APCs. This then initiates an inflammatory cascade resulting in the activation of CNS resident cells (microglia and astrocytes), the recruitment of additional inflammatory cells (macrophages, NK cells etc) and antibody production by plasma cells that are involved in myelin and axonal damage (Zamvil and Steinman., 2003; Constantinescu *et al*., 2011).

While many immune cells from the systemic inflammatory compartment migrate to the CNS via BBB during MS/EAE and contribute towards the disease pathogenesis, there are many CNS resident cells that are either targeted during the disease or that directly take part in augmenting and inhibiting the disease. Neurons are the major type of cells that make up the CNS. They don't directly participate in the MS/EAE pathogenesis at the early stage of MS/EAE the axons and the neurons are mostly protected, however as the disease progress, they are often damaged through direct or indirect targeting and gradual

neuroaxonal loss occurs which correlates with the clinical symptoms of progressive paralysis. The augmented CNS inflammation, and demyelination of the axon, makes the neurons more vulnerable to damage (Correale *et al*., 2015). Astrocytes on the other hand are the second most abundant CNS resident cells and have demonstrated to undergo activation and proliferation in the WM lesion during CNS inflammation, suggesting playing a critical role in disease progression. Microglia is regarded as the resident immune macrophages of the CNS, which play an important role in inflammatory and immune responses in MS/EAE (Ponomarev *et al*., 2005), and often get activated at very early stage of CNS injury (Kreutzberg., 1996; Luo *et al*., 2017). Destruction of myelin in the CNS has been associated with activated macrophage and microglia in the pathogenesis of MS/EAE (Benveniste *et al*., 1997; Lassmann *et al*., 2007).

In chapter 3, we investigated the expression of IL-16 cytokine in the lymphoid organs and in the CNS under normal and inflammatory conditions using EAE animal model. Our data suggested an increased percentage of IL-16^{+} cells in the lymphoid tissues of both PBS and MOG_{35-55} immunised mice in comparison to the naïve control group. In CNS we demonstrated increased percentage of IL-16^{+} cells in MOG_{35-55} immunised mice in comparison to both naïve and PBS controls and the levels were associated with EAE clinical severity and CNS inflammation. Furthermore, while IL-16 expression was primarily observed in the GM of CNS in all groups of mice, its expression in the WM (particularly in lesions) was only observed in tissues of EAE mice. The altered pattern of IL-16 expression in the CNS of EAE mice suggests a possible change of its expression level and cellular localisation in tissues during inflammation. High levels of IL-16 expression in CNS lesions indicate IL-16 is ikely to be expressed by immune cells (T cells, macrophages, monocytes etc) as well as the CNS resident cells (astrocytes, neurons or microglia). Identification of the phenotype of cells expressing IL-16 in the CNS and in the periphery would help to understand the role of the molecule in CNS inflammation.

Therefore, the aims of this chapter are:

Aim 1: To identify the phenotype of IL-16 expressing immune cells within spleen and lymph node tissues, and whether this changes during systemic and CNS inflammation.

Aim 2: To determine the phenotype of IL-16 expressing CNS resident and infiltrating immune cells with or without CNS neuroinflammation.

4.2 Results

In this chapter we have carried out double fluorescence immunohistochemistry on lymphoid and CNS tissues to distinguish the cell types expressing IL-16. Since we did not observe any difference in percentage of IL-16$^+$ cells within the lymphoid tissues of MOG_{35-55} immunised group over the course of EAE, therefore we have only included the naïve, and PBS or MOG_{35-55} immunised mice at day 16 post immunisation for co-localisation study in lymphoid organs. However, for studies in CNS we have included both naïve and PBS day 16 controls as well as all the time points of EAE mice (day 12, 16 and 26).

4.2.1 IL-16 expression on CD45$^+$ cells in spleen and lymph node tissues

Having established that IL-16 is expressed by spleen and lymph node cells in all the examined animal groups, we next used double immunofluorescence staining with CD45 and IL-16 in the spleen and lymph node tissues of naïve, PBS day 16 and EAE day 16 mice and studied the whether systemic and CNS inflammation changes the expression pattern of IL-16. Expression of IL-16 by CD45$^+$ cells was observed in both spleen (Figure 4.1) and lymph node (Figure 4.2) tissues from all groups of mice, and there was an increase in the CD45$^+$IL-16$^+$ cells in PBS and EAE tissues. However not all CD45$^+$ cells co-expressed IL-16 and only some IL-16$^+$ cells were co-localised with CD45$^+$ cells. We next quantified the percentage of CD45$^+$IL-16$^+$ cells out of the total CD45$^+$ cell population within the comparable ROI in the tissue sections using the Image J. In the spleen tissues of PBS day 16 (16 ± 1%) and EAE day 16 (20 ± 1%) mice the percentages were significantly higher compared to that of naïve (4 ± 0.5%) mice. But there was no difference between the PBS day 16 and EAE day 16 mice groups (Figure 4.1D).

In the lymph node tissues, the percentage of CD45$^+$ IL-16$^+$ cells were 20 ± 1% and 20 ± 1.8% respectively for PBS day 16 and EAE day 16 groups, both significantly higher in comparison to naïve (4 ± 0.5%) mice. Again, there was no difference between PBS day 16 and EAE groups (Figure 4.2D).

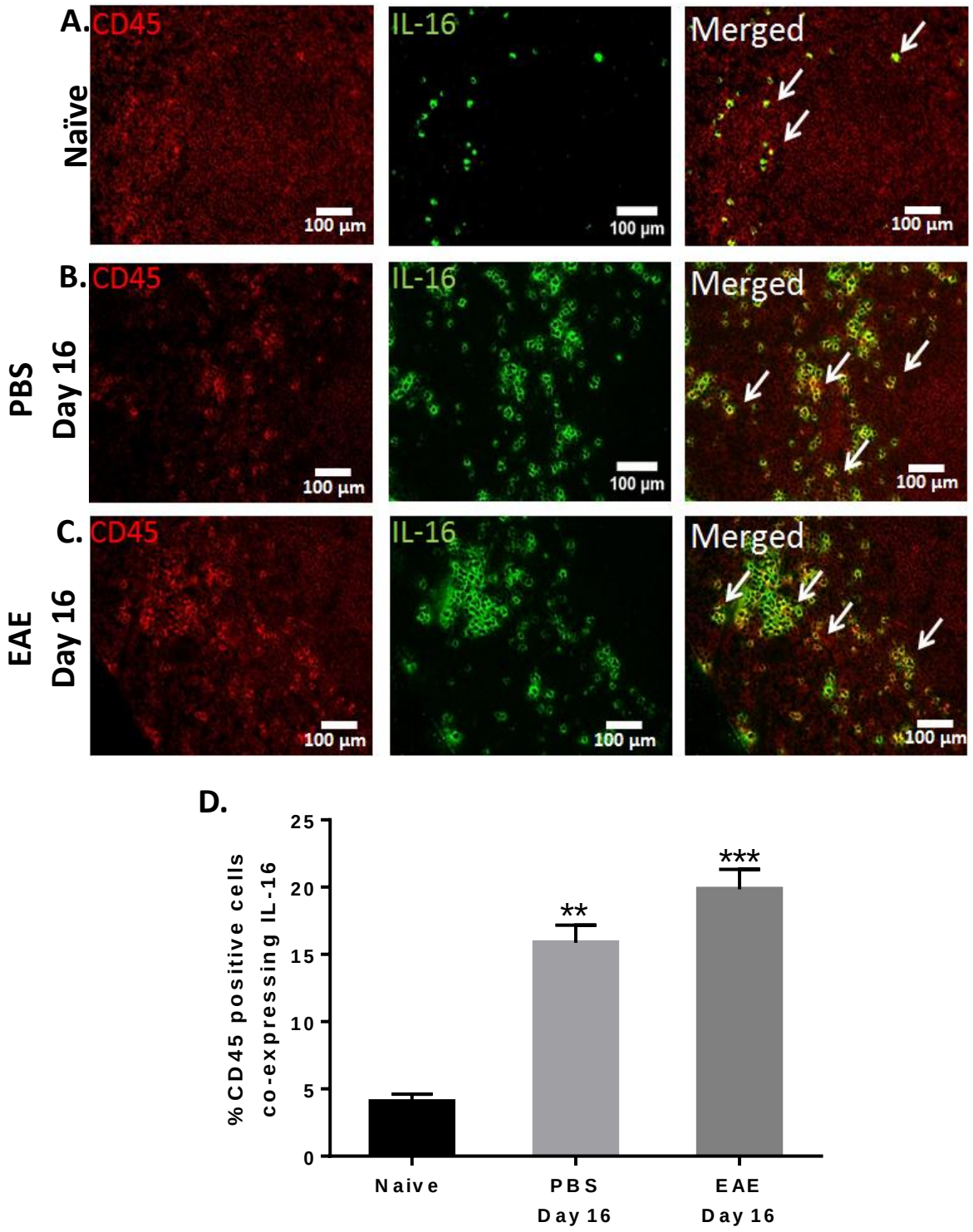

Figure 4.1: Expression of IL-16 by CD45⁺ cells in the spleen tissues of naïve, PBS and EAE mice*. Lymph nodes were harvested from* ***(A)*** *naïve, and* ***(B)*** *PBS or* ***(C)*** *MOG_{35-55} immunised mice at day 16 post immunisation and the tissues stained with anti-IL-16 (Green) and anti-CD45 (Red). Data are representative of each group. n=3 for all groups. Images X20 magnification, scale bars = 100µm.* ***(D)*** *Percentage of IL-16 expressing $CD45^+$ cells within the total $CD45^+$ cell population in the spleen tissue sections of naïve, PBS and EAE spleen tissues has been quantified using the cell counter tool of Image J software and result expressed as mean ± S.E.M. Statistical significance was determined by one-way ANOVA with Bonferroni post-hoc**P <0.01, ***P<0.001 versus naïve.*

.

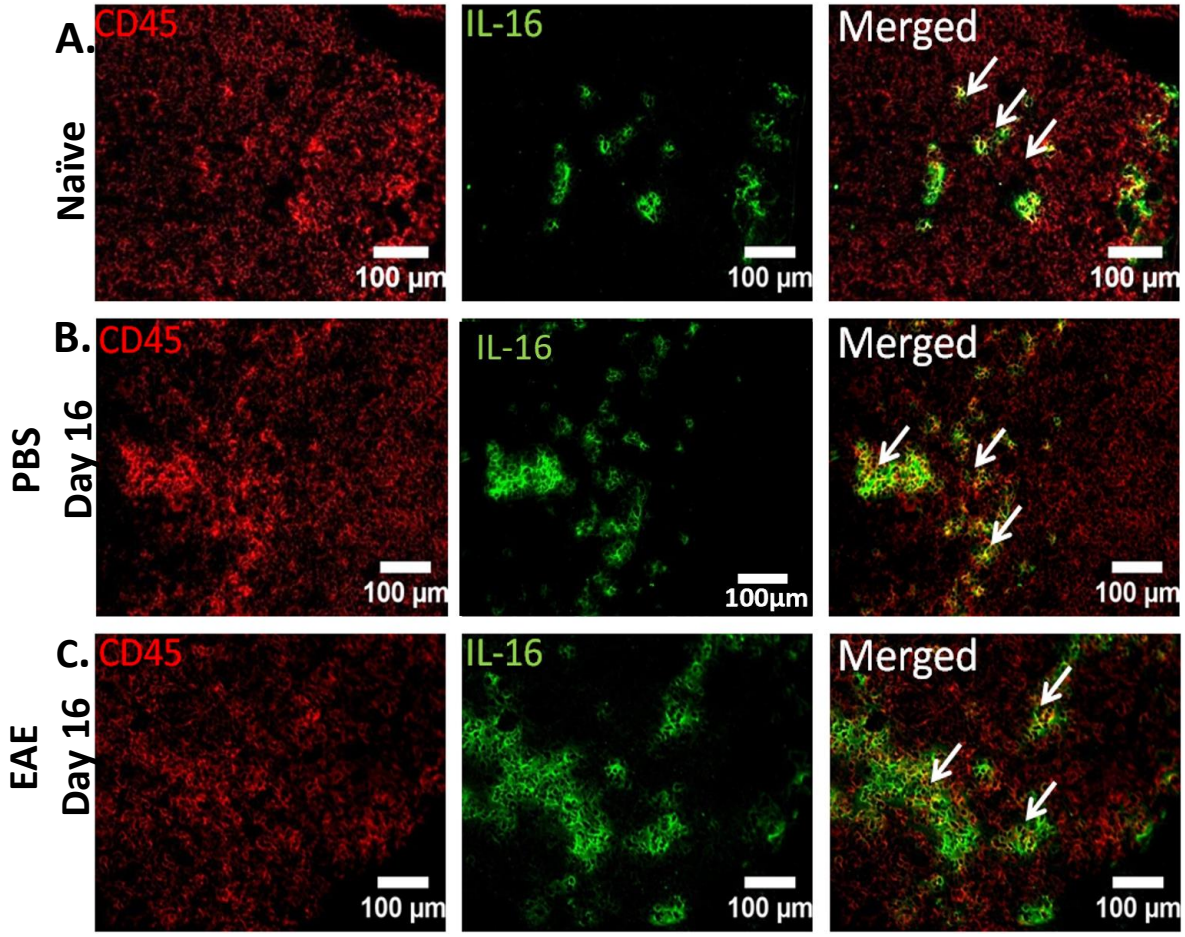

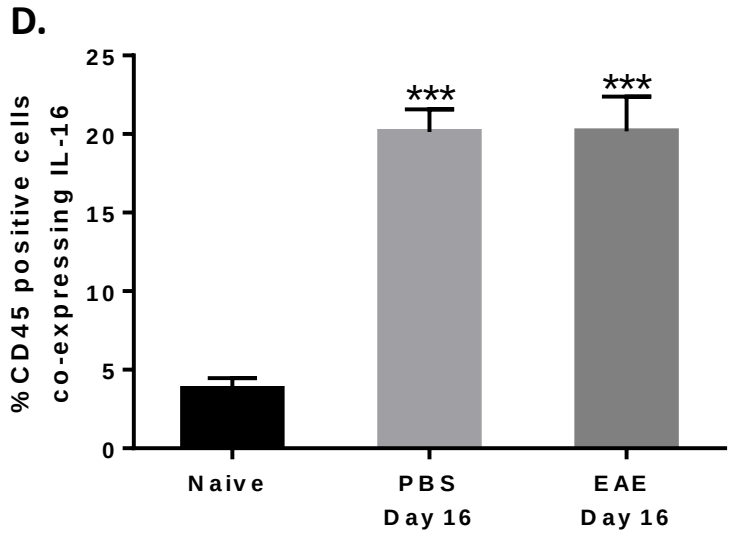

Figure 4.2: ***Expression of IL-16 by CD45⁺ cells in the lymph node tissues of naïve, PBS and EAE mice***. *Lymph nodes were harvested from* ***(A)*** *naïve and* ***(B)*** *PBS or* ***(C)*** *MOG_{35-55} immunised mice at day 16 post immunisation and the tissues stained with anti-IL-16 (Green) and anti-CD45 (Red). Data are representative of each group. n=3 for all groups. Images X20 magnification, scale bars = 100µm.* ***(D)*** *Percentage of IL-16 expressing $CD45^+$ cells within the total $CD45^+$ cell population in naïve, PBS and EAE lymph node tissues has been quantified using the cell counter tool of Image J software and result expressed as mean ± S.E.M. Statistical significance was determined by one-way ANOVA with Bonferroni post-hoc. ***P<0.001 versus naïve.*

4.2.2 IL-16 expression on $CD4^+$ cells in spleen and lymph node tissues

Following the observation of immune cells (CD45) co-expressing IL-16, next we wanted to determine the specific types of the immune cells such as $CD4^+$ T cells, which is the key mediator of MS/EAE disease, and CD4 is also the receptor required for IL-16 signalling and function.

IL-16 was observed to be expressed by some $CD4^+$ cells in both spleen (Figure 4.3) and lymph node (Figure 4.4) tissues from the three different mice groups. However not many IL-16^+ cells were co-localised with $CD4^+$ cells and therefore the percentage of $CD4^+$ IL-16^+ cells were comparatively low as confirmed through analysis of the percentage of the IL-16^+ $CD4^+$ cells out of the total $CD4^+$ cells, in the comparable ROI of spleen tissue sections. However, the percentage of IL-16^+ $CD4^+$ cells in the PBS day 16 (4 ± 0.5%) and EAE day 16 (5 ± 0.3%) mice was significantly higher compared to that of naïve (1.3 ± 0.2%) mice. And there was no difference between PBS day 16 and EAE day 16 mice group mice (Figure 4.3D).

In lymph node tissues, the percentage of IL-16^+ $CD4^+$ cells in the EAE day 16 (7 ± 1%) but not the PBS day 16 (6 ± 1%) mice was significantly higher compared with that of the naïve (1 ± 0.3%) mice. And no difference was observed between PBS day 16 and EAE mice (Figure 4.4D).

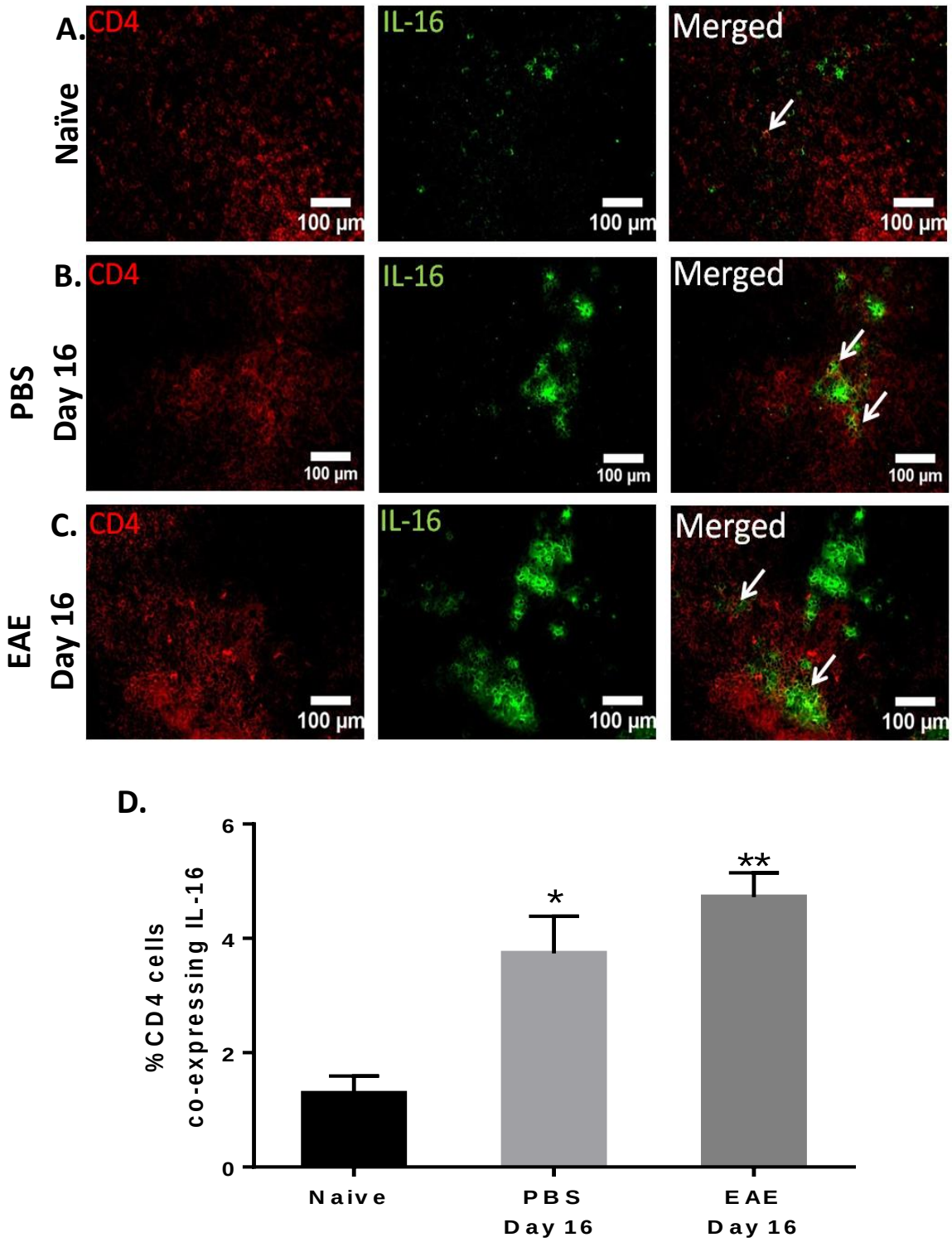

Figure 4.3: Expression of IL-16 by CD4⁺ cells in the spleen tissues of naïve, PBS and EAE mice. *Spleens were harvested from* ***(A)*** *naïve and* ***(B)*** *PBS or* ***(C)*** *MOG_{35-55} mice at day 16 post immunisation and the tissues were stained with anti-IL-16 (Green) and anti-CD4 (Red). Data are representative of each group. n=3 for all groups. Images X20 magnification, scale bars = 100µm.* ***(D)*** *Percentage of IL-16 expressing $CD4^+$ cells within the total $CD4^+$ cell population in naïve, PBS and EAE spleen tissues has been quantified using the cell counter tool of Image J software and result expressed as mean ± S.E.M. Statistical significance was determined by one-way ANOVA with Bonferroni post-hoc. *P<0.05, **P <0.01 versus naïve.*

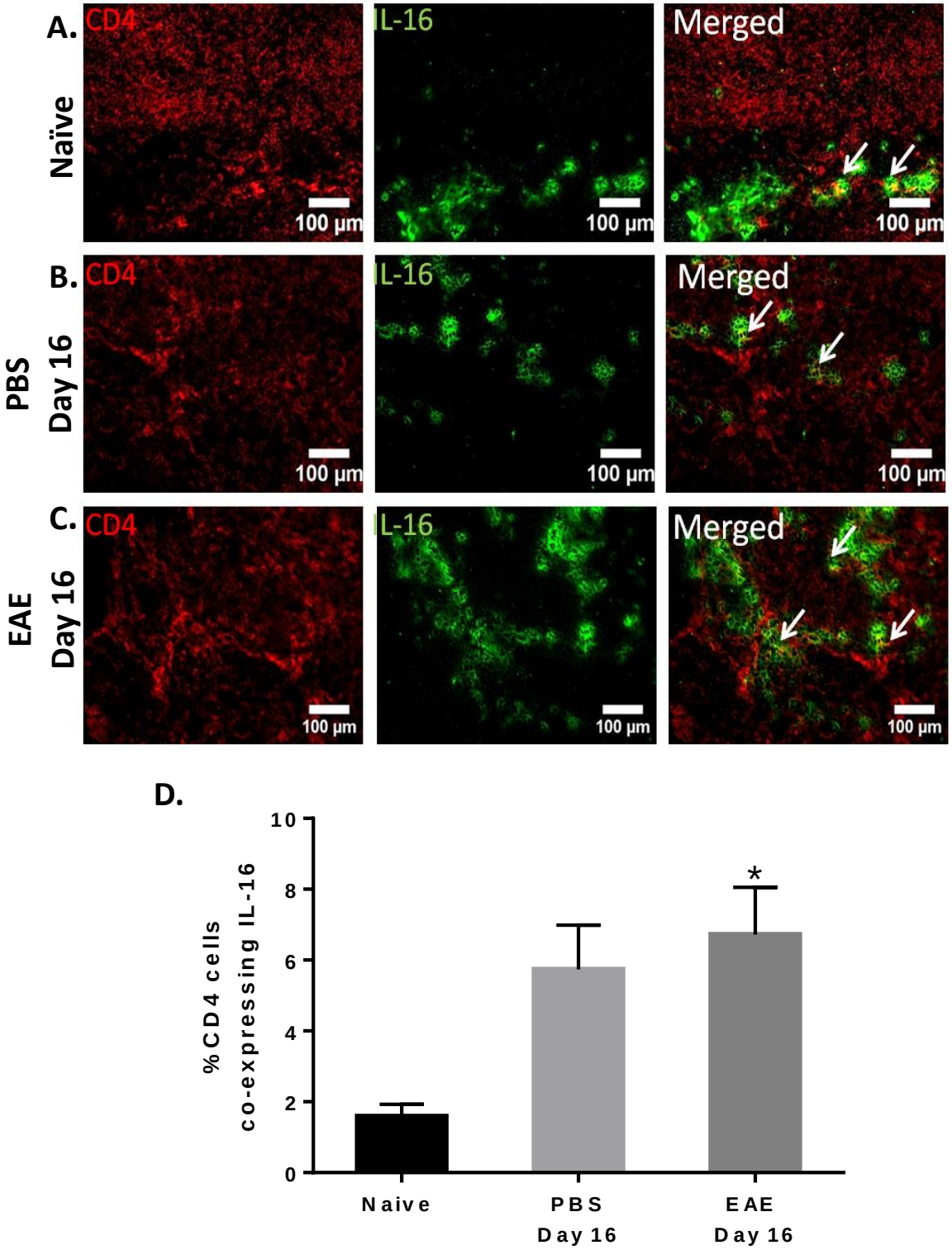

Figure 4.4: Expression of IL-16 by CD4⁺ cells IL-16 in the lymph node tissue s of naïve, PBS and EAE mice*. Lymph nodes were harvested from* ***(A)*** *naïve and* ***(B)*** *PBS or* ***(C)*** *MOG_{35-55} immunised mice at day 16 post immunisation and the tissues were stained with anti-IL-16 (Green) and anti-CD4 (Red). Data are representative of each group. n=3 for all groups. Images X20 magnification, scale bars = 100µm.* ***(D)*** *Percentage of IL-16 expressing $CD4^+$ cells within the total $CD4^+$ cell population in naïve, PBS and EAE lymph node tissues has been quantified using the cell counter tool of Image J software and result expressed as mean ± S.E.M. Statistical significance was determined by one-way ANOVA with Bonferroni post-hoc. *P<0.05 versus naïve.*

4.2.3 IL-16 expression by Th1 and Th17 splenic cells during EAE

IL-16 is thought to be predominantly produced by T cells and with co-localisation staining we have demonstrated that some $CD4^+$ cells express IL-16 in both spleen and lymph nodes of naïve, PBS and MOG immunised mice. To further determine the type of T cell subsets involved in producing IL-16, we next utilised FACS analysis to assess the expression of IL-16 in $CD4^+$ subsets: Th1 and Th17 cells on splenocytes derived from PBS and MOG_{35-55} immunised mice at day 16 post immunisation.

Our data revealed the percentage of IL-16 expressing $CD4^+$ cells out of the total $CD4^+$ population was significantly increased in MOG_{35-55} immunised mice with 1.4 ± 0.11% in comparison to 0.76 ± 0.07% in the PBS immunised mice group (Figure 4.5A). But when we assessed the percentage of $CD4^+$ cells within the total spleen cell population, there was no significant difference between the PBS (10.4 ± 0.3%) and MOG_{35-55} (11.6 ± 0.8%) immunised groups (Figure 4.5B) which is consistent to our data in Chapter 3.

To determine if the Th17 and Th1 subsets express IL-16, CD4 population was gated and expression of IL-16 by IL-17 and IFN-γ expressing cells was analysed. When we assessed Th17 cells, no difference in percentage of $CD4^+$ cells expressing IL-17 alone or IL-17 and IL-16 together was observed between the PBS day 16 (3.1 ± 0.1% and 1.3 ± 0.2% respectively) and the EAE day 16 (3.3 ± 0.6% and 1.9 ± 0.2% respectively) groups (Figure 4.5C).

Similar pattern of expression was also observed in Th1 cells, with no difference in the percentage of $CD4^+$ cells expressing IFN-γ alone or IFN-γ and IL-16 together between the PBS day 16 (3.2 ± 0.3% and 2.7 ± 0.2% respectively) and EAE day 16 (3.4 ± 0.3% and 3.1 ± 0.2% respectively) MOG immunised groups (Figure 4.5D).

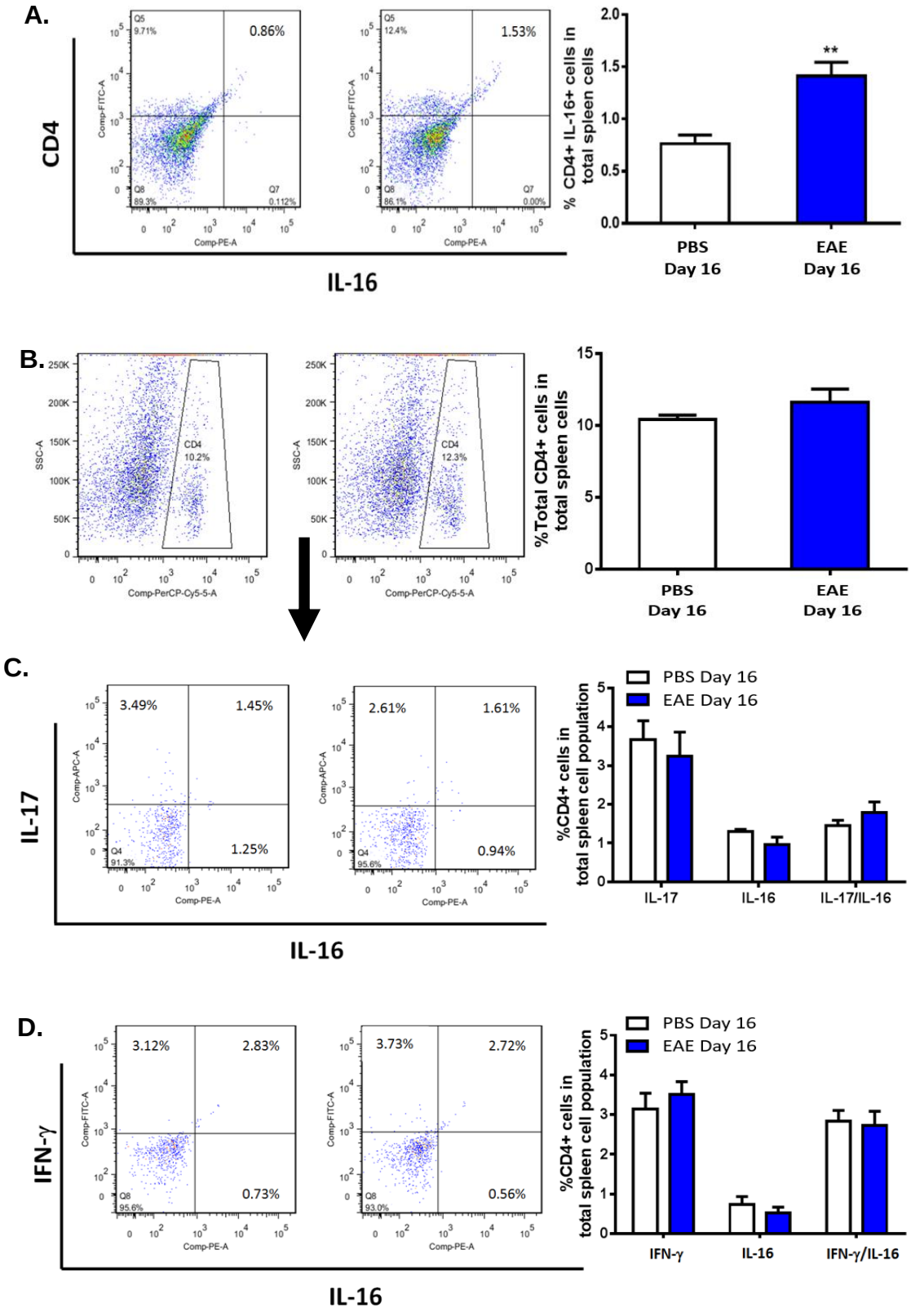

Figure 4.5 IL-16 expression by Th1 and Th17 CD4+ T cell subsets within the spleen: *Spleen cells collected from PBS and MOG_{35-55} immunised mice at day 16 post immunisation was stained for FACS analysis of (A) CD4 and IL-16, (B) CD4, (C) IL-17 and IL-16, and (D) IFN-γ and IL-16. Data are representative of each group, PBS n=5 and EAE n=5. Result illustrated as mean ± S.E.M. Statistical significance was determined by one-way ANOVA with Bonferroni post hoc test **P <0.01 versus PBS.*

4.2.4 IL-16 expression on CD11b$^+$ cells in spleen and lymph nodes tissues

The fact that some but not all IL-16$^+$ cells are CD4$^+$ T cells suggest IL-16 is also expressed by other immune cells. We utilised double fluorescence staining with CD11b and IL-16 in the spleen and lymph node tissues of naïve, PBS day 16 and EAE day 16 mice and studied is expression by monocytes/macrophages.

IL-16 was observed to be expressed by some but not all CD11b$^+$ cells in both spleen (Figure 4.6) and lymph node (Figure 4.7) tissues in all three mice groups. However similar to CD4$^+$ cells, not many CD11b$^+$ cells expressed IL-16. We next quantified the percentage of CD11b$^+$ cells expressing IL-16 out of the total CD11b$^+$ cells in the comparable ROI in the tissue sections. In the PBS day 16 (34 ± 2%) and EAE day 16 (37 ± 2%) mice the percentage CD11b$^+$ IL-16$^+$ cells were significantly higher compared to that of naïve (23 ± 0.7%) mice spleen tissues. But there was no difference between the PBS day 16 and EAE day 16 mice groups (Figure 4.6D).

Similarly, the percentage of CD11b$^+$ IL-16$^+$ cells out of the total CD11b$^+$ cells in the comparable ROI in the lymph node tissues of PBS day 16 (28 ± 1%) and EAE day 16 (30 ± 0.8%) mice was significantly higher in comparison to that of the naïve (15 ± 1%) mice. And there was no difference between the PBS and EAE (Figure 4.7D).

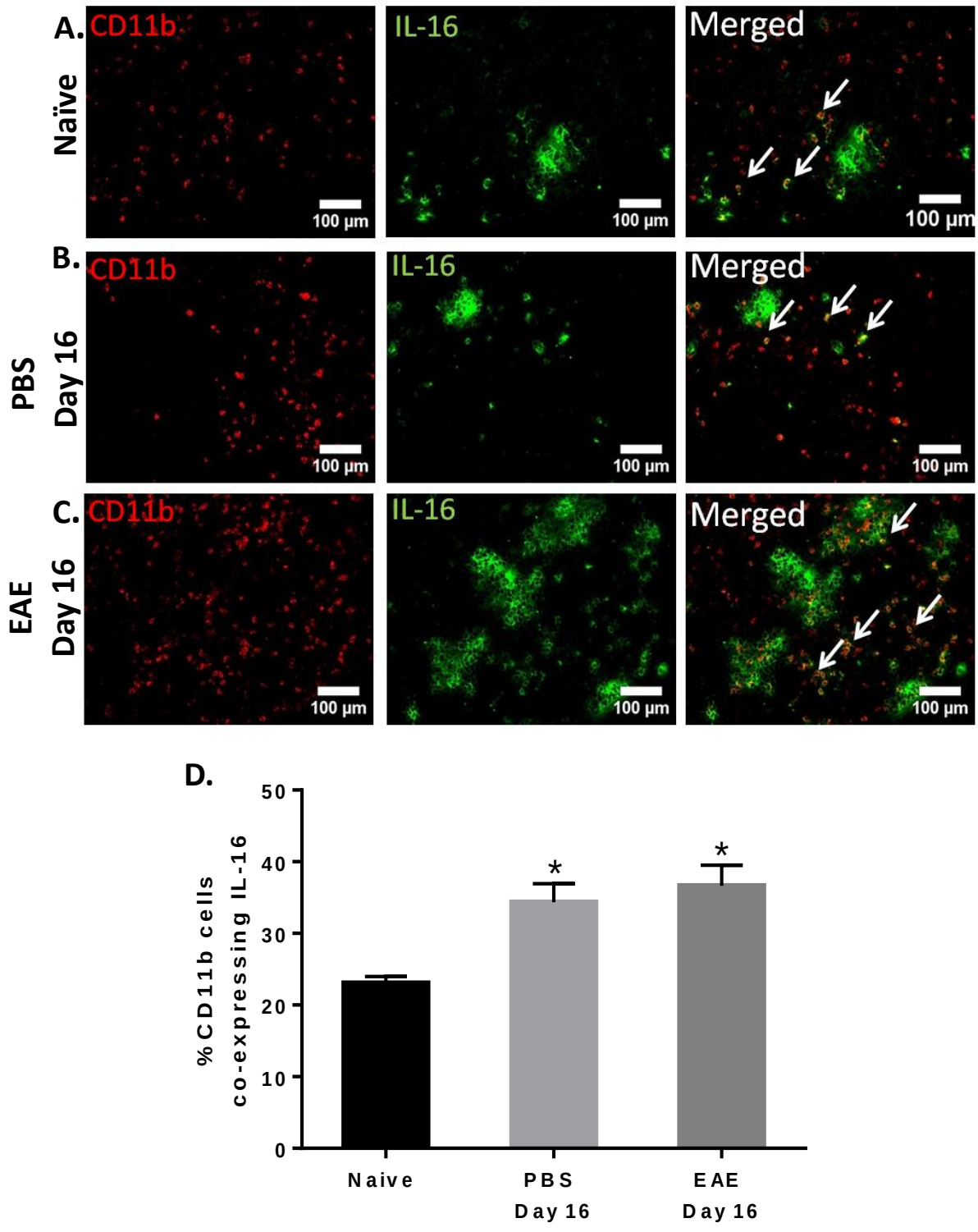

Figure 4.6: ***Expression of IL-16 by CD11b⁺ cells in the spleen tissues of naïve, PBS and EAE mice.*** *Spleen were harvested from* ***(A)*** *naïve* ***(B)*** *PBS and* ***(C)*** *MOG_{33-55} immunised mice at day 16 post immunisation and the tissues were stained with anti-IL-16 (Green) and anti-CD11b⁺ (Red). Data are representative of each group. n=3 for all groups. Images X20 magnification, scale bars = 100µm.* ***(D)*** *Percentage of IL-16 expressing CD11b⁺ cells within the total CD11b⁺ cell population in naïve, PBS and EAE spleen tissues has been quantified using the cell counter tool of Image J software and result expressed as mean ± S.E.M. Statistical significance was determined by one-way ANOVA with Bonferroni post-hoc. *P<0.05 versus naïve.*

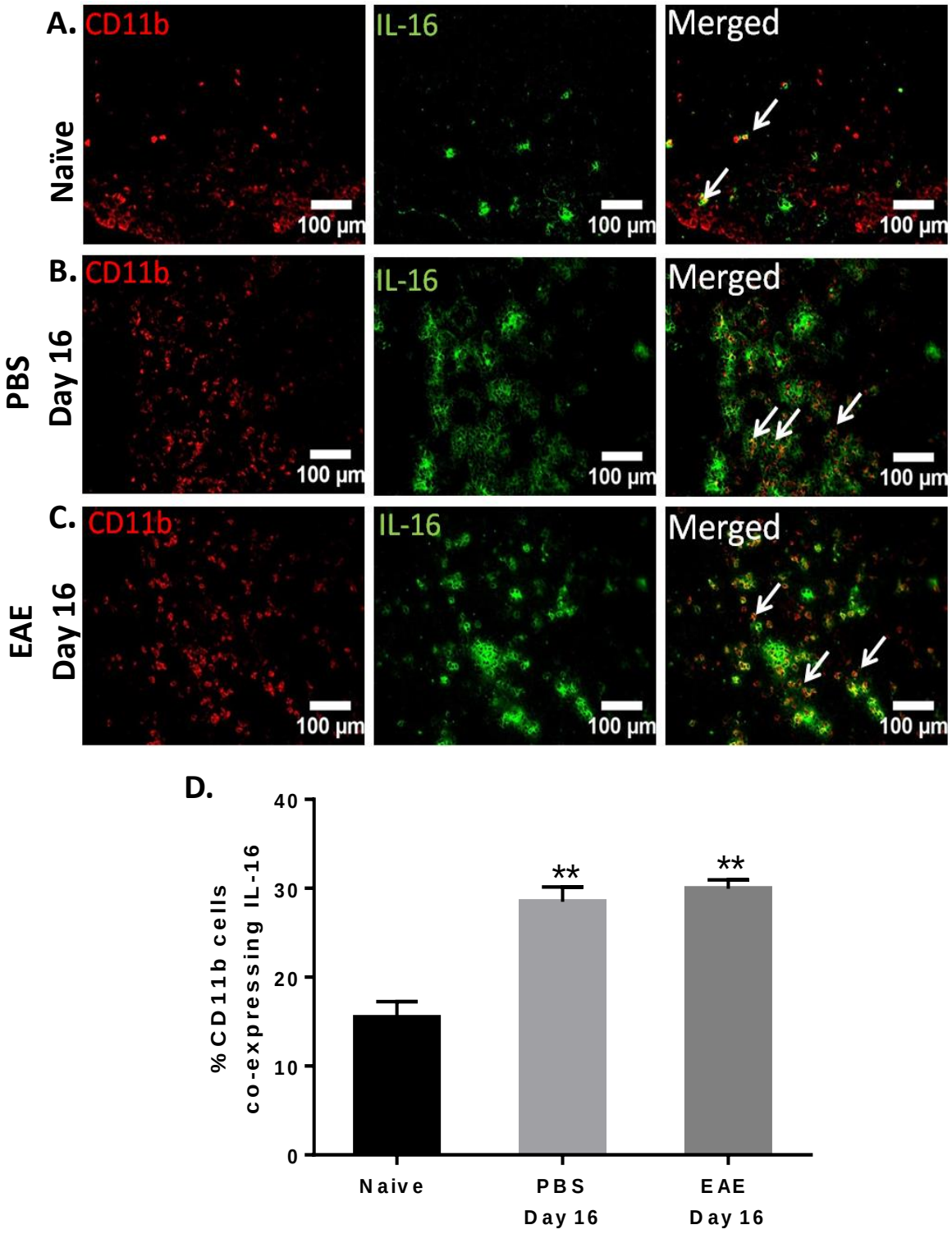

Figure 4.7: ***Expression of IL-16 by CD11b$^+$ cells in the lymph node tissues of naïve, PBS and EAE mice.*** *Lymph nodes harvested from* ***(A)*** *naïve and* ***(B)*** *PBS or* ***(C)*** *MOG_{35-55} immunised mice at day 16 post immunisation and the tissues were stained with anti-IL-16 (Green) and anti-CD11b$^+$ (Red). Data are representative of each group. n=3 for all groups. Images X20 magnification, scale bars = 100µm.* ***(D)*** *Percentage of IL-16 expressing CD11b$^+$ cells within the total CD11b$^+$ cell population in naïve, PBS and EAE lymph node tissues has been quantified using the cell counter tool of Image J software and result expressed as mean ± S.E.M. Statistical significance was determined by one-way ANOVA with Bonferroni post-hoc. **P <0.01 versus naïve.*

4.2.5 IL-16 expression on F4/80^{+} cells in spleen and lymph node tissues

We next utilised double immunofluorescence staining with F4/80 and IL-16 to examine if mature macrophages express IL-16 in the spleen and lymph node tissues of naïve, PBS day 16 and EAE day 16 mice.

IL-16 was observed to be expressed by some F4/80^{+} cells in both spleen (Figure 4.8) and lymph node (Figure 4.9) tissues in all three mice groups. Quantification of the percentage of F4/80^{+}IL-16^{+} cells out of the total F4/80^{+} cells in the comparable ROI in tissues sections demonstrated that spleen tissues from EAE day 16 (13 ± 0.3%) mice had significantly higher percentage of F4/80^{+}IL-16^{+} cells than that of the naïve (9 ± 1%) mice, however there was no difference between the PBS day 16 (12% ± 0.4%) and the naïve controls or EAE day 16 mice groups (Figure 4.8D).

Lymph node tissues of PBS day 16 (9 ± 0.9%) and EAE day 16 (10 ± 0.3%) mice demonstrated significantly higher co-expression with F4/80 in comparison to the lymph node tissues of naïve (5 ± 0.6%) mice, but there was no difference between the co-expression observed with in the lymph node tissues of PBS day16 and EAE day 16 mice groups (Figure 4.9D).

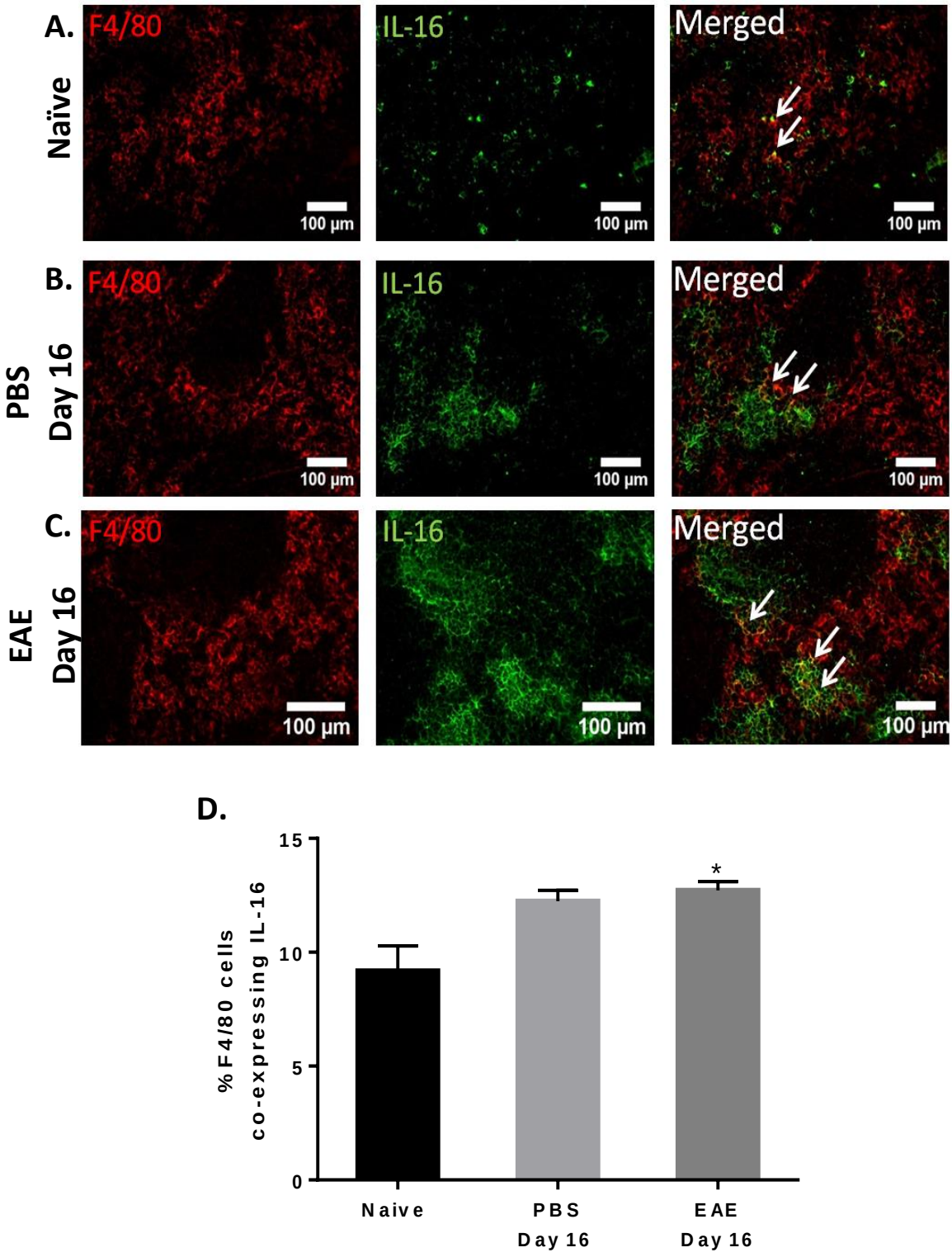

Figure 4.8: Expression of IL-16 by F4/80⁺ cells in the spleen tissues of naïve, PBS and EAE mice. *Spleens were harvested from **(A)** naïve and **(B)** PBS or **(C)** MOG_{35-55} immunised mice at day 16 post immunisation and the tissues were stained with anti-IL-16 (Green) and anti-F4/80⁺ (Red). Data are representative of each group. n=3 for all groups. Images X20 magnification, scale bars = 100µm. **(D)** Percentage of IL-16 expressing F4/80⁺ cells within the total F4/80⁺ cell population in naïve, PBS and EAE spleen tissues has been quantified using the cell counter tool of Image J software and result expressed as mean ± S.E.M. Statistical significance was determined by one-way ANOVA with Bonferroni post-hoc. *P<0.05 versus naïve.*

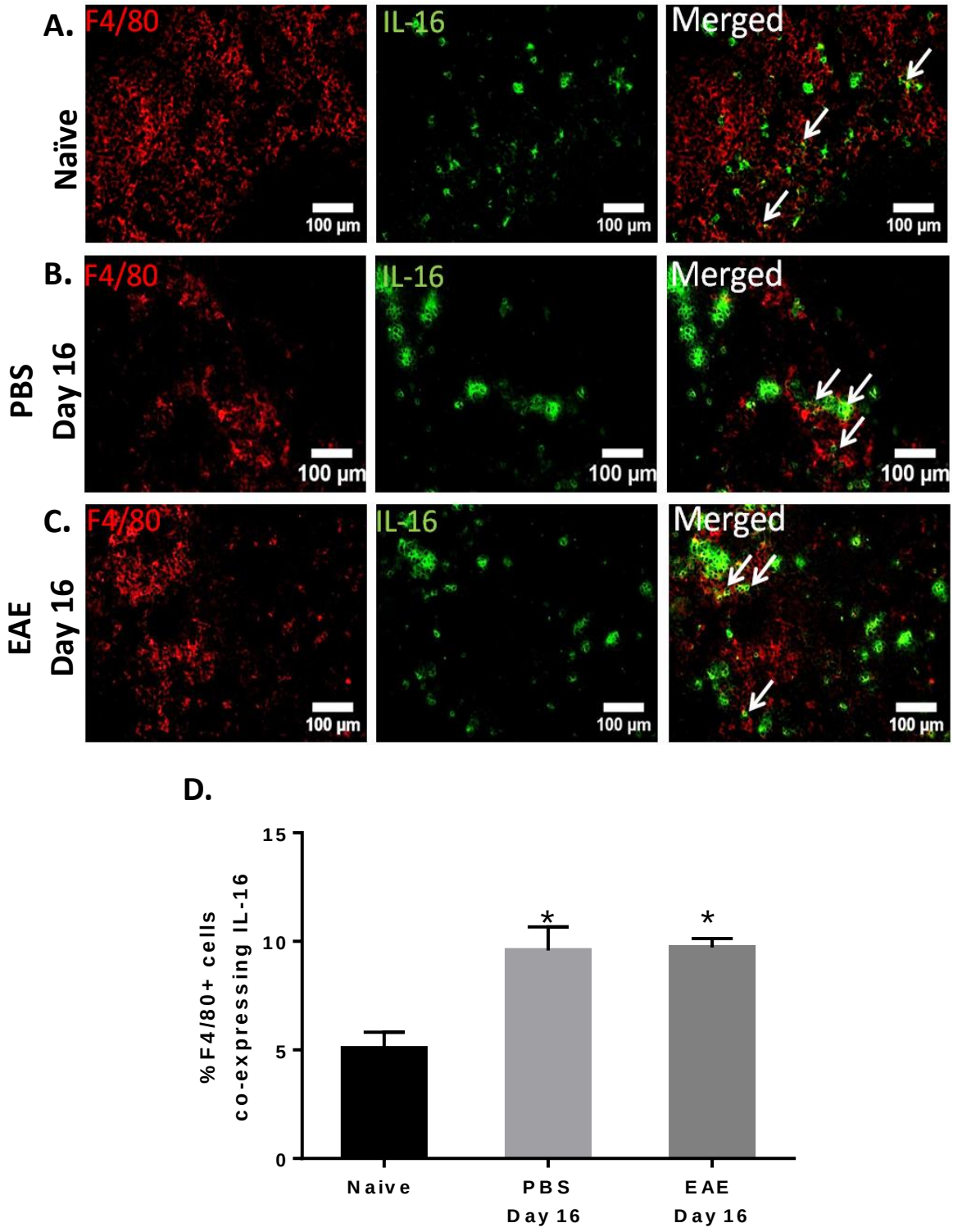

Figure 4.9: ***Expression of IL-16 by F4/80⁺ cells in the lymph node tissues of naïve, PBS and EAE mice****. Lymph nodes were harvested from* ***(A)*** *naïve and* ***(B)*** *PBS or* ***(C)*** *MOG_{35-55} immunised mice at day 16 post immunisation and the tissues were stained with anti-IL-16 (Green) and anti-F4/80⁺ (Red). Data are representative of each group. n=3 for all groups. Images X20 magnification, scale bars = 100µm.* ***(D)*** *Percentage of IL-16 expressing F4/80⁺ cells within the total F4/80⁺ cell population in naïve, PBS and EAE lymph node tissues has been quantified using the cell counter tool of Image J software and result expressed as mean ± S.E.M. Statistical significance was determined by one-way ANOVA with Bonferroni post-hoc. *P<0.05 versus naïve.*

4.2.6 Expression of IL-16 on CD45$^+$ cells in spinal cord tissues

The infiltrating immune cells forming the lesions in the CNS include a variety of activated immune cells such as CD4$^+$ and CD8$^+$ T cells, B cells, and monocytes/macrophages. In chapter 3 we have demonstrated the accumulation of immune cells within the lesions of EAE spinal cord tissue sections and IL-16 is shown to be expressed by several types of immune cells in the spleen and lymph nodes (Figures 4.1-4.9). Next, we investigated if these infiltrating immune cells in the CNS tissues expressed IL-16 using double immunofluorescence staining in tissues of naïve mice, PBS immunised mice at day 16 post immunisation and MOG_{35-55} immunised mice at day 12, day 16 and day 26 post immunisation.

There was no co-localisation of IL-16 with CD45 within the white matter of naïve and PBS spinal cord tissue sections due to the absence of both CD45 and IL-16 within this region. However, IL-16 was expressed by CD45$^+$ cells within the lesions predominantly in the white matter of spinal cord tissues in all EAE group mice (Figure 4.10). Quantification of the percentage of CD45$^+$ IL-16$^+$ cells out of the total CD45$^+$ cells in the comparable ROI revealed no difference between the naïve and PBS day 16 mice. However, spinal cord tissue sections from EAE day 12 (14 ± 1%) and EAE day 16 (15 ± 1%) demonstrated significantly higher percentage in comparison to the EAE day 26 (8 ± 0.9%) mice (Figure 4.10F).

A. Naïve

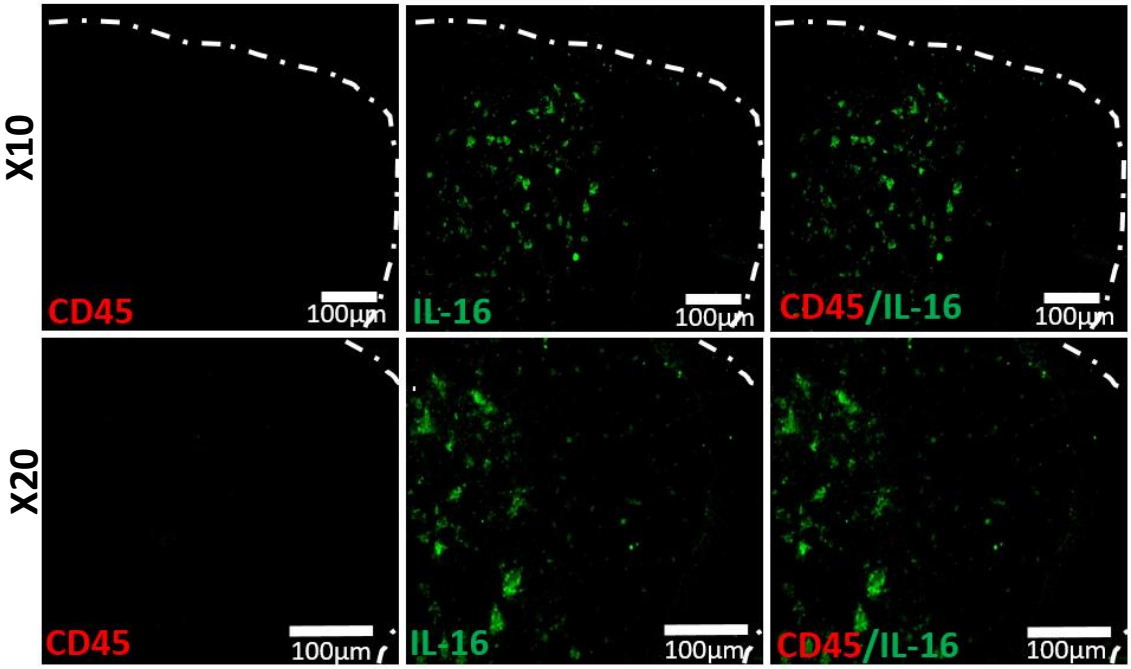

B. PBS Day 16

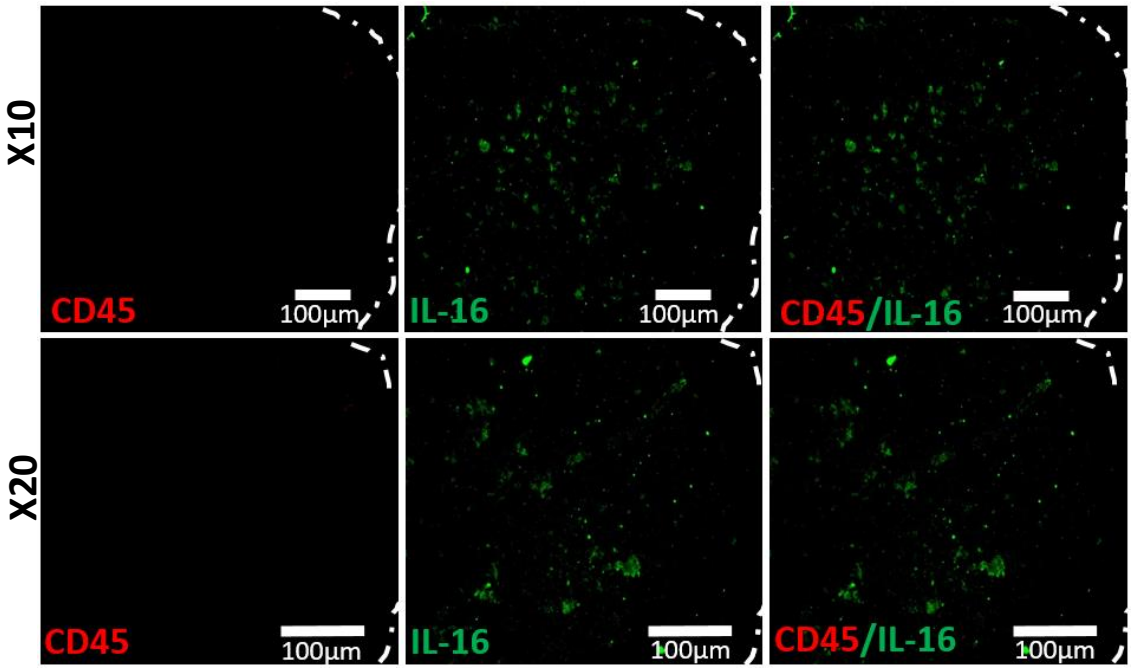

C. EAE Day 12

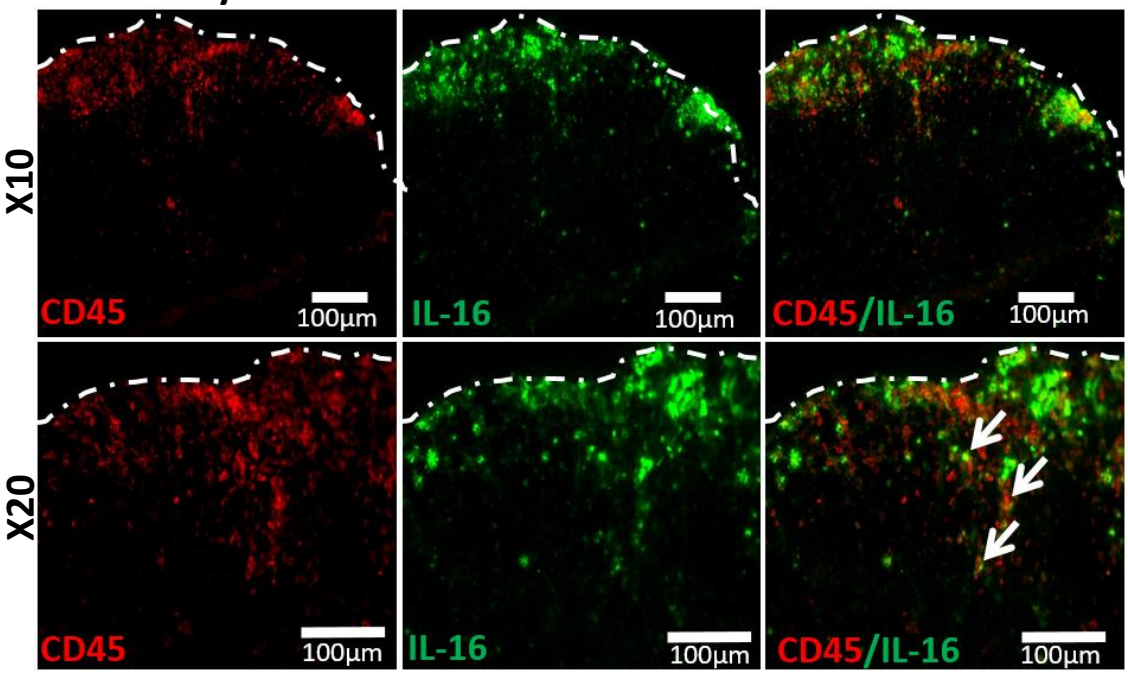

D. EAE Day 16

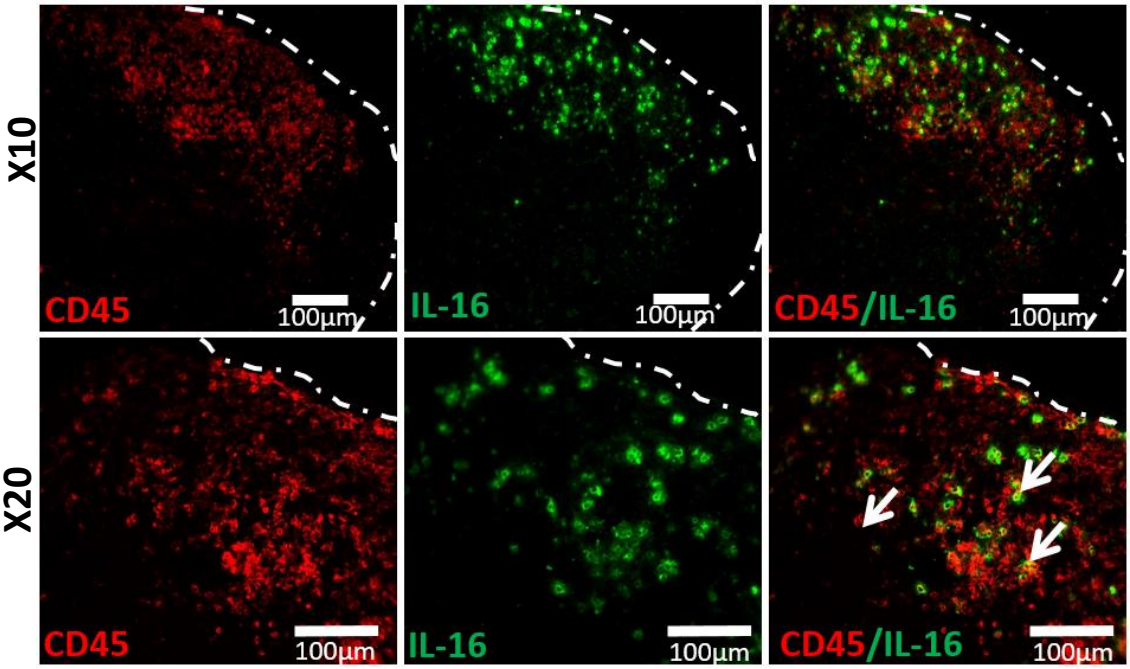

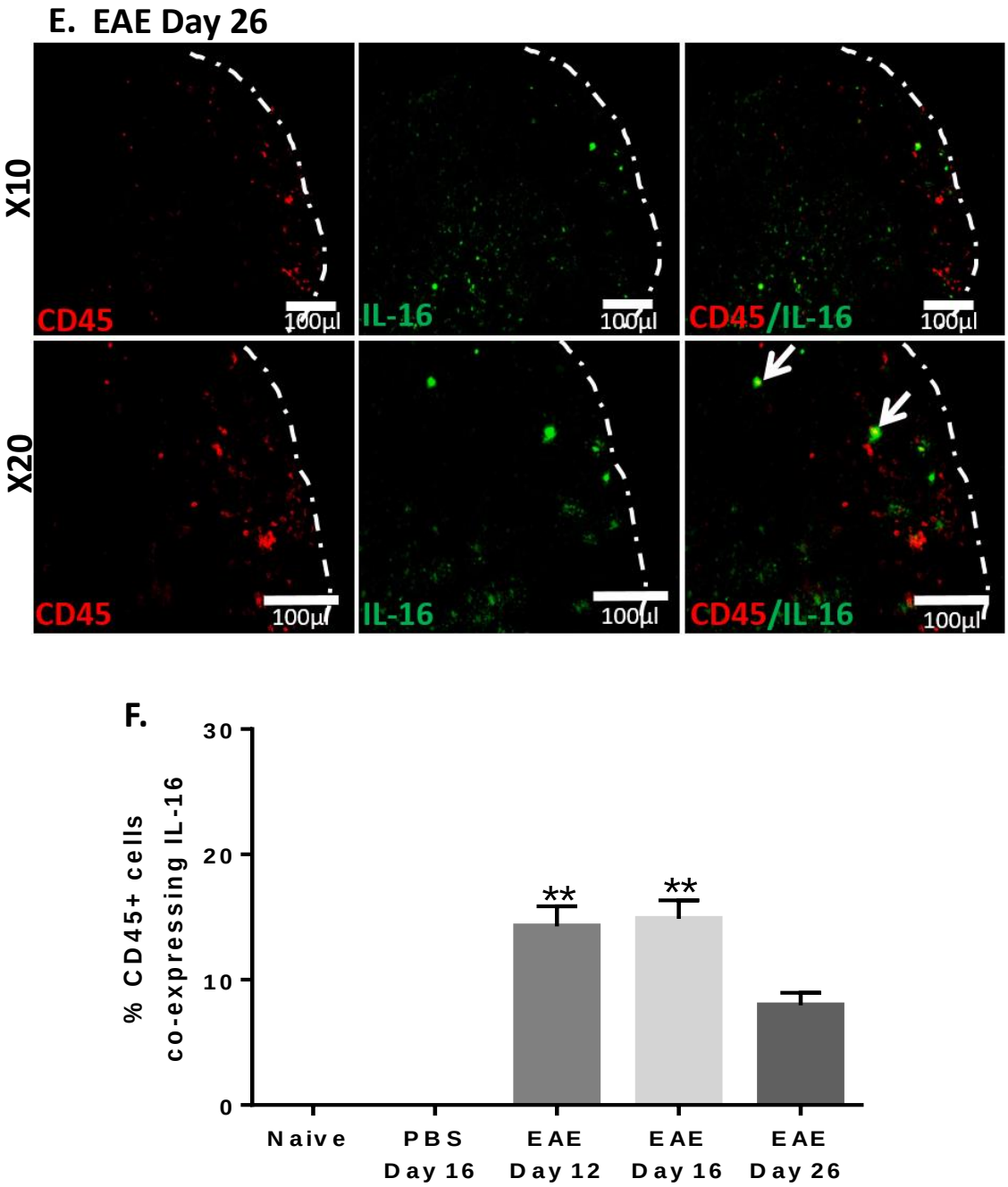

Figure 4.10: Expression of IL-16 by CD45⁺ cells in the spinal cord tissues of naïve, PBS and EAE mice. *Spinal cords were harvested from **(A)** naïve **(B)** PBS day 16 and EAE **(C)** day 12 **(D)** day 16 and **(E)** day 26 mice and the tissues were stained with anti-IL-16 (Green) and anti-CD45⁺ (Red). Data are representative of each group. n=5 for all groups. Primary images x10 and secondary images X20 magnification, scale bars = 100µm. Dotted white line indicating the edge of the tissue section **(F)** Percentage of IL-16 expressing CD45⁺ cells within the total CD45⁺ cell population in naïve, PBS and EAE spinal cord tissues has been quantified using the cell counter tool of Image J software and result expressed as mean ± S.E.M. Statistical significance was determined by one-way ANOVA with Bonferroni post-hoc. **P <0.01 versus EAE day 26.*

4.2.7 IL-16 expression on $CD4^+$ cells in spinal cord tissues

$CD4^+$ T cells are the key immune cells that are thought to orchestrate and drive the immune response resulting in inflammation within CNS during MS/EAE. T cells not specific for myelin antigens can enter the CNS but only T cells specific for CNS antigens are able to persist within the CNS and initiate the recruitment of other inflammatory cells (Nowak *et al*., 2009; Sayed *et al*., 2010).

Having shown that the spinal cord of naïve and PBS immunised mice had no $CD45^+$ cells to express IL-16 and that many $CD45^+$ cells in the spinal cord of MOG_{35-55} immunised co-expressed IL-16, we next planned to examine the specific phenotype of infiltrating immune cells using double immunofluorescence staining. Out data showed that $CD45^+$ cells were absent within the spinal cord tissue sections of naïve and PBS (day 16) mice, so we didn't include them while examining the co-expression by $CD4^+$ cells or any other specific immune cells. Our data demonstrated IL-16 was expressed by some $CD4^+$ cells within the lesions predominantly in the white matter of spinal cord tissues from MOG_{35-55} immunised mice (Figure 4.11).

We next quantified the percentage of $CD4^+IL\text{-}16^+$ cells out of the total $CD4^+$ cell population in the comparable ROI. In the spinal cord tissues of EAE day 12 (19 ± 0.6%) and EAE day 16 (15 ± 0.4%) mice the percentage was significantly higher compared to that of EAE resolution stage mice at day 26. But there was no difference between the EAE day 12 and EAE day 16 mice groups (Figure 4.11D).

A. EAE Day 12

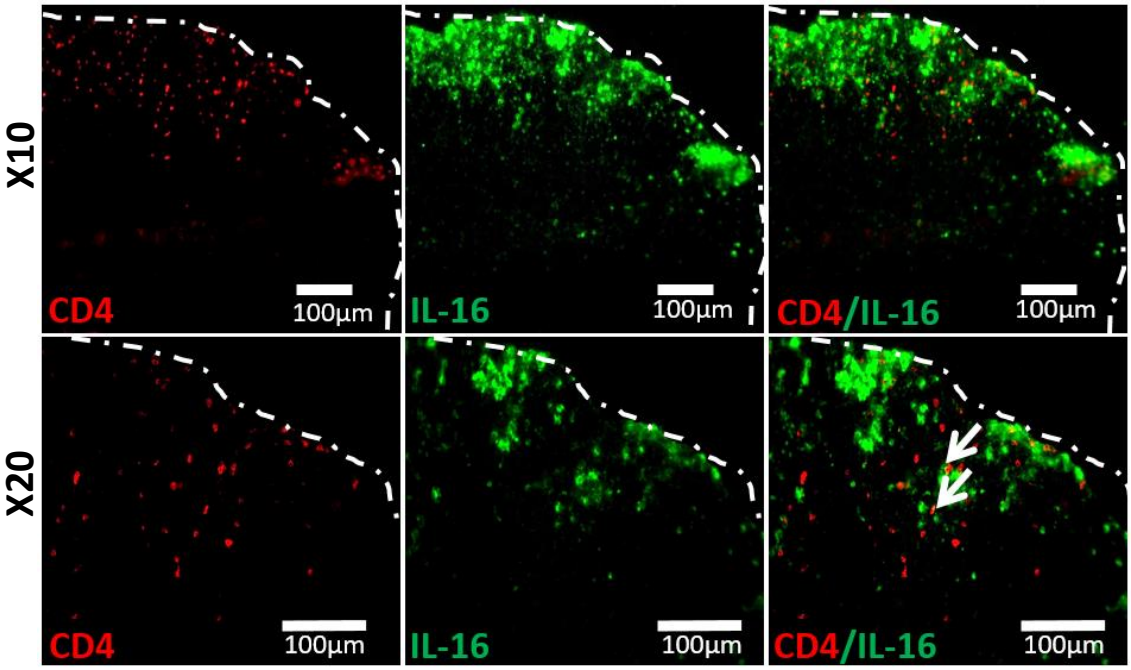

B. EAE Day 16

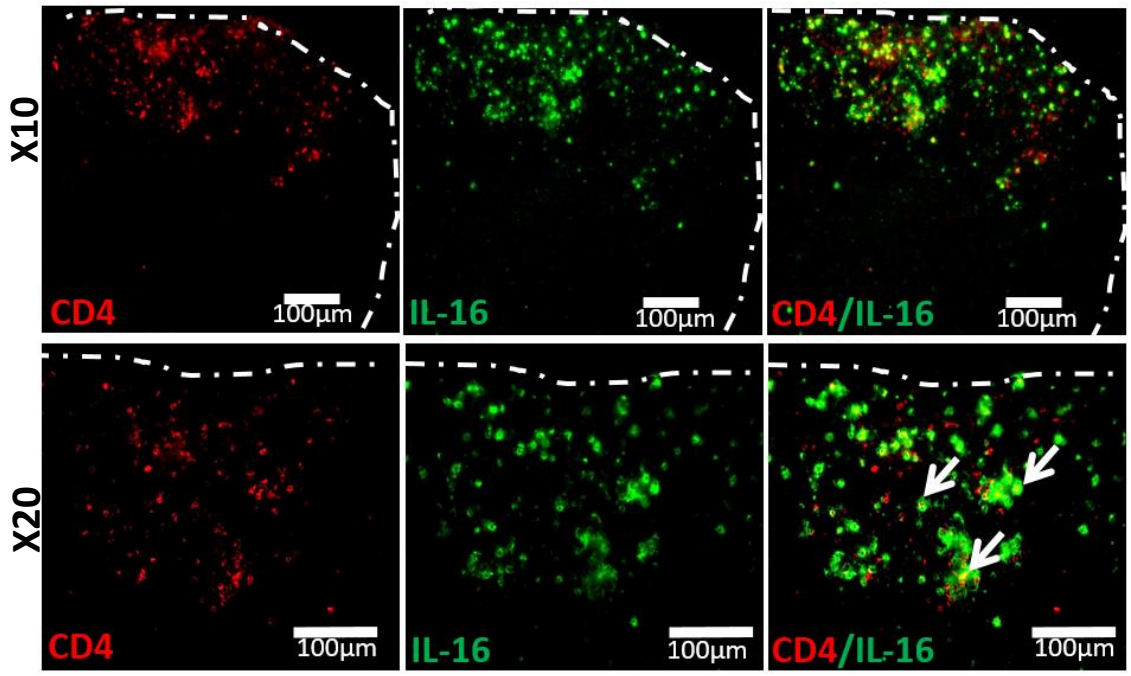

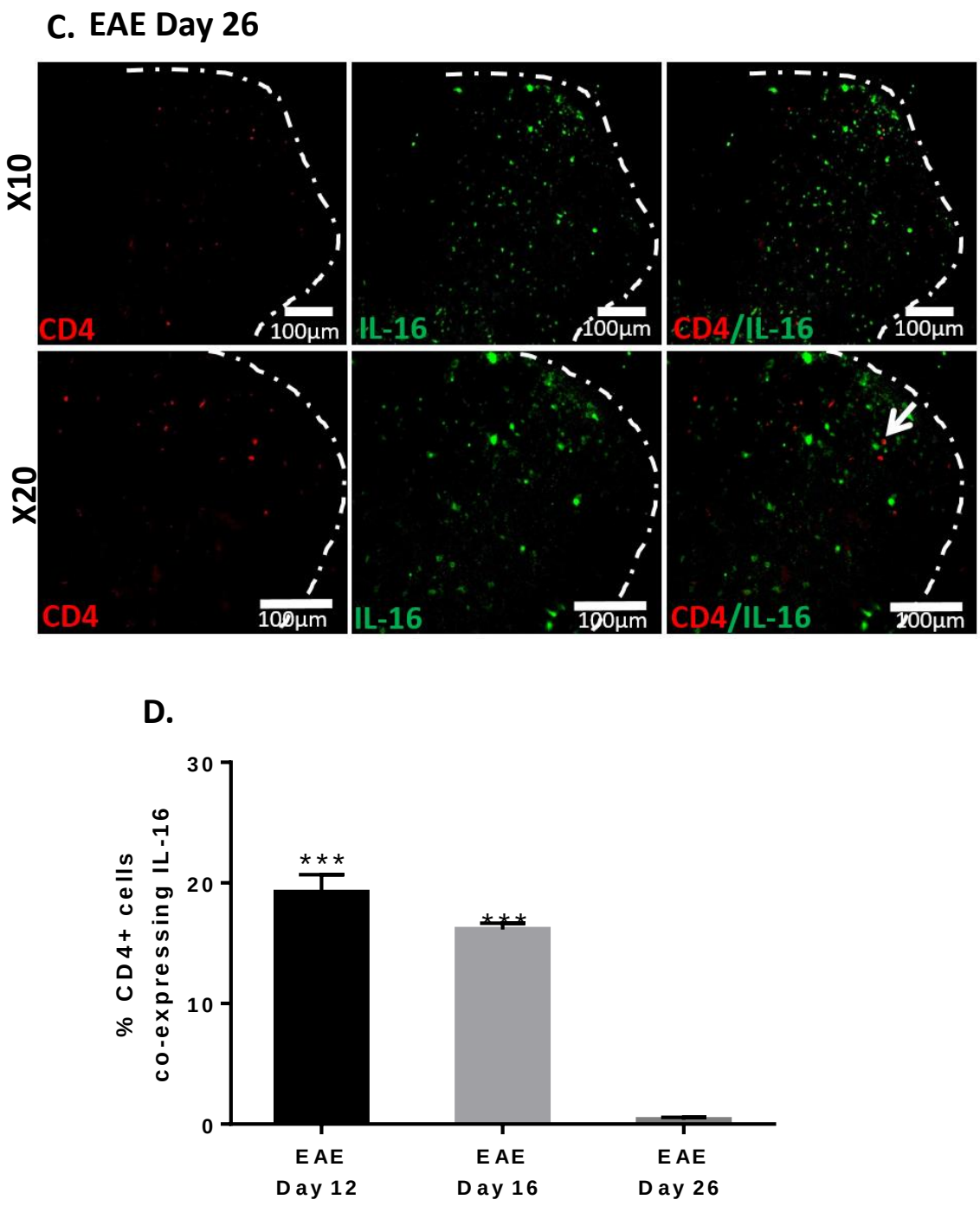

Figure 4.11: Expression of IL-16 by CD4⁺ cells in the spinal cord tissues of naïve, PBS and EAE mice*. Spinal cords were harvested from EAE* ***(A)*** *day 12,* ***(B)*** *day 16 and* ***(C)*** *day 26 mice and the tissues were stained with anti-IL-16 (Green) and anti-CD4 (Red). Data are representative of each group. n=5 for all groups. Primary images x10 and secondary images x20 magnification, scale bars = 100µm. Dotted white line indicating the edge of the tissue section.* ***(D)*** *Percentage of CD4⁺ cells expressing IL-16 within the total CD4⁺ cell population in naïve, PBS and EAE spinal cord tissues has been quantified using the cell counter tool of Image J software and result expressed as mean ± S.E.M. Statistical significance was determined by one-way ANOVA with Bonferroni post-hoc. ***P <0.001 versus EAE day 26.*

4.2.8 IL-16 expression on $CD11b^+$ cells in spinal cord tissues

In MS/EAE apart from T cells many immune cells including monocyte/macrophages infiltrate into the CNS from the periphery and local activation of microglia and macrophages occurs, which actively participate in initiating inflammation and demyelination.

Having shown that $CD4^+$ cells expressed IL-16 within the spinal cord of MOG_{35-55} immunised mice we next examined the co-expression of IL-16 with $CD11b^+$ cells (Figure 4.12). Our data demonstrated IL-16 was expressed by $CD11b^+$ cells predominantly within the lesion in the white matter of spinal cord tissues of MOG_{35-55} immunised mice. Quantification of the percentage of $CD11b^+IL-16^+$ cell out of the total $CD11b^+$ cells in the comparable ROI revealed that the percentage of both EAE day 12 (23 ± 1%) and EAE day 16 (21 ± 1%) mice was significantly higher in comparison to that of EAE day 26 (9 ± 0.9%) mice. However, there were no differences between the EAE day 12 and EAE day 16 mice groups (Figure 4.12D).

A. EAE Day 12

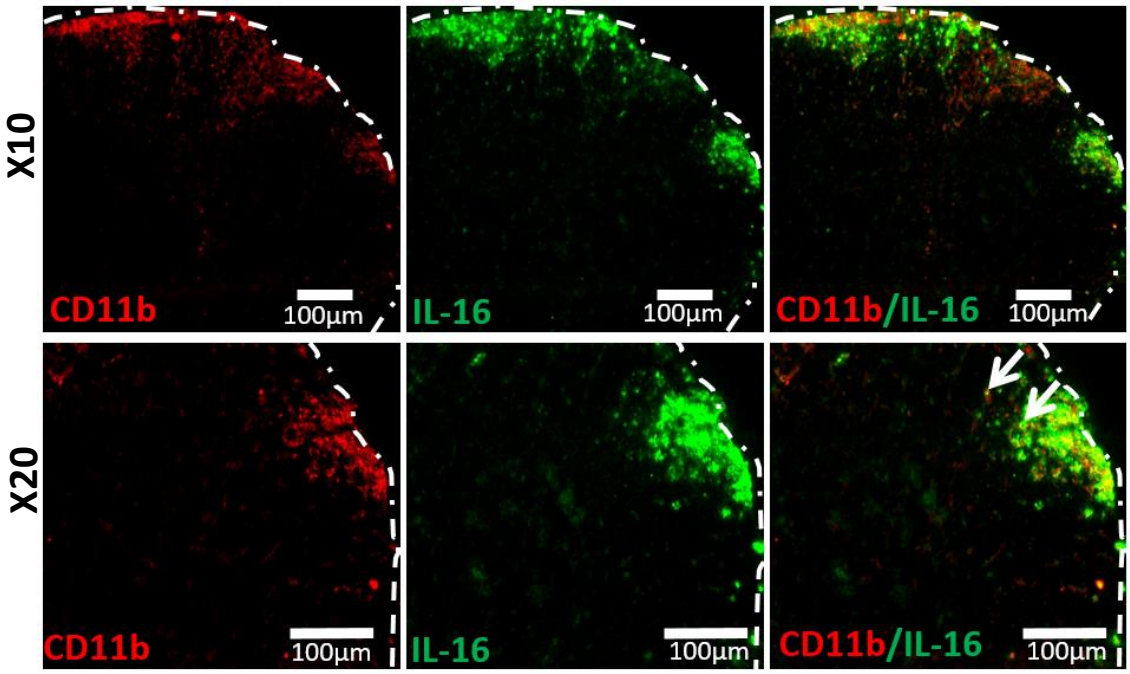

B. EAE Day 16

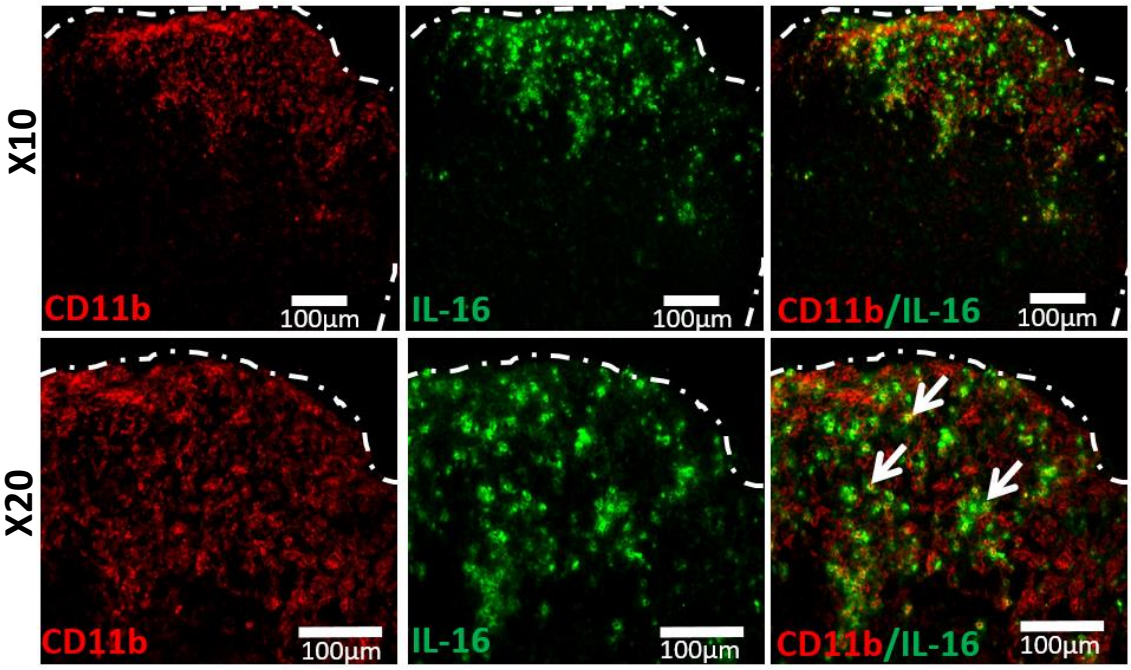

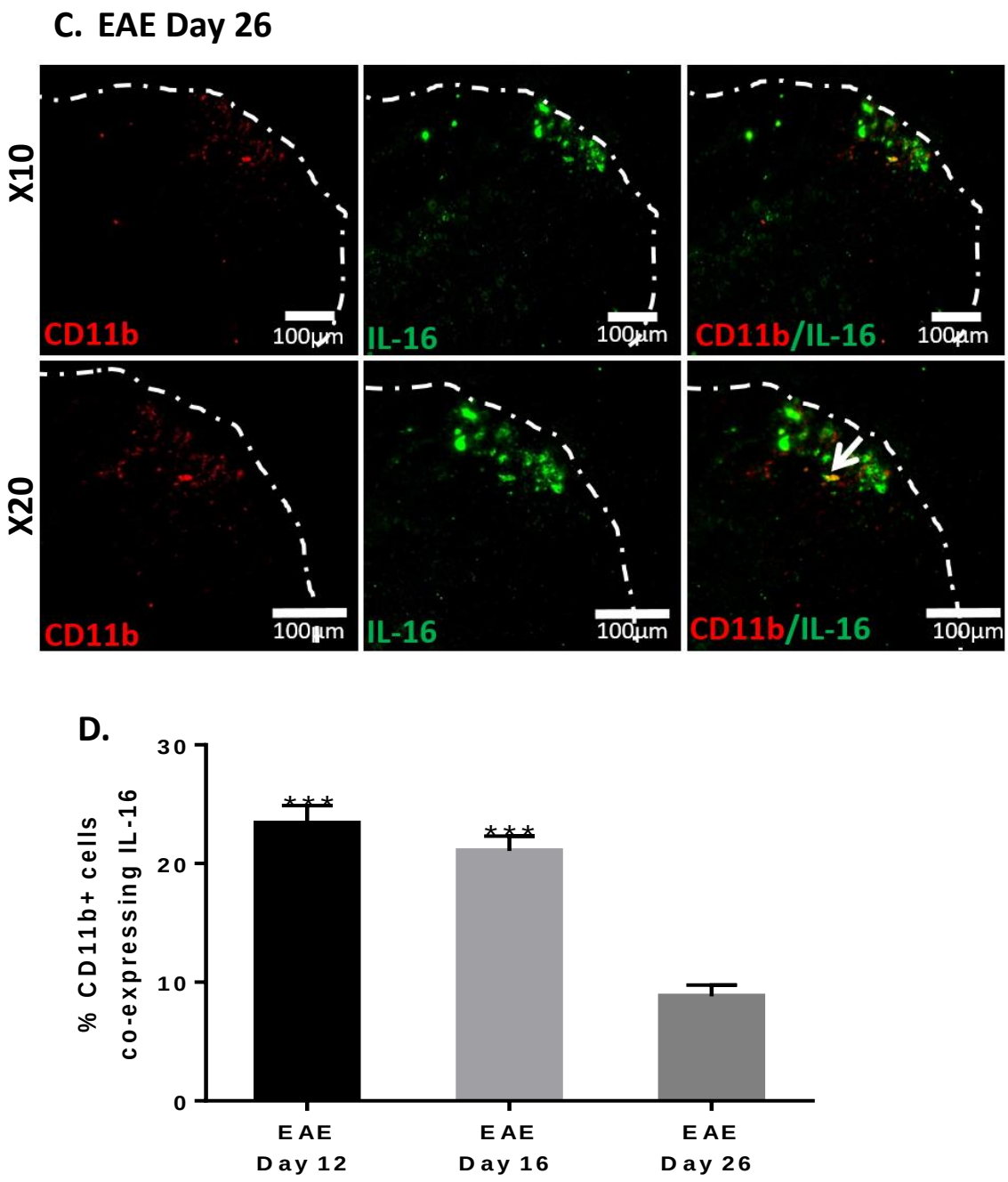

Figure 4.12: Expression of IL-16 by CD11b⁺ cells in the spinal cord tissues of naïve, PBS and EAE mice*. Spinal cords were harvested from EAE* ***(A)*** *day 12,* ***(B)*** *day 16 and* ***(C)*** *day 26 mice and the tissues were stained with anti-IL-16 (Green) and anti-CD11b (Red). Data are representative of each group. n=5 for all groups. Primary images x10 and secondary images x20 magnification, scale bars = 100µm. Dotted white line indicating the edge of the tissue section.* ***(D)*** *Percentage of CD11b⁺ cells expressing IL-16 within the total CD11b⁺ population in naïve, PBS and EAE spinal cord tissues has been quantified using the cell counter tool of Image J software and result expressed as mean ± S.E.M. Statistical significance was determined by one-way ANOVA with Bonferroni post-hoc. ***P <0.001 versus EAE day 26.*

4.2.9 IL-16 expression on F4/80$^+$ cells in spinal cord tissues

Following the examination of CD11b$^+$ macrophage/microglia cells expressing IL-16, we next examined the co-expression of IL-16 with F4/80$^+$ mature macrophages. Our data demonstrated IL-16 was expressed by F4/80$^+$ cells predominantly within the lesion in the white matter of spinal cord tissues from MOG_{35-55} immunised mice (Figure 4.13). Quantification of percentage F4/80$^+$ cells expressing IL-16 out of the total F4/80$^+$ cells, of the comparable ROI in the spinal cord tissue sections revealed both EAE day 12 (10 ± 0.7%) and EAE day 16 (5 ± 0.6%) mice had significantly higher percentage of F4/80$^+$ cells expressing IL-16 in comparison to that of EAE day 26 (1 ± 0.7%) mice. Furthermore, the percentage of co-expressing cells in the spinal cord tissues of EAE day 12 mice was significantly higher in comparison to that of EAE day 16 mice (Figure 4.13D).

A. EAE Day 12

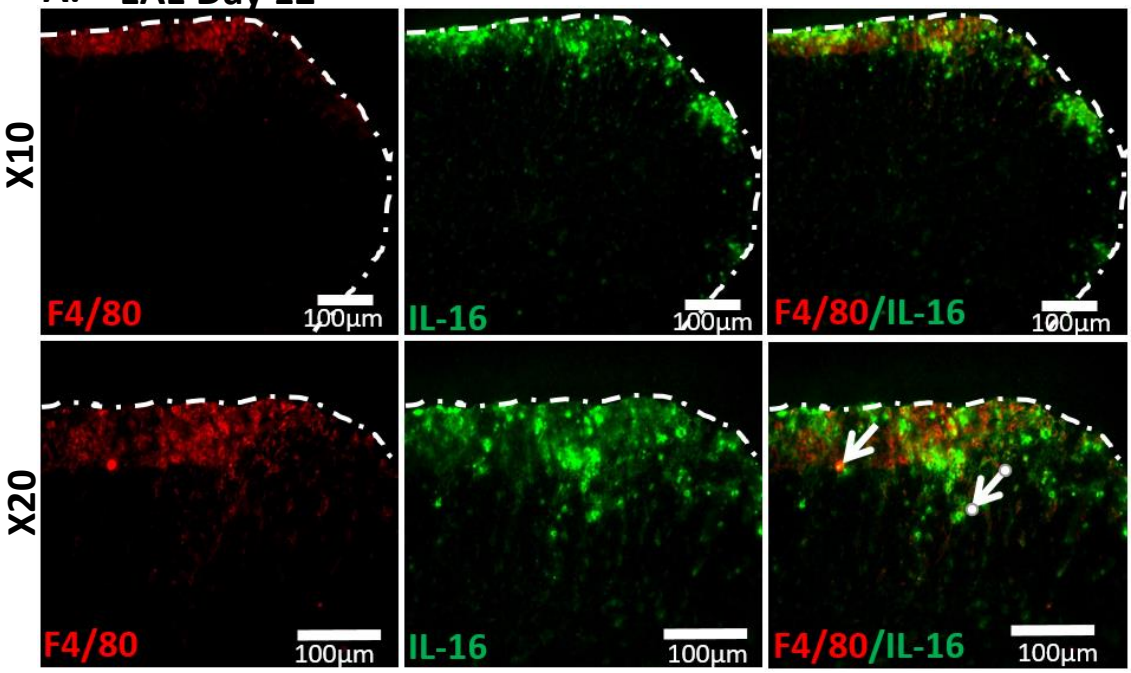

B. EAE Day 16

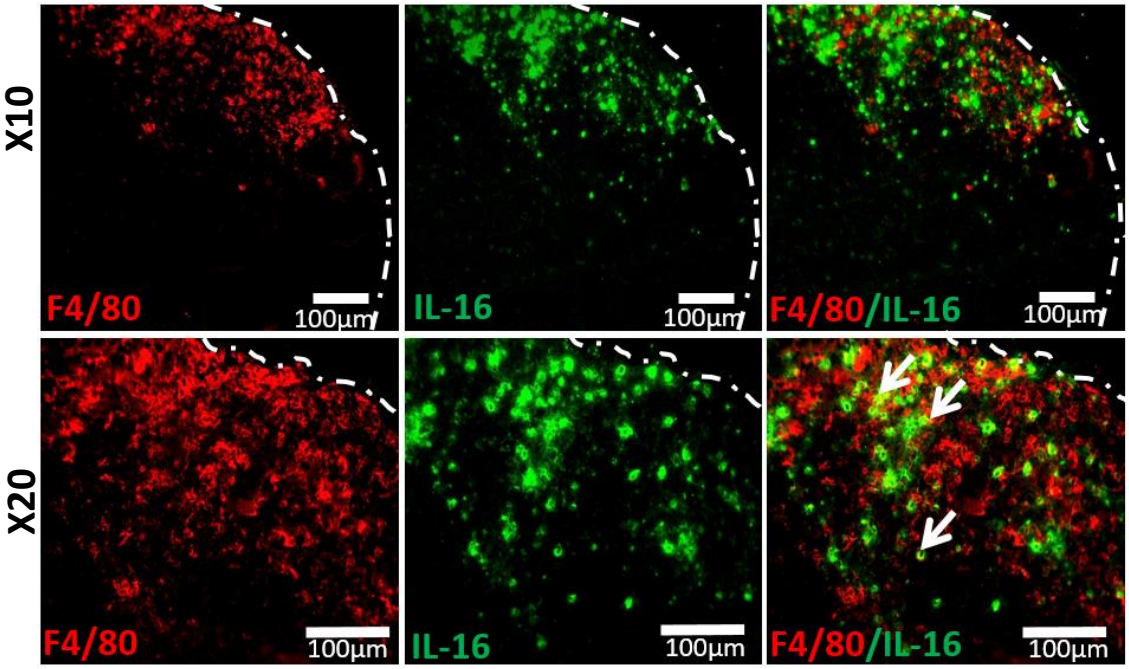

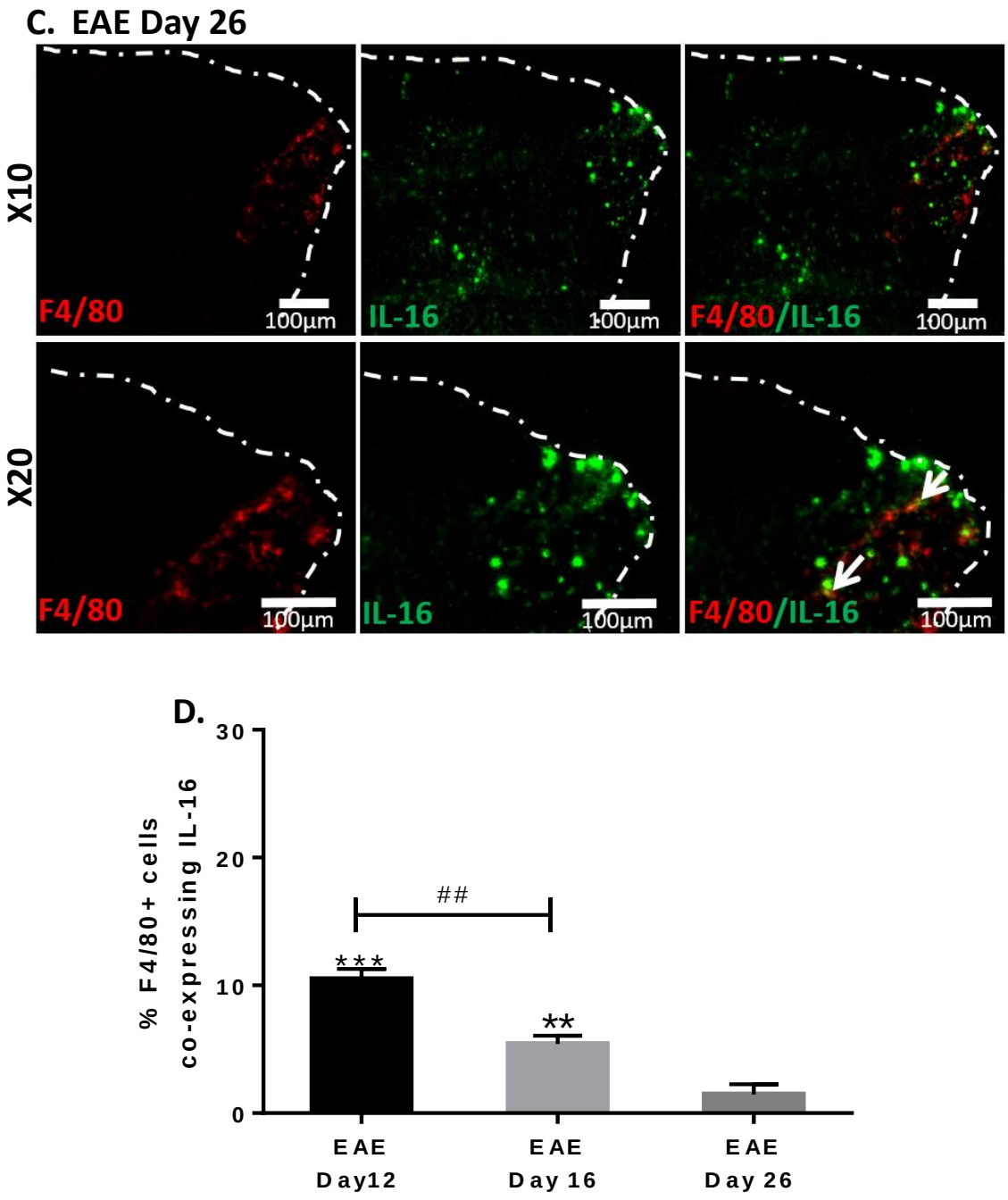

Figure 4.13: Expression of IL-16 by F4/80⁺ cells in the spinal cord tissues of naïve, PBS and EAE mice. *Spinal cords were harvested from EAE* ***(A)*** *day 12,* ***(B)*** *day 16 and* ***(C)*** *day 26 mice and the tissues were stained with anti-IL-16 (Green) and anti-F4/80 (Red). Data are representative of each group. n=5 for all groups. Primary images x10 and secondary images X20 magnification, scale bars = 100µm. Dotted white line indicating the edge of the tissue section.* ***(D)*** *Percentage of F4/80⁺ cells expressing IL-16 within the total F4/80⁺ cell population in naïve, PBS and EAE spinal cord tissues has been quantified using the cell counter tool of Image J software and result expressed as mean ± S.E.M.in naïve, PBS and EAE spinal cord tissues has been quantified using the cell counter tool of Image J software and result expressed as mean ± S.E.M. Statistical significance was determined by one-way ANOVA with Bonferroni post-hoc. ***P <0.001 versus EAE day 26; ##P<0.01 versus EAE day 16.*

4.2.10 IL-16 expression on neurons in spinal cord tissues

Although IL-16 was clearly expressed by immune cells in the periphery lymphoid organs and infiltrating into the CNS tissues, constitutive expression of IL-16 in the spinal cord and brain tissues suggests its expression by CNS resident cells. Thus, next we studied the colocalization of IL-16 with neurons and glia cells in the CNS tissues under normal and diseased condition.

Neurons being the major type of CNS resident cells do not play an active role in the pathogenesis of MS/EAE. However, as a result of MS/EAE pathology the demyelination of axons makes both neurons and axons vulnerable to damages. So, we wanted to examine if neurons in the spinal cord tissue sections expressed IL-16. And to investigate this, we utilised double immunofluorescence staining with NeuN (marker for neurons that stains nucleus and the cytoplasm of most neurons) and IL-16 in spinal cord tissues of naïve mice, PBS immunised mice at day 16 post immunisation and MOG_{35-55} immunised mice at day 12, day 16 and day 26 post immunisation. To further investigate if the expression pattern changes over the course of the disease and with the extent of the disease, here we have included tissues collected from all three time points of the EAE disease course.

IL-16 was observed to be expressed by $NeuN^+$ cells within the grey matter of spinal cord tissues of all groups of mice examined (Figure 4.14). As there are no neuronal cell bodies within the white matter, so NeuN expressing IL-16 was not observed in that region of spinal cord. Quantification of the percentage of $NeuN^+$ cells expressing IL-16 expressing out of the total $NeuN^+$ cells, within the comparable ROI in the spinal cord tissue sections, did not demonstrate any differences between the naïve (34 ± 23%) and PBS day 16 (33 ± 23%) mice groups. Spinal cord tissue sections collected from EAE day 12 (33 ± 2 %), EAE day 16 (35 ± 3%) and EAE day 26 (33 ± 2%) mice groups also had similar percentage of $NeuN^+$ $IL\text{-}16^+$ cells as observed in the control groups (Figure 4.14F).

A. Naïve

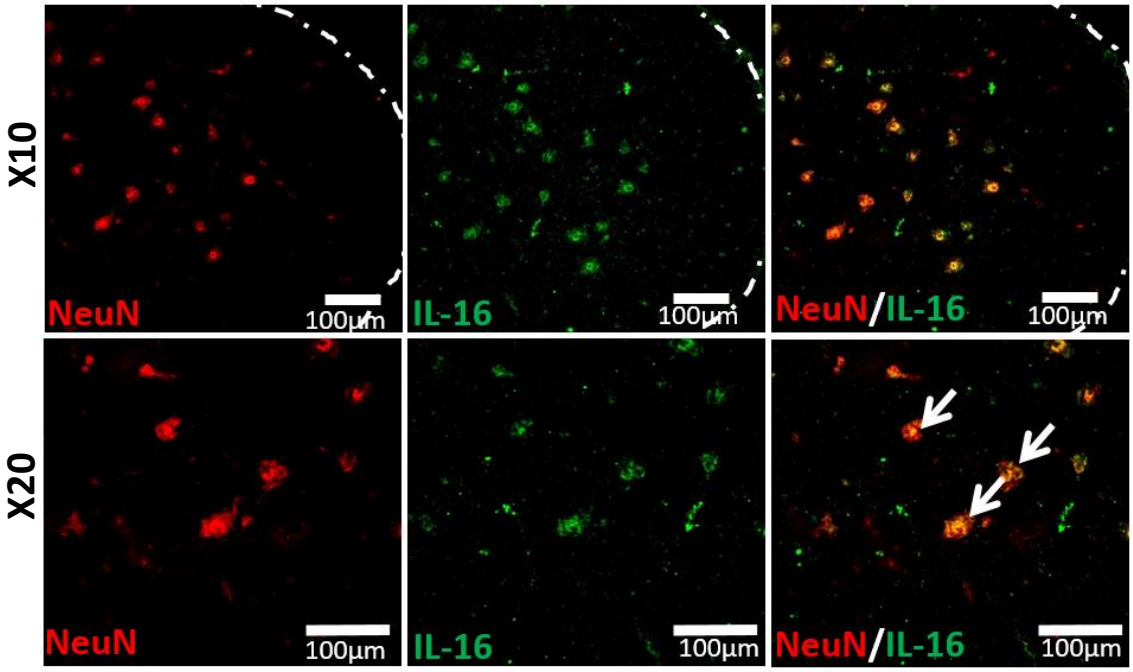

B. PBS Day 16

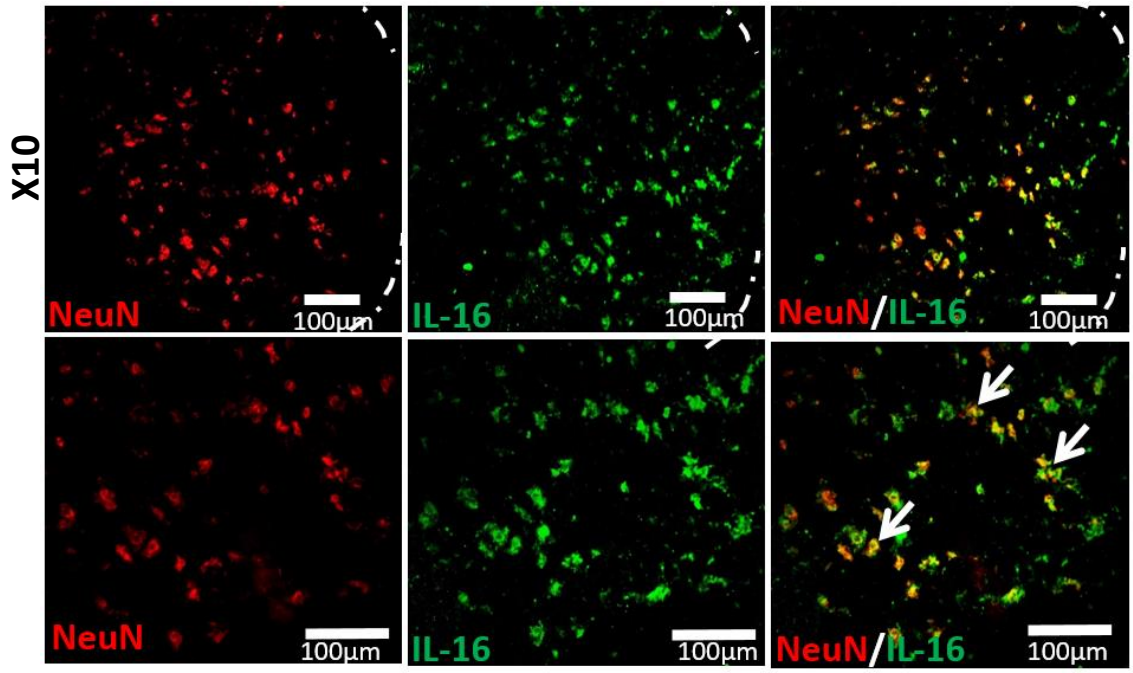

C. EAE Day 12

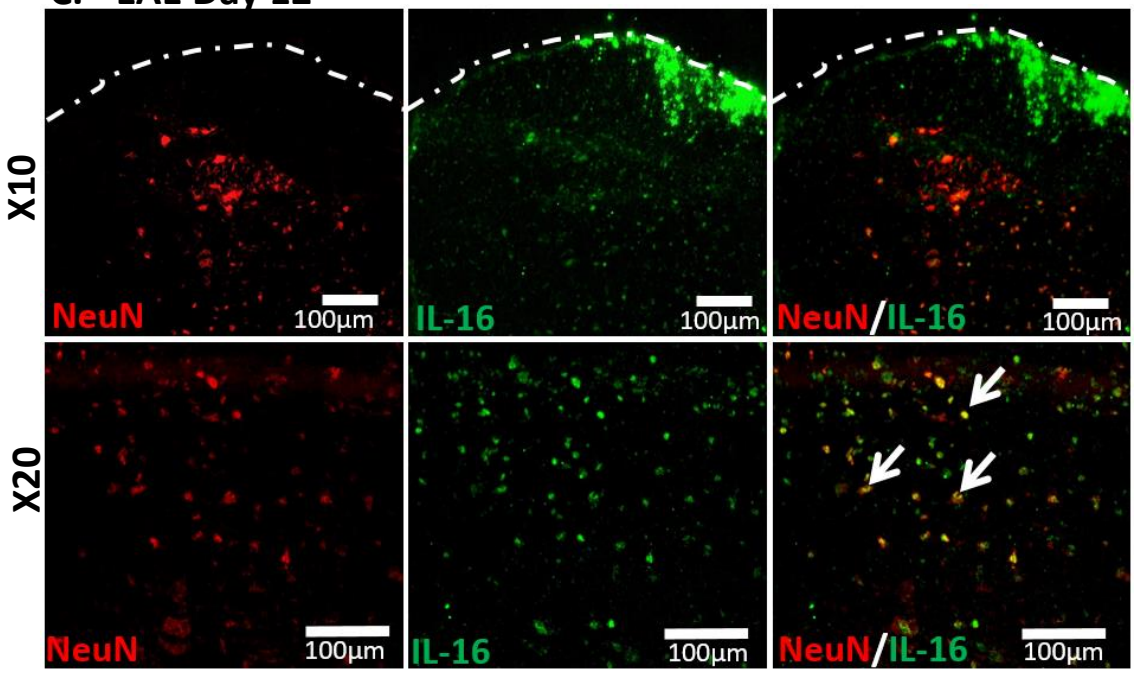

D. EAE Day 16

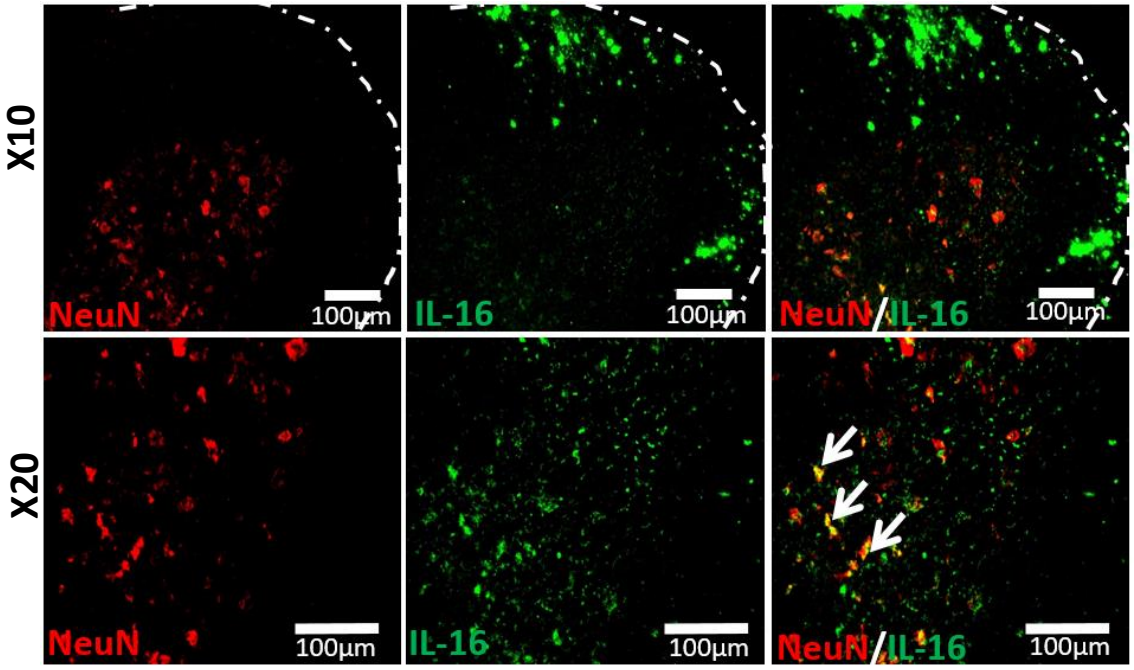

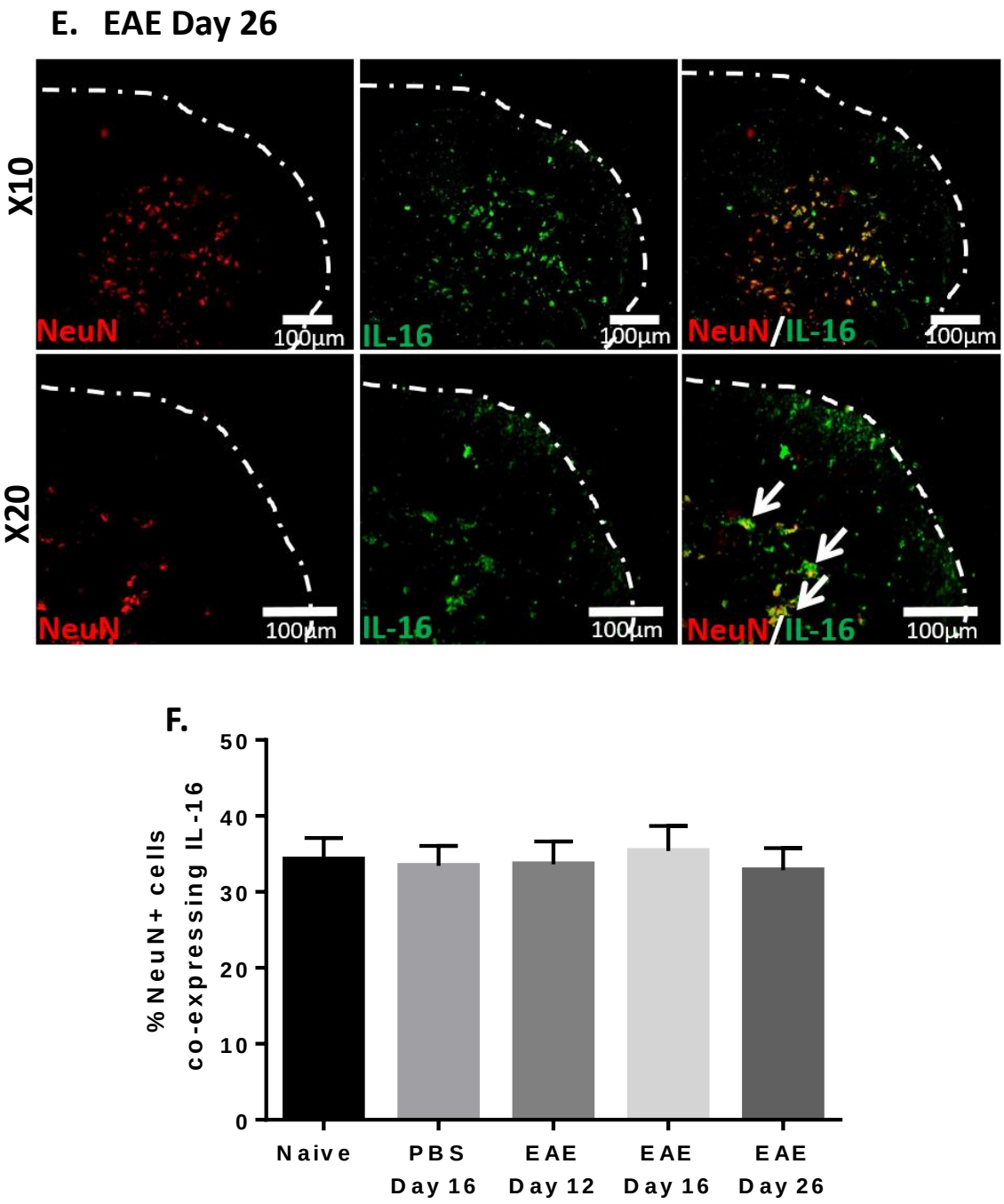

Figure 4.14: Expression of IL-16 by NeuN⁺ cells in the spinal cord tissues of naïve, PBS and EAE mice*. Spinal cords were harvested from* ***(A)*** *naïve* ***(B)*** *PBS day 16 and EAE* ***(C)*** *day 12* ***(D)*** *day 16 and* ***(E)*** *day 26 mice and the tissues were stained with anti-IL-16 (Green) and anti-NeuN (Red). Data are representative of each group. n=5 for all groups. Primary images x10 and secondary images X20 magnification, scale bars = 100µm. Dotted white line indicating the edge of the tissue section.* ***(F)*** *Percentage of IL-16 expressing NeuN⁺ cells within the total NeuN⁺ cell population in naïve, PBS and EAE spinal cord tissues has been quantified using the cell counter tool of Image J software and result expressed as mean ± S.E.M. Statistical significance was determined by one-way ANOVA with Bonferroni post-hoc.*

4.2.11 IL-16 expression on astrocytes in spinal cord tissues

Apart from the neurons, glial cells are also predominantly found in the CNS. Astrocytes are the star shaped glial cells which intertwine with all other neighbouring neuronal and non-neuronal cells in the CNS by filling the space between neurons. Activation and proliferation of astrocytes during MS/EAE have a critical contribution in augmenting inflammation and disease progression. To investigate the expression of IL-16 by astrocytes we next utilised double immunofluorescence staining with GFAP (marker for astrocytes) and IL-16 in the spinal cord tissue sections.

Our data demonstrated IL-16 was expressed by $GFAP^+$ cells predominantly within the lesion in the white matter of spinal cord tissues sections of MOG_{35-55} immunised mice (Figure 4.15). There was no co-localisation of IL-16 with GFAP within the white matter in the spinal cord tissue sections of naïve and PBS day 16 mice due to the absence of IL-16 within this region. Quantification of the percentage of $GFAP^+IL\text{-}16^+$ cells out of the total $GFAP^+$ cells in the comparable ROI revealed no difference between the naïve and PBS day 16 mice. However, both spinal cord tissue sections of EAE day 12 (22 ± 2%) and EAE day 16 (23 ± 12%) mice demonstrated significantly higher percentage in comparison to the EAE day 26 (3 ± 0.52%) mice (Figure 4.15D).

A. Naïve

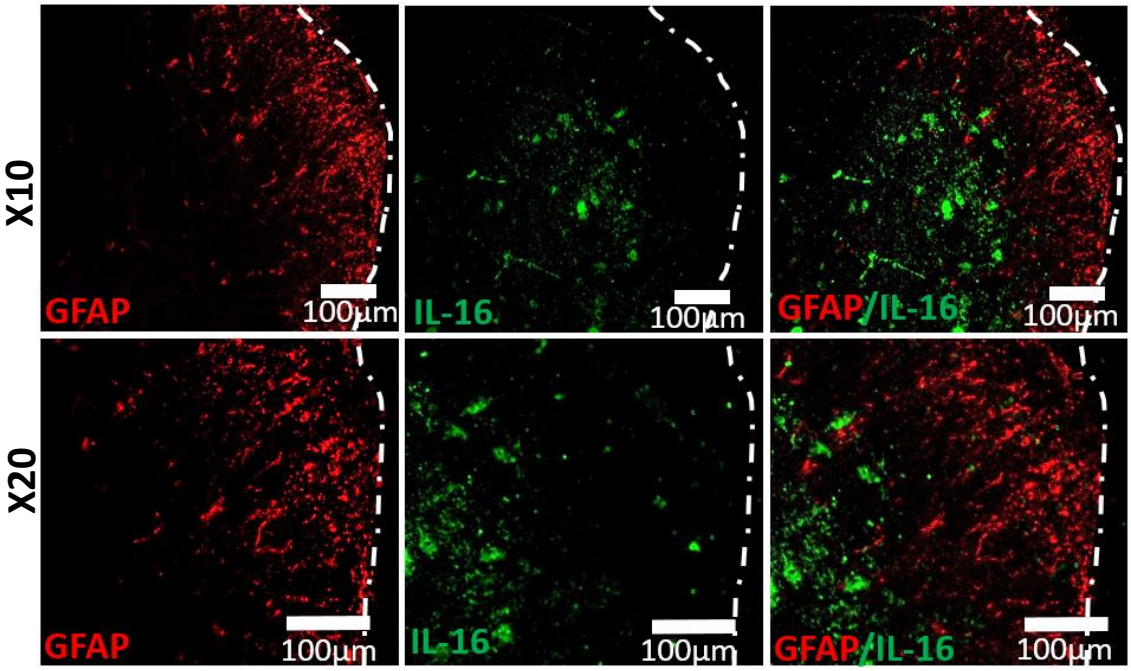

B. PBS Day 16

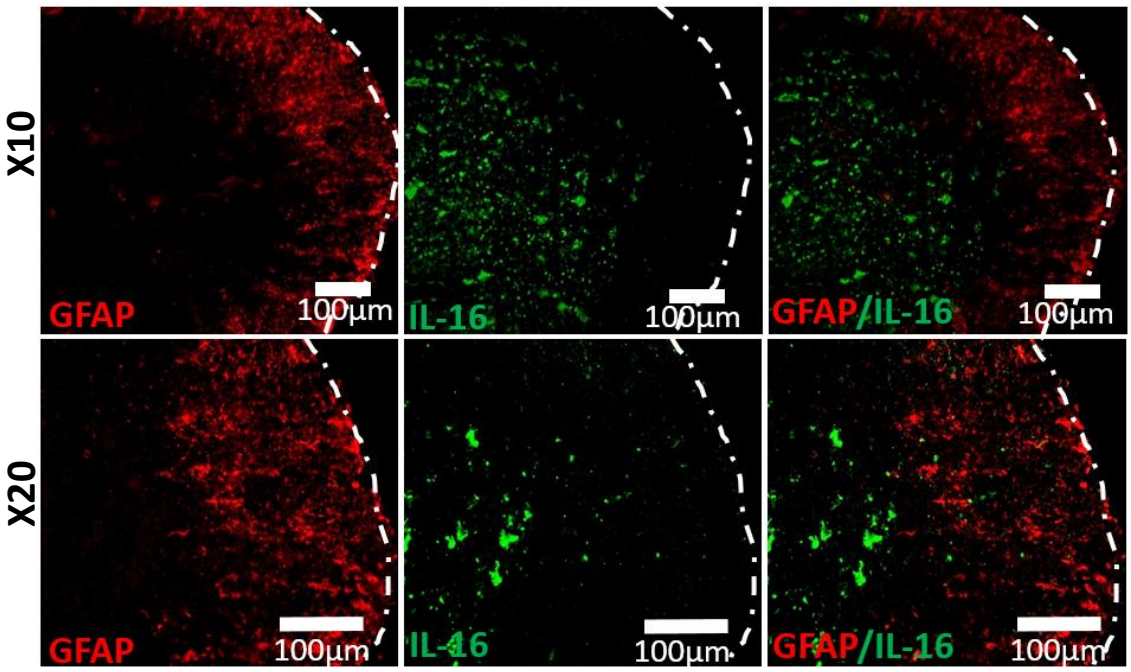

C. EAE Day 12

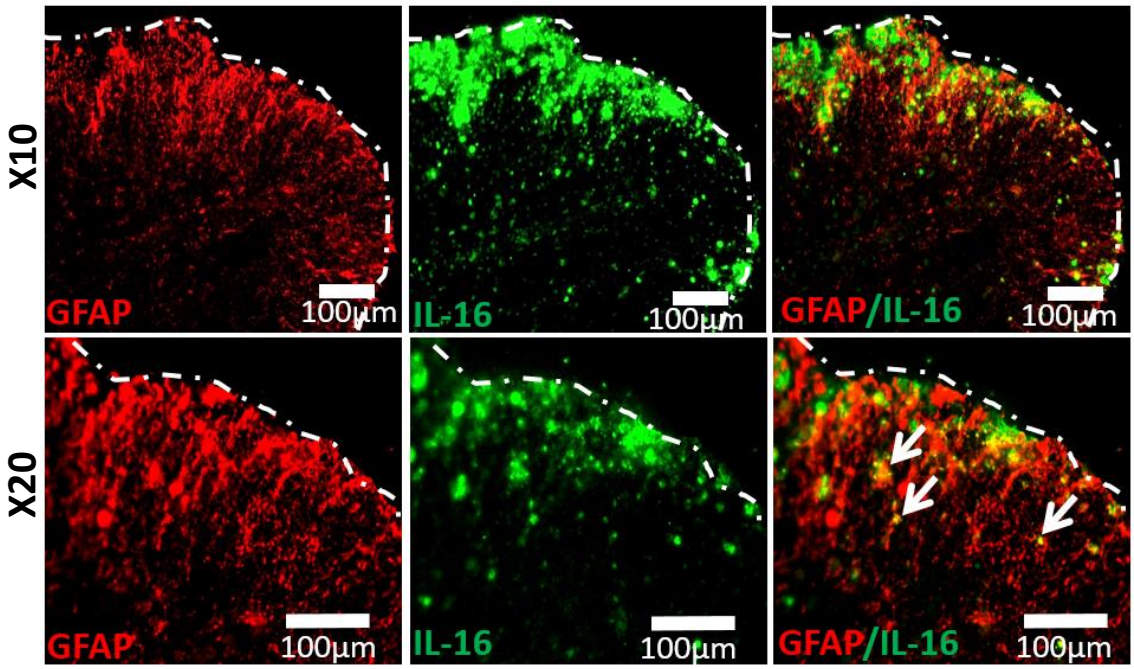

D. EAE Day 16

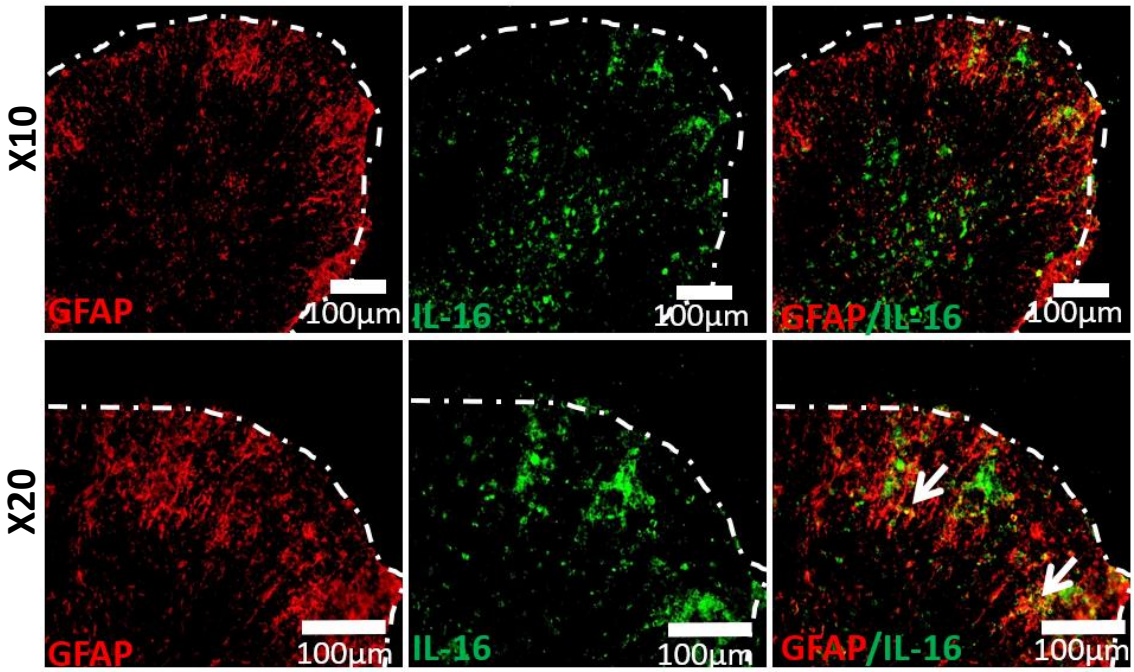

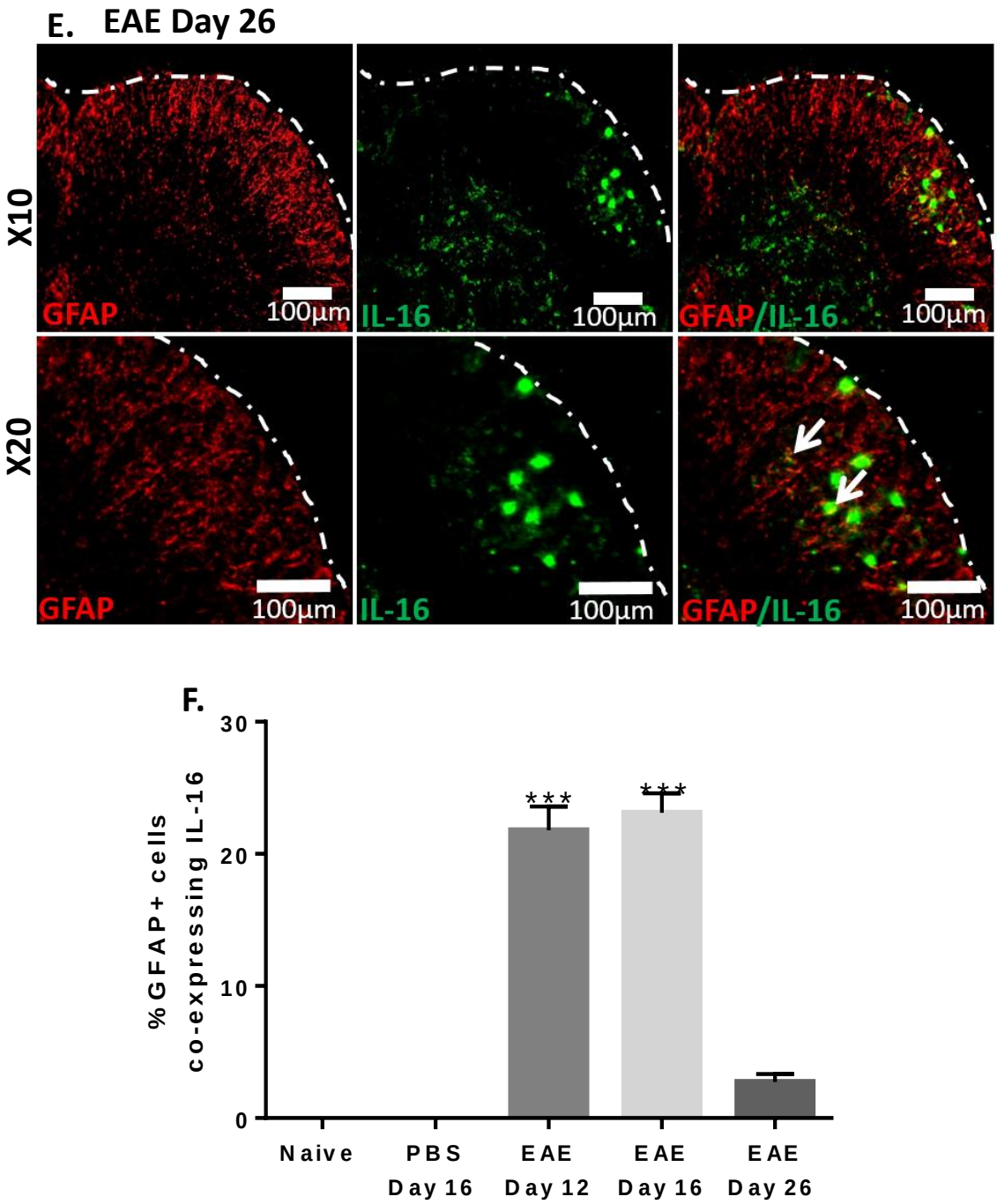

Figure 4.15: Expression of IL-16 by GFAP⁺ cells in the spinal cord tissues of naïve, PBS and EAE mice. *Spinal cords were harvested from* ***(A)*** *naïve* ***(B)*** *PBS day 16 and EAE* ***(C)*** *day 12* ***(D)*** *day 16 and* ***(E)*** *day 26 mice and the tissues were stained with anti-IL-16 (Green) and anti-GFAP (Red). Data are representative of each group. n=5 for all groups. Primary images x10 and secondary images X20 magnification, scale bars = 100µm. Dotted white line indicating the edge of the tissue section.* ***(F)*** *Percentage of IL-16 expressing GFAP⁺ cells within the total GFAP⁺ cell population in naïve, PBS and EAE spinal cord tissues has been quantified using the cell counter tool of Image J software and result expressed as mean ± S.E.M. Statistical significance was determined by one-way ANOVA with Bonferroni post-hoc. ***P <0.001 versus EAE day 26.*

4.2.12 IL-16 expression on CD45$^+$ cells in brain tissues

Earlier we have demonstrated that CD45$^+$ cells co-expressed IL-16 predominantly within the lesions of spinal cord tissues from MOG_{35-55} immunised mice, to investigate if this is consistent within the brain tissues, we next examined the co-expression of IL-16 with CD45$^+$ cells in brain tissue sections collected from control and EAE mice. IL-16 co-expression with CD45 and various other immune cell markers was specifically assessed within the regions of hippocampus (area near dentate gyrus) (Figure 4.16) and the cerebellum (white mater) (Figure 4.17) where the cellular infiltration and lesions were observed in this EAE model.

Our data demonstrated IL-16 was expressed by CD45$^+$ cells predominantly within the lesion in the hippocampus (area near dentate gyrus was studied) and the cerebellum (white matter) of brain tissues from MOG_{35-55} immunised mice. There was no co-localisation of IL-16 on CD45$^+$ cells within the naïve and PBS day 16 hippocampus (area near dentate gyrus) or the cerebellum (white matter) of the brain tissue sections due to the absence of CD45$^+$ cells within this region. Quantification of the percentage of CD45$^+$IL-16$^+$ cells out of the total CD45$^+$ cell population within the comparable ROI in the hippocampus revealed no difference between the naïve and PBS day 16 mice. However, the percentage of CD45$^+$IL-16$^+$ cells in the EAE mice at day 12 and day 16 was significantly higher with 19 ± 1% and 22 ± 1% respectively in comparison to that of EAE day 26 mice, which had 3.4 ± 3% of CD45$^+$ cells co-expressing IL-16 (Figure 4.16F).

In the cerebellum (white matter), quantification revealed significantly higher percentage of CD45$^+$ cells co-expressing IL-16 in EAE mice at day 12 (24 ± 2%) and day 16 (28 ± 1%) in comparison to EAE mice at day 26 (5.6 ± 4.4%) (Figure 4.17F).

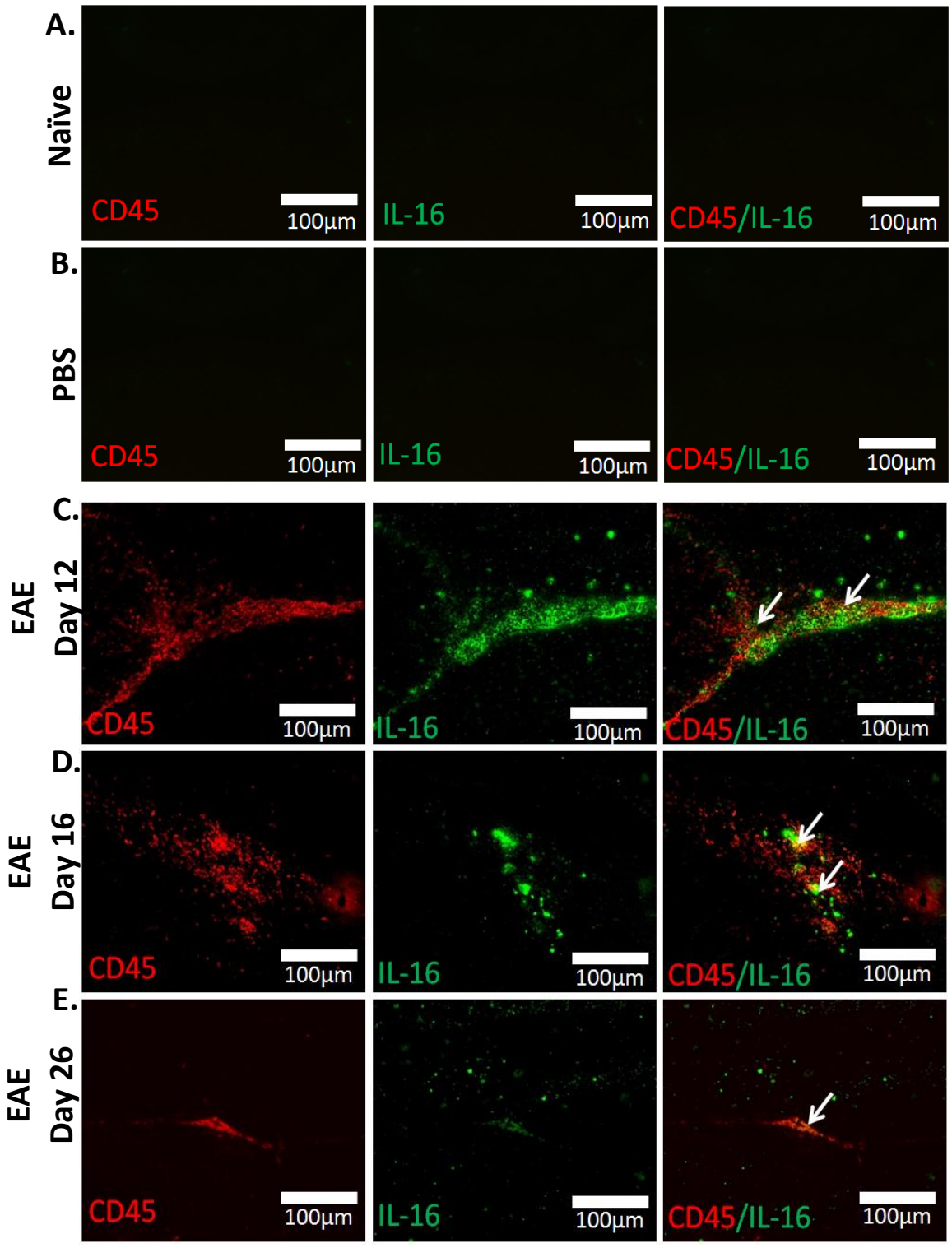
A.
Naïve
CD45
100µm
IL-16
100µm
CD45/IL-16
100µm
B.
PBS
CD45
100µm
IL-16
100µm
CD45/IL-16
100µm
C.
EAE
Day 12
CD45
100µm
IL-16
100µm
CD45/IL-16
100µm
D.
EAE
Day 16
CD45
100µm
IL-16
100µm
CD45/IL-16
100µm
E.
EAE
Day 26
CD45
100µm
IL-16
100µm
CD45/IL-16
100µm

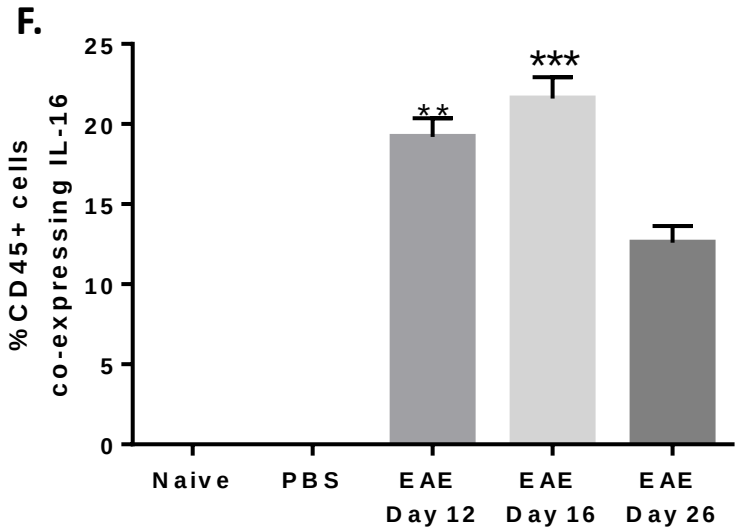

Figure 4.16: Expression of IL-16 by CD45⁺ cells in the hippocampus (area near dentate gyrus) of naïve, PBS and EAE mice*. Brains were harvested from* ***(A)*** *naïve* ***(B),*** *PBS day 16 and EAE* ***(C)*** *day 12,* ***(D)*** *day 16 and* ***(E)*** *day 26 mice and the tissues were stained with anti-IL-16 (Green) and anti-CD45 (Red). Data are representative of each group. n=5 for all groups. Scale bars of the images = 100µm.* ***(F)*** *Percentage of CD45⁺ cells expressing IL-16 in naïve, PBS and EAE hippocampus (area near dentate gyrus) has been quantified using the cell counter tool of Image J software and result expressed as mean ± S.E.M. Statistical significance was determined by one-way ANOVA with Bonferroni post-hoc. **P <0.01, ***P <0.001 versus EAE day 26.*

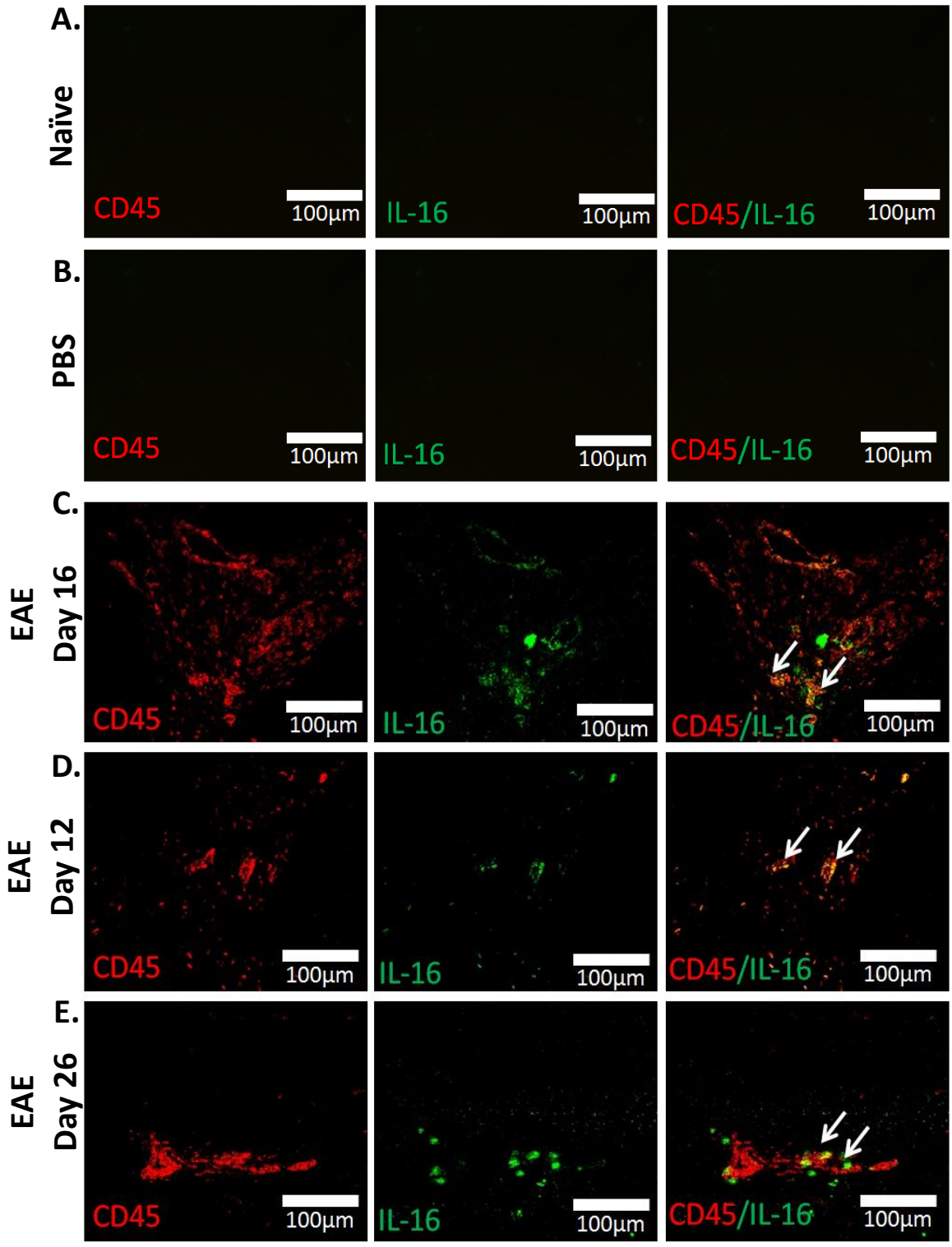
A.
Naïve
CD45
100µm
IL-16
100µm
CD45/IL-16
100µm
B.
PBS
CD45
100µm
IL-16
100µm
CD45/IL-16
100µm
C.
EAE
Day 16
CD45
100µm
IL-16
100µm
CD45/IL-16
100µm
D.
EAE
Day 12
CD45
100µm
IL-16
100µm
CD45/IL-16
100µm
E.
EAE
Day 26
CD45
100µm
IL-16
100µm
CD45/IL-16
100µm

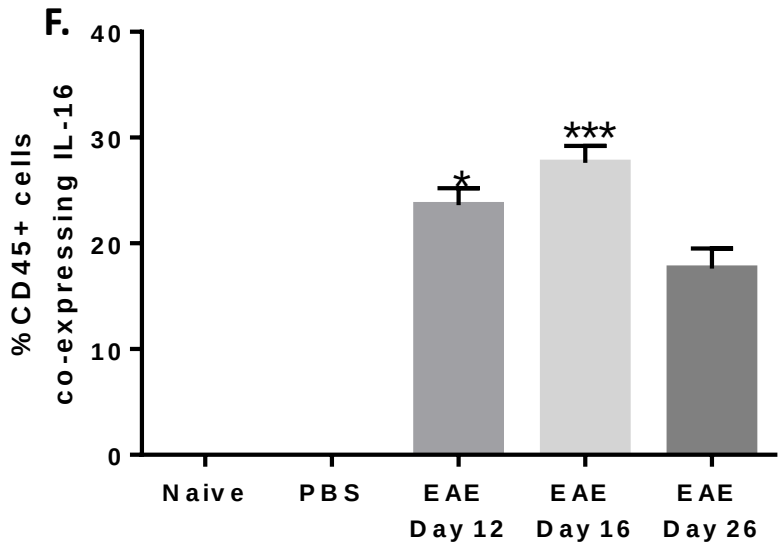

Figure 4.17: Expression of IL-16 by CD45⁺ cells in the cerebellum (white matter) of naïve, PBS and EAE mice*. Brains were harvested from* ***(A)*** *naïve,* ***(B)*** *PBS day 16 and EAE* ***(C)*** *day 12,* ***(D)*** *day 16 and* ***(E)*** *day 26 mice and the tissues were stained with anti-IL-16 (Green) and anti-CD45 (Red). Data are representative of each group. n=5 for all groups. Scale bars of the images = 100µm.* ***(F)*** *Percentage of CD45⁺ cells expressing IL-16 in naïve, PBS and EAE cerebellum (white matter) has been quantified using the cell counter tool of Image J software and result expressed as mean ± S.E.M. Statistical significance was determined by one-way ANOVA with Bonferroni post-hoc. *P <0.05, ***P <0.001 versus EAE day 26.*

4.2.13 IL-16 expression on $CD4^+$ cells in brain tissues.

Some $CD4^+$ cells have been observed to co-express IL-16 within the spinal cord of MOG_{35-55} immunised mice, to determine if such expression is consistent within the brain, we next examined the co-expression of IL-16 with $CD4^+$ cells in brain tissues. Our data showed that $CD45^+$ cells were absent within the brain tissues sections of naïve and PBS day 16 mice, so these tissues were not included in our study examining the co-expression of IL-16 with various immune cells. As mentioned in section 4.2.13, IL-16 co-expression was specifically assessed within the regions of hippocampus (near the dentate gyrus) (Figure 4.18) and the cerebellum (white mater) (Figure 4.19).

Our data demonstrated IL-16 was expressed by $CD4^+$ cells predominantly within the lesion in the hippocampus and cerebellum of brain tissue sections from MOG_{35-55} immunised mice. Quantification of the percentage of $CD4^+$IL-16 cells out of the total $CD4^+$ cells in the comparable ROI revealed both EAE mice at day 12 (14 ± 1%) and day 16 (14 ± 2%) had significantly higher percentage in comparison to the EAE mice at day 26 which didn't demonstrate any $CD4^+$ cells co-expressing IL-16.

In the cerebellum, quantification revealed significantly higher percentage of $CD4^+$ cells co-expressing IL-16 in EAE mice at day 12 (27 ± 1%) and day 16 (31 ± 1%) in comparison to EAE mice at day 26 which didn't demonstrate any $CD4^+$ cells co-expressing IL-16.

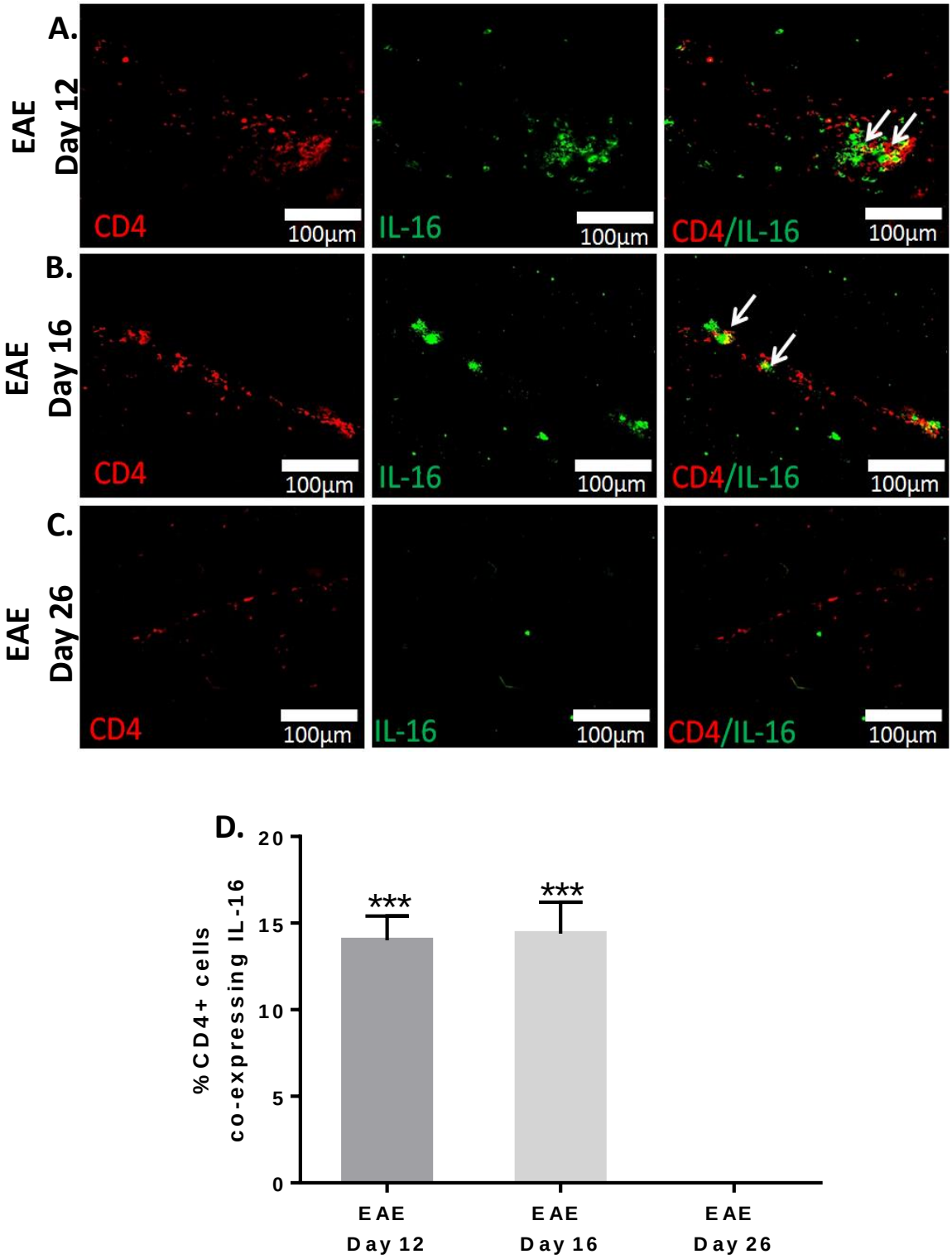

Figure 4.18: Expression of IL-16 by CD4⁺ cells in the hippocampus (area near dentate gyrus) of EAE mice*. Brains were harvested from EAE* ***(A)*** *day 12,* ***(B)*** *day 16 and* ***(C)*** *day 26 mice and the tissues were stained with anti-IL-16 (Green) and anti-CD4 (Red). Data are representative of each group. n=5 for all groups. Scale bars of the images = 100µm.* ***(D)*** *Percentage of CD4⁺ cells expressing IL-16 in naïve, PBS and EAE hippocampus (area near dentate gyrus) has been quantified using the cell counter tool of Image J software and result expressed as mean ± S.E.M. Statistical significance was determined by one-way ANOVA with Bonferroni post-hoc. ***P <0.001 versus EAE day 26.*

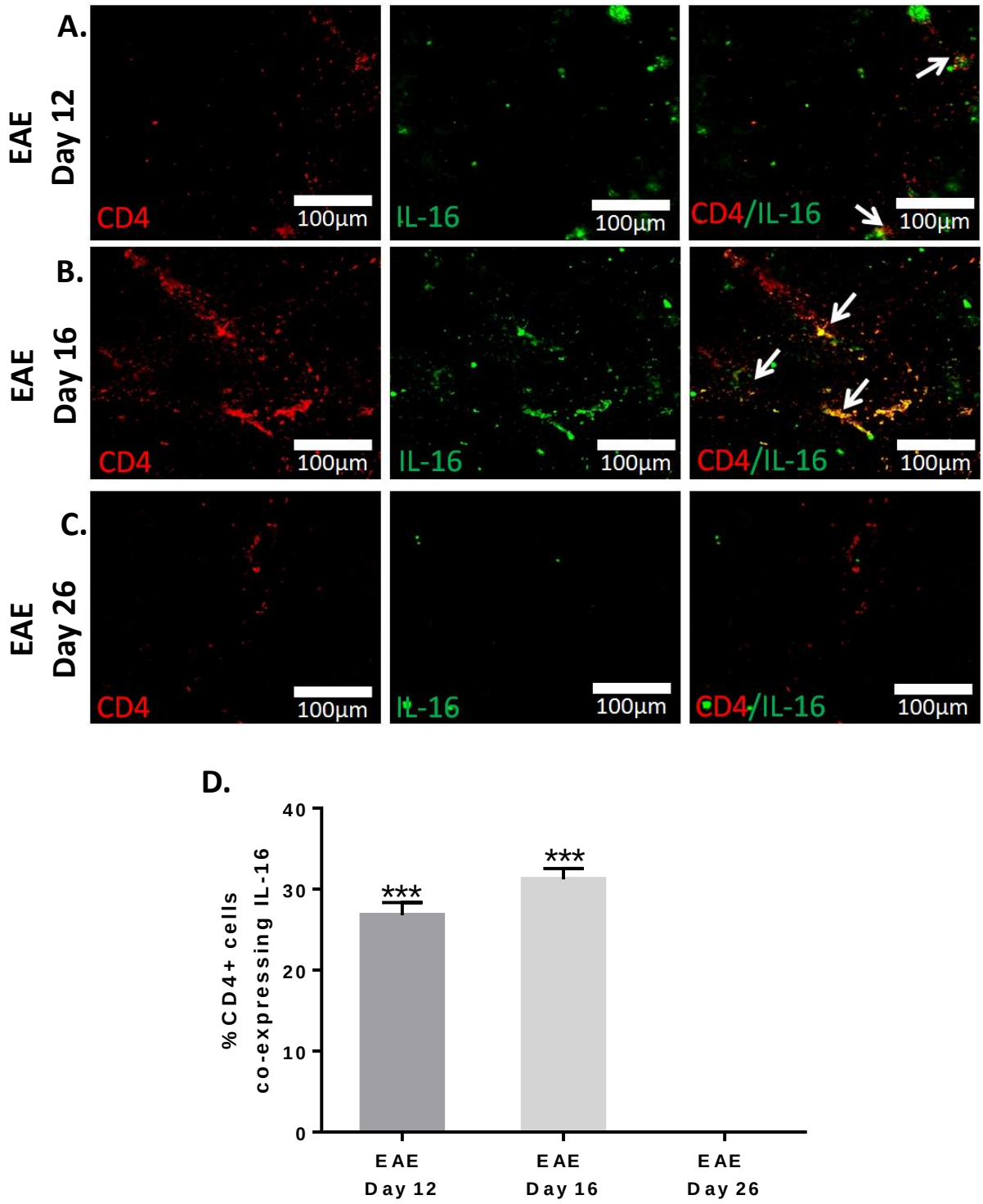

Figure 4.19: Expression of IL-16 by CD4⁺ cells in the cerebellum (white matter) of EAE mice. *Brains were harvested from EAE* ***(A)*** *day 12,* ***(B)*** *day 16 and* ***(C)*** *day 26 mice post immunisation and the tissues were stained with anti-IL-16 (Green) and anti-CD4 (Red). Data are representative of each group. n=5 for all groups. Scale bars of the images = 100µm.* ***(D)*** *Percentage of CD4+ cells expressing IL-16 in naïve, PBS and EAE cerebellum (white matter) has been quantified using the cell counter tool of Image J software and result expressed as mean ± S.E.M. Statistical significance was determined by one-way ANOVA with Bonferroni post-hoc. ***P <0.001 versus EAE day 26.*

4.2.14 IL-16 expression on CD11b$^+$ cells in brain tissues.

Having shown that CD11b$^+$ cells co-expressed IL-16 within the spinal cord of MOG_{35-55} immunised mice we also utilised double immunofluorescence staining in brain tissue sections to examine the co-expression of IL-16 with CD11b$^+$ cells. IL-16 co-expression was specifically assessed within the regions of hippocampus (area near the dentate gyrus) (Figure 4.20) and the cerebellum (white mater) (Figure 4.21).

Our data demonstrated IL-16 was expressed by CD11b$^+$ cells predominantly within the lesion in the area near the dentate gyrus and the white matter of cerebellum regions of brain tissue sections from MOG_{35-55} immunised mice. Quantification of the percentage of CD11b$^+$ cells expressing IL-16 out of the total CD11b$^+$ cells in the comparable ROI revealed both EAE mice at day 12 (50 ± 3%) and day 16 (59 ± 3%) had significantly higher percentage of CD11b$^+$ IL-16$^+$ cells in comparison to the EAE mice at day 26 which didn't demonstrate any CD11b$^+$ cells co-expressing IL-16 (Figure 4.20D).

In the cerebellum (white matter), quantification revealed significantly higher percentage of CD11b$^+$ cells co-expressing IL-16 in EAE mice at day 12 (50 ± 3%) and day 16 (59 ± 3%) in comparison to EAE mice at day 26 which didn't demonstrate any CD11b$^+$ cells co-expressing IL-16. And the co-expression was significantly higher in EAE day 12 mice in comparison to the EAE day 16 mice (Figure 4.21D).

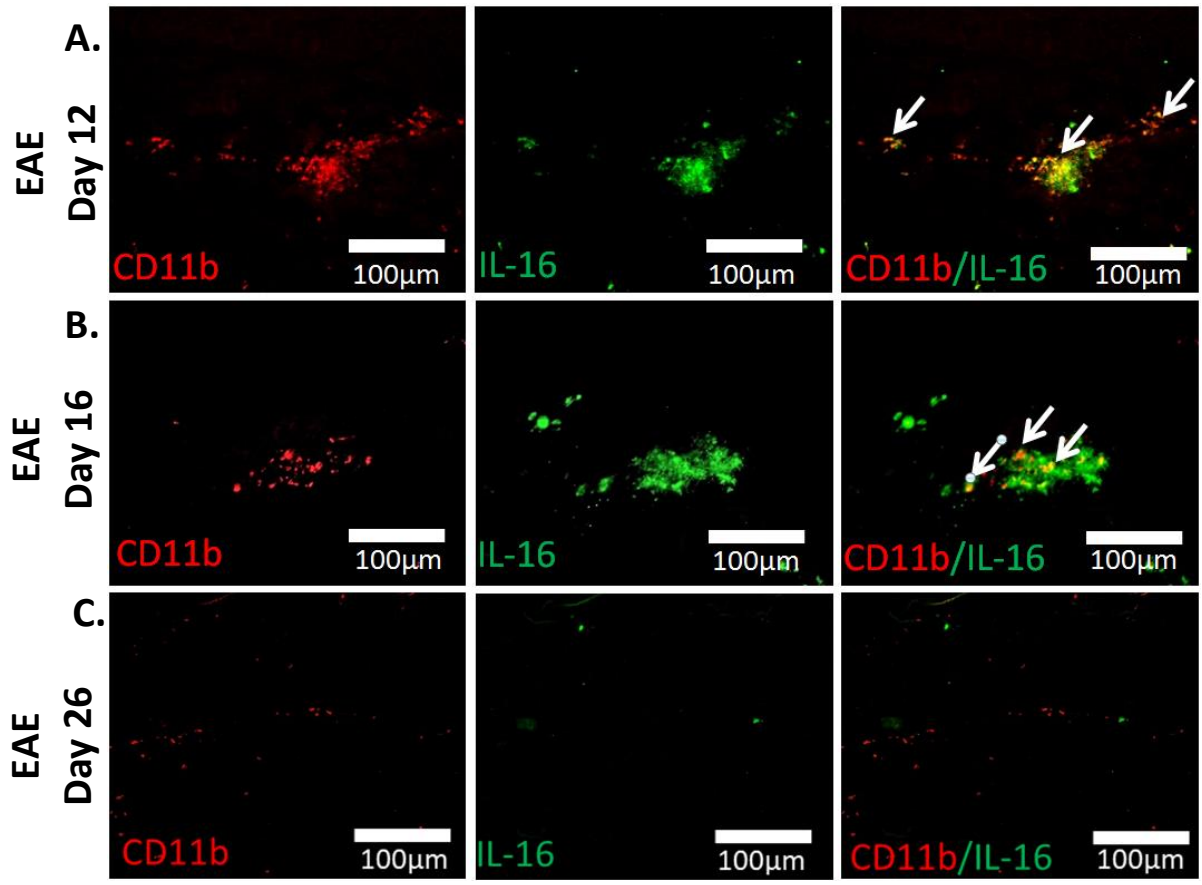

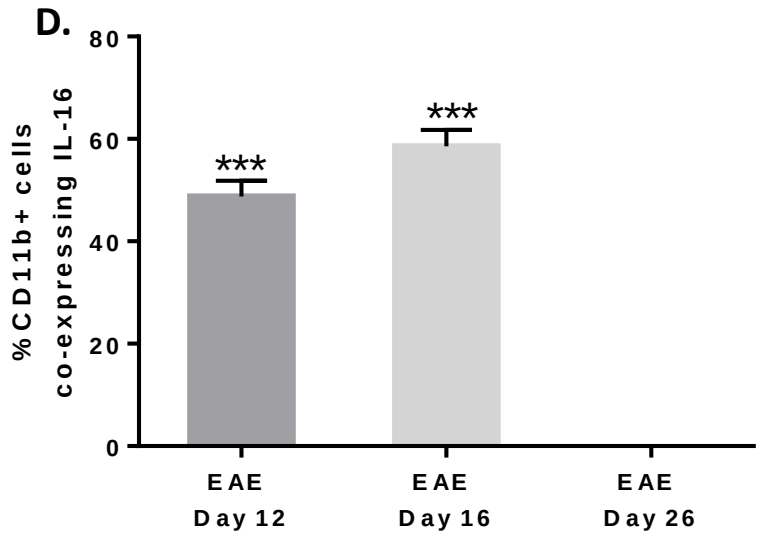

Figure 4.20: Expression of IL-16 by CD11b⁺ cells in the hippocampus (area near dentate gyrus) of EAE mice*. Brains were harvested from EAE* ***(A)*** *day 12,* ***(B)*** *day 16 and* ***(C)*** *day 26 mice and the tissues were stained with anti-IL-16 (Green) and anti-CD11b (Red). Data are representative of each group. n=5 for all groups. Scale bars of the images = 100µm.* ***(D)*** *Percentage of CD11b⁺ cells expressing IL-16 in naïve, PBS and EAE hippocampus (area near dentate gyrus) has been quantified using the cell counter tool of Image J software and result expressed as mean ± S.E.M. Statistical significance was determined by one-way ANOVA with Bonferroni post-hoc. ***P <0.001 versus EAE day 26.*

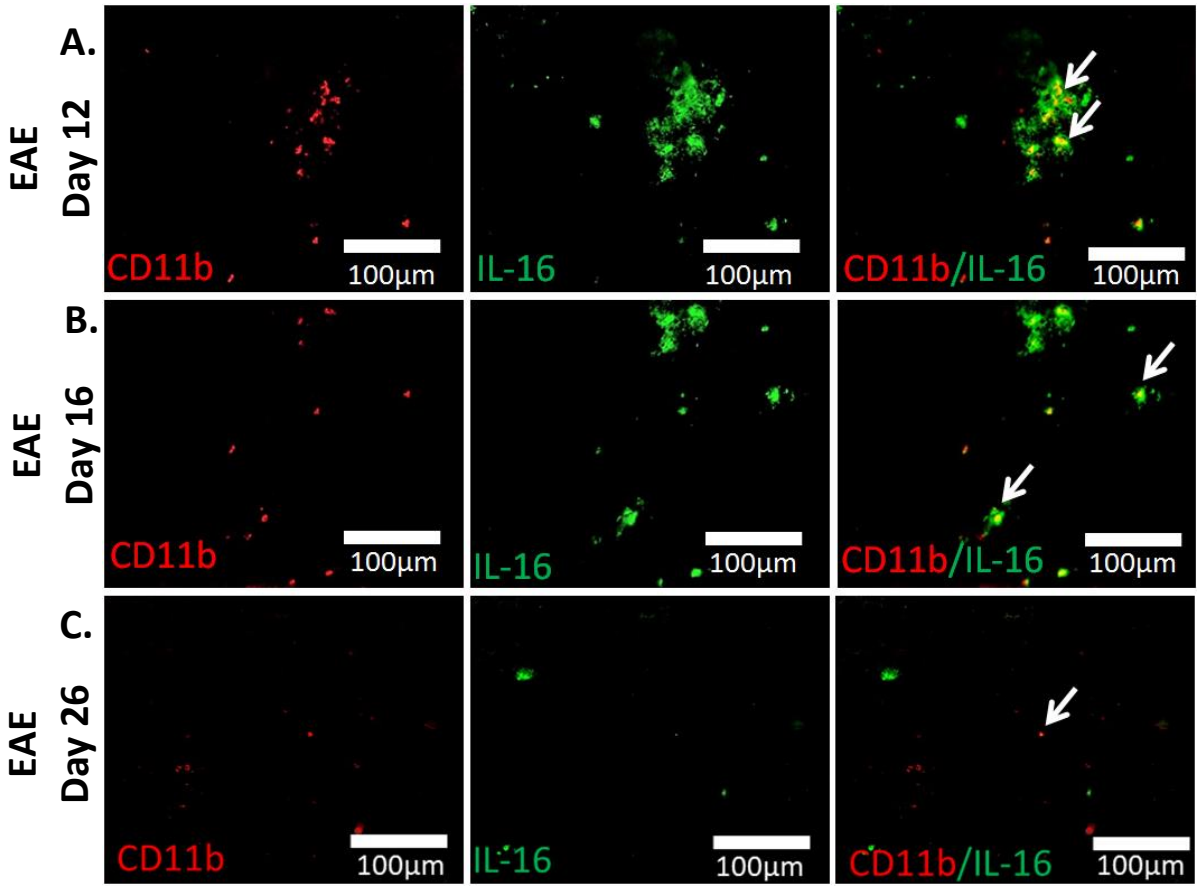

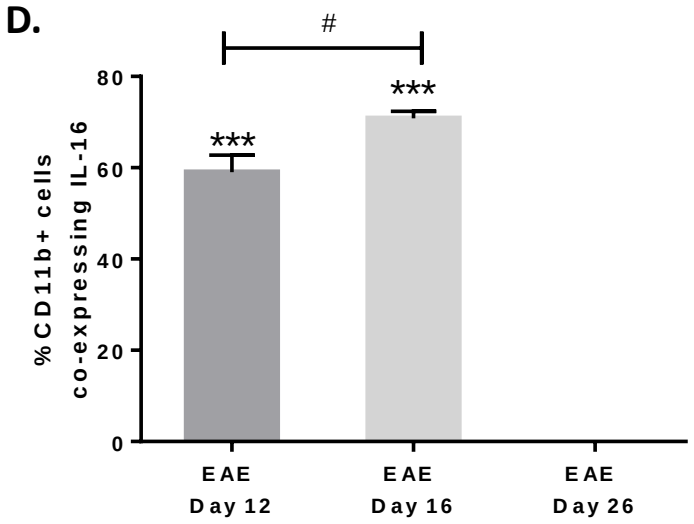

Figure 4.21: Expression of IL-16 by CD11b⁺ cells in the cerebellum (white matter) of EAE mice. *Brains were harvested from EAE (A) day 12, (B) day 16 and (C) day 26 mice and the tissues were stained with anti-IL-16 (Green) and anti-CD11b (Red). Data are representative of each group. n=5 for all groups. Scale bars of the images = 100µm. (G) Percentage of CD11b+ cells expressing IL-16 in EAE cerebellum (white matter) has been quantified using the cell counter tool of Image J software and result expressed as mean ± S.E.M. Statistical significance was determined by one-way ANOVA with Bonferroni post-hoc. ***P <0.001 versus EAE day 26; #P <0.05 versus EAE day 12.*

4.2.15 IL-16 expression on F4/80^{+} cells in brain tissues

Expression of IL-16 by F4/80^{+} cells was studied next using immunofluorescence staining in brain tissue section of EAE day 12, day 16 and day 26 mice. Surprisingly our data revealed the absence of F4/80^{+} cells within the brain tissue sections of all three time points of EAE mice, thus no co-expression with IL-16 was observed in either the hippocampus (area near dentate gyrus) (Figure 4.22) or the cerebellum (white matter) (Figure 4.23).

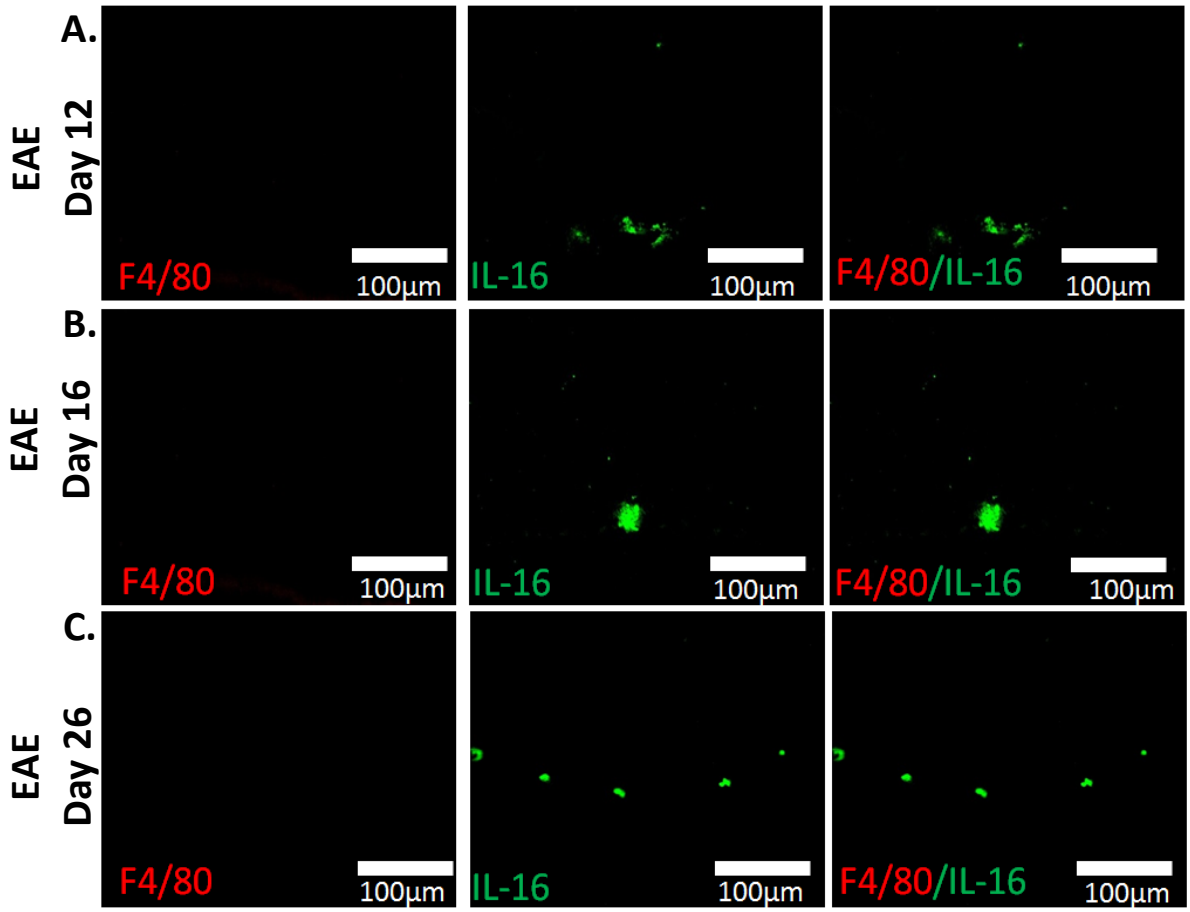

Figure 4.22: F4/80^{+} cells were undetected and did not express IL-16 in the hippocampus (area near dentate gyrus) of EAE mice*. Brains were harvested from EAE* ***(A)*** *day 12,* ***(B)*** *day 16 and* ***(C)*** *day 26 mice and the tissues were stained with anti-IL-16 (Green) and anti-F4/80 (Red). Data are representative of each group. n=5 for all groups. Images X20 magnification, scale bars = 100µm.*

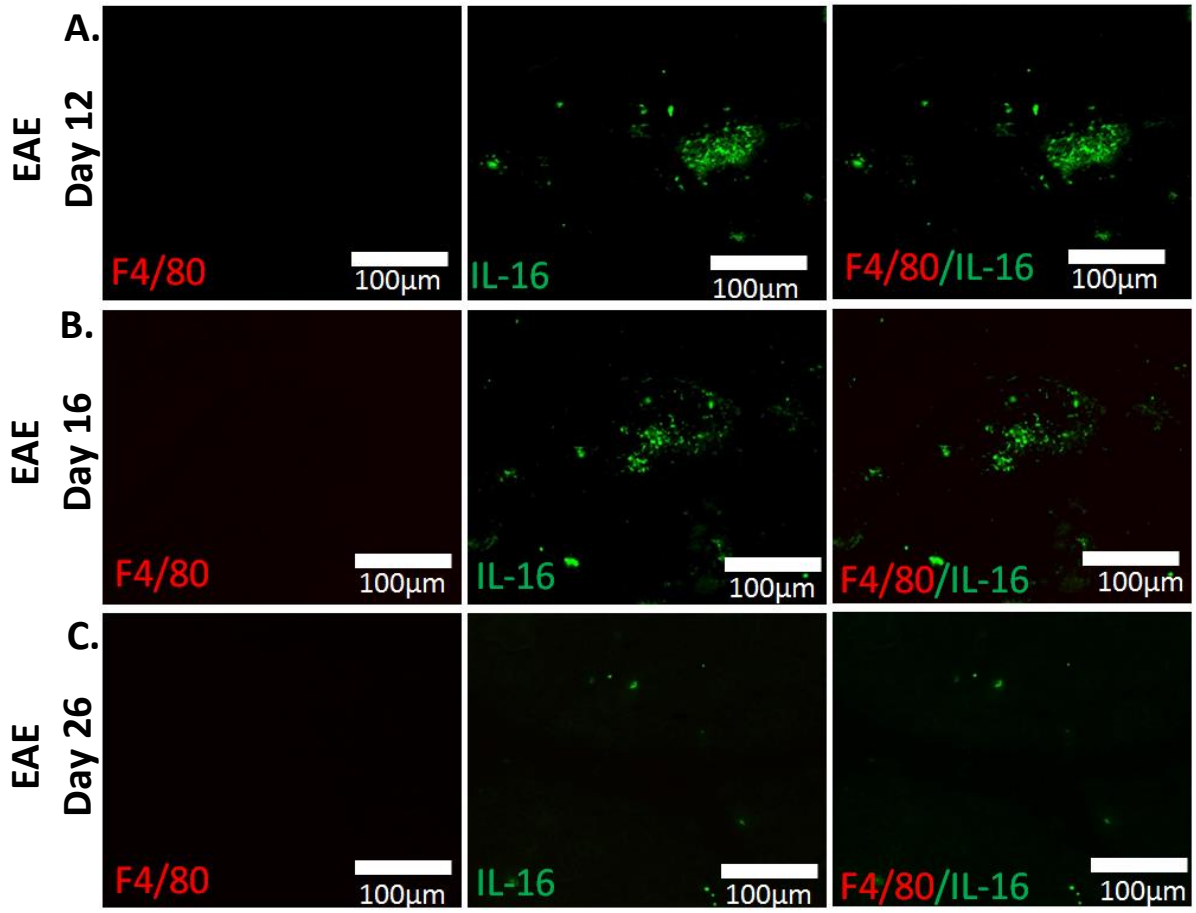

Figure 4.23: F4/80^{+} cells were undetected and did not express IL-16 in the cerebellum (white matter) of EAE mice*. Brains were harvested from EAE* ***(A)*** *day 12,* ***(B)*** *day 16 and* ***(C)*** *day 26 mice and the tissues were stained with anti-IL-16 (Green) and anti-F4/80 (Red). Data are representative of each group. n=5 for all groups. Images X20 magnification, scale bars = 100µm.*

4.2.16 IL-16 expression on neurons in brain tissues

In this chapter we have shown that the neurons expressed IL-16 in the spinal cord tissue sections, to investigate if this is consistent within the brain tissues, we next utilised double immunofluorescence staining to examine the co-expression of IL-16 with NeuN in brain tissue sections. IL-16 co-expression was specifically assessed within the pyramidal layer of CA3 region of the hippocampus (Figure 4.24) and the granular layer and the Purkinje cells of the cerebellum (Figure 4.25) mainly because the neurons in these regions demonstrated the expression of IL-16 as shown in Chapter 3.

Our data again confirmed that IL-16 was expressed by neurons within the brain tissue sections from naïve, PBS day 16, EAE (day 12, 16 and 26) mice groups. Quantification of the percentage $NeuN^+$ $IL\text{-}16^+$ cells out of the total $NeuN^+$ cells, within the comparable ROI in the pyramidal layer of CA3 region of hippocampus, did not demonstrate any difference between the naïve (52 ± 2%) and PBS (49 ± 3 %) mice. Brain tissue sections from EAE mice at day 12 (48 ± 3%), day 16 (48 ± 2 %) and day 26 (47 ± 2%) also had similar levels of percentage as with the other two mice groups (Figure 4.24F).

Similarly, co-expression quantified within the ROI in the GL and Purkinje cell of cerebellum did not demonstrate any difference between naïve (26 ± 2%), PBS day 16 (28 ± 2%) mice and any of the EAE mice at day 12 (29 ± 2%), day 16 (28 ± 2 %) and day 26 (30 ± 2 %) (Figure 4.25F).

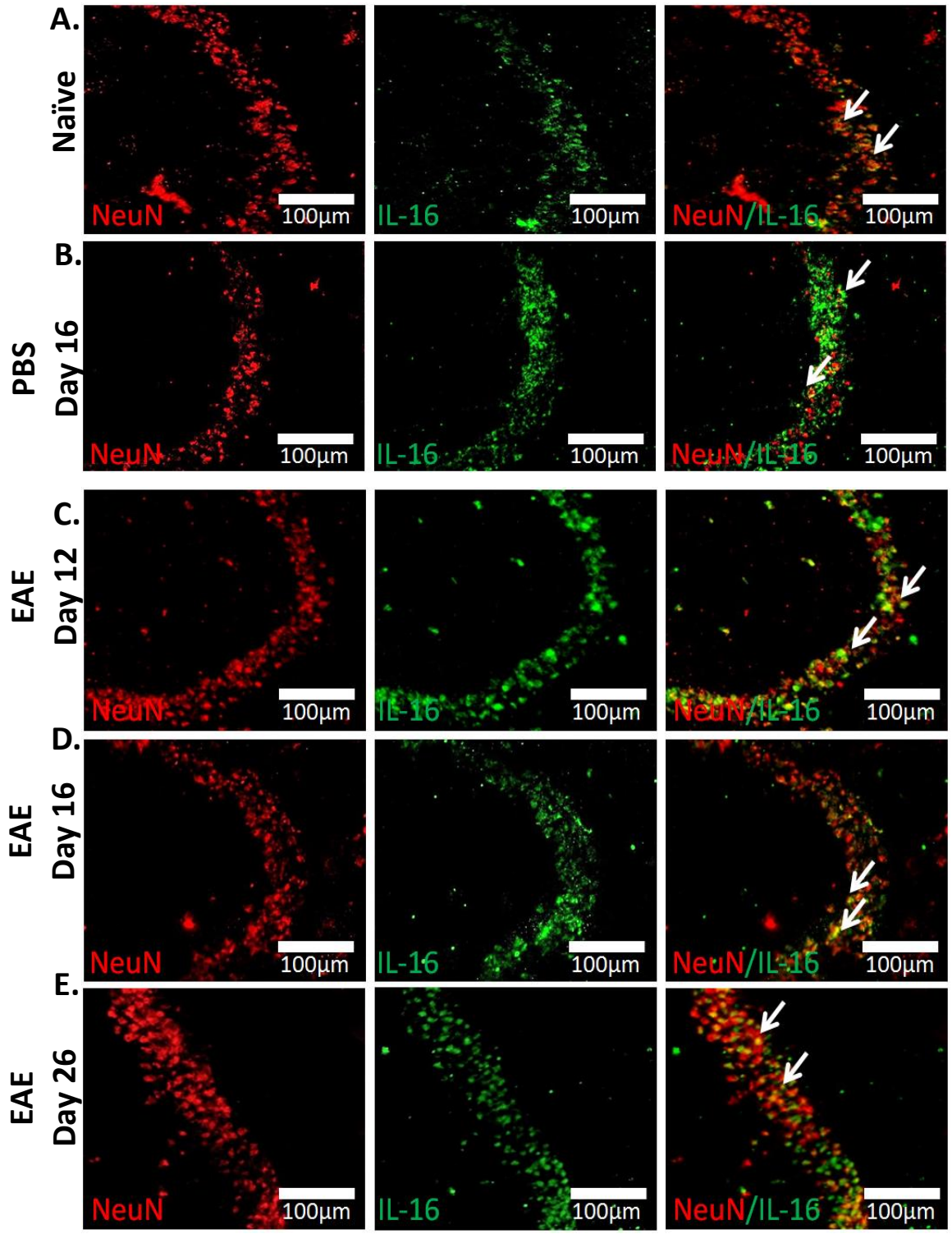
A.
Naïve
NeuN
100µm
IL-16
100µm
NeuN/IL-16
100µm
B.
PBS
Day 16
NeuN
100µm
IL-16
100µm
NeuN/IL-16
100µm
C.
EAE
Day 12
NeuN
100µm
IL-16
100µm
NeuN/IL-16
100µm
D.
EAE
Day 16
NeuN
100µm
IL-16
100µm
NeuN/IL-16
100µm
E.
EAE
Day 26
NeuN
100µm
IL-16
100µm
NeuN/IL-16
100µm

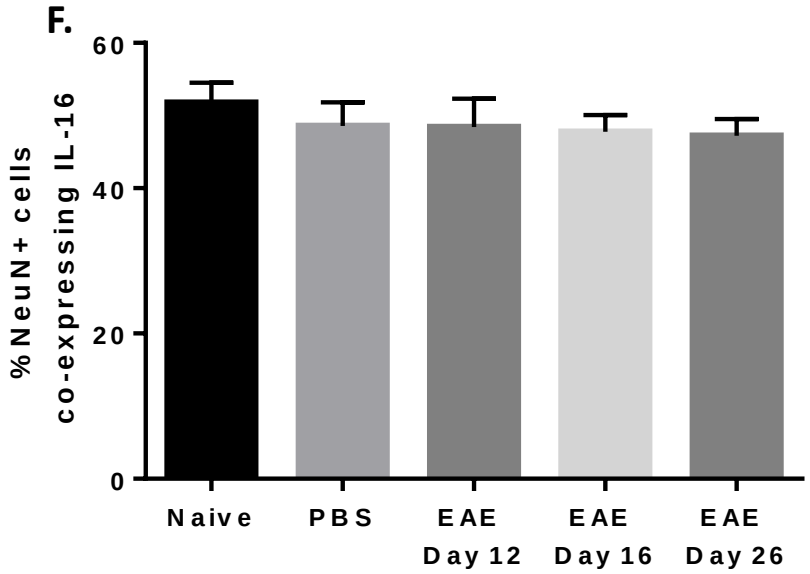

Figure 4.24: Expression of IL-16 by NeuN$^+$ cells in the in the hippocampus (pyramidal cells in CA3 region) of naïve, PBS and EAE mice. *Brains were harvested from* ***(A)*** *naïve,* ***(B)*** *PBS day 16 and EAE* ***(C)*** *day 12,* ***(D)*** *day 16, and* ***(E)*** *day 26 mice and the tissues were stained with anti-IL-16 (Green) and anti-NeuN (Red). Data are representative of each group. n=5 for all groups. Scale bars of the images = 100µm.* ***(F)*** *Percentage of NeuN$^+$ cells expressing IL-16 in naïve, PBS and EAE hippocampus (pyramidal cells in CA3 region) has been quantified using the cell counter tool of Image J software and result expressed as mean ± S.E.M. Statistical significance was determined by one-way ANOVA with Bonferroni post-hoc.*

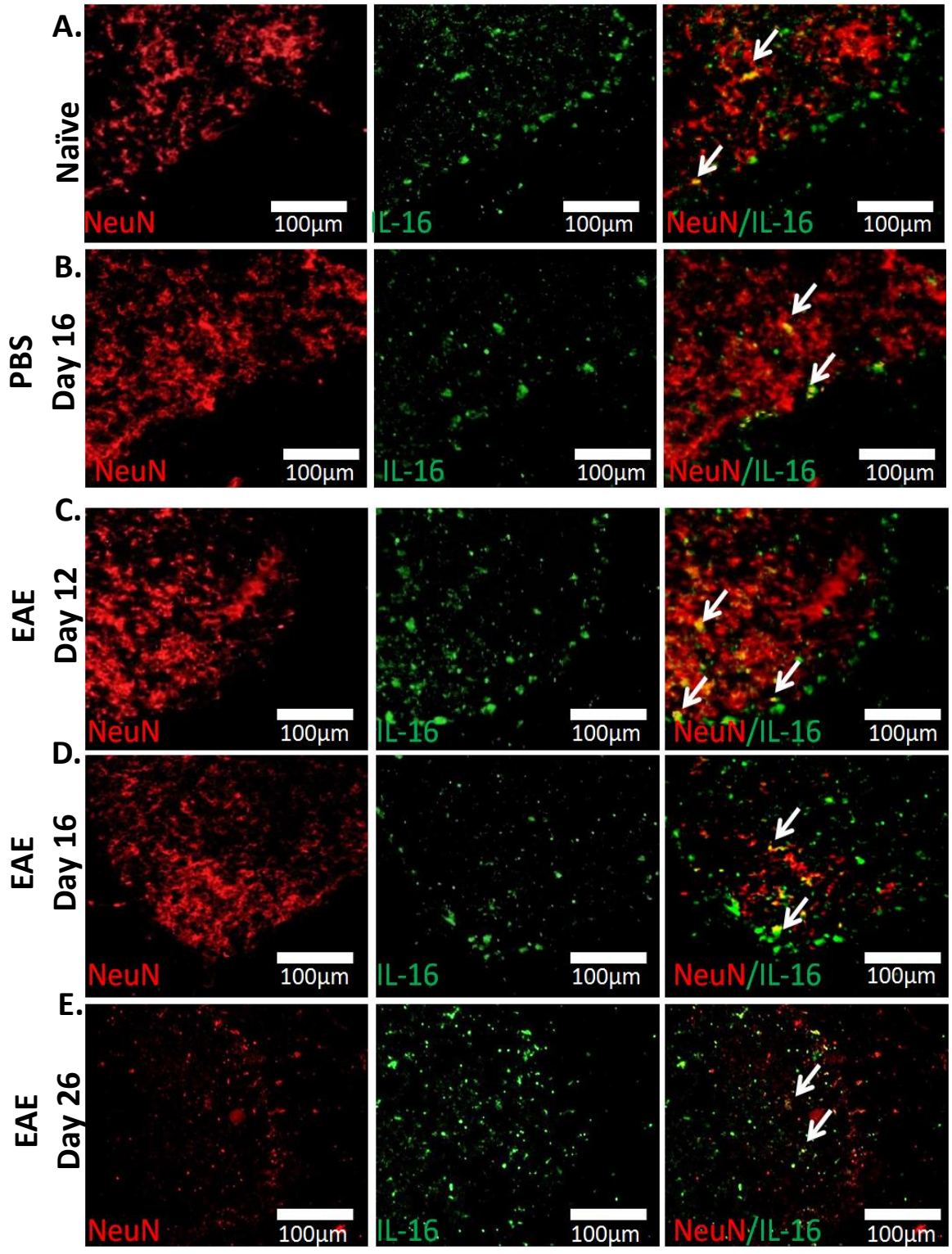
A.
Naïve
NeuN
100µm
IL-16
100µm
NeuN/IL-16
100µm
B.
PBS
Day 16
NeuN
100µm
IL-16
100µm
NeuN/IL-16
100µm
C.
EAE
Day 12
NeuN
100µm
IL-16
100µm
NeuN/IL-16
100µm
D.
EAE
Day 16
NeuN
100µm
IL-16
100µm
NeuN/IL-16
100µm
E.
EAE
Day 26
NeuN
100µm
IL-16
100µm
NeuN/IL-16
100µm

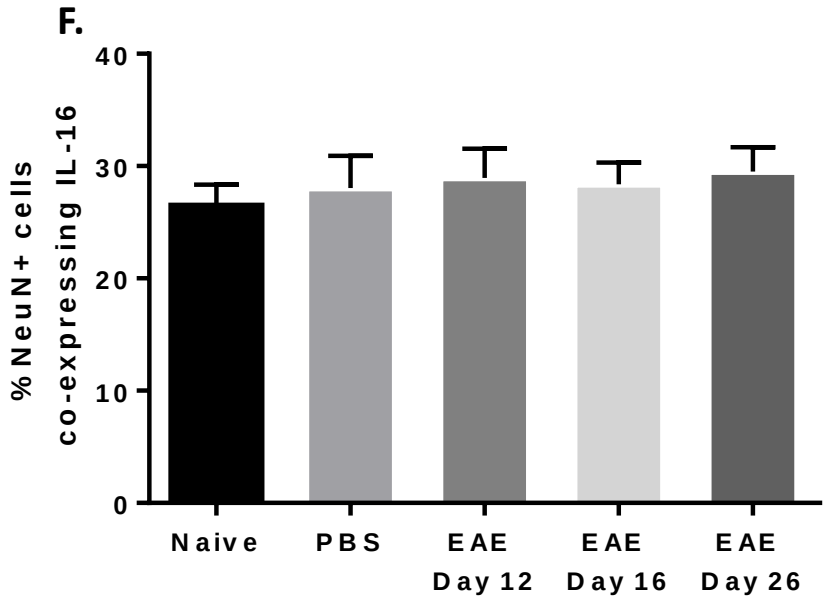

Figure 4.25: Expression of IL-16 by NeuN$^+$ cells in the cerebellum (granule cells in the granular layer and Purkinje cells) of naïve, PBS and EAE mice. *Brains were harvested from* ***(A)*** *naïve,* ***(B)*** *PBS day 16, and EAE* ***(C)*** *day 12* ***(D)*** *day 16 and* ***(E)*** *day 26 mice and the tissues were stained with anti-IL-16 (Green) and anti-NeuN (Red). Data are representative of each group. n=5 for all groups. Scale bars of the images = 100µm.* ***(F)*** *Percentage of NeuN$^+$ cells expressing IL-16 in naïve, PBS and EAE cerebellum (granule cells in the granular layer and Purkinje cells) has been quantified using the cell counter tool of Image J software and result expressed as mean ± S.E.M. Statistical significance was determined by one-way ANOVA with Bonferroni post-hoc.*

4.2.17 IL-16 expression on astrocytes in brain tissues

Earlier in this chapter we have shown that during EAE, astrocytes within the lesion of the white matter of EAE spinal cord tissue sections co-expressed IL-16. Here we examined the co-expression of IL-16 with GFAP in the brain tissues of control and EAE mice. IL-16 co-expression was specifically assessed within the region where the cellular infiltration and lesions were observed in the hippocampus (area near the dentate gyrus) (Figure 4.26) and the cerebellum (white mater) (Figure 4.27).

There was no co-localisation of IL-16 on astrocytes within the naïve and PBS day 16 hippocampus (area near dentate gyrus) or the cerebellum (white matter) of the brain tissue sections due to the absence of IL-16 within this region (Figure 4.26 A and B). Our data demonstrated IL-16 was expressed by astrocytes predominantly within the lesion in the brain tissue sections from MOG_{35-55} immunised mice (Figure 4.26 C, D and E). Quantification of percentage $GFAP^+$ $IL\text{-}16^+$ cells out of the total $GFAP^+$ cells within the comparable ROI in the hippocampus (area near dentate gyrus) of the brain tissue sections revealed that EAE mice at day 12 (19 ± 1%) and day 16 (22 ± 1%) had significantly higher percentage of $GFAP^+$ cells expressing IL-16 within the hippocampus in comparison to the mice at day 26 (11 ± 1%) (Figure 4.26F)

Similarly, co-expression quantified within the ROI in the cerebellum (white matter) of the brain tissues demonstrated EAE mice at day 12 (25 ± 1%) and day 16 (29 ± 1%) had significantly higher co-expression in comparison to EAE mice at day 26 (20 ± 1 %). However, EAE mice at day 16 demonstrated significantly higher percentage of co-expressing cell population in comparison to EAE day 12 mice (Figure 4.27F).

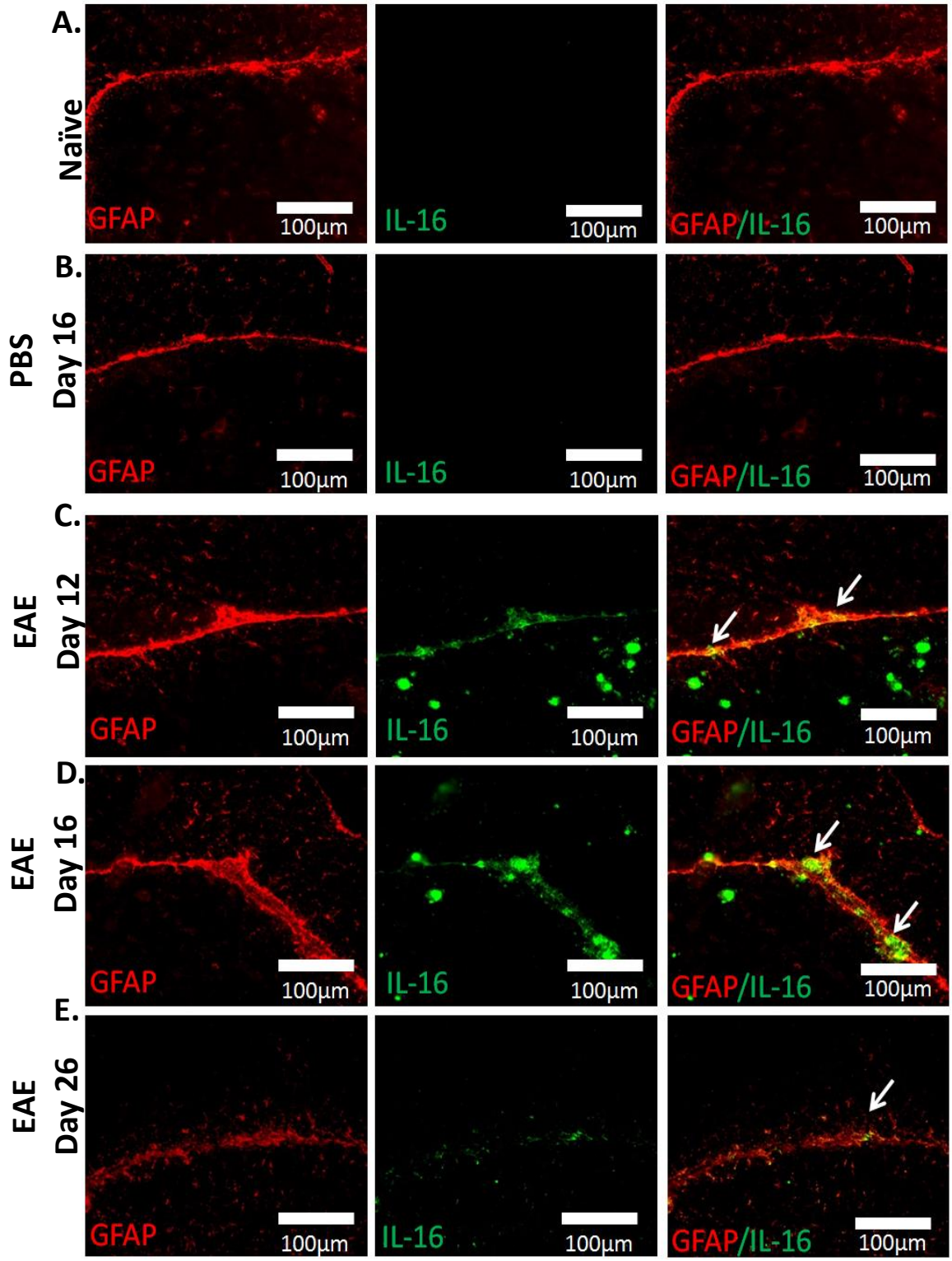
A.
Naïve
GFAP
100µm
IL-16
100µm
GFAP/IL-16
100µm
B.
PBS
Day 16
GFAP
100µm
IL-16
100µm
GFAP/IL-16
100µm
C.
EAE
Day 12
GFAP
100µm
IL-16
100µm
GFAP/IL-16
100µm
D.
EAE
Day 16
GFAP
100µm
IL-16
100µm
GFAP/IL-16
100µm
E.
EAE
Day 26
GFAP
100µm
IL-16
100µm
GFAP/IL-16
100µm

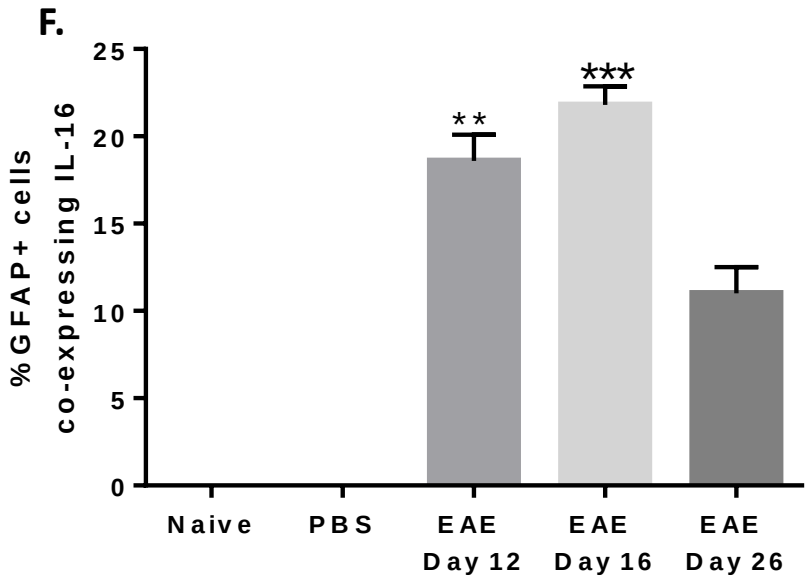

Figure 4.26: Expression of IL-16 by GFAP⁺ cells in the hippocampus (area near dentate gyrus) of naïve, PBS and EAE mice*. Brains were harvested from* ***(A)*** *naïve,* ***(B)*** *PBS day 16, and EAE* ***(C)*** *day 12* ***(D)*** *day 16 and* ***(E)*** *day 26 mice and the tissues were stained with anti-IL-16 (Green) and anti-GFAP (Red). Data are representative of each group. n=5 for all groups. Scale bars of the images = 100µm.* ***(F)*** *Percentage of GFAP⁺ cells expressing IL-16 in naïve, PBS and EAE hippocampus (area near dentate gyrus) has been quantified using the cell counter tool of Image J software and result expressed as mean ± S.E.M. Statistical significance was determined by one-way ANOVA with Bonferroni post-hoc. **P <0.01, ***P <0.001 versus EAE day 26.*

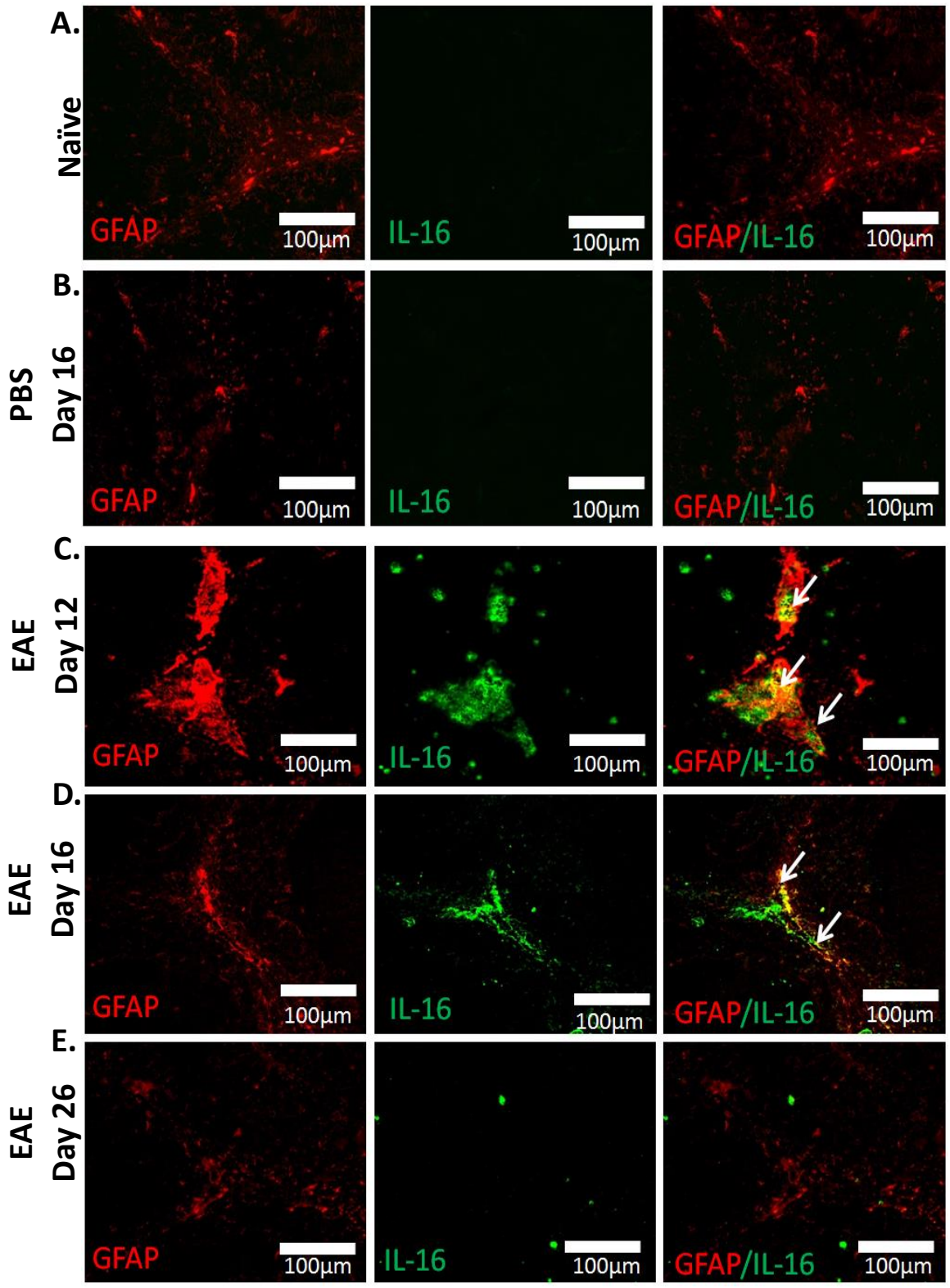
A.
Naïve
GFAP
100µm
IL-16
100µm
GFAP/IL-16
100µm
B.
PBS
Day 16
GFAP
100µm
IL-16
100µm
GFAP/IL-16
100µm
C.
EAE
Day 12
GFAP
100µm
IL-16
100µm
GFAP/IL-16
100µm
D.
EAE
Day 16
GFAP
100µm
IL-16
100µm
GFAP/IL-16
100µm
E.
EAE
Day 26
GFAP
100µm
IL-16
100µm
GFAP/IL-16
100µm

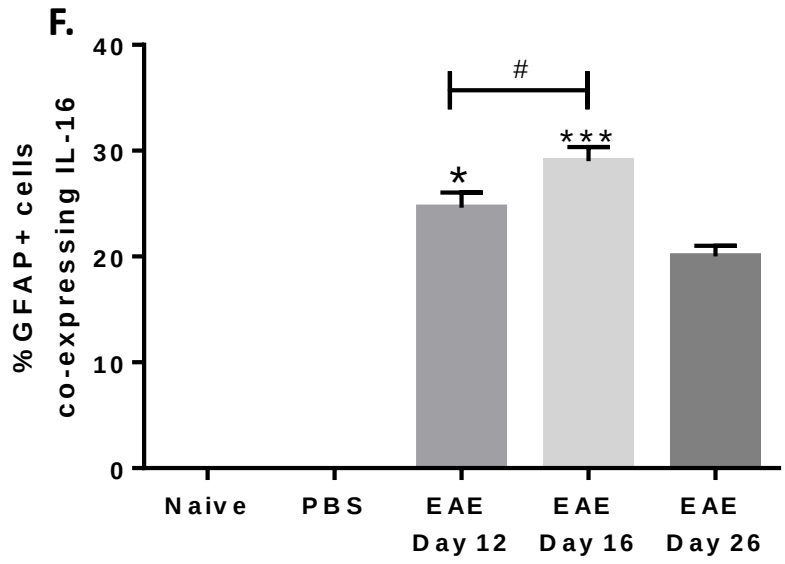

Figure 4.27: Expression of IL-16 by GFAP⁺ cells in the cerebellum (white matter) of naïve, PBS and EAE mice*. Brains were harvested from* ***(A)*** *naïve,* ***(B)*** *PBS day 16 and EAE* ***(C)*** *day 12,* ***(D)*** *day 16 and* ***(E)*** *day 26 mice and the tissues were stained with anti-IL-16 (Green) and anti-GFAP (Red). Data are representative of each group. n=5 for all groups. Scale bars of the images = 100µm.* ***(F)*** *Percentage of GFAP⁺ cells expressing IL-16 in naïve, PBS and EAE cerebellum (white matter) has been quantified using the cell counter tool of Image J software and result expressed as mean ± S.E.M. Statistical significance was determined by one-way ANOVA with Bonferroni post-hoc. *P <0.05, ***P <0.001 versus EAE day 26; #P <0.05 versus EAE day 12.*

4.2.18 Summary of IL-16 expression by immune cells in lymphoid organs and CNS

Earlier in this chapter we have shown co-expression of IL-16 on different immune cells in the spleen, lymph node and CNS tissues of MOG_{35-55} immunised mice at different stages of EAE. Here we have compared the percentage of IL-16 expression in various immune cells in these tissues collected from MOG_{35-55} immunised mice at day 16 after immunisation to determine the immune cell population with highest level of IL-16 expression during CNS inflammation.

Our data revealed that co-expression of IL-16 was significantly higher on $CD11b^+$ cells in comparison to the $CD4^+$ and $F4/80^+$ cells in all the different types of tissues we have assessed.

In spleen (Figure 4.28A) 37 ± 1% of the total $CD11b^+$ cells co-expressed IL-16 while only 5 ± 1% of the total $CD4^+$ cells and 13 ± 1% of the total $F4/80^+$ cells co-expressed IL-16. Similar trend of co-expression was also observed in the lymph node (Figure 4.28B), with 30 ± 0.5% of total $CD11b^+$ cells co-expressing IL-16 whereas only 7 ± 0.5% of the total $CD4^+$ cells and 10 ± 0.3% of the total $F4/80^+$ cells co-expressed IL-16.

In spinal cord (Figure 4.28C), 21 ± 0.5% of the total $CD11b^+$ cells co-expressed IL-16, however 17 ± 0.5% of the total $CD4^+$ cells and 5 ± 0.6% of the total $F4/80^+$ cells co-expressed IL-16.

In the hippocampus (Figure 4.28D) 58 ± 1% of the total $CD11b^+$ cells co-expressed IL-16, while only 14.4% of the total $CD4^+$ cells co-expressed IL-16. $F4/80^+$ cells were not detected in the brain, so no co-localisation was observed with F4/80. In the cerebellum (Figure 4.28E) 70 ± 1% of total $CD11b^+$ cells co-expressed IL-16 and 31 ± 1% of total $CD4^+$ cells co-expressed IL-16.

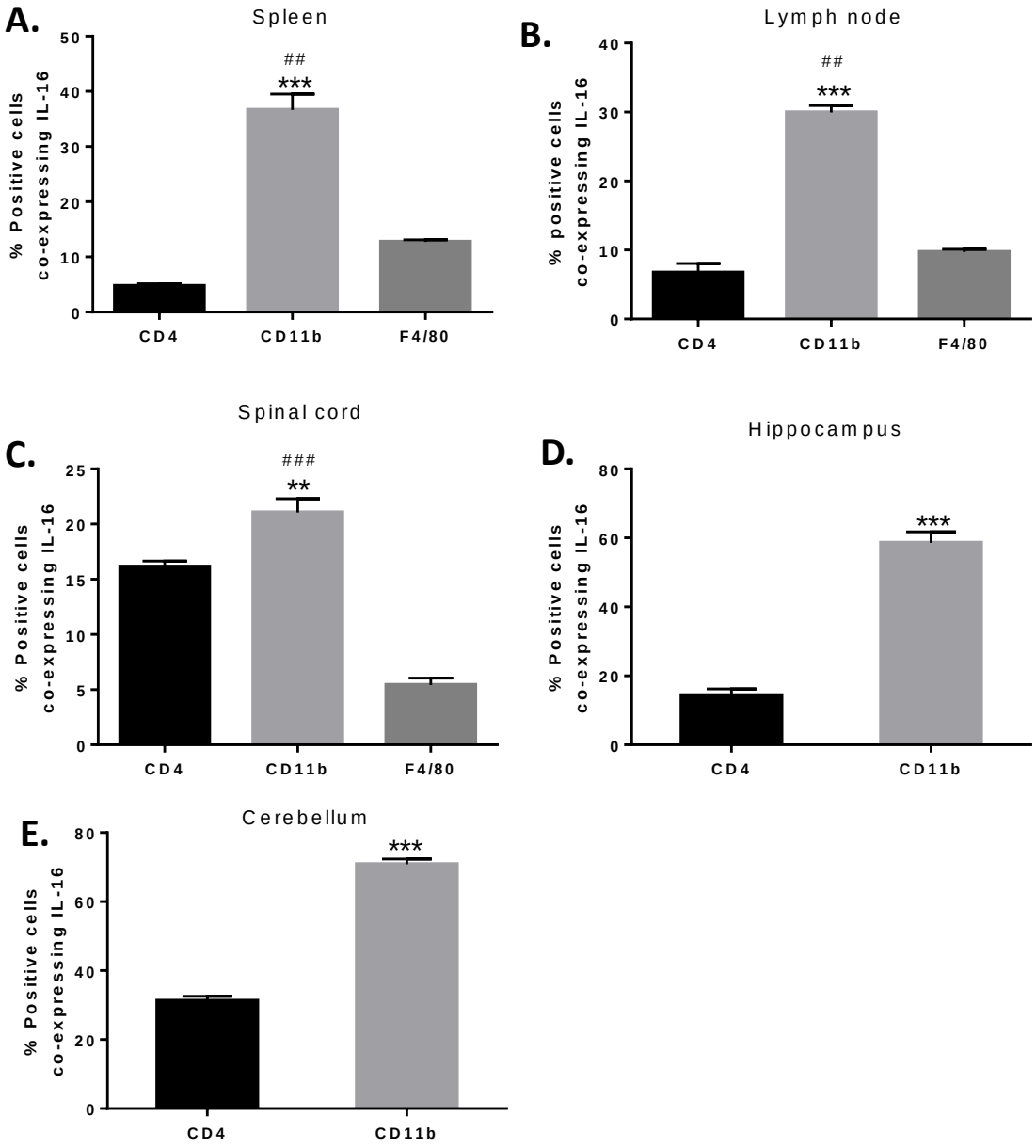

Figure 4.28: Increased co-expression of IL-16 on CD11b$^+$ cells in comparison to CD4$^+$ and F4/80$^+$ cells. *Percentage CD11b$^+$ cells co-expressing IL-16 in **(A)** spleen, **(B)** lymph node, **(C)** spinal cord and **(D)** brain tissues from MOG$_{35-55}$ immunised mice at day 16 post immunisation was higher than that of CD4$^+$ and F4/80$^+$. Percentage positive cells co-expressing IL-16 has been quantified using the cell counter tool of Image J software and result expressed as mean ± S.E.M. n=5 for all group. Statistical significance was determined by one-way ANOVA with Bonferroni post-hoc. **P <0.01, ***P <0.001 versus CD11b$^+$ cells; $^{###}$P <0.001, $^{##}$P <0.01 versus F4/80$^+$ cells.*

4.2.19 IL-16 expression and production by CD11b$^+$ cells

As CD11b$^+$ cells were observed to be the dominant cell population with highest co-expression of IL-16, suggesting CD11b$^+$ cells may be the main mediating cells for the function of IL-16 during CNS inflammation, so next we wanted to study if CD11b$^+$ cells secrete IL-16 after an inflammatory stimulus.

Before checking the cell function we utilised double immunofluorescence staining in isolated CD11b$^+$ cells from spleen, blood and CNS cell suspensions of EAE day 16 mice to examine if they expressed IL-16. Our data demonstrated co-localisation of IL-16 in the CD11b$^+$ cells isolated from spleen (Figure 4.29A), blood (Figure 4.29B) and CNS tissues (Figure 4.29C). However not all CD11b$^+$ cells expressed IL-16 while all IL-16 was co-localised with CD11b$^+$ cells here as there should be no other cells after the isolation process.

To examine if CD11b$^+$ cells produced IL-16, CD11b$^+$ cells were isolated and cultured (spleen 10 x 10^6 /ml; blood 2.5 X 10^6 /ml; and CNS 0.5 x 10^6 /ml) for 24 hours with either media alone or media supplemented with LPS (50 µg/ml) and supernatants were harvested for ELISA assay to assess the levels of production of IL-16. CD11b$^+$ cells isolated from spleen cell suspension produced 2776.1 ± 185.7 pg/ml and 2755.2 ± 178.7 pg/ml of IL-16 respectively when cultured with media alone and upon LPS stimulation, with no significant difference between the media and LPS cultures for both tissue cells (Figure 4.30A). CD11b$^+$ cells isolated from whole blood cells produced 140.0 ± 3.5 pg/ml of IL-16 when cultured with media alone and again LPS stimulation did not alter the production of IL-16, with CD11b$^+$ cells producing 150.6 pg/ml of IL-16 (Figure 4.30B). Similarly, IL-16 production by CD11b$^+$ cells isolated from CNS cell suspension was also unaltered upon LPS stimulation, with cells cultured with media alone produced 987.8 ± 137.3 pg/ml of IL-16 while stimulated cells produced 898.0 ± 93.7 pg/ml of IL-16 (Figure 4.30C). Interestingly the amount of IL-16 produced per million cells in the spleen, blood and CNS varies dramatically (Figure 4.30D), with CNS CD11b$^+$ cells (media: 796 ± 187.4 pg/ml; LPS: 1975.5 ± 274.6 pg/ml) producing the highest levels of IL-16 in comparison to spleen (media: 277.61 ± 18.77 pg/ml; LPS: 275.52 ± 17.82 pg/ml) and blood (media 56 ± 8.75 pg/ml ; 60.24 ± 9.08 pg/ml) CD11b$^+$ cells. The data indicate

the potential different functions of CD11b^{+} cells depending on the tissues they reside.

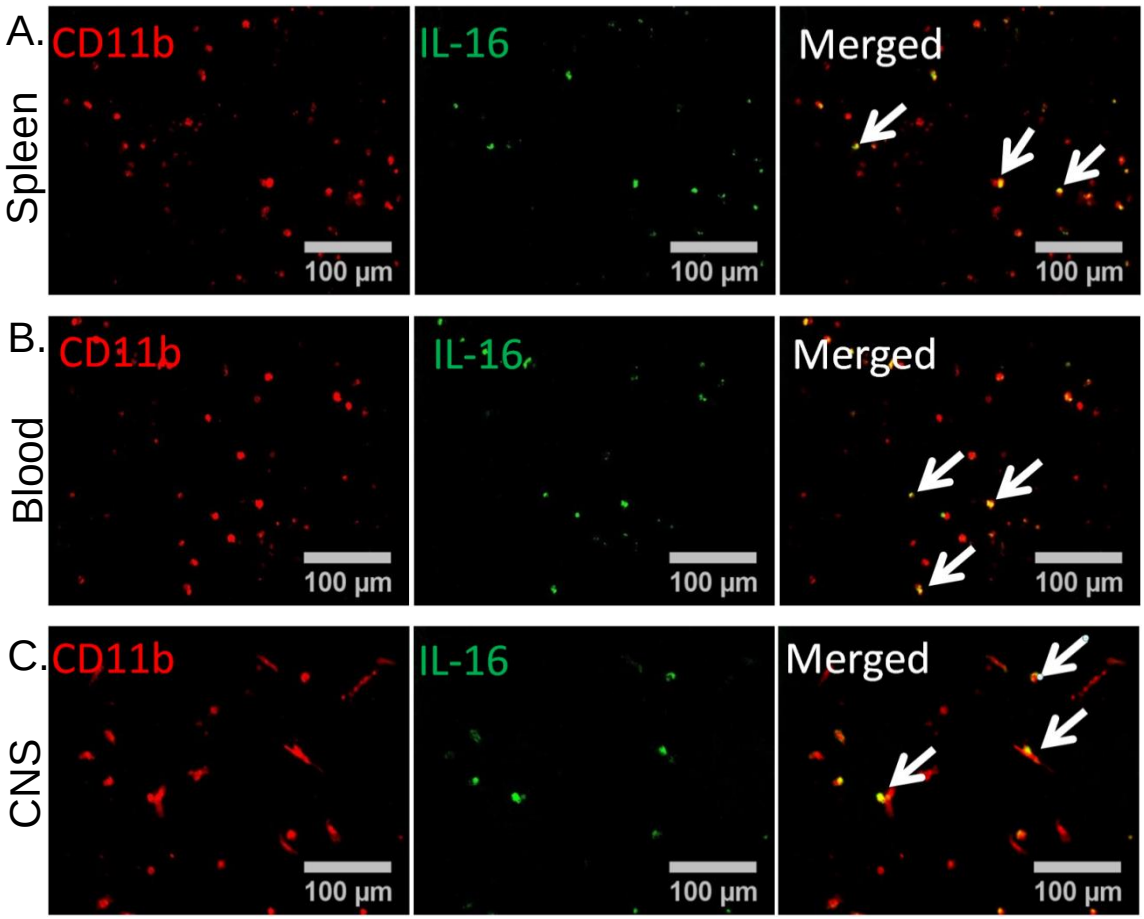

Figure 4.29: CD11b^{+} cells isolated from spleen, blood and CNS of EAE mice co-expressed IL-16*. CD11b^{+} cells were isolated from* ***(A)*** *spleen* ***(B)*** *blood* ***(C)*** *CNS cell suspension of EAE mice were stained with anti-IL-16 (Green) and anti-CD11b (Red). Data are representative of each group. n=2 for all groups. Images X20 magnification, scale bars = 100µm.*

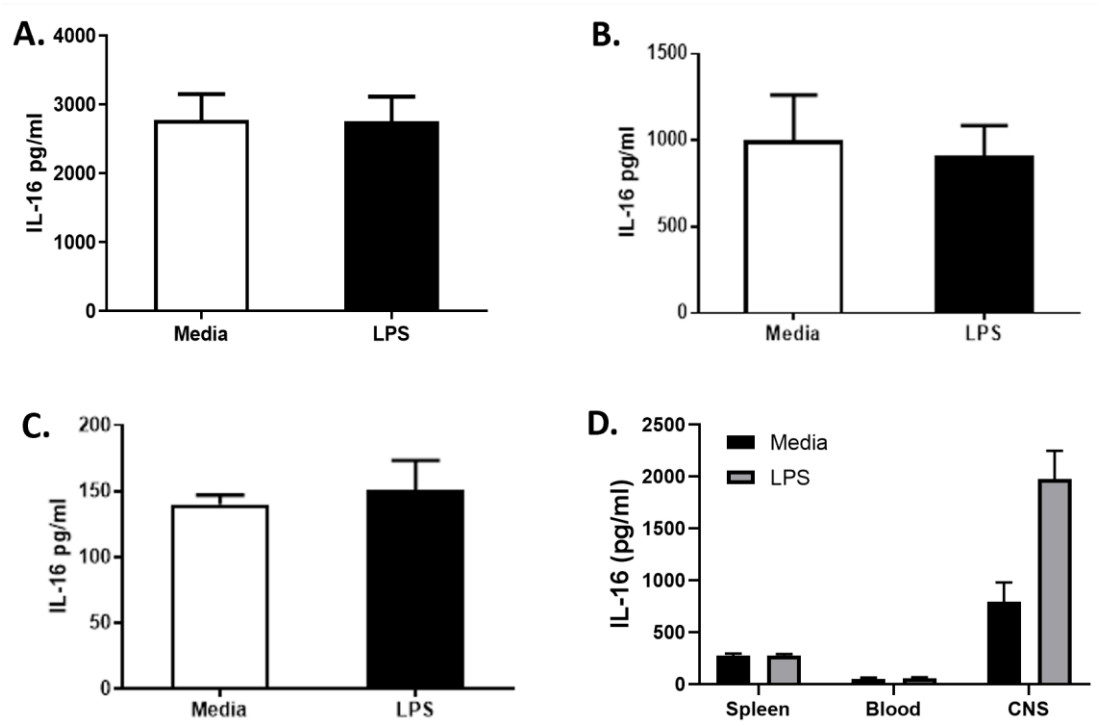

Figure 4.30: IL-16 production by CD11b$^+$ isolated from of EAE mice was unaltered upon LPS stimulation*. CD11b$^+$ cells were isolated from* ***(A)*** *spleen,* ***(B)*** *blood and* ***(C)*** *CNS cells suspension and incubated either with media alone or media containing LPS (50 µg/ml) and then checked for IL-16 production.* ***(D)*** *Graph represents the level of IL-16 produced per million cells of spleen, blood and CNS. n=2 for all group. Result illustrated as mean ± S.E.M.*

4.3 Discussion

Despite the recent research on IL-16 in MS/EAE (Skundric *et al*., 2005; Skundric *et al*., 2015), the precise cellular source and expression levels of IL-16 have not been conclusively determined. In this chapter we proceeded to identify the cellular sources of IL-16 in tissues collected from mice immunised with PBS or MOG_{35-55}. Our study in this chapter demonstrates that IL-16 protein is expressed by various immune cells in the lymphoid tissues and by CNS resident cells as well as infiltrating immune cells in the CNS tissues. Consistent with previous study where IL-16 up-regulation has been observed in the peripheral lymphoid organs (lymph node and spleen) and CNS tissues collected from mice with relapsing EAE (Skundric *et al*., 2005), we have also observed elevated level of IL-16 expression in MOG_{35-55} immunised mice when compared with naïve controls. In spleen and lymph nodes both EAE (day 16) and PBS (day 16) mice had the elevated levels of IL-16 in comparison to naïve control. Whereas in the CNS of EAE mice at onset (day 12) and peak (day 16) stage of the disease had the highest percentage of IL-16 expression in comparison to both naïve and PBS (day 16) controls, with increased expression predominantly within the lesion. While quantification of $IL\text{-}16^+$ cells without including the EAE lesion, demonstrated similar percentage of $IL\text{-}16^+$ cells in both EAE and control mice groups. This observation in CNS tissues indicated that the expression of IL-16 by some CNS resident cells was unaltered with or without neuroinfammation.

Previously many studies have indicated the expression of various cytokines by neurons in the CNS including IFN-γ, IL-1β, IL-6 and TNF-α, which have been linked to the modulation of synaptic plasticity, learning and memory as well as inflammation-related CNS disorders such as MS (Donzis & Tronson, 2014; Gruol, 2015; Vezzani & Viviani, 2015). Expression of IL-16 particularly within the grey matter of the CNS tissues indicated the possibility of its expression by CNS resident neurons. To investigate this further, we utilised double fluorescence staining in the CNS tissues with NeuN (a neuronal marker) and IL-16. In our study we have observed co-localisation of IL-16 with $NeuN^+$ cells in the CNS tissues of naïve, PBS or EAE mice and the quantification confirmed similar number of $NeuN^+$ cells co-expressing IL-16 in these mice within the

spinal cord (Figure 4.14) as well as in the hippocampus (Figure 4.24) and the cerebellum (Figure 4.25) of the brain. Our data is consistent with previous study by Kurschner *et al*., (1999), who have demonstrated the expression of NIL-16 (a larger neural-specific splice variant of the lymphocyte IL-16) in post-mitotic neurons of the mammalian hippocampus and cerebellum. While the study mentioned that NIL-16 is a cytosolic protein which has been only detected in hippocampus and the cerebellum, we observed IL-16 expression on neurons in the hippocampus, cerebellum as well as other regions (data not shown) of the murine brain. This expression pattern may be due to an IL-16 antibody that is not selective for NIL-16 but is nevertheless interesting given the proposed role of IL-16 in MS/ EAE. Furthermore, we are the first to demonstrate the expression of IL-16 on neurons within the murine spinal cord tissues. It is unclear how NIL-16 contributes in maintenance of neuronal homeostasis and in regulation of autoimmune mediated neuroinflammation but, what is known about NIL-16 is that it get processed by caspase 3 similar to that of lymphocyte IL-16 and once released NIL-16 serve as a signalling molecule through interaction with CD4 expressed on neurons. In our study we have observed the expression of CD4 in the CNS of EAE mice only, but not in any of the control mice, suggesting the function of IL-16 in CNS possibly through CD4 dependent and independent pathways.

While we did not observe any change in IL-16 expression by neurons within the grey matter of the CNS tissues from naïve, PBS and MOG_{35-55} immunised mice, however the number of other types of cells expressing IL-16 within white matter regions of EAE spinal cords and brain demonstrated a significant increase in comparison to the controls. As increased IL-16^{+} cells in the EAE spinal cord and brain was localised within the white matter regions where most immune cell infiltration are observed, and lesions develops during EAE pathogenesis, we hypothesized that IL-16 is likely expressed by infiltrating immune cells and possibly activated CNS resident cells present in the lesions in the CNS. To confirm this, we utilised co-localisation staining with cell types that are known to be present at high levels in EAE inflammatory lesions in the white matter using antibodies again GFAP; an astrocytic marker, CD45; an immune cell marker, CD4; T cell marker and CD11b/F4/80, monocytes/macrophage and microglia marker.

Astrocytes being the CNS resident cell, are well documented to have association with MS/EAE pathogenesis and the reactivity of astrocyte around inflammatory lesions are extensive (Correale & Farez., 2015). During EAE activated astrocytes can produce IL-1 which targets vascular endothelial growth factor A (VEGF-A) in astrocytes and induces the loss of BBB function and eventually leads to CNS inflammation (Argaw *et al*., 2006; Argaw *et al*., 2009). Furthermore, activated astrocytes also induces or up-regulates astrocytic secretion of cytokines such as TNF-α, IL-1β, and IL-6 which have been linked to CNS inflammation during MS (Ponath *et al*., 2018). Furthermore, astrocytes in MS/EAE play a dual function by promoting axonal degeneration and demyelination but also creating a tolerant environment to aid remyelination (Williams *et al*., 2007). While no previous reports have demonstrated the expression of IL-16 by astrocytes, we did not observe any $GFAP^+$ cells co-expressing IL-16 within the spinal cord (Figure 4.15 A and B) and brain (Figure 4.26 + 4.27 A and B) tissues of naïve and PBS control mice. To the best of our knowledge, this study is the first to determine the expression of IL-16 on $GFAP^+$ astrocytes within the lesions in spinal cord (Figure 4.15 C, D and E) and brain (Figure 4.26 + 4.27 C, D and E) tissue sections of MOG_{35-55} immunised mice. The data suggest IL-16 may be involved in specific astrocyte function during the development of neuroinflammation. Apart from the astrocytes, CD45 immune cells population consisting $CD4^+$, $CD11b^+$ and $F4/80^+$ cells are also present at high levels in EAE inflammatory lesions that predominantly occur in the white matter, which we support here. Before investigating the expression of IL-16 by these immune cells in the CNS tissues, we examined the lymphoid tissues to identify whether the phenotype of IL-16 expressing immune cells within spleen and lymph node, changes during systemic and CNS inflammation. In agreement with previous study which indicated that IL-16 is synthesized by a various immune cell (Cruikshank *et al*., 2000), we have also observed co-expression of IL-16 with $CD45^+$ cells in the lymphoid issues (Figure 4.1 and 4.2).

Lesions found in the CNS are the main pathological hallmarks of MS/EAE which is consist of inflammatory cells, demyelination, reduced oligodendrocyte numbers, transected axons, and gliosis (Duffy *et al*., 2014). After substantial discoveries it is now accepted hypothesis that MS/EAE is mediated by activation of autoreactive myelin-specific T cells that enter the CNS and initiate

and/or propagate a chronic inflammatory response (Compston and Coles, 2008). In the peripheral immune system naive $CD4^+$ T cells differentiate into effector T helper cells under the influence of IL-12, IL-6, and TGF-β secreted by APCs (macrophages/microglia, DCs, and B cells) and co-stimulatory molecules (CD40, CD80, CD86) present on APCs. Once in the CNS, activated T cells and M1 macrophages/microglia promote demyelination, axonal damage, and the formation of disease plaques, while M2 macrophages/microglia and Tregs have anti-inflammatory, regulatory properties and inhibit disease progression by facilitating tissue repair (Zamvil & Steinman., 2003; Constantinescu *et al*., 2011; Cheng *et al*., 2017).

Even though previous studies have repeatedly mentioned that IL-16 originates from T cells, DCs and eosinophils (Cruikshank *et al*., 2000, Skundric *et al*., 20005b), here in our study we have demonstrated co-expression of IL-16 with $CD11b^+$ (Figure 4.6 and 4.7) and $F4/80^+$ (Figure 4.8 and 4.9) monocytes and macrophages in addition to $CD4^+$ cells (Figure 4.3 and 4.4) in the lymphoid tissues of naïve, PBS and EAE mice. We observed increased percentage of immune cells (CD45) and its different phenotype CD4, CD11b and F4/80 expressing IL-16 in the lymphoid tissues of PBS (day 16) and EAE (day 16) in comparison to the naïve mice. With $CD4^+$ T cells and its subsets Th17 and Th1 being the key producer of pro-inflammatory cytokines IL-17 and IFN-γ and the main contributors in MS/EAE initiation and progression, we next utilised FACS analysis on spleen cells derived from PBS and MOG_{35-55} immunised mice at day 16 post immunisation, to determine the type of T cell subsets (Th1 and Th17) involved in producing IL-16. We have observed an increased percentage of $CD4^+$ cells to be $IL\text{-}16^+$ during EAE in comparison to PBS (Figure 4.5A). While previously over 70% of unstimulated human peripheral blood $CD4^+$ cells have been detected to be $IL\text{-}16^+$ (Chupp *et al*., 1998, Ren *et al*., 2005), the percentage is low in the tissues we studied. However, this may be due to the cells originating from different organs, as for our studies we have used spleen cells, whereas previous studies are on cells from blood. It is also possible that difference in research method and analysis may have caused the discrepancy. In 2014 Nischwitz and colleagues demonstrated mRNA expression of IL-16 in MOG_{35-55} stimulated Th17 and Th1 cells derived from spleen $CD4^+$ T cells of naïve 2D2 mice (Nischwitz *et al*., 2014). In agreement with the

literature, in our present study we report IL-16 expression on Th17 (IL-17) (Figure 4.5C) and Th1 (INF-γ) (Figure 4.5D) in both PBS and MOG_{35-55} immunised groups. However, during EAE there was no significant difference in cells expressing both IL-16 and Th17/Th1 in comparison to PBS. This could be possibly because both PBS and EAE mice are systemically activated, however comparison with naïve mice would have further confirm that if this is due to the systemic inflammation.

In our study increased expression of IL-16 on immune $CD4^+$ T cells and macrophages was also observed in the CNS lesions of EAE mice. The data confirm the previous findings that in the CNS of two different strains of EAE mice (relapsing remitting F1 and low relapsing B6), IL-16 has been found to be elevated within the lesion in comparison to the controls, and the elevation of IL-16 within the lesion has been correlated with the levels of infiltrated $CD4^+$ cells (Skundric *et al*., 2005). Furthermore, co-immuno-precipitation of IL-16 with CD4 was also observed in the CNS of both the relapsing EAE mice (Skundric *et al*., 2005b). IL-16 was up-regulated within the CNS of EAE mice of both F1 and B6 background, and the level was peaked during the active stage of the disease but reduced during the remission stage of the disease, consistent with the clearance of infiltrating cells from the CNS (Skundric *et al*., 1993; Skundric *et al*., 2005). Even though IL-16 in the EAE lesions has been repeatedly studied with $CD4^+$ cells and correlated with the $CD4^+$ cell infiltration, in the MS lesions, $CD3^+$, $CD4^+$ and $CD8^+$ T cells, B cells, DCs and occasionally activated resident microglia has been also demonstrated to be the major cellular sources of intrathecally produced IL-16 (Skundric *et al*., 2005a; Skundric *et al*., 2006). This present study is the first to demonstrate co-expression of IL-16 with CD45 immune cells population, $CD11b^+$ and $F4/80^+$ apart from $CD4^+$ cells in the spinal cord and brain tissues of EAE mice.

Although MS is a disease of CNS, both brain and spinal cord are involved in immunopathogenesis, lesions were predominantly localised in the spinal cord tissues in the EAE model used for this study. Despite the reduced lesion and levels of infiltrating immune cells, the brain undergoes damage which leads to decreased mobility and cognitive impairment. In consistent with the literature we have also observed massive lesion and expression of IL-16 in the white

matter of the EAE spinal cord tissues with elevated percentage of $CD45^+$ immune cells (Figure 4.10) and its different subtypes; $CD4^+$(Figure 4.11), $CD11b^+$ (Figure 4.12) and $F4/80^+$ (Figure 4.13) cells expressing IL-16 in a monophasic trend over the course of the EAE. However, brain tissues had comparatively smaller lesion with less infiltrating immune cells observed within the cerebellum and hippocampus. Furthermore we observed the similar monophasic trend in percentage of $CD45^+$ cells expressing IL-16 (Figure 4.16 and 4.17) in EAE over the course of the disease but as we checked for the different phenotypes of immune cells;CD4 (Figure 4.18 and 4.19) and CD11b (Figure 4.20 and 4.21) we found them co-expressing IL-16 only at the onset (day 12) and the peak (day 16) stage of EAE, however no co-localisation of IL-16 was observed with the $F4/80^+$ cells (Figure 2.22 and 4.23). In both spinal cord and brain tissues during the peak stage of the EAE at day 16 we observed the highest IL-16 co-expression with CD45 immune cell population and with all other assessed phenotypes of infiltrating immune cells (except F4/80 in the brain tissues).

In addition, CNS tissues from both EAE onset (day 12) and EAE peak (day 16) demonstrated the highest co-expression of IL-16 with infiltrating immune cells in comparison to the EAE resolution (day 26) mice which had little to none accumulation of infiltrating immune cells in the CNS. In agreement with the previous studies our finding clearly indicates the correlation of IL-16 expression level with the levels of the infiltrating immune cells, and therefore the severity of neuroinflammation in the CNS. But as we further analysed our data to identify which phenotype of infiltrating immune cells expressed the highest percentage of IL-16 in the lymphoid organs (Figure 4.28) and CNS tissues (Figure 4.28), we found the percentage of IL-16 co-expression with $CD11b^+$ cells was higher in comparison to $CD4^+$ and $F4/80^+$ cell population, suggesting during MS/EAE $CD11b^+$ cells might be the main mediating cells for IL-16's action in the CNS. According to Skundric *et al* (2005) the low relapsing EAE model (B6 mice) with less infiltrating $CD4^+$ T cells but more macrophages did not demonstrate IL-16 expression in spinal cord during the acute stage of the disease as macrophages do not readily produce IL-16, however relapsing-remitting EAE model (F1 mice) with higher high numbers of infiltrating $CD4^+$ T cells in the spinal cord lesions expressed the highest amount of IL-16, as T

cells constitutively contains pro-IL-16 and upon cleavage with activated Caspase-3 they secrete bioactive IL-16 (Skundric *et al*., 2005). Whilst previous finding correlated the production of IL-16 to infiltrating $CD4^+$ T cells and also established infiltrating $CD4^+$ T cells as the main producer of IL-16 during EAE, but with our EAE disease model we observed appreciable levels of infiltration of both $CD4^+$ and $CD11b^+$ cells and the percentage of cells co-expressing IL-16 was higher with $CD11b^+$ than that of the $CD4^+$ cells. This should be noted that even though CD11b is a commonly used marker for microglia/macrophage, it is basically a cell surface integrin of many leukocytes including monocytes, neutrophils, natural killer cells, granulocytes and macrophages (McFarland *et al*., 1992). Based on what we observed in our co-expression study within the CNS it could be potentially other subtypes of cells with CD11b integrin on their cell surface, apart from microglia/macrophage co-expressing IL-16 in the CNS lesion during EAE. Further research required for better understanding this.

As we have observed the $CD11b^+$ cells expressing the highest amount of IL-16 in all tissues from different organs so, next we isolated $CD11b^+$ cells from spleen, blood and CNS tissues from day 16 EAE mice and further confirmed the expression of IL-16 (Figure 4.29). LPS is an initiator of classical activation in macrophages/microglia (Song *et al*., 2003) via TLR4 receptors expressed on the surface of monocyte/microglia (Zhou *et al*., 2005). Once activated these cells migrate to sites of inflammation where they encounter and degrade pathogens (Mosser *et al*., 2003). LPS-treated cells along with untreated cells, are commonly used to study the production cytokine by activated macrophages/microglia (Schutte *et al*., 2009). Similarly, as an approach to identify if activated $CD11b^+$ cells produce altered levels of IL-16, we cultured our isolated $CD11b^+$ cells and stimulated with LPS, and measured IL-16 using ELISA. While cells cultured in media alone produced higher levels of IL-16, surprisingly we did not observe any difference between the unstimulated and stimulated groups (Figure 4.30). These data indicate $CD11b^+$ cells during EAE express IL-16, but they are not releasing or secreting further amount of IL-16 through the TLR4 pathway which usually initiates the production of pro-inflammatory cytokine by macrophages. The above data together with our findings of the consistent levels of IL-16 production by medium or antigen stimulated T

cells suggest IL-16 is a unique cytokine, which behaves differently from other immunomodulatory cytokines. However, this could be due to the inability of *in vitro* culture system to mimic the activation *in vivo* which showed increased IL-16 in neuroinflammation.

In summary, we have established that IL-16 is expressed by various immune cells in the lymphoid organs and by the CNS resident and infiltrating immune cells in the CNS during EAE. And the expression levels of IL-16 in the CNS changes over the course of the disease with IL-16 being more prominent at the peak stage. Furthermore, the correlation of IL-16$^+$ cells with the severity of EAE indicates a role of IL-16 in the CNS neuroinflammation.

We have also demonstrated that the co-expression of IL-16 with all the assessed infiltrating immune cells correlated with the level of co-expression observed in the lymphoid tissues from EAE mice. And both Th1 and Th17 cells being the main mediator of EAE exhibited, similar levels of IL-16$^+$ cell percentage in the spleen cells of PBS and EAE mice. The high percentage of CD11b$^+$ cells expressing IL-16 suggest monocytes and macrophages may be the main mediating cells for the function of IL-16 during CNS inflammation in our EAE disease model. In addition, we have demonstrated co-expression of IL-16 with neurons and astrocytes of the CNS resident cells. The findings in this chapter suggest a role by IL-16 in CNS inflammation possibly through the complex interactions of the immune and CNS cells. However, the exact function of IL-16 in the CNS under normal and diseased conditions are not clear and require further investigation.

5. Investigating the function of rIL-16 in primary hippocampal cultures

5.1 Introduction

It is well documented that immune factors including cytokines and chemokines play a vital role within the peripheral immune system, but it is now established that these immune factors play a critical role in the CNS under normal physiological as well as pathophysiological conditions (Spooren *et al*., 2011; Arisi, 2014). While the CNS has been once considered an immune privileged site, it is now accepted to have communication with the immune system, with the innate and adaptive immune system contributing in CNS development, function and disease progression (Louveau *et al*., 2015). The cytokines and chemokines produced by the peripheral immune system usually get trafficked to the CNS via BBB, unlike the immune factors, there are neuroimmune factors (cytokines and chemokines) that are released by CNS resident cells such as astrocytes and microglia (Kettenmann *et al*., 2011; Smith *et al*., 2012; Jensen *et al*., 2013; Choi *et al*., 2014) and occasionally by neurons depending on the condition and the physiological state (Tsakiri *et al*., 2008; Wei *et al*., 2013). In general, the production of these neuroimmune factors is low, and in steady state conditions they assist in physiological functions including neurite outgrowth, neurogenesis, synaptic pruning, neurotransmission and synaptic plasticity (Vezzani & Viviani, 2015). However, elevated levels of these neuroimmune factors have been observed during many neuroinflammatory diseases including Alzheimer's disease (AD) and MS, (Zheng *et al*., 2016; Laurent *et al*., 2018; Selles *et al*., 2018, Zephir,2018) and have been shown to impair neuronal activity and viability. During CNS inflammation many neuroimmune factors are produced (Dong & Benveniste 2001; Fitch & Silver, 2008), making the situation even more complex, and making it difficult to identify the exact cell source and the exact target of these neuroimmune factors. To achieve a clear understanding on the potential role of these factors, it is necessary to

study them individually and identify the exact function which can also contribute in development of new therapeutic strategies.

In the previous chapters, it has been demonstrated that IL-16 is expressed in the CNS of control mice under normal physiological conditions as well as at elevated levels in EAE mice. Having established that IL-16 is widely expressed by neurons in the CNS under physiological and pathophysiological conditions, we next wanted to determine its function in the CNS by examining whether it modulates neuronal excitability and synaptic activity. In addition to the immune system-derived IL-16 (Chupp *et al*., 1998; Keane *et al*., 1998), a neuronal form of IL-16 (NIL-16) has been also identified in the CNS (Kurschner & Yuzaki 1999). NIL-16 is a multi-PDZ domain protein expressed only in post-mitotic neurons of the hippocampus and cerebellum (Kurschner & Yuzaki 1999). NIL-16 is identified and characterized as a longer splice variant of the immune cell-derived IL-16 precursor protein and unlike immune system derived IL-16, NIL-16 has two additional PDZ domains located within the neuron-specific N-terminal region (Fenster *et al*., 2007). NIL-16 has dual functions in the nervous system, by serving as a signalling molecule that is secreted after cleavage by caspase-3 and as a cytosolic scaffolding protein that is involved in clustering and anchoring neurotransmitter receptors /ion channels in the plasma membrane (Ponting *et al*., 1997; Sheng and Wyszynski *et al*., 1997; Kurschner & Yuzaki 1999). Using a yeast two-hybrid approach, it was shown that the N-terminal region of NIL-16 selectively interacts with a variety of neuronal ion channels, including subunits of NMDA receptor subunits (NR2A-D), inward rectifier and voltage-gated K^+ channels (Kir2.1, 2.3 and Kir4.1, 4.2), as well as the Ca^{2+} channel α1C subunit and A-type K^+ channel subunits (Kv4.1–3) (Kurschner & Yuzaki., 1999). In addition, co-expression of NIL-16 with Kv4.2 in COS-7 cells induces Kv4.2 to form dense intracellular clusters and results in a significant reduction in whole-cell A-type current densities (Fenster *et al*., 2007).

A study by Fenster *et al* (2010) has demonstrated that IL-16 treatment on cerebellar granule neurons (CGNs) can result in CD4-dependent up regulation of the transcription factor Fos. Furthermore, IL-16 treatment on CGNs also led to increased neurite outgrowth, both in presence and absence of CD4 receptors

(Fenster *et al*., 2010). In addition, previous work from our laboratory revealed a neuroprotective role of IL-16 in an excitotoxicity model, with brain slices protected against kainate- and oxygen-glucose deprivation (OGD)-induced neuronal cell death in presence of IL-16 (Shrestha *et al*., 2014). Furthermore, we have established that IL-16 is present in the CNS under normal physiological conditions, while its receptor CD4 is absent. Despite IL-16 being reported to interact with multiple ion channels, its function on neuronal excitability and synaptic transmission is yet to be investigated and therefore, the exact role of IL-16 in CNS remains unclear and it remains be determined what role IL-16 plays both under normal physiological condition and during CNS disorder.

Therefore, the aims of this chapter were:

Aim 1: To determine the consequence of rIL-16 treatment on hippocampal neuronal excitability and synaptic activity.

Aim 2: To assess the expression and subcellular localisation of IL-16 and its putative receptor, CD4, in primary hippocampal cultures.

5.2 Results

5.2.1 rIL-16 treatment significantly reduced sEPSC frequency and amplitude in primary mouse hippocampal cultures

Having shown the presence of IL-16 in the CNS of naïve mice under normal physiological condition, we examined the consequence of IL-16 treatment on neuronal synaptic activity in primary mouse hippocampal cultures. In this chapter we utilised patch clamp electrophysiology to investigate the effect of rIL-16 treatment on synaptic activity by monitoring sEPSCs. A previous study from our laboratory demonstrated that conditioned media from mouse lymphocyte preparations (LCM) contains IL-16 (Shrestha *et al*., 2014). Based on that finding, another colleague from our laboratory recently established, following an 18h incubation, LCM contains 360 ± 51 pg/ml of IL-16. Thus, to investigate the function of IL-16, we exposed our primary hippocampal mouse culture to 300pg/ml of rIL-16. Treatment of rIL-16 (300 pg/ml, 1h) impaired sEPSC frequency to 21.6 ± 6.4% of vehicle control (n=8, $p< 0.001$, Figure 5.1 A-C), an effect that was absent when rIL-16 was denatured (dIL-16) prior to application (97.0 ± 16.0% of vehicle control, n=6 neurons, Figure 5.1 A-C). In addition, rIL-16 treatment reduced sEPSC amplitude (58.3 ± 6.0% of vehicle control, n=8 patch neurons, $p<0.05$, Figure 5.1 2A, B & D) with dIL-16 treatment having no effect (99.5 ± 7.2% of vehicle control, n=6 neurons).

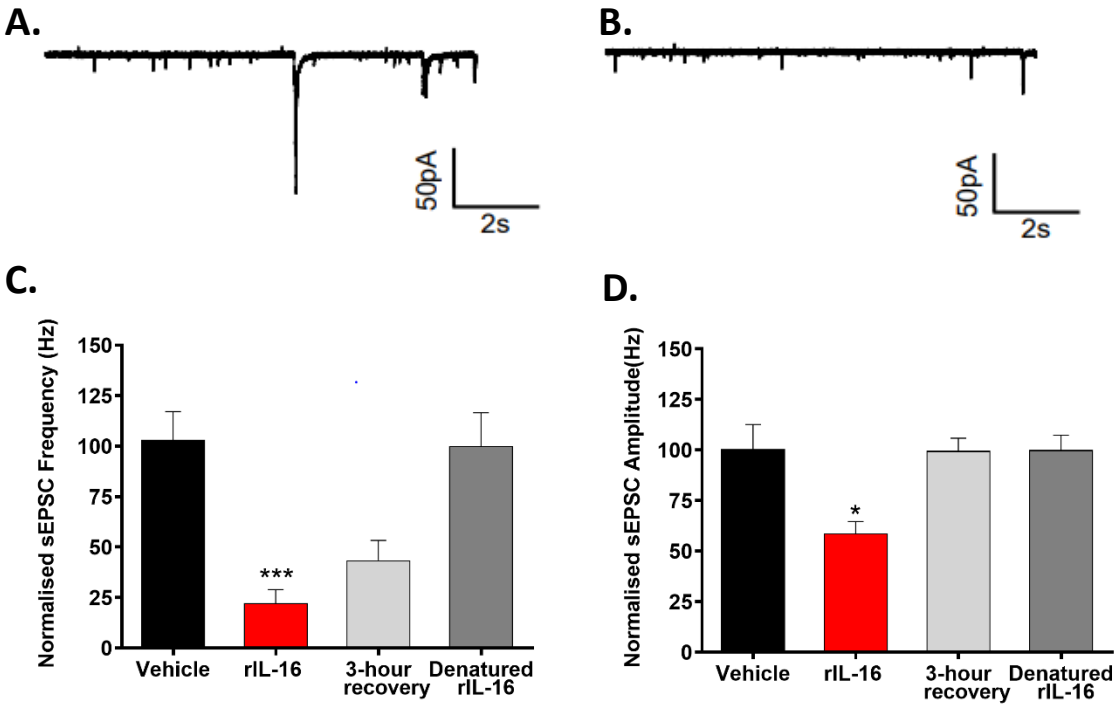

Figure 5.1: rIL-16 treatment significantly reduced sEPSC frequency and amplitude. *Representative traces displaying sEPSCs in* ***(A)*** *the absence and* ***(B)*** *presence of rIL-16 (300 pg/ml, 1h) respectively.* ***(C + D)*** *Bar charts revealing the effect of rIL-16 (300 pg/ml, 1h) on sEPSC frequency and amplitude respectively. n= number of neurons from at least 5 different cultures illustrated as mean ± S.E.M. Significance determined by one-way ANOVA with Bonferroni post hoc test. *P < 0.05 vs vehicle control, ***P < 0.001 vs vehicle control*.

5.2.2 rIL-16 treatment decreased S831 but not S845 GluA1 phosphorylation in primary mouse hippocampal cultures

Protein phosphorylation is one of the key mechanisms required for regulating ionotropic glutamate receptors and plays an essential role in receptor expression as well as in modulating the functional properties of the ionotropic receptors (Wnag et al., 2014). With rIL-16 significantly reducing both the frequency and amplitude of sEPSCs compared to vehicle controls, we next utilised western blot technique on our primary hippocampal culture and examined GluA1 subunit expression and its phosphorylation state following exposure to rIL-16. GluA1 S831 phosphorylation was decreased in rIL-16 (300pg/ml, 1h) treated cultures (54.8 ± 6.7% of vehicle control, n=3, $p<0.05$, Figure 5. 2 B) whereas GluA1 (105.1 ± 27.4% of vehicle control, n=3, Figure 5.2 A) and GluA1 S845 phosphorylation (74.1 ± 19.3% of vehicle control, n=3, Figure 5.2 C) were unaffected by rIL-16 treatment.

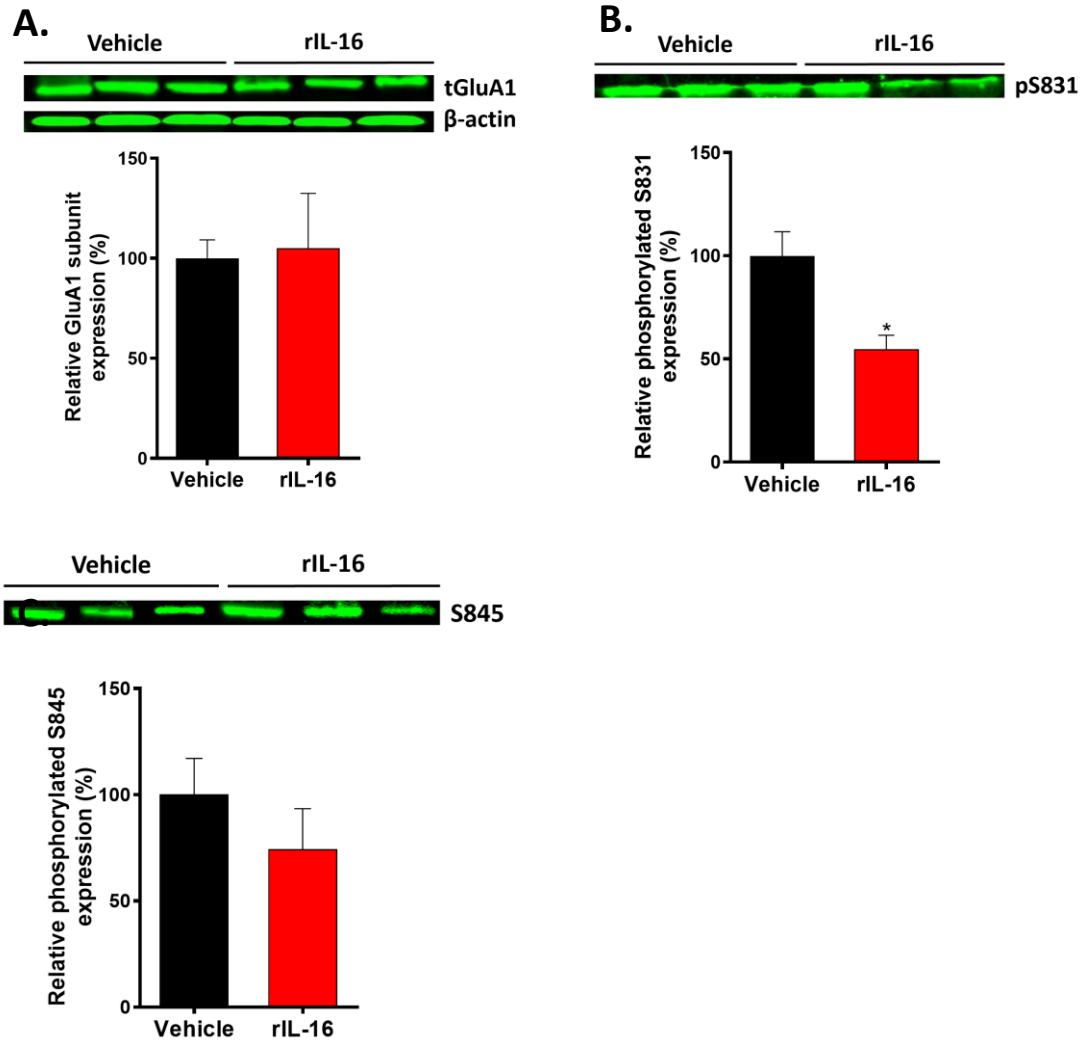

Figure 5.2: rIL-16 treatment reduced S831 but not S845 GluA1 phosphorylation. *Representative image and bar chart show* ***(A)*** *no differences between the expression of GluA1 subunit in vehicle control and rIL-16 treated cultures,* ***(B)*** *significant reduction in S831 GluA1 phosphorylation in rIL-16 treated cultures compared to vehicle controls, and* ***(C)*** *no difference in S845 GluA1 phosphorylation in vehicle control and rIL-16 treated cultures. Data taken from 3 different cultures illustrated as mean ± S.E.M. Significance determined by one-way ANOVA with Bonferroni post hoc test. *P < 0.05 vs vehicle control.*

5.2.3 rIL-16 treatment significantly reduced Na^+ currents, but not K^+ currents in primary mouse hippocampal cultures

Having established that rIL-16 impairs sEPSC frequency and amplitude, using patch clamp electrophysiology, we also examined whether IL-16 modulation of Na^+ and K^+ channel function contributed to these effects. rIL-16 (300 pg/ml, 1h, n=16) significantly impaired Na^+ current density ($P<0.001$, Figure 5.3 C & E) compared to vehicle controls (n=15) with peak Na^+ current density (at -40mV) being 9.7 ± 1.8% of vehicle control (n=16, $p<0.001$, Figure 5.3 C & E). rIL-16 inhibition of Na^+ current density was partially reversed upon a 3h washout (n=9, $P<0.05$) with peak Na^+ current density being 40.5 ± 6.9% of vehicle control (n=16, $P<0.05$, Figure 5.3 E). Corresponding to the effects observed on sEPSC frequency and amplitude, exposure to denatured rIL-16 had no effect on Na^+ current density with peak Na^+ current density being 103.2 ± 11.1% of vehicle control (n=9, Fig. 3C). In contrast to the effects of IL-16 on Na^+ current density, K^+ current density was unaffected following rIL-16 exposure with peak K^+ current density (at +30mV) being 82.6 ± 16.4% of vehicle control (Figure 5.3 D & F).

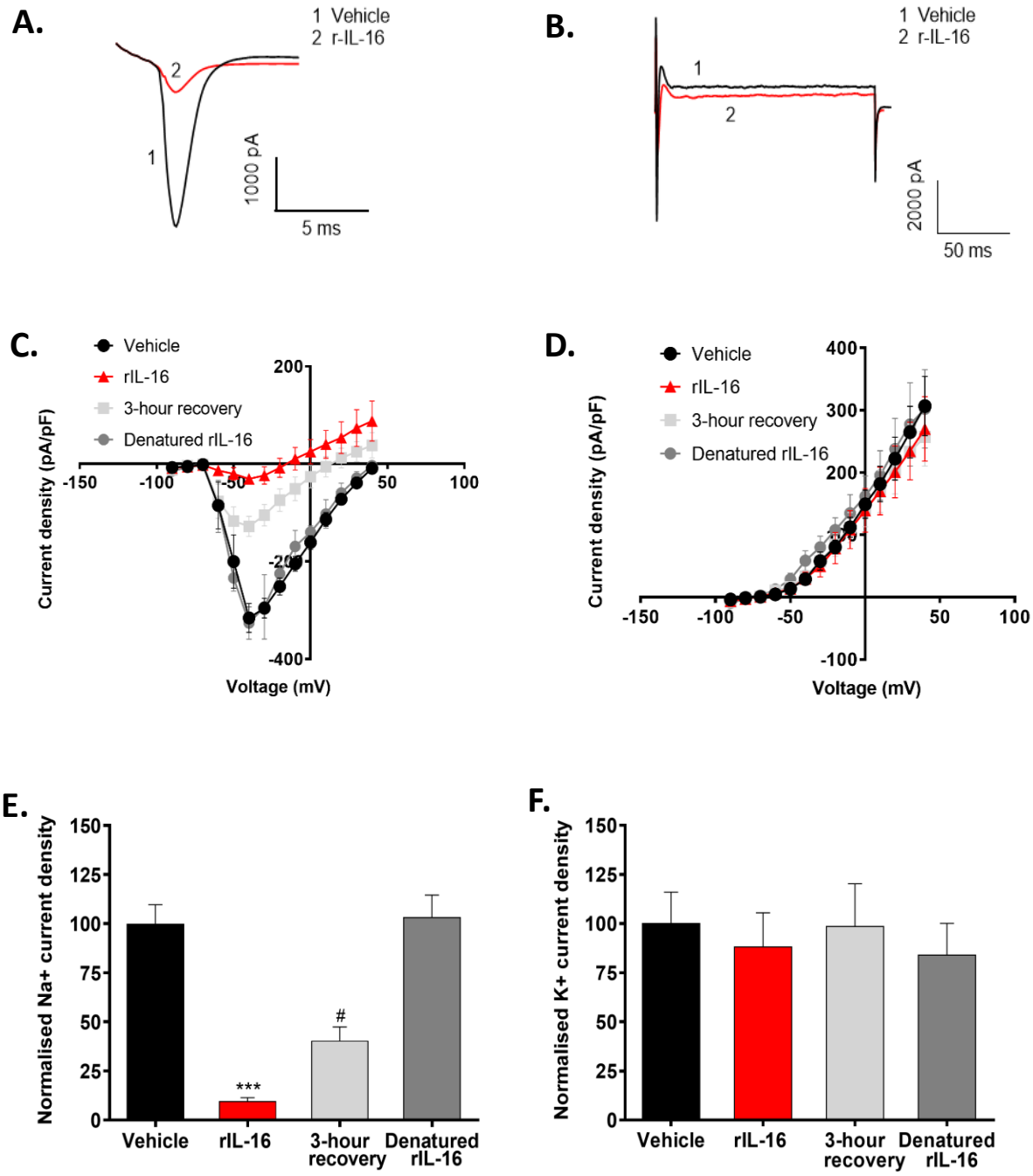

Figure 5.3: rIL-16 treatment inhibited Na+ channel but not K+ channel function in primary mouse hippocampal cultures. *Representative traces of* ***(A)*** *Na^+ currents and* ***(B)*** *K^+ currents in the absence and presence of IL-16.* ***(C + D)*** *I-V curve revealing rIL-16 (300 pg/ml, 1h) inhibits Na^+ current density but has no effect on K^+ current density.* ***(E + F)*** *Bar chart summarising the effect of rIL-16 on peak Na^+ current density but no effect of rIL-16 on peak K^+ current density. Data taken from at least 3 different cultures illustrated as mean ± S.E.M. Significance determined by one-way ANOVA with Bonferroni post hoc test. ***P < 0.001 vs vehicle control, $^{\#}P$ < 0.05 vs rIL-16.*

5.2.4 rIL-16 treatment did not alter Na^+ channel expression in primary mouse hippocampal cultures

With rIL-16 significantly reducing Na^+ current density, we next utilised western blotting on our primary hippocampal cultures to investigate whether this effect is due to altered Na^+ channel expression. However, rIL-16 treatment (300pg/ml, 1h) revealed no change in total Na^+ channel expression (89.8 ± 8.2% of vehicle control, n=3, Figure 5.4) when compared to vehicle control.

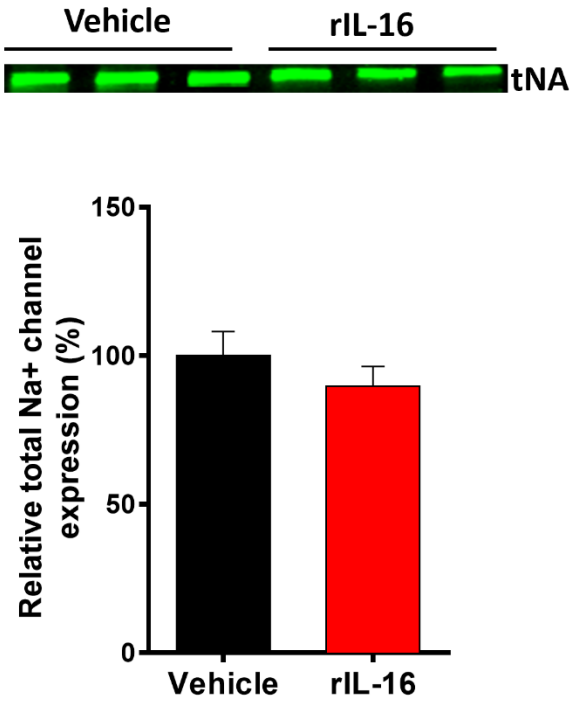

Figure 5.4: rIL-16 treatment had no effect on Na^+ channel expression. *Representative image and bar chart show no differences between total sodium channel expression in vehicle control and rIL-16 treated cultures. Data taken from 3 different cultures illustrated as mean ± S.E.M. Significance determined by one-way ANOVA with Bonferroni post hoc test.*

5.2.5 IL-16 actions on primary mouse hippocampal cultures were CD4-independent

Having shown that IL-16 exposure impairs neuronal excitability and synaptic activity and given that IL-16 is proposed to mediate its effects via both CD4-dependent and independent mechanisms (Kurschner and Yuzaki, 1999; Fenster *et al*., 2010), we next examined both IL-16 and CD4 expression in our primary hippocampal cultures. Immunocytochemical staining was performed to examine IL-16 expression and determine the cellular localisation of IL-16 in mouse primary hippocampal cultures (11-13 DIV). Epifluorescent microscopy revealed that IL-16 was expressed in neurons as shown by co-expression with the neuronal somatodendritic marker, MAP-2 (Figure 5.5 A) and the neuronal nuclei marker, NeuN (Figure 5.5 B). However, co-expression of IL-16 with NeuN confirmed IL-16 is expressed only in the cell body of the neurons but not in the dendrites. Furthermore, co-staining with astrocytic marker, GFAP revealed IL-16 was not expressed by astrocytes as no co-expression was observed with GFAP (Figure 5.5 C). However, CD4 expression was not observed in neither neuron (Figure 5.6 A) nor astrocytes (Figure 5.6 B) under our experimental conditions, whereas positive CD4 staining was evident in control lymphocyte preparations (Figure. 5.6 C).

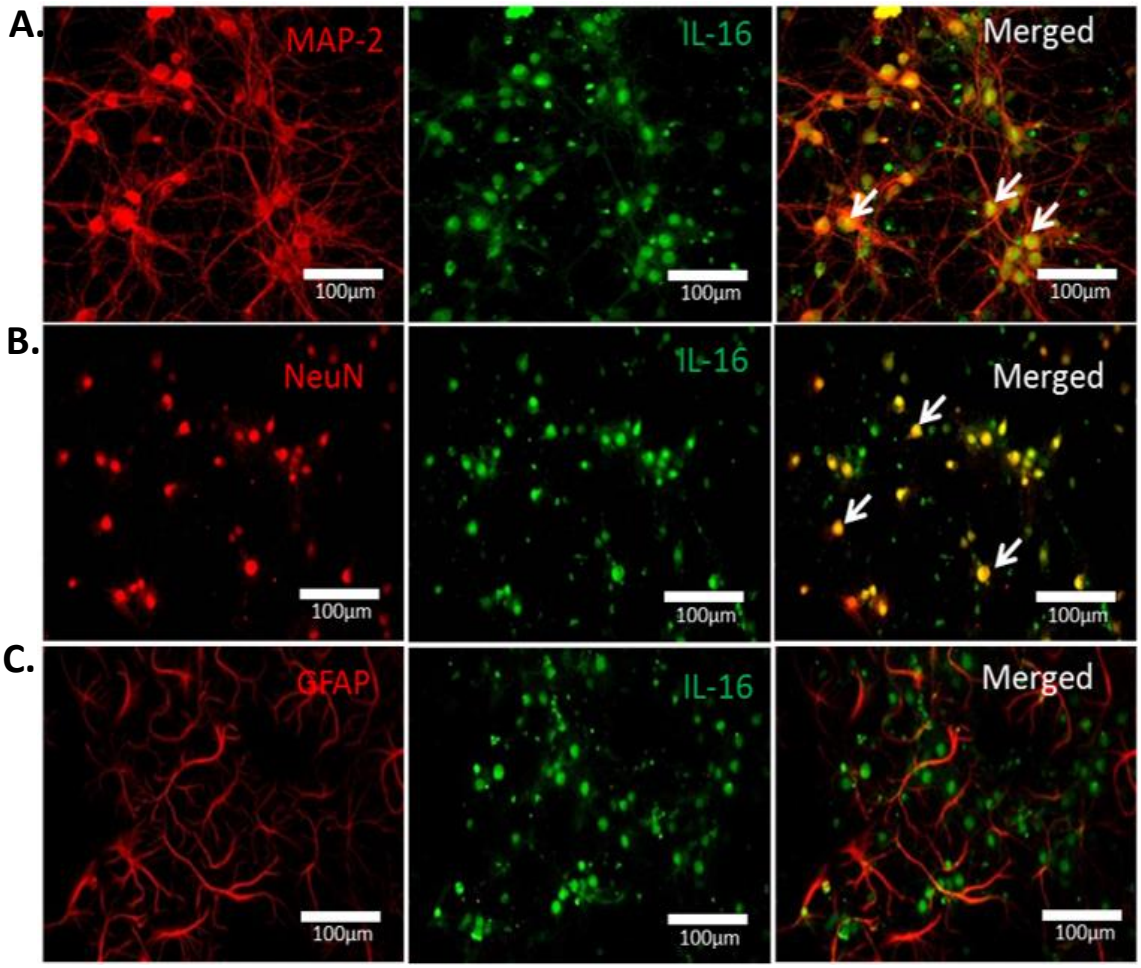

Figure 5.5: Expression of IL-16 by neurons but not by astrocytes in primary mouse hippocampal cultures. *Representative images showing* ***(A)*** *MAP-2 (red) and IL-16 (green) and a merged image (yellow) revealing IL-16 expression by neurons,* ***(B)*** *NeuN (red) and IL-16 (green) and a merged image (yellow) revealing IL-16 expression is restricted to the cell body.* ***(C)*** *Astrocytes (red) do not express IL-16 (green). Images are representative of 5 different cultures. Magnification x20, scale bar.*

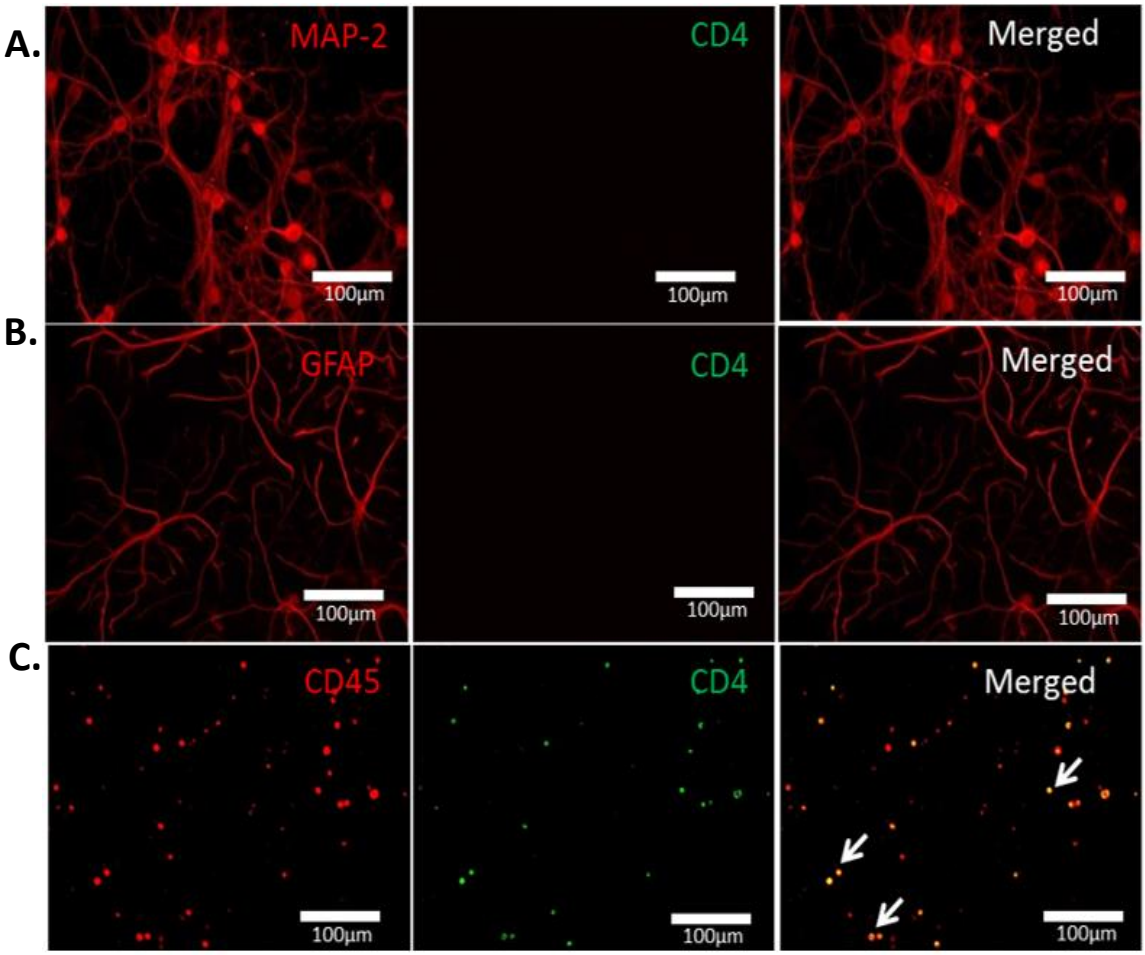

Figure 5.6: CD4 was undetected in primary mouse hippocampal cultures. *Representative images showing* ***(A)*** *MAP-2 (red) and CD4 (green) and a merged image reveal no CD4 expression in neurones.* ***(B)*** *GFAP (red) and CD4 (green) and a merged image reveal no CD4 expression in astrocytes.* ***(C)*** *CD45 (red) and CD4 (green) and a merged image (yellow) revealing CD4 expression by CD45^{+}ve lymph node derived immune cells. Magnification x20, scale bar.*

5.3 Discussion

Involvement of IL-16 in the development of MS and CNS inflammation has been proposed and well documented in several studies. However, most studies suggest a critical role of IL-16 in exacerbation of CNS inflammation, whereas previously our laboratory showed a neuroprotective role of IL-16 in an excitotoxicity model (Shrestha *et al*., 2014). To elucidate how IL-16 functions and protects the neurons under excitotoxic conditions, first we need to understand how IL-16 functions in steady state condition, and as an approach to investigate the function of IL-16 we incubated primary mouse hippocampal cultures with rIL-16 (300ng/ml) for 1 hour at 37 ºC, 5% CO_2 in an incubator and carried out patch clamp electrophysiology. To the best of our knowledge, no previous studies have shown the effects of rIL-16 on neuronal excitability and synaptic activity or the mechanisms underlying the effects within the CNS. Patch clamp electrophysiology allowed us to determine if rIL-16 is involved in spontaneous neurotransmitter release (sEPSCs) and in modulation of ion channels. We demonstrated that exposure of mouse hippocampal cultures to rIL-16, resulted in a significant decrease in both sEPSC frequency and amplitude (Figure 5.1 C + D), suggesting a role of IL-16 in modulating synaptic activity, through reduction of both sEPSC frequency and amplitude. It is well established that a change in the frequency suggests a presynaptic locus of action, possibly via impairing spontaneous release (Han and Stevens, 2009), whereas alteration in amplitude suggests postsynaptic mechanism of action including alterations in AMPA receptor surface expression (Turrigiano, 2012).Thus we thought that rIL-16 may be regulating the surface expression of AMPA receptor through internalisation and this may be a possible mechanism through which IL-16 acts. To determine whether AMPA receptor internalisation accounts for the changes seen in the rIL-16 treated neurons, western blot analysis was utilised to measure the cell surface expression of GluR1 in neurons of our primary mouse hippocampal culture system. Our data demonstrated no significant differences in levels of GluA1 expression in rIL-16 treated cultures in comparison to the vehicle control (Figure 5.2 A). As we didn't observe any difference in GluA1 levels between the rIL-16 treated cultures and the vehicle treated controls (Figure 5.7 A, B), we next investigated the levels

of phosphorylated S845 (pS845) GluA1 and S831 (pS831) GluA1, as the serine residues S831 and S845 in GluA1 C-terminal of AMPARs are the major phosphorylation sites, with S831 phosphorylated by protein kinase C (PKC) and calmodulin dependent protein kinase II (CaMKII), and S845 phosphorylated by protein kinase A (PKA) (Mao *et al*., 2011; Lu and Roche *et al*., 2012). Our data demonstrated cultures treated with rIL-16 had reduced GluA1 S831 phosphorylation (Figure 5.2 B) with no effect observed on S845 phosphorylation (Figure 5.2 C). S831 phosphorylation leads to membrane insertion of AMPARs and trafficking of receptors to synaptic membrane to strengthen the excitatory connection, hence in our study we have observed reduced phosphorylation in this site, which may be an underlying cause for reduced sEPSCs amplitude (Lu and Roche *et al*., 2012). While this is the first time that IL-16 have been demonstrated to modulate GluA1, but interaction of IL-16 with other glutamate receptor subtypes have been observed previously, with NIL-16 co-immunoprecipitating with the NR2A NMDA subunit when both were overexpressed in cell lines (Kurschner and Yuzaki, 1999). Furthermore, there are several reports on cytokines including IL-1β, IL-6 and TNF-α increasing and/or decreasing glutamate receptor function and expression (O'Connor and Coogan, 1999; Viviani *et al*., 2003; Yang *et al*., 2005; Liu *et al*., 2013; Wigerblad *et al*., 2017), suggesting that modulation of glutamate receptor function and expression, is a common mechanism of action utilised by many cytokines and not just distinctive to IL-16. It is well known that in hippocampal cultures, spontaneous glutamate release acts on postsynaptic receptors to mediate sEPSCs, but it has been also observed that synaptically-driven action potential firing also contributes to the spontaneous neurotransmitter release (Chanaday and Kavalali, 2018). So, next we examined whether IL-16 modulates Na^+ and K^+ channel function. We revealed for the first time that exposure to rIL-16 for 1 hour impairs Na^+ channel function (Figure 5.3 C+ E) but K^+ channel function remains unaltered (Figure 5.3 D + F). Furthermore, we have also showed that the inhibition of Na^+ channel function is not due to reduced Na^+ channel expression (Figure 5.4). While we are the first to show reduction in Na^+ channel function in primary mouse hippocampal culture upon rIL-16 exposure, there are several reports on other cytokines including IL-1β (Liu *et al*., 2006; Zhou *et al*., 2011) and TNF-α (Chen *et al*., 2015; Leo *et al*., 2015) being involved in

modulating Na^+ channel function in both peripheral and central neurons. In contrast to our understanding regarding Na^+ channel function, we observed no effect on steady state K^+ current upon rIL-16 treatment, which contradicts previous studies where NIL-16 have been observed to interact with multiple K^+ channel subtypes including members of the Kir2 and Kir4 family via its PDZ domain (Kurschner and Yuzaki, 1999) and furthermore, reduced surface expression of Kv4.2 subunit of A-type K^+ channels was also observed in the presence of NIL-16 in both COS-7 and hippocampal neurons (Fenster *et al*., 2007). Thus, our data suggest that exposure to rIL-16 can impair neuronal excitability via inhibition of Na^+ channel function but is without effect on K^+ channel function. IL-16 is proposed to modulate neuronal function through both CD4-dependent and -independent pathways (Kurschner and Yuzaki, 1999; Fenster *et al*., 2010). We also examined the reported selective IL-16 expression within our primary mouse hippocampal culture and under our experimental conditions, IL-16 was observed to be expressed in the neuron (Figure 5.5 A + B) but not in the astrocytes (Figure 5.5 C), and our finding is consistent with previous study that showed cerebellar granule neurons and hippocampal neurons contain NIL-16, a larger splice variant of immune cytokine IL-16 (Kurschner and Yuzaki, 1999; Skundric *et al*., 2006). However, we demonstrated that CD4 was absent in mouse hippocampal cultures (Figure 5.6 A + B) indicating that the observed synaptic effect by IL-16 were CD4-independent. This result is consistent with our previous finding in chapter 3, where we have shown CD4 was undetected in the CNS tissues from naïve C57BL/6J mice. In a recent study, CD4 was observed to expressed by CGNs, however this was absent in CD4-deficient mice (Fenster *et al*., 2010). Increased *c-fos* expression following IL-16 treatment was absent in CD4-deficient mice, whereas increased neurite outgrowth was still present, indicating that IL-16 mediates its effects through both CD4-dependent and independent pathways. Furthermore, it has been also proposed that IL-16 interaction with immune cells is CD4-independent (Mathy *et al*., 2000), thus our finding that IL-16 mediates its effects in mouse hippocampal cultures via CD4-independent mechanisms is in agreement with these studies and further supports the idea that other receptors may exist for IL-16 function.

In summary, we provide evidence that exposure of mouse primary hippocampal cultures to rIL-16 impairs neuronal excitability and synaptic activity via CD4-independent mechanisms. These data extend our current understanding of how IL-16 modulates CNS function under normal physiological condition and highlight that IL-16 does not function solely as a CD4-dependent chemoattractant, but also has direct CD4-independent effects on neuronal function.

6. General Discussion

Over the past two decades a growing number of studies have shown an involvement of immune regulatory factors in the CNS function and disease. The immune system functions in a unique way within the CNS in comparison to the peripheral organs. The CNS which was once considered an immune privileged site, is now accepted to have bidirectional communication between the CNS and the immune system, with the innate and adaptive immune system involved in modulating the action, differentiation, and survival of neuronal cells, while the neurotransmitter and neuropeptide release play a crucial role in influencing the immune response (Szelény, 2001).

Cytokines are the key signalling molecules that are involved in complex communications between the immune system and the CNS. They are inflammatory mediators that are categorised as either pro- or anti-inflammatory cytokines (Szelényi, 2001; Deverman and Patterson, 2009). By binding to their receptors on immune cells, cytokines exhibit a variety of roles including modulating cell viability, cell proliferation, cytokine secretion, phagocytosis, cell adhesion and cell migration. In addition to coordinating innate and adaptive immune responses throughout the body, cytokines and their receptors are also present in the CNS under both normal and pathological state (Szelény, 2001). Over expression of various cytokines in the CNS tissues is a common feature of many neurotoxic and neurodegenerative disorders (Szelény, 2001).

Within the CNS, while cytokines are often released by infiltrating immune cells during inflammatory CNS disorders, CNS resident cells including astrocytes, microglia and neurons, can also produce and release cytokines (Arisi, 2014). These cytokines are involved in a complex cross-talk between the immune and CNS cells and modulate several physiological functions including neurite outgrowth, neurogenesis, synaptic development and synaptic plasticity (Vezzani & Viviani, 2015; de Miranda *et al*., 2017; Levin & Godukhin, 2018). Inflammation in CNS disrupts the normal pathway which maintains the homeostatic environment (Tansey and Wyss-coray, 2008), thus may function as a trigger to reveal the previously existing problems or worsen the previous functional

defaults in the CNS, and eventually leads to various clinical symptoms for neurological dysfunctions (Deverman & Patterson, 2009). Furthermore, immune cell infiltration into the CNS territory and elevated levels of immune cytokines have been considered an important part of the pathological process in many neuroinflammatory and neurodegenerative disorders such as like AD and MS (Schwartz *et al*., 2014). Recent studies have demonstrated that during CNS injuries and recovery, these cytokines play an important role in activation of glia through altered gene expression (Farina *et al*., 2007; Rothhammer & Quintana., 2015). They also mediate inflammatory processes that increase the BBB permeability, initiate the apoptosis of oligodendrocytes, astrocytes and neuronal cells, and damage myelin and myelinated axons (Tansey & Wyss-coray, 2008).

In addition to their immune-regulating properties, cytokines may also direct neurotoxic and neuroprotective effects (Tansey & Wyss-coray, 2008). Whether a cytokine has helpful or harmful effects depends entirely on the cell source from where it is released, and the dynamics, degree of cytokine release, pathophysiological circumstance and the presence of other factors that are expressed along with it (Deverman & Patterson, 2009). To date we have limited knowledge regarding the functions of cytokines in CNS under normal and diseased conditions. Studies of the pro-inflammatory cytokines such as TNF-α and IL-1β suggest that they not only regulate neuroinflammation but also perform a distinct set of CNS specific functions within the brain and the spinal cord which include modulation of synaptic plasticity, learning and memory (Gosselin & Rivest, 2007; Donzis &Tronson, 2014; Gruol, 2015). In addition to these cytokines, other cytokines including IL-16 a formerly identified lymphocyte chemoattractant factor (Center *et al*., 1982) and a natural soluble ligand to the CD4 molecule, have been also linked to neuroinflammatory disease. IL-16 was identified as a T-cell-derived cytokine that induces CD4-dependent migration and proliferation of immune cells (Center and Cruickshank., 1982, Parada *et al*., 1998, Liu *et al*., 1999), it is also produced by other immune cells including B cells and monocytes (Kaser *et al*., 2000; Elssner *et al*., 2004). Based on its potential in recruiting $CD4^+$ cells, IL-16 is considered an inflammatory cytokine and has been implicated in the regulation of many

immune-mediated diseases including MS/EAE (Glass *et al*., 2006). Interestingly, in addition to its role in inflammation, the neuronal variant IL-16 protein, NIL-16, has been found to be selectively expressed in hippocampal and cerebellar neurons, and is cleaved by caspase-3 similar to pro-IL-16 in immune cells and results in the release of mature IL-16 (Kurschner & Yuzaki., 1999). Furthermore, NIL-16 induces the upregulation of the transcription factor c-fos, (Kurschner and Yuzaki, 1999; Fenster *et al*., 2010), enhances neurite outgrowth (Fenster *et al*., 2010) and interacts with neurotransmitter receptors and several ion channel proteins (Kurschner & Yuzaki., 1999; Fenster *et al*., 2007). In addition, we recently revealed that immune cell-derived IL-16 is neuroprotective against kainate- and oxygen-glucose deprivation (OGD)-induced excitotoxicity in organotypic slice cultures (Shrestha *et al*., 2014). Despite recent findings, the exact role of IL-16 in CNS function and its involvement in CNS diseases remains unclear.

Therefore, the main purpose of our study was to examine the expression and distribution of IL-16 in the CNS tissues and investigate whether the expression levels correlate with the severity of neuroinflammation in EAE. To get an insight into its function in the CNS, we also determined its effect on neuronal excitability and synaptic transmission under physiological conditions using primary mouse hippocampal cultures. We hope that this investigation has provided new knowledge about the potential role of IL-16 in the CNS under normal and diseased conditions. In this chapter, we have summarised the major findings of this study, followed by the general discussion.

6.1 Major findings

The major findings in this thesis are listed below:

1. Spleen/lymph node cells from EAE and control mice constitutively produced IL-16.

2. IL-16 and CD4 expression was observed in spleen and lymph node tissues of EAE and control mice.

3. $CD45^+$ $CD4^+$ $CD11b^+$ and $F4/80^+$ cells in spleen and lymph node tissues of both EAE and control mice expressed IL-16.

4. Serum levels of IL-16 correlated with EAE progression.

5. Elevated levels of IL-16 was observed in the spinal cord and brain homogenates of EAE mice in comparison to the controls.

6. Increased IL-16 and CD4 expression was observed in the spinal cord and brain (hippocampus and cerebellum) tissues during EAE. IL-16 expression was also observed in control spinal cord and brain tissues, while CD4 expression was absent.

7. Infiltrating $CD45^+$, $CD4^+$, $CD11b^+$ cells as well as CNS resident astrocytes expressed IL-16 in the spinal cord and brain (hippocampus and brain) tissues during EAE.

8. spinal cord and brain (hippocampus and brain) tissues during EAE.

9. IL-16 expression was also observed on infiltrating $F4/80^+$ cells in spinal cord tissues but not in brain tissues during EAE.

10. IL-16 expression was also observed on CNS resident neurons in the spinal cord and brain (hippocampus and cerebellum) tissues of both EAE and control mice.

11. $CD11b^+$ cells co-expressed the highest percentage of IL-16 in lymphoid and CNS tissues of EAE day 16 mice.

12. $CD11b^+$ cells isolated from EAE spleen, blood and CNS expressed IL-16, but did not secrete elevated levels of IL-16 upon LPS stimulation in comparison to unstimulated cells.

13. rIL-16 treatment significantly reduced sEPSC frequency and amplitude in primary mouse hippocampal cultures.

14. rIL-16 treatment decreased S831 but not S845 GluA1 phosphorylation in primary mouse hippocampal cultures.

15. rIL-16 treatment significantly reduced Na^+ current, but not K^+ current in primary mouse hippocampal cultures.

16. rIL-16 treatment did not alter Na^+ channel expression in primary mouse hippocampal cultures.

17. IL-16 actions on primary mouse hippocampal cultures were CD4-independent.

6.1.1 IL-16 and its receptor CD4 in the CNS, spleen and lymph node

In this study, to determine whether IL-16 is involved in the development of CNS inflammation, we comparatively analysed the levels of expression and distribution of IL-16 and its receptor CD4 in the lymphoid and CNS tissues of EAE mice. In good agreement with previous reports (Chupp *et al*., 1998; Schwab *et al*., 2001; Skundric *et al*., 2005; Skundric *et al*., 2006), our study confirmed elevated expression of IL-16 and CD4 in the CNS, and the expression levels correlated with the severity of clinically active disease stages in EAE. While previous report indicated the expression of IL-16 in the CNS tissues from MS patients/ EAE mice using western blot analysis (Skundric *et al*., 2005; Skundric *et al*., 2006), here in this study we showed both extent of expression and distribution through immunohistochemistry (Chapter 3). Consistent with previous studies (Skundric *et al*., 2005; Skundric *et al*., 2006), our study has indicated CNS expression of IL-16 in both grey and white matter of EAE mice while its expression in the tissues of naïve and PBS control mice was only limited within the grey matter (Chapter 3).

Furthermore, a previous study has established the comparison in expression levels of IL-16 during the acute, remission, relapse and chronic stages of two different relapsing EAE model (severe relapsing-remitting [(B6 x SJL) F1], and low-relapsing (B6)) and demonstrated the highest level of IL-16 at relapsing stage of the disease in both models (Skundric *et al*., 2005). However here in our study we have established a comparison between the onset, peak and resolution stages of the EAE and in agreement with a previous study in MS patients (Skundric *et al*., 2006) our study demonstrated IL-16 expression to be notably higher in the white matter lesion of EAE mice, with IL-16 being most prominent during the peak stage of the disease.

In addition, for the first time we have also revealed that IL-16 expression levels were similar in the grey matter of both the EAE and control mice. When we assessed CNS expression of CD4 we found similar pattern of expression within white matter lesion of EAE mice, but CD4 was absent in the naïve and PBS controls. Furthermore, in consistent with previous reports (Skundric *et al*.,

2005; Skundric *et al*., 2006) CNS expression of IL-16 corresponded to increased CD4 expression in EAE mice (Chapter 3). Previous studies also demonstrated that mice treated with anti-IL-16 showed to have reduced number of $CD4^+$ T cells and improved paralysis and histopathology of relapsing EAE (Skundric *et al*., 2005). Thus, expression of similar levels of IL-16 and CD4 in the CNS of EAE mice agrees with previous findings that IL-16 is a $CD4^+$ cell-specific chemoattractant cytokine (Center *et al*., 1982; Skundric *et al*., 2005), and further suggest that the additional activities of IL-16 during the CNS inflammation in the regions of CNS white matter are likely through mediating $CD4^+$ T cells.

Increased IL-16 expression in the CNS lesions during EAE disease stages suggested that infiltrating inflammatory cells may produce IL-16. Indeed, our study revealed IL-16 to be expressed by infiltrating $CD45^+$ immune cells in the lesions of CNS tissues (Chapter 4) and further investigations suggested that IL-16 is expressed by infiltrating $CD4^+$ cells (Chapter 4) which agrees with previous report (Skundric *et al*., 2016). Furthermore, our study also demonstrated IL-16 expression by infiltrating $CD11b^+$ cells and occasionally by infiltrating $F4/80^+$ cells (Chapter 4), possibly due to less extensive infiltration by $F4/80^+$ cells in the CNS than that of $CD11b^+$ cells. Infiltrating $CD4^+$IL-16^+ and $CD11b^+$IL-16^+ and $F4/80^+$IL-16^+ cells were observed throughout the white matter of spinal cord. Similarly, in the brain $CD4^+$IL-16^+ cells $CD11b^+$IL-16^+ cells were observed most frequently around blood vessels penetrating white matter and scattered within the white matter parenchyma, however we did not observe $F4/80^+$ cells infiltrations in the brain. Thus, despite previous study confirming $CD4^+$ cells being the key local source of IL-16 in the CNS during EAE (Skundric *et al.,* 2005), our data support increased levels of IL-16 production in the CNS after neuroinflammatory response are predominantly by monocytes and macrophages.

Furthermore, in contrast to previous observation where activated macrophages did not produce IL-16 (Cruikshank *et al*., 2000), we observed reduced IL-16 production by infiltrating macrophages (Chapter 4). However, production of IL-16 by microglia during CNS infarction has been previously reported

(Schwab *et al*., 2001). And microglia have been previously identified within the lesion site in MS tissues (Ulvestad *et al*., 1994), which are involved in tissue destruction through expression and production of inflammatory cytokines including TNF-α, IL-1β, IL-2, IL-6 and IL-12, as well as scavenging of dead cells and myelin debris, and tissue repair (Goldmann & Prinz 2013). As microglia cells often express low levels of CD11b, our data of increased expression of IL-16 by CD11b+ cells at onset and peak stage of disease in EAE mice also support the expression of IL-16 by microglia cells. While we were unable to further confirm the co-localization of IL-16 by Iba-1 expressing microglia cells, we used a culture system to determine whether $CD11b^+$ cells produce IL-16. Surprisingly, when we analysed IL-16 secretion by in-vitro LPS stimulated $CD11b^+$ cells isolated from blood, spleen and CNS of EAE mice, we did not observe any difference in secretion of IL-16 between the stimulated or unstimulated $CD11b^+$ cells. As we did not check if poly(I:C) stimulated $CD11b^+$ cells secrete IL-16, so it is difficult to come to any conclusion regarding the mechanistic secretion of IL-16 and whether the cells respond differently *in vivo* and *in vitro*, thus further investigation is required.

Although this study supports the role of $CD11b^+$ cells in producing IL-16 in CNS of EAE mice, some other CNS resident cells also elaborate and locally release IL-16. We examined IL-16 production by CNS resident neurons and astrocytes. IL-16 expression by $NeuN^+$ cells were observed in the CNS of both EAE and control mice, particularly within the grey matter. Although previously no other studies have reported the co-localisation of IL-16 immunoreactivity with neurons, but it is known that there is a neuronal form of IL-16, NIL-16, a longer splice variant of immune IL-16 that is contained only within the neurons of the cerebellum and the hippocampus (Kurschner *et al*., 1999), which supports our observation of IL-16 expression in $NeuN^+$ cells. IL-16 expression has been also observed with $GFAP^+$ cells in the white matter lesion however only during EAE. It is a well-established that astrocytes (Allaman *et al*., 2011; Nair *et al*., 2008) undergo activation through altered gene expression, hypertrophy and proliferation and release various cytokines during MS (Farina *et al*., 2007; Rothhammer & Quintana., 2015). It is therefore likely that the increased ex-

pression of IL-16 observed with $GFAP^+$ cells only in EAE mice is due the presence of activated astrocytes in EAE lesion. Following that we also tried to check some other CNS resident cells including oligodendrocyte (olig1/olig2) and microglia (Iba1) for the production of IL-16, however it was unsuccessful due to limitation of time and antibody specificity issues. As we observed the highest IL-16 co-expression with $CD11b^+$ but comparatively lower with $F4/80^+$ cells, analysis of IL-16 co-expression with microglia-specific markers such as Iba1 would have been useful to investigate the contribution of microglia in the production of IL-16 and EAE regulation.

Consistent with previous reports (Chupp et., al 1998; Schwab *et al*., 2001, Skundric *et al*., 2005), our study has also confirmed the expression of IL-16 within the spleen and lymph node tissues. Like CNS, (Skundric *et al*., 2005), highest levels of expression were observed in the peripheral lymphoid organs of EAE onset and peak mice in comparison to the controls. In addition, similar pattern of CD4 expression was also observed in the tissues of both the EAE and control mice, further suggesting a correlation between the lymphoid and CNS expression of IL-16 and its receptor CD4. Despite reporting the correlation of IL-16 expression and the extent of CD4 expression in the lymphoid tissues of EAE mice, we did not observe any difference in IL-16 secretion by splenocytes or lymphocytes obtained from EAE and naïve or PBS mice upon in-vitro incubation with or with of MOG_{35-55}. In 2014, Nischwitz and colleagues using real-time PCR revealed MOG_{35-55} specific Th17 cells expressed more IL-16 than Th1 cells, however, when we utilised FACS analysis in spleen cells obtained from EAE and PBS mice we did not observe a significant difference in IL-16 expression by Th1 and Th17 subset of T cells, between the EAE and the control groups. This may indicate MOG_{35-55} specific auto-reactive $CD4^+$ T cells or its subset Th1 or Th17 are not the main producer of IL-16 in EAE, unlike other MS/EAE specific cytokines such as IL-6, IL-10, IL-17 and IFN-γ which have been observed to be produced by EAE splenocytes and lymphocytes upon in-vitro MOG_{35-55} stimulation.

From this current study what we understand is that peripheral inflammation increases expression and release of IL-16 by different immune cells which in

turn induces activated CD4 cell migration into CNS. Following the CNS infiltration, the $CD4^+$ T cells further recruit/activate other immune cells and local cells such as astrocytes, which releases more IL-16 in the CNS, and further induces CD4+ T cell migration thus act as a contributor in MS/EAE pathogenesis.

6.1.2 Function of IL-16 signalling pathway in CNS

Meanwhile in our study we have also established that neurons extensively expressed IL-16 within the grey matter of CNS under normal physiological condition in naïve mice, which suggested IL-16 may have a role in neuron functions. As we investigated further, we established a novel finding of IL-16 mediating its effects in mouse hippocampal cultures via CD4-independent mechanisms. In this study by using the primary hippocampal cultures, we established IL-16 modulates synaptic activity through the reduction of both sEPSC frequency and amplitude indicating a postsynaptic mechanism of action (Chapter 5). It is well established that GluA1 phosphorylation is required for the expression in the postsynaptic membrane (Henley and Wilkinson, 2016), and we further demonstrated IL-16 exposure reduced GluA1 S831 phosphorylation but had no effect on S845 phosphorylation or total GluA1 in the primary mouse hippocampal cultures, which indicates that reduced postsynaptic GluA1 expression underlies the IL-16 modulation of sEPSCs (Chapter 5). Because many other cytokines including IL-1β, IL-6 and TNF-α can increase or decrease the glutamate receptor function and expression (O'Connor and Coogan, 1999; Nelson *et al*., 2001; Viviani *et al*., 2003; Yang *et al*., 2005; Liu *et al*., 2013; Wigerblad *et al*., 2017), the modulation of glutamate receptor function and expression is not unique to IL-16. It is rather a common mechanism of action utilised by many cytokines.

It is well documented that sEPSCs are mediated by spontaneous glutamate release acting on postsynaptic receptors, and synaptically-driven action potential firing also contributes to the spontaneous neurotransmitter release observed in hippocampal cultures (Gan *et al*., 2011; Chanaday and Kavalali,

2018). In our study we have established that IL-16 impairs neuronal excitability via inhibition of Na^+ channel function but is without effect on K^+ channel function and the inhibition of Na^+ channel function is not due to reduced Na^+ channel expression (Chapter 5). While we are the first to demonstrate the effect of IL-16 effect on Na^+ channel, but there are reports of other cytokines including IL-1β (Liu *et al*., 2006; Zhou *et al*., 2011) and TNF-α (Chen *et al*., 2015; Leo *et al*., 2015) regulating Na^+ channel function in both peripheral and central neurons. Many studies have reported that blocking of Na^+ channels can prevent axonal degeneration within white matter tracts in a variety of disease models (Stys et al., 1992, Imaizumi et al., 1998, Agrawal, et al., 1996, Rosenberg et al., 1999, Garthwaite, et al., 2002), including EAE (Kapoor et al.,2003; Lo et al., 2003). So, the role of IL-16 in reducing Na^+ channel function can be beneficial during EAE.

Previous study demonstrated NIL-16 interacts with multiple K^+ channel subtypes including members of the Kir2 and Kir4 family via its PDZ domain (Kurschner and Yuzaki, 1999). Furthermore, Kv4.2 expression is reduced in the presence of NIL-16 in both COS-7 and hippocampal neurons (Fenster *et al*., 2007). However, in the present study, IL-16 exposure had no effect on the steady state outward K+ current observed in hippocampal neurons (Chapter 5).

To identify if the effect of IL-16 observed in the hippocampal culture is due its interaction with CD4 receptor, we also examined IL-16 and CD4 expression within our culture system. In consistent with our previous observation in the CNS of naïve and PBS mice, under our experimental conditions in mouse hippocampal cultures, IL-16 expression was observed in neurons, and CD4 was absent (Chapter 5), indicating that the observed effects were CD4-independent. It has been proposed that IL-16 modulates neuronal function through both CD4-dependent and -independent pathways (Kurschner and Yuzaki, 1999; Fenster *et al*., 2010). A very recent study demonstrated the presence of CD4 in CGNs using western blot, but this was absent in CD4-deficient mice (Fenster *et al*., 2010). Furthermore, while NIL-16 induced the upregulation of the transcription factor c-fos, (Kurschner and Yuzaki, 1999; Fenster *et al*., 2010),

enhanced neurite outgrowth (Fenster *et al*.,2010) and interacts with neurotransmitter receptors and several ion channel proteins (Kurschner & Yuzaki., 1999; Fenster *et al*., 2007), this effect was absent in CD4-deficient mice, whereas increased neurite outgrowth was still present. The findings indicate that IL-16 mediates its effects through both CD4-dependent and independent pathways. Another study also proposed that IL-16 interacts with immune cells via a CD4-independent manner (Mathy *et al*., 2000). Hence our finding that IL-16 mediates its effects in mouse hippocampal cultures via CD4-independent mechanisms agrees with this and further supports the idea that other receptors may exist for IL-16 function. Therefore, it is likely IL-16 contributes to the CNS function under normal physiological condition through mediating CNS resident cells.

6.2 Future Work

Increased expression of IL-16 in the CNS during EAE, and the correlation observed between the levels of IL-16 in the CNS and the extent of infiltrating immune cells has confirmed IL-16 may have an important function in the development of CNS inflammation. Furthermore, we have shown that IL-16 impairs neuronal excitability and synaptic activity via CD4-independent mechanisms in primary mouse hippocampal cultures. Further investigations are required to fully elucidate the exact action and the underlying mechanisms of IL-16 in both the immune and the CNS systems during the development of EAE before considering it a potential novel therapeutic target in the treatment of MS.

- When we assessed the production of IL-16 by splenocytes and observed a constant level of IL-16 with no significant difference between the EAE and the control groups cultured in the media or media supplemented MOG_{35-55} groups. This was unusual in comparison to the antigen specific production of many other important cytokines (IL-17, IFN-γ, IL-16 and IL-10) we have assessed, which are known for MS/EAE pathogenesis. It is not clear whether the difference of IL-16 levels between the treatment

groups were too small to be assessed by ELISA, thus in the future qPCR can be an useful method to check this.

- We have utilised FACS analysis and assessed the expression of IL-16 in $CD4^+$ cells and two MS/EAE relevant T-cell subsets: Th1 and Th17 cells on splenocytes derived from PBS and MOG_{35-55} immunised mice mainly because of the previous findings in the area. However, it is not known whether Treg cells express IL-16 and we did not assess Treg cells which are also relevant to MS/EAE and are known for playing protective role during inflammation through production of anti-inflammatory cytokines. Since we did not observe any difference between the Th1 and Th2 cells expressing IL-16, so accessing Treg cells for IL-16 expression will help us better understand and compare all the T cell subsets and will also allow us to establish whether IL-16 have a pathogenic or protective role in MS/EAE.

- We have established expression of IL-16 in the CNS during EAE by infiltrating immune cells including $CD4^+$, $CD11b^+$ and $F4/80^+$ cells and CNS resident cells including neurons and astrocytes, however as we analysed the percentage of each type of cells co-expressing IL-16 we found there were still a good percentage of $IL\text{-}16^+$ cells which did not co-localise with any of the assessed cell types. On other hand, we rarely observed any co-localization of $CD11c^+$ (marker for dendritic cells), $CD8^+$ (marker for CD8 T cells), B^+ cells with IL-16 during our study (data not shown) and were unable to repeat these experiments further due to the time limitation and antibody availability. Similarly, determining the expression of IL-16 by other CNS resident cells relevant to MS/EAE such as Iba1 (marker specific to microglia), olig1 and olig2 (marker for mature and progenitor oligodendrocyte) will allow us to improve our understanding of contribution of different CNS resident cell types in IL-16 expression and in CNS inflammation and progression of MS/EAE.

- We have demonstrated IL-16 modulates neuronal excitability and synaptic activity via CD4-independent mechanisms in primary mouse hippocampal cultures. However, in a very recent study IL-16 has been shown to induce

migration in human lung epithelial cells (A549) via the CD9 receptor (Blake *et al*., 2018). Therefore, by utilising immunohistochemistry or western blot techniques it would be interesting to check if this receptor is expressed in the mouse hippocampal cultures used in our study and test for the effect of rIL-16 on these receptors. The findings also add the complexity of IL-16 action in CNS inflammation with its potential effect on epithelial cells.

- Finally, we have established that IL-16 expression level correlates with CNS inflammation, and $CD11b^{+}$ cells as the main source of IL-16 in our EAE model. While our current findings support IL-16 as a contributor to MS/EAE pathogenesis, we are not certain the exact function of IL-16 and the underlying mechanisms. This would require further investigation.

6.3 Conclusion

In summary, although we established an expression and distribution pattern for IL-16 and CD4 in CNS and peripheral lymphoid tissues during EAE and also established that $CD11b^{+}$ cells as the main source of IL-16 during EAE, many questions still remains unclear, including the processing of IL-16 in the CNS *in vivo*, as well as the molecular mechanism underlying the mediatory roles of IL-16 in CNS, and whether IL-16 is beneficial or detrimental under pathophysiological conditions. And thus, merits further initiatives and research approaches to determine the function of IL-16 in modulating MS/EAE. However, our novel findings suggest IL-16 is produced by mainly neurons in the CNS in-vitro and modulate neuronal excitability and synaptic transmission despite the absence of its receptor CD4 in the CNS under normal physiological condition. These data extend our current understanding of how IL-16 modulates CNS function and highlight that IL-16 does not function solely as a CD4-dependent chemoattractant, but also has direct CD4-independent effects on neuronal function. In conclusion we can say IL-16 is a shared molecule between the immune and nervous systems engaged in the regulation of CNS inflammation as well as the neuronal and synaptic functions. Thus, like many other cytokines IL-16 is clearly involved in neuroimmune cross-talk.

References

Abbott, N. *et al*., 2010. Structure and function of the blood-brain barrier. Neurobiol. Dis., 37(1),13–25.

Allaman, I. *et al*., 2011. Astrocyte neuron metabolic relationships: for better and for worse. Trends in Neurosci., 34(2), 76-87.

Aloisi, F., 2001. Immune functions of microglia. Glia., 36, 165-79.

Amedei, A. *et al*., 2012. Multiple Sclerosis: The Role of Cytokines in Pathogenesis and in Therapies. International J. Molecul Sci., 13(12),13438–13460.

Amiry-Moghaddam, M. *et al*., 2004. Anchoring of aquaporin-4 in brain: Molecular mechanisms and implications for the physiology and pathophysiology of water transport. Neurosci.,129, 997-1008.

Anggono, V. & Huganir, R.L., 2012.Regulation of AMPA receptor trafficking and synaptic plasticity. Curr. Opin. Neurobiol., 22, 461-469.

Argaw, A.T. *et al*., 2009. VEGF-mediated disruption of endothelial CLN-5 promotes blood-brain-barrier breakdown. Proc Natl Acad Sci USA., 106(6), 1977–82.

Argaw, A.T. *et al*., 2006. IL-1beta regulates blood-brain-barrier permeability via reactivation of the hypoxia-angiogenesis program. J Immunol., 177(8), 5574–5584.

Arisi, G.M., 2014. Nervous and immune systems signals and connections: cytokines in hippocampus physiology and pathology. Epilepsy Behav., 38,43-7.

Ascher, P. *et al*., 1988. N-methyl-D-aspartate-activated channels of mouse central neurones in magnesium-free solutions. J. Physiol., 399, 207-226.

Aspelund, A. *et al*., 2015 A dural lymphatic vascular system that drains brain interstitial fluid and macromolecules. J Exp Med., 212,991–999.

Bailey, S.L. *et al*., 2007. CNS myeloid DCs presenting endogenous myelin peptides 'preferentially' polarize $CD4^+$ Th17 cells in relapsing EAE. Nat. Immunol., 8, 172-180.

Banchereau, J. & Steinman, R.M., 1998. Dendritic cells and the control of immunity. Nat., 392,245-252.

Bankston, A.N. *et al*., 2013. Oligodendroglia and neurotrophic factors in neurodegeneration. Neurosci Bull., 29, 216-228.

Barela, A.J. *et al*., 2006. An epilepsy mutation in the sodium channel SCN1A that decreases channel excitability. J. Neurosci., 26, 2714-2723.

Bartholomäus I, et al., 2009. Effector T cell interactions with meningeal vascular structures in nascent autoimmune CNS lesions. Nature, 462,94–98.

Becher, B. *et al*., 2002.Experimental autoimmune encephalitis and inflammation in the absence of interleukin-12. J. Clin., Invest. 110, 493–497.

Bechtold, D.A. *et al*., 2004. Axonal protection using flecainide in experimental autoimmune encephalomyelitis. Annals Neurol.,55, 607–16.

Bentivoglio, M. & Kristensson K., 2014. Tryps and trips: cell trafficking across the 100-year-old blood-brain barrier. Trends Neurosci., 37,325–333.

Benveniste, E.N., 1997. Role of macrophages/microglia in multiple sclerosis and experimental allergic encephalomyelitis. J. Molecul. Med., 75(3),165–173.

Berman, J.S. *et al*., 1985. Chemoattractant lymphokines specific for the helper/inducer T-lymphocyte subset. Cell Immunol., 95(1),105-12.

Bernacki, J. et al., 2008. Physiology and pharmacological role of the blood-brain barrier. Pharmacol Reports., 60, 600-622.

Bettelli, E. *et al*., 2008. Th17: The third member of the effector T cell Trilogy Estelle. Current Opinions in Immunol., 19(6),652–657.

Bican, O. *et al*., 2013. The spinal cord: a review of functional neuroanatomy. Neurologic Clinics., 31, 1–18.

Biedermann, T. *et al*., 2004. Th1 and Th2 lymphocyte development and regulation of Th cell-mediated immune responses of the skin. J. Investigative Dermtlgy Sympos Proceedings., 9(1), 5–14.

Billiau, A. & P. Matthys., 2001. Modes of action of Freund's adjuvants in experimental models of autoimmune diseases. J. Leukoc boil., 70,849-860.

Biou V. *et al*., 2008.Endocytosis and recycling of AMPA receptors lacking GluR2/3. PNAS., 105, 1038-1043.

Black, J.A. *et al*., 2007. Exacerbation of experimental autoimmune encephalomyelitis after withdrawal of phenytoin and carbamazepine. Annals Neurol., 62:21–33.

Black, J.A. & Waxman, S.G., 2008. Phenytoin protects central axons in experimental autoimmune encephalomyelitis. J Neurological Sci., 274,57–63.

Blaschke, S. *et al*., 2001. Interleukin 16 expression in relation to disease activity in rheumatoid arthritis. Rheumatol (Oxford)., 40,474-475.

Biedermann, T. *et al*., 2004. Th1 and Th2 lymphocyte development and regulation of Th cell-mediated immune responses of the skin. Journal of Investigative Dermatology Symposium Proceedings., 9(1),5–14.

Bliss, T.V.P & Cooke, S.F.2011.Long-term potentiation and long-term depression: a clinical perspective. Clinics., 66, 3-17.

Bliss, V.P & Collingridge, G.L., 2013. Expression of NMDA receptor dependent LTP in the hippocampus: bridging the divide. Molec Brain., 6, 5-18.

Blum, J.S. *et al*., 2013. Pathways of antigen processing. Annual Review of Immunology., 31,443–73.

Boulter, J. *et al*., 1990. Molecular cloning and functional expression of glutamate receptor subunit genes. Sci., 249, 1033-1037.

Bradl, M. & Lassmann, H., 2012. Oligodendrocytes: biology and pathology. Annu Rev Immunol., 30,221-41.

Brandl, M. & Lassmann, H., 2010. Oligodendrocytes: biology and pathology. Acta Neuropathol.,119, 37-53.

Brehm, M. a. *et al*., 2005. Rapid Production of TNF- following TCR Engagement of Naive CD8 T Cells. J. Immunol., 175(8), 5043–5049.

Broder, M.S. *et al*., 2017. The Cost of Hematopoietic Stem-Cell Transplantation in the United States. Am Health Drug Benefits., 10(7): 366–374.

Brown, D.A and Sawchenko P.E, et al., 2007. Time course and distribution of inflammatory and neurodegenerative events suggest structural bases for the pathogenesis of experimental autoimmune encephalomyelitis. J Comp Neurol 2007, 502,236–260.

Burns, J., et al., 1983.Isolation of myelin basic protein reactive T-cell lines from normal human blood. Cell Immunol., 81,435-40.

Burman, J. et al., 2017. Autologous haematopoietic stem cell transplantation for neurological diseases. J Neurol Neurosurg Psychiatry., 89(2): 147–155.

Caldwell, J.H. *et al*., 2000. Sodium channel Na(v)1.6 is localized at nodes of ranvier, dendrites, and synapses. Proceedings of the National Academy of Sciences of the United States of America., 97(10), 5616–20.

Cao, C. *et al*., 1999. Lipopolysaccharide injected into the cerebral ventricle evokes fever through induction of cyclooxygenase-2 in brain endothelial cells. J. Neurosci.,19:716-725.

Carlson, N.G. *et al*., 1999. Inflammatory cytokines IL-1 alpha, IL-1 beta, IL-6, and TNF-alpha impart neuroprotection to an excitotoxin through distinct pathways. J. Immunol., 163(7), 3963–3968.

Center, D.M. & Cruikshank, W., 1982. Modulation of lymphocyte migration by human lymphokines. I. Identification and characterization of chemoattractant activity for lymphocytes from mitogen-stimulated mononuclear cells. J. Immunol., 128(6), 2563–2568.

Cepok, S. *et al*., 2005. Short-lived plasma blasts are the main B cell effector subset during the course of multiple sclerosis. Brain: A J. Neurology, 128(7).,1667–76.

Cesta, M., 2006. Normal Structure, Function, and Histology of the Spleen., Toxicol Pathol., 34(5), 455–465.

Chupp, G. L., *et al*., 1998. Tissue and T cell distribution of precursor and mature IL-16. J. Immunol., 161:3114.

Chittajallu, R. *et al*., 1999. Kainate receptors: subunits, synaptic localization and function. TiPS., 20, 26-35.

Choi, S.S. *et al*., 2014.Humanastrocytes: secretome profiles of cytokines and chemokines. PLoS One., 9, e92325.

Christensen, J. R. *et al*., 2013. Systemic Inflammation in Progressive Multiple Sclerosis Involves Follicular T-Helper, Th17- and Activated B-Cells and Correlates with Progression. PLoS One., 8(3), e57820.

Christophi, G.P. *et al*., 2009. Modulation of macrophage infiltration and inflammatory activity by the phosphatase SHP-1 in virus-induced demyelinating disease. J. Virol., 83,522–39.

Chupp, G.L *et al*., 1998. Tissue and T-cell distribution of precursor and mature IL-16. J Immunol., 161,3114e9.

Coles, J. *et al*., 1999. Monoclonal antibody treatment exposes three mechanisms underlying the clinical course of multiple sclerosis. Ann. Neurol, 46 (3), 296–304.

Comabella, M. & Khoury, S. J., 2012. Immunopathogenesis of multiple sclerosis. Clinical Immunology.,142(1), 2-8.

Compston, A. & Coles, A., 2008. Multiple sclerosis. The Lancet., 372, 1502-1517.

Constantinescu, C.S. *et al*., 2011. Experimental autoimmune encephalomyelitis (EAE) as a model for multiple sclerosis (MS). Bri. J. Pharmacol., 164(4),1079–1106.

Cools, N. *et al*., 2007. Balancing between immunity and tolerance: An interplay between dendritic cells, regulatory T cells, and effector T cells. J. Leukoc Biol., 82, 1365–1374.

Copits, B. a, & Swanson, G. T., 2013. Kainate receptor post-translational modifications differentially regulate association with 4.1N to control activity-dependent receptor endocytosis., J. Biolcl. Chem, 288, 8952–65.

Correale. J and Farez. M.F., 2015. The Role of Astrocytes in Multiple Sclerosis., Progression Front Neurol., 6,180.

Costantino C.M *et al*., 2008. Multiple sclerosis and regulatory T cells., J. Clin Immunol., 8(6), 697-706.

Craner, M.J. *et al*., 2004. Co-localization of sodium channel Nav1.6 and the sodium-calcium exchanger at sites of axonal injury in the spinal cord in EAE. Brain., 127(2), 294–303.

Cross, A.H. & Raine, CS., 1990.Serial adoptive transfer of murine experimental allergic encephalomyelitis: successful transfer is dependent on active disease in the donor. J. Neuroimmunol., 28,27–37.

Cruikshank, W. & Center, D.M., 1982. Modulation of lymphocyte migration by human lymphokines. II. Purification of a lymphotactic factor (LCF). J. Immunol.,128(6),2569–74.

Cruikshank, W. W. *et al*., 1991. Center D. M. J. Immunol.146, 2928–2934.

Cruikshank, W.W. *et al*., 2000. Interleukin-16. J Leukoc Biol, 67(6), 757-66.

Cserr, H.F. *et al*., 1992. Drainage of brain extracellular fluid into blood and deep cervical lymph and its immunological significance. Brain Pathol Zurich Switz. 2,269–276.

Dacher, M. & Nugent, F.S., 2011. Morphine-induced modulation of LTD at GABAergic synapses in the ventral tegmental area. Neuropharmacol., 61, 1166-1171.

Danbolt, N. C., 2001.Glutamate uptake. Prog. Neurobiol., 65, 1-105.

Deb, C. *et al*., 2010. $CD8^+$ T cells cause disability and axon loss in a mouse model of multiple sclerosis. PloS one., 5(8), e12478.

Decimo, I. *et al*., 2012. Meninges: from protective membrane to stem cell niche. Am J Stem Cells.,1,92–105.

Derrick, P. *et al*., 2012. Mouse Models of Multiple Sclerosis: Experimental Autoimmune Encephalomyelitis and Theiler's Virus-Induced Demyelinating Disease Methods. Mol Biol., 900, 381–401.

Donzis, E.J., and Tronson, N.C., 2014. Modulation of learning and memory by cytokines: signaling mechanisms and long term consequences. Neurobiol Learn Mem., 115,68-77.

Dinarello, C.A., 2007. Historical insights into cytokines. European Journal of Immunology., 37, S34-45.

Duncan, I.D. *et al*., 2011.The myelin mutants as models to study myelin repair in the leukodystrophies. Neurotherap., 8, 607-624.

Emond, M.R. *et al*., 2010. AMPA receptor subunits define properties of state-dependent synaptic plasticity. J. Physiol., 588, 1929-1946.

Eng, L.F. *et al*., 1996. Inflammation in EAE: Role of chemokine/cytokine expression by resident and infiltrating cells. Neurochem. Res., 21(4),511–525.

Erta, M. *et al*., 2012. Interleukin-6, a major cytokine in the central nervous system. Int.J.Biol.Sci., 8, 1254–1266.

Farias, A.S. *et al*., 2012. Proteome analysis of spinal cord during the clinical course of monophasic experimental autoimmune encephalomyelitis. Proteom., 12(17), 2656–62.

Farina, C. *et al*., 2007. Astrocytes are active players in cerebral innate immunity, Trends in Immunol., 28, 138-145.

Fenster, C.P. *et al*., 2007. Modulation of Kv4.2 K^+ currents by neuronal interleukin-16, a PDZ domain-containing protein expressed in the hippocampus and cerebellum. Brain Research, 1162(1), 19–31.

Ferber, I.A. et al., 1996. Mice with a Disrupted IFN-y Gene Are Susceptible to the Induction of Experimental Autoimmune Encephalomyelitis (EAE). J. Immunol., (156), 0–2.

Fern, R. et al., 1993. Pharmacological protection of CNS white matter during anoxia: actions of phenytoin, carbamazepine, and diazepam. J Pharmacol ExpTher., 266,1549–55.

Fex Svenningsen, A. et al., 2003. Rapid method for culturing embryonic neuron-glial cell co-cultures. J. Neurosci. Res., 72(5), 565–73.

Fields, R.D.& Stevens-Graham, B., 2002. New insights into neuron-glia communication., 298, 556-62.

Fillatreau, S. et al., 2002. B cells regulate autoimmunity by provision of IL-10. Nat. Immunol., 10(3),944–950.

Fleischer, B., 1986. Lysis of bystander target cells after triggering of human cytotoxic T lymphocytes. European Journal of Immunology., 16(8), 1021–1024.

Fletcher, J.M. *et al*., 2010. T cells in multiple sclerosis and experimental autoimmune encephalomyelitis. Clin. Exp. Immunol., 162(1), 1–11.

Fodstad, H., 2002. The neuron saga. International Congress Series., 1247,645-650.

Ford, M.L.& Evavold, B.D., 2005. Specificity, magnitude, and kinetics of MOGspecific $CD8^+$ T cell responses during experimental autoimmune encephalomyelitis. Eur. J. Immunol.,35,76-85.

Franz, J.K. *et al*., 1998. Interleukin-16 produced by synovia fibroblast, mediates chemoattraction for $CD4^+$T lymphocytes in rheumatoid arthritis. Eur. J.Immunol., 28, 2661-2671.

Freund, J. &Mc Dermott K., 1942. Proc. Soc. Exp. Biol. Med., 49, 548-553.

Freund, J. *et al*., 1947. Isoallergic encephalomyelitis and radiculitis in Guinea pigs after one injection of brain and mycobacteria in water-in-oil emulsion. J. Exp. Med., 57,179-194.

Freund, J., 1947 Ann. Rev., Microbiol.,1, 291.

Freund, J., 1956 Adv. Tuberc. Res., 7, 130.

Friese, M. a.& Fugger, L., 2009. Pathogenic $CD8^+$ T cells in multiple sclerosis. Ann. Neurol., 66, 132–141.

Funfschilling, U. *et al*., 2012. Glycolytic oligodendrocytes maintain myelin and long term axonal integrity. Nat., 485: 517-521.

Gan, J. *et al*., 2011. Indirect modulation of neuronal excitability and synaptic transmission in the hippocampus by activation of proteinase-activated receptor-2, Bri. J. Pharmacol, 163(5), 984–94.

Ghirnikar, R.S. *et al*., 1998. Inflammation in traumatic brain injury: role of cytokines and chemokines. Neurochem. Resear., 23(3), 329–340.

Gijbels. K. *et al*., 1990. Interleukin 6 production in the central nervous system during experimental autoimmune encephalomyelitis. Eur. J. Immunol., 20, 233–235.

Giralt, M. *et al*., 2013. Induction of atypical EAE mediated by transgenic production of IL-6 in astrocytes in the absence of systemic IL-6, Glia, 61,587–600.

Glass,W. *et al*.,2006. Not-So-Sweet Sixteen: The Role of Il-16 in infectious and Immune-Mediated Inflammatory Disease. J. Interfer. Cytok Resear., 26, 511-520.

Goh, J.J. & Manahan-Vaughan, D.,2015. Role of inhibitory autophosphorylation of calcium/calmodulin-dependent kinase II (αCAMKII) in persistent (>24 h) hippocampal LTP and in LTD facilitated by novel object-place learning and recognition in mice. Behav. Brain Res., 285, 79-88.

Goldmann, T. &Prinz, M., 2013. Role of microglia in CNS autoimmunity,Clin. Dev. Immunol.,208093.

Gosselin, D. & Rivest, S., 2007, Role of IL-1 and TNF in the brain: twenty years of progress on a Dr. Jekyll/Mr. Hyde duality of the innate immune system. Brain. Behavr. Immun., 21, 281–9.

Grueter, B.A & Winder, D.G., 2009. Metabotropic Glutamate Receptors (mGluRs): Functions, Encyclopedia of Neurosci., 7, 795-800.

Hagman, S., 2011. Inflammatory Biomarkers in Multiple Sclerosis, University of Tampere.

Gruol D.L., 2015. IL-6 regulation of synaptic function in the CNS. Neuropharmacology., 96,42-54.

Halassa, M. M. *et al*., 2007. The tripartite synapse: roles for gliotransmission in health and disease. Trends in Molec. Med., 13, 54-63.

Halt, A.R., 2012.CaMKII binding to GluN2B is critical during memory consolidation. The EMBO J., 31, 1203-1216.

Hanisch, U.K. & Kettenmann, H., 2007. Microglia: active sensor and versatile effector cells in the normal and pathologic brain, Nat. Neurosci., 10, 1387-1394.

Harrington, L. E., *et al*., 2005. Interleukin 17-producing CD4+ effector T cells develop via a lineage distinct from the T helper type 1 and 2 lineages., Nat. Immunol., 6(11), 1123–1132.

Hartline, D.K. & Colman, D.R., 2007. Rapid conduction and the evolution of giant axons and myelinated fibers. Curr. Biol., 17, 29-35.

Hauben, E. *et al*., 2000. Passive or Active Immunization with Myelin Basic Protein Promotes Recovery from Spinal Cord Contusion. J. Neurosci., 20(17), 6421–6430.

Hawkins, B. T. & Davis, T. P.,2005. The Blood-Brain Barrier/Neurovascular Unit in Health Pharmacol Rev., 57(2), 173-85.

Heneka, M. T. & O'Banion, M. K., 2007.Inflammatory processes in Alzheimer's disease. J. Neuroimmunol., 184, 69-91.

Hendrix S. & Nitsch, R., 2007. The role of T helper cells in neuroprotection and regeneration. J Neuroimmunol., 184,100-12.

Hille, B. 2001. Chapter 1 - Ion channels of excitable membranes. University of Washington.

Hofstetter, H.H. *et al*., 2002.Pertussis toxin modulates the immune response to neoantigens injected in incomplete Freund's adjuvant: induction of Th1 cells and experimental autoimmune encephalomyelitis in the presence of high frequencies of Th2 cells. J. Immunol.,169,117-125.

Höftberger, R. *et al*., 2004.Expression of Major Histocompatibility Complex Class I Molecules on the Different Cell Types in Multiple Sclerosis Lesions. Brain Pathol., 14, 43–50.

Hohlfeld, R. *et al*., 2007.Dual role of inflammation in CNS disease. Neurol., 68, S58–S63.

Howard, L.M & Miller S.D., 2001. Autoimmune intervention by CD154 blockade prevents T cell retention and effector function in the target organ. J Immunol., 166,1547–1553.

Imaizumi, T., Kocsis, J. D. & Waxman, S. G. 1998. Resistance to anoxic injury in the dorsal columns of adult rat spinal cord following demyelination. Brain Res., 779, 292–296.

In book: Autoimmune Diseases – Contributing Factors, Specific Cases of Autoimmune Diseases, and Stem Cell and Other Therapies Chapter: Central Nervous System Resident Cells in Neuroinflammation.

Jäger, A. *et al*., 2009. Th1, Th17, and Th9 effector cells induce experimental autoimmune encephalomyelitis with different pathological phenotypes. J. Immunol., 183, 7169–7177.

Jagessar, S.A. *et al*., 2012. B-Cell Depletion Abrogates T Cell-Mediated Demyelination in an Antibody-Nondependent Common Marmoset Experimental Autoimmune Encephalomyelitis Model. J of Neuropathol and Exper Neurol., 71(8),716–728.

Jensen, C.J. *et al*., 2013.Immune players in the CNS: the astrocyte. J. Neuroimmune Pharmacol., 8, 824–839.

Jiang, H.R. et al., 2012. IL-33 attenuates EAE by suppressing IL-17 and IFN-γ production and inducing alternatively activated macrophages. Eur J Immunol., 42(7):1804-14.

Jonas, P., 2000. The Time Course of Signalling at Central Glutamatergic Synapses. News in Physiological Sciences: An International Journal of Physiology Produced Jointly by the International Union of Physiological Sciences and the American Physiological Society., 15, 83–89.

Jun, W. *et al*., 2017. Distribution and function of voltage-gated sodium channels in the nervous system. Channels., 11:6, 534-554.

Kabat, E.A. *et al*., 1946. Rapid production of acute disseminated encephalomyelitis in rhesus monkeys by injection of brain tissue with adjuvants. Sci., 104, 362-363.

Kabat, E.A. *et al*., 1947.The rapid production of acute disseminated encephalomyelitis in rhesus monkeys by injection of heterologous and homologous brain tissue with adjuvants. J. Exp. Med., 85,117-129.

Kandel, E. R., 2000. The brain and behaviour, In: Principles of Neural Science. New York, McGraw-Hill, 1-14.

Kandel, E. R., 2000. The brain and behaviour, In: Principles of Neural Science. New York, McGraw-Hill, 7-18.

Kandel, E. R., 2000. Nerve cells and behaviour, In: Principles of Neural Science. New York, McGraw-Hill, 19 - 35.

Kandel, R. *et al*, 2000. Principles of Neural Science, 4th edition, 7-9.

Kang, J. *et al*., 1998. Astrocyte-mediated potentiation of inhibitory synaptic transmission. Nat. Neurosci.,1, 683-692.

Kapoor, R., *et al*., 2003. Blockers of sodium and calcium entry protect axons from nitric oxide-mediated degeneration. Ann. Neurol., 53, 174–180.

Karcher, D. *et al*., 1982. Antibodies-restricted heterogeneity in serum and cerebrospinal fluid of chronic relapsing experimental allergic encephalomyelitis. J Neuroimmunol., 2, 93–106.

Kawakami, N. *et al*., 2004. The activation status of neuroantigen-specific T cells in the target organ determines the clinical outcome of autoimmune encephalomyelitis. J. Exp. Med., 199,185–197.

Kawanokuchi, J. *et al*., 2008. Production and functions of IL-17 in microglia. J. Neuroimmunol.,194, 54-61.

Keane, J. *et al*., 1998. Conservation of structure and function between human and murine IL-16. J Immunol., 160: 5945-5954.

Kennedy, M.K. *et al*., 1992. Analysis of cytokine mRNA expression in the CNS of mice with experimental autoimmune encephalomyelitis reveals that IL-10 mRNA correlates with recovery. J. Immunol.,149, 2496-505.

Kessels, H.W & Malinow, R.,2009. Synaptic AMPA receptor plasticity and behaviour. Neur., 61, 340-350.

Kettenmann, H. *et al*., 2011.Physiology of microglia. Physiol. Rev., 91, 461–553.

Kew, J. N. C. & Kemp, J. a., .2005. Ionotropic and metabotropic glutamate receptor structure and pharmacology. Psychopharmacol., 179, 4–29.

Kida, S., *et al*., 1993. CSF drains directly from the subarachnoid space into nasal lymphatics in the rat. Anatomy, histology and immunological significance. Neuropathol Appl Neurobiol.,19,480–488.

Kilimuik, P.A. *et al*., 1999. IL-16 as an anti-inflammatory cytokine in rheumatoid synovitis. J. Immunol., 162, 4295-4299.

Kim, C. & Tse, H.Y., 1993. Adoptive transfer of murine experimental autoimmune encephalomyelitis in SJL.Thy-1 congenic mouse strains. J. Neuroimmunol., 46,129–136.

Kintner, D. B. *et al*., 2004. Increased tolerance to oxygen and glucose deprivation in astrocytes from Na(+)/H(+) exchanger isoform 1 null mice." Amer. J. Physiol. Cell. Physiol., 287, 12-21.

Kivisäkk, P. *et al*., 1999. High numbers of perforin mRNA expressing CSF cells in multiple sclerosis patients with gadolinium-enhancing brain MRI lesions. Acta Neurologica Scandinavica., 100 (1),18–24.

Knopf, P.M. *et al*., 1998. Antigen-dependent intrathecal antibody synthesis in the normal rat brain: tissue entry and local retention of antigen-specific B cells. J. Immunol., 161(2), 692–701.

Kofuji, P. & Newman, E. A., 2004. Potassium buffering in the central nervous system. Neurosci., 129(4), 1043-1054.

Kohm, P. *et al*., 2002. Cutting Edge: $CD4^{+}CD25^{+}$ Regulatory T Cells Suppress Antigen-Specific Autoreactive Immune Responses and Central Nervous System Inflammation During Active Experimental Autoimmune Encephalomyelitis. J. Immunol.,169,4712–4716.

Kotter, M.R. *et al*., 2006. Myelin impairs CNS remyelination by inhibiting oligodendrocyte precursor cell differentiation. J. Neurosci., 26, 328–32.

Kreutzberg, G. W., 1996. Microglia: a sensor for pathological events in the CNS. Trends Neurosci., 19 (8), 312-318.

Kroenke, M.A. *et al*., 2008. IL-12- and IL-23-modulated T cells induce distinct types of EAE based on histology, CNS chemokine profile, and response to cytokine inhibition. J. Exp. Med., 205:1535–1541.

Kukley, M.*et al*., 2010. The fate of synaptic input to NG2 glial cells: neurons specifically downregulate transmitter release onto differentiating oligodendroglial cells. J Neurosci., 30, 8320-8331.

Kurschner, C. & Yuzaki, M., 1999. Neuronal interleukin-16 (NIL-16): a dual function PDZ domain protein. J Neuroscience., 19(18), 7770–7780.

Laberge, S. *et al*., 1996. Secretion of IL-16 (lymphocyte chemo-attractant factor) from serotonin-stimulated $CD8^+$ T cells *in vitro*, J. Immunol (Baltimore, Md.: 1950), 156(1), 310–5.

Langrish, C.L. *et al*., 2005. IL-23 drives a pathogenic T cell population that induces autoimmune inflammation. J. Exp. Med., 201, 233-240.

Lard, L.R. *et al*., 2002. Elevated IL-16 levels in patients with systemic lupus erythematosus are associated with disease severity but not with genetic susceptibility to lupus. Lupus., 11,181-185.

Lassmann, H. *et al*., 2007. The immunopathology of multiple sclerosis: an overview. Brain Pathol., 17, 210-8.

Lavi, E. & Constantinescu, C., 2005. Experimental Models of MS,ed. Springer.

Lee, H. & Kirkwood, A.,2011. AMPA receptor regulation during synaptic plasticity in hippocampus and neocortex, Seminars in cell and developmental biology, 22, 514-520.

Lee, J.M. & Olitsky, P.K., 1955. Simple method for enhancing development of acute disseminated encephalomyelitis in mice, Soci. Exp. Biol. Med., 89,263-266.

Lee, S. *et al*., 1998. Possible pathogenic role of IL-16 on SLE: with reference to HIV-1 infection, Ryumachi, 38,747-751.

Lee, S. *et al*.,1998. Circulating interleukin-16 in systemic lupus erythematosus, Br.J. Rheumatol., 37,1334-1337.

Lees, J.R and A. H., 2007. Cross, A little stress is good: IFN-γ, demyelination, and multiple sclerosis. J. Clin. Invest, 117(2), 297–299.

Lees, J.R. *et al*., 2008.Regional CNS responses to IFN-gamma determine lesion localization patterns during EAE pathogenesis. J. Exp. Med.,205, 2633– 2642.

Lees,J. R. & Cross, A. H., 2007. A little stress is good: IFN-γ, demyelination, and multiple sclerosis. J. Clin. Invest., 117(2),297–299.

Lehner, P.J. & Cresswell, P., 2004. Recent developments in MHC-class-I-mediated antigen presentation. Current Opinion in Immunol., 16(1), 82–89.

Lerma, J., 2006. Kainate receptor physiology. Current Opinion in Pharmacol., 6, 89–97.

Levite, M., 2017. Glutamate, T cells and multiple sclerosis Neural Transm.124:775–798.

Lindsey, J.W., 2005. EAE: History, Clinical Signs, and Disease Course, Exp. Model. Multip. Sclero.,1–9.

Linthicum, D.S. *et al*.,1982. Acute experimental autoimmune encephalomyelitis in mice. I. Adjuvant action of Bordetella pertussis is due to vasoactive amine sensitization and increased vascular permeability of the central nervous system. Cell. Immunol.,73,299-310.

Lisman, J. *et al*., 2012. Mechanisms of CaMKII action in long-term potentiation. Nat. Rev. Neurosci., 13, 169-182.

Liu, W. *et al*., 2010. It's all about change: The antigen-driven initiation of B-cell receptor signaling. Cold Spring Harbor Perspectives in Biology., 2,1–12.

Lo, A. C., *et al.,* 2003. Phenytoin protects spinal cord axons and preserves axonal conduction and neurological function in a model of neuroinflammation in vivo., J. Neurophysiol. 90, 3566–3571.

López-Muñoz, F. *et al*., 2006. Neuron theory, the cornerstone of neuroscience, on the centenary of the Nobel Prize award to Santiago Ramón y Cajal. Brain Research Bulletin., 70, 391-405.

Louveau, A. *et al*., 2015. Structural and functional features of central nervous system lymphatic vessels, Nature., 523, 337–341.

Louveau, A. *et al*., 2015 Revisiting the concept of CNS immune privilege Trends Immunol., 36(10), 569–57.

Lu, W. & Roche, K.W., 2012. Post translational regulation of AMPA receptor trafficking and function. Curr.Opin. Neurobiol., 22, 470–479.

Lucchinetti, C. *et al*., 2000. Heterogeneity of multiple sclerosis lesions: implications for the pathogenesis of demyelination. Annals of Neurology., 47(6), 707–717.

Lumen learning 2017, accessed 9 April 2019, https://courses.lumenlearning.com/wm-biology2/chapter/spinal-cord/.

Lüscher, C. *et al*., 1999. Role of AMPA Receptor Cycling in Synaptic Transmission and Plasticity. Neuron., 24, 649-658.

Mackenzie, I.S. *et al*., 2014. Incidence and prevalence of multiple sclerosis in the UK 1990-2010: a descriptive study in the General Practice Research Database. J. Neurol. Neurosur. Psychiat., 85(1),76–84.

Maimone, D. *et al*., 1997. IL-6 detection in multiple sclerosis brain. J. Neurol. Sci., vol. 146, 59–65.

Malmeström, C. *et al*., 2006. IL-6 and CCL2 levels in CSF are associated with the clinical course of MS: Implications for their possible immunopathogenic roles J. Neuroimmunol., 175,176–182.

Mao, L.M. *et al*., 2011. Post- translational modification biology of glutamate receptors and drug addiction. Front. Neuroanatom., 5, 19.

Marmiroli, P. & Cavaletti, G., 2012.The Glutamatergic Neurotransmission in the Central Nervous System, Curr. Medicnl. Chem., 19, 1269-1276.

Mars, L. T. *et al*., 2011. Contribution of CD8 T lymphocytes to the immunopathogenesis of multiple sclerosis and its animal models. Biochim. Biophys. Acta., 1812(2), 151–161.

Martiney, J.A. *et al*., 1998. Prevention and treatment of experimental autoimmune encephalomyelitis by CNI-1493, a macrophage-deactivating agent,J. Immunol., 160, 5588–5595.

Mathy, N.L. *et al*., 2000. Interleukin-16 stimulates the expression and production of pro inflammatory cytokines by human monocytes. Immunol., 100 (1), 63-9.

Matsumura, K. & Yamagata, K., 1996. Endothelial cells of the rat brain vasculature express cyclooxygenase-2 mRNA in response to systemic interleukin-1 ~: a possible site of prostaglandin synthesis responsible for fever (COX-2). Brain Research., 733,263–272.

Matsushita,T. *et al*., 2008. Regulatory B cells inhibit EAE initiation in mice while other B cells promote disease progression. J. Clin. Invest.,10, 3420–3430.

Matusevicius, D. *et al*., 1998. Interleukin-12 and perforin mRNA expression is augmented in blood mononuclear cells in multiple sclerosis. Scandinavian journal of Immunology., 47(6), 582–590.

Mauri, C. and Bosma, A., 2010.Immune regulatory function of B cells. Acta Neuropathol., 119(1), 37-53.

Mayadevi, M. *et al*., 2015. Molecular Mechanisms in Synaptic Plasticity

Mayer, M.L., 2006. Glutamate receptors at atomic resolution. Nat., 440, 456-462.

McCallum K. *et al*., 1987.T cell subsets in multiple sclerosis. Gradients at plaque borders and differences in non-plaque regions. Brain., 110, 1297–1308.

Mccarthy, D.P. *et al*., 2012. Autoimmunity., 900,1–19.

McFadden, C. *et al*., 2007. Preferential migration of T regulatory cells induced by IL-16. J. Immunol., 179(10), 6439–45.

McFarland, H.F & Martin, R. 2007. Multiple sclerosis: a complicated picture of autoimmunity, Nat Immunol.,8, 913-919.

McFarland, H. I. *et al*., 1992. CD11b (Mac-1): a marker for $CD8^+$ cytotoxic T cell activation and memory in virus infection. J Immunol., 149 (4), 1326-1333.

McGeachy, M. J., 2005. Natural Recovery and Protection from Autoimmune Encephalomyelitis: Contribution of $CD4^+CD25^+$ Regulatory Cells within the Central Nervous System. J. Immunol., 175(5), 3025–3032.

Meldrum, B S., 2000. Glutamate as a Neurotransmitter in the Brain: Review of Physiology and Pathology American Society for Nutritional Sciences, 1007S-1015S.

Menard, L.C. *et al*., 2007. B cells amplify IFN-gamma production by T cells via a TNF-alpha-mediated mechanism. J of Immunol., 179(7),4857–4866.

Merrill, J. E. *et al*., 1992. Inflammatory leukocytes and cytokines in the peptide-induced disease of experimental allergic encephalomyelitis in SJL and B10.PL mice, Proc. Natl. Acad. Sci. U. S. A., 89, 574–578.

Michelucci, A. *et al*., 2009.Characterization of the microglial phenotype under specific pro-inflammatory and anti-inflammatory conditions: Effects of oligomeric and fibrillar amyloid-β. J. Neuroimmunol., 210, 3-12.

Miller, S.D. *et al*., 2007. Experimental Autoimmune Encephalomyelitis in the Mouse. Current Proto. Immunol., 15.1(3), 1–26.

Mills, K.H., 2011. TLR-dependent T cell activation in autoimmunity. Nat. Rev. Immunol.,11,807-822.

Minagar, A. & Alexander, J.S., 2003. Blood-brain barrier disruption in multiple sclerosis. Mult Scler., 9, 540-549.

Mor, F. & Cohen, I.R., 2006. How special is a pathogenic CNS autoantigen? Immunization to many CNS self-antigens does not induce autoimmune disease. J Neuroimmunol., 174,3-11.

Morgan, I.M., 1947. Allergic encephalomyelitis in monkeys in response to injection of normal monkey nervous tissue, J. Exp. Med., 85, 1331-140.

Morell. P and Quarles R. H. The Myelin Sheath Basic Neurochemistry: Molecular, Cellular and Medical Aspects. 6th edition.

Morris-Downes, M.M. *et al*., 2002. Pathological and regulatory effects of anti-myelin antibodies in experimental allergic encephalomyelitis in mice. J of Neuroimmunol., 125(1-2),114–124.

Morrison, L.R., 1947. Disseminated encephalomyelitis experimentally produced by the use of homologous antigen. Arch. Neurol. Psych., 58,391-416.

Mosser, D. M., 2003.The many faces of macrophage activation. J Leukoc Biol., 73,209–212.

Muraro, P.A. et al., 2017. Autologous haematopoietic stem cell transplantation for treatment of multiple sclerosis. Nat Rev Neurol., 13(7):391-405

MStrust 2019, accessed 1 February 2019, https://smart.servier.com

Nair, A. *et al*., 2008. Astrocytes in multiple sclerosis: a product of their environment. Cellular and Molec. Life Sci., 65, 2702–2720.

Napoli, I. & Neumann, H., 2009. Microglial clearance function in health and disease, Neurosci., 158,1030-1038.

Newcombe, J., 2007.Glutamate Receptor Expression in Multiple Sclerosis Lesions. Brain Pathology., 1015-6305.

Nischwitz, S., *et al*., 2014.Interferon β-1a reduces increased interleukin-16 levels in multiple sclerosis patients. Acta Neurol Scand.,130, 46–52

Nicoletti, F. *et al*., 2011. Metabotropic glutamate receptors: From the workbench to the bedside. Neuropharmacol., 60, 1017–1041.

Nikolaev, M.V. *et al*., 2012. Influence of external magnesium ions on the NMDA receptor channel block by different types of organic cations. Neuropharmacol., 62, 2078-2085.

Nowak, E.C. *et al*., 2009. IL-9 as a mediator of Th17-driven inflammatory disease. The Journal of experimental medicine, 206(8), 1653–1660.

Oh, J.W. *et al*., 1999.Cytokine regulation of CC and CXC chemokine expression by human astrocytes. J Neurovirol., 5,82-94.

Ohya, W. *et al*., 2007. Hepatocyte growth factor (HGF) promotes oligodendrocyte progenitor cell proliferation and inhibits its differentiation during postnatal development in the rat. Brain Research., 1147:51–65.

Olitsky, P.K. and R.H. Yager., 1949. Experimental disseminated encephalomyelitis in white mice. J. Exp. Med., 90,213-223.

Orthmann-Murphy, J. L. *et al*., 2008. Gap junctions couple astrocytes and oligodendrocytes. J. Molec. Neurosci., 35,101-116.

Ostby, I. *et al*., 2009. Astrocytic mechanisms explaining neural-activityinduced shrinkage of extra neuronal space. PLoS Computnal. Biol., 5, e1000272.

Panitch, H.S. *et al*., 1987. Exacerbations of Multiple Sclerosis Interferon. The Lancet, 893–895.

Parada, N. A. *et al*., 1996. IL-16- and other CD4 ligand-induced migration is dependent upon protein kinase C. Cell Immunol., 168(1),100–106.

Parpura, V., Heneka, M.T., *et al.*, 2012. Glial cells in (patho)physiology. J Neurochem., 121, 4-27.

Patrick, J., 1972. University of Strathclyde. Tribology International., 5(2), 85.
Pereda, A.E.,2014. Electrical synapses and their functional interactions with chemical synapses. Nat. Rev. Neurosci., 15, 250-263.

Peron, J.P.S. *et al*., 2012. Central Nervous System Resident Cells in Neuroinflammation : A Brave New World.

Perry, V.H., 2004. The influence of systemic inflammation on inflammation in the brain: implications for chronic neurodegenerative disease. Brain. Behav. Immun., 18(5), 407–13.

Persidsky, Y. *et al*., 2006. Blood-brain barrier: structural components and function under physiologic and pathologic conditions. J. Neuroimm. Pharmacol., 1,223-236.

Piccio, L. *et al*., 2002. Molecular mechanisms involved in lymphocyte recruitment in inflamed brain micro vessels: critical roles for P-selectin glycoprotein ligand-1 and heterotrimeric G (i)-linked receptors. Journal of immunology, 168(4),1940–9.

Pinheiro, P. S., & Muller, C., 2008. Presynaptic glutamate receptors: physiological functions and mechanisms of action. Nat. Rev. Neurosci., 9, 423–36.

Pitsikas, N., 2014. The metabotropic glutamate receptors: potential drug targets for the treatment of anxiety disorders?. European Journal of Pharmacology., 15, 723.

Platt, S. R., 2007. The role of glutamate in central nervous system health and disease--a review. Vet. J., 173, 278–286.

Ponath, G., *et al*. 2018. The Role of Astrocytes in Multiple Sclerosis. Front Immunol., 9, 217.

Ponting, C.P. *et al*., 1997. PDZ domains: targeting signalling molecules to sub membranous sites. BioEssays., 19:469–479.

Pristerà, A. *et al*., 2012.Association between Tetrodotoxin Resistant Channels and Lipid Rafts Regulates Sensory Neuron Excitability. PLoS ONE., 7: E40079.

Pritchard, J. *et al*., 2002. Igs from patients with Graves' disease induce the expression of T cell chemoattractant their fibroblast. J. Immunol.,168,942-950.

Raine, C.S. *et al*., 1984. Adoptively transferred chronic relapsing experimental autoimmune encephalomyelitis in the mouse, Neuropathol. Analy., Lab Invest. 51,534–546.

Raine, C. S. 1984 Morphology of myelin and myelination. In P. Morell (ed.), Myelin, 2nd ed. 1–41.

Ransohoff, R. M. & Cardona, A. E., 2010. The myeloid cells of the central nervous system parenchyma. Nat., 468, 253-262.

Ransohoff, R.M. *et al*., 1993. Astrocyte expression of mRNA encoding cytokines IP-10 and JE/MCP-1 in experimental autoimmune encephalomyelitis. FASEB J., 7,592-600.

Rasband, M.N. & Shrager, P., 2000. Topical Review Ion channel sequestration in central nervous system axons. J. Physiol., 525, 63–73.

RBPAonline.com 2018, accessed 1 October 2018, https://rbpaonline.com.

Reboldi, A. *et al*., 2009. C-C chemokine receptor 6-regulated entry of TH-17 cells into the CNS through the choroid plexus is required for the initiation of EAE. Nat. Immunol., 10, 514-523.

Reddy, J.*et al*., 2005. Cutting edge: $CD4^+CD25^+$ regulatory T cells contribute to gender differences in susceptibility to experimental autoimmune encephalomyelitis. J. Immunol.,175:5591–5595.

Ren, F. *et al*., 2005. $CD4^+$ Lymphocytes Pro-IL-16 Regulation in Activated Murine. J Immunol., 174, 2738-2745.

Renno, T. *et al*., 1995. TNF-alpha expression by resident microglia and infiltrating leukocytes in the central nervous system of mice with experimental allergic encephalomyelitis. Regulation by Th1 cytokines. J. Immunol., 154,944–953.

Rivers, T.M. *et al*., 1933. Observations on attempts to produce acute disseminated encephalomyelitis in monkeys. J. Exp. Med., 58, 39-53.

Rivest, S., 2009. Regulation of innate immune responses in the brain. Nat. Rev. Immunol., 9, 429–439.

Russi, A.E. & Brown, M.A., 2015. The meninges: new therapeutic targets for multiple sclerosis. Transl Res J Lab Clin Med. 165,255–269.

Rosenberg, L. J et al., 1999. Effects of the Sodium Channel Blocker Tetrodotoxin on Acute White Matter Pathology After Experimental Contusive Spinal Cord Injury, J. Neurosci. 19, 6122–6133.

Roosendaal, *et al*., 2010.Structural and functional hippocampal changes in multiple sclerosis patients with intact memory function, Radiol, 255 (2), 595-604.

Sad, S *et al*., 1995. Cytokine-induced differentiation of precursor mouse CD8+ T cells into cytotoxic $CD8^+$ T cells secreting Th1 or Th2 cytokines. Immunity, 2(3),271–279.

Sakaguchi, S., 2004. Naturally arising CD4+ regulatory T cells for immunologic self-tolerance and negative control of immune responses. Annual Review of Immunology., 22,531–562.

Sambasivarao, S. V., 2013. NIH Public Access, 18(9), 1199–1216.

Samoilova, E.B. *et al*., 1998. IL-6-deficient mice are resistant to experimental autoimmune encephalomyelitis: roles of IL-6 in the activation and differentiation of autoreactive T cells, J. Immunol., 161(12), 6480-6.

Sandwick, S., 2012. Suppression of Experimental Autoimmune-Encephalomyelitis by Myeloid-Derived Suppressor Cells Suppression.

Sawcer, S. *et al*., 2011. Genetic risk and a primary role for cell-mediated immune mechanisms in multiple sclerosis, Nat., 476(7359), 214–219.

Sayed, B. a. *et al*., 2010. Meningeal mast cells affect early T cell central nervous system infiltration and blood-brain barrier integrity through TNF: a role for neutrophil recruitment? Journal of immunology., 184(12): 6891–6900.

Schwartz, M. & Raposo, C. 2014. Protective Autoimmunity: A Unifying Model for the Immune Network Involved in CNS Repair, Neurosci Rev J Bringing Neurobiol Neurol Psychiatry. 20:343–358.

Schwartz M and Baruch K, 2014 Breaking peripheral immune tolerance to CNS antigens in neurodegenerative diseases: Boosting autoimmunity to fight-off chronic neuroinflammation. Journal of Autoimmunity., 54,8-14.

Schluesener, H.J. *et al*., 1996. Leukocyte chemotactic factor, a natural ligand to CD4, is expressed by lymphocytes and microglial cells of the MS plaque, J. Neurosci. Res., 44(6),606–611.

Schutte, R. J., *et al*., 2009. Cytokine profiling using monocytes/macrophages cultured on common biomaterials with a range of surface chemistries. J Biomed Mater Res A., 88(1), 128–139.

Segal, B.M. *et al*., 1998. An interleukin (IL)-10/IL-12 Immunoregulatory circuit controls susceptibility to autoimmune disease. J Exp Med., 187: 537-546.

Serada, S. *et al*., 2008. IL-6 blockade inhibits the induction of myelin antigen-specific Th17 cells and Th1 cells in experimental autoimmune encephalomyelitis. Proc. Natl. Acad. Sci. U. S. A.,105(21), 9041–9046.

Shechter, R. *et al*., 2009. Infiltrating blood-derived macrophages are vital cells playing an anti-inflammatory role in recovery from spinal cord injury in mice. PLoS Med., 6, 7, e1000113.

Sheng, M. & Wyszynski M., 1997. Ion channel targeting in neurons. BioEssays., 19:847–853.

Skundric, D. S. *et al*., 1993. Homing of T cells to the central nervous system throughout the course of relapsing experimental autoimmune encephalomyelitis in Thy-1 congenic mice. J Neuroimmunol., 46, 113-121.

Skundric, D.S. *et al*., 2005. Anti-IL-16 therapy reduces $CD4^+$ T-cell infiltration and improves paralysis and histopathology of relapsing EAE, J. Neurosci. Res., 79(5), 680-93.

Skundric, D.S. *et al*., 2005. Increased levels of bioactive IL-16 correlate with disease activity during relapsing experimental autoimmune encephalomyelitis (EAE). J. Autoimmun., 25(3), 206–14.

Skundric, D.S. *et al*., 2006. Production of IL-16 correlates with CD4+ Th1 inflammation and phosphorylation of axonal cytoskeleton in multiple sclerosis lesions. J. Neuroinflamm., 3, 13.

Skundric, D.S. *et al*., 2015. Current Concepts of Interleukin-16 (IL-16) in the Onset and Progression of Multiple Sclerosis. Innov. Immunol., 16,1–17.

Skundric, D.S. *et al*., 2015. Emerging role of IL-16 in cytokine-mediated regulation of multiple sclerosis. Cytok., 1–15.

Smart servier medical art 2005, accessed 1 October 2018, https://smart.servier.com

Smith, J.A., *et al*., 2012. Role of pro-inflammatory cytokines released from microglia in neurodegenerative diseases. Brain Res Bull., 87, 10–20.

Schmitt C. et al., 2012. Brain leukocyte infiltration initiated by peripheral inflammation or experimental autoimmune encephalomyelitis occurs through pathways connected to the CSF-filled compartments of the forebrain and midbrain J of Neuroinflammation., 9,187.

Sonobe, Y. *et al*., 2007. Chronological changes of CD4 (+) and CD8 (+) T cell subsets in the experimental autoimmune encephalomyelitis, a mouse model of multiple sclerosis. The Tohoku J. Exp. Med., 213(4), 329–339.

Song, E. W., *et al*., 2000. Influence of alternatively and classically activated macrophages on fibrogenic activities of human fibroblasts. Cell Immunol., 204, 19–28.

Spassky, N. *et al*., 2001. Sonic hedgehog-dependent emergence of oligodendrocytes in the telencephalon: evidence for a source of oligodendrocytes in the olfactory bulb that is independent of PDGFRα signaling. 5004:4993–5004.

Spooren, A. *et al*., 2011. Interleukin-6, a mental cytokine. Brain Res.Rev., 67, 157–183.

Sprengel, R., 2006. Role of AMPA receptors in synaptic plasticity, Cell Tissue Res., 326, 447-455.

Sriram, S. & Steiner, I.,2005. Experimental allergic encephalomyelitis: a misleading model of multiple sclerosis, Ann Neurol.,58, 939–945.

Steinman, L.,2007. A brief history of T (H) 17, the first major revision in the T(H)1/T(H)2 hypothesis of T cell-mediated tissue damage, Nat. Med.,13, 139-145.

Stinissen, P. *et al*., 1998. Myelin reactive T cells in the autoimmune pathogenesis of multiple sclerosis,Mult.Scler.,4,203-211.

Streit, W. J. *et al*., 1999. Reactive microgliosis,Prog.Neurobiol., 57(6), 563-581.

Stys, P.K. *et al*., 1992. Tertiary and quaternary local aesthetics protect CNS white matter from anoxic injury at concentrations that do not block excitability. J Neurophysiol; 67(1),236–40.

Stys, P.K. *et al*., 1992.Ionic mechanisms of anoxic injury in mammalian CNS white matter: role of Na^+ channels and Na^+–Ca^{2+} exchanger. J Neurosci 12,430–439.

Sun, D. *et al*., 1997. Expression of chemokine genes in rat glial cells: the effect of myelin basic protein-reactive encephalitogenic T cells. J. Neurosci. Res., 48, 192-200.

Sun, D. *et al*., 2001. Myelin antigen-specific $CD8^+$ T cells are encephalitogenic and produce severe disease in C57BL/6 mice. J. Immunol.166, 7579-7587.

Sun, D. *et al*., 2003. Encephalitogenic activity of truncated myelin oligodendrocyte glycoprotein (MOG) peptides and their recognition by $CD8^+$ MOG-specific T cells on oligomeric MHC class I molecules. Int. Immunol.,15,261-268.

Swanborg, R.H., 1995. Experimental autoimmune encephalomyelitis in rodents as a model for human demyelinating disease. Clin Immunol Immunopathol., 77, 4–13.

Takeshita, Y. & Ransohoff R.M., 2012. Inflammatory cell trafficking across the blood-brain barrier: chemokine regulation and *in vitro* models. Immunol Rev., 248,228–239.

Takahashi, Y. *et al*., 2013. Circumventricular organs and fever. Amer. J. Physiol., 273, 1690–1695.

Tambuyzer, B.R., 2009. Microglia: gatekeepers of central nervous system immunology. J. Leukoc. Biol., 85, 352–370.

Tian, L. *et al*., 2012. Neuroimmune crosstalk in the central nervous system and its significance for neurological diseases, J. Neuroinflamm., 9,155.

Tong, G. *et al*., 2008. Modulation of NMDA Receptor Properties and Synaptic Transmission by the NR3A Subunit in Mouse Hippocampal and Cerebrocortical. Neurons, J. Neurophysiol., 99, 122-132.

Tornes, L., *et al*., 2014. Multiple Sclerosis and the Cerebellum, Neurol.Clin., 32, 957-977.

Tsakiri, N. *et al*., 2008. Mechanisms of interleukin-6 synthesis and release induced by interleukin-1 and cell depolarisation in neurones. Mol. Cell. Neurosci., 37, 110–118.

Turrigiano, G. G., 2008. The Self-Tuning Neuron: Synaptic Scaling of Excitatory Synapses, Cell, 135, 422–435.

Tzartos, J.S., *et al* 2008. Interleukin-17 production in central nervous system-infiltrating T cells and glial cells is associated with active disease in multiple sclerosis. Am. J. Pathol, 172, 146–155.

Tzingounis, A. V, & Nicoll, R. a., 2004. Presynaptic NMDA receptors get into the act. Nat. Neurosci., 7, 419–20.

Vaknin, I.et al., 2011. Excess circulating alternatively activated myeloid (M2) cells accelerate ALS progression while inhibiting experimental autoimmune encephalomyelitis. PLoS One., 6, e26921.

Van Oosten BW, et al., 1997. Treatment of multiple sclerosis with the monoclonal anti-CD4 antibody cM-T412: results of a randomized, double-blind, placebo-controlled, MR-monitored phase II trial. Neurology., 49(2), 351-7.

Van, H.J. et al., 2011. Radical changes in multiple sclerosis pathogenesis. (BBA) - Molecular Basis of Disease., 1812, 141-150.

Velásquez-Lopera, M.M. et al., 2008. Human spleen contains different subsets of dendritic cells and regulatory T lymphocytes. Clin. Exp. Immunol., 154(1), 107–14.

Vezzani, A. and Viviani, B., 2015. Neuromodulatory properties of inflammatory cytokines and their impact on neuronal excitability. Neuropharmacology., 96, 70-82.

Viglietta, V. *et al*., 2004. Loss of functional suppression by $CD4^{+}CD25^{+}$ regulatory T cells in patients with multiple sclerosis. Journal of experimental biology., 199(7), 971–979.

Walsh, J.T. *et al*., 2014. Regulatory T cells in central nervous system injury: a double-edged sword. J Immunol Baltim Md., 193,5013–5022.

Wang, P.Y. *et al*., 2011. Functional NMDA Receptors at Axonal Growth Cones of Young Hippocampal Neurons, J. Neurosci., 31, 9289-9297.

Wang, X. *et al*., 2006. Astrocytic Ca^{2+} signalling evoked by sensory stimulation *in vivo*, Nat. Neurosci., 9, 816-823

Waxman, S.G. *et al*., 1992. Ultra-structural concomitants of anoxic injury and early post-anoxic recovery in rat optic nerve. Brain Res., 574:105–19.

Waxman, S.G. *et al*., 1992. Ultrastructural concomitants of anoxic injury and early post-anoxic recovery in rat optic nerve. Brain Res., 574:105–119.

Wei, X.H. *et al*., 2013. The up-regulation of IL-6 in DRG and spinal dorsal horn contributes to neuropathic pain following L5 ventral root transection. Exp. Neurol., 241, 159–168.

Weier, K. *et al*., 2015. The Role of the Cerebellum in Multiple Sclerosis .The Cerebellum. Springer Science, 14(3), 364-74.

Weil, Z.M. *et al*., 2008. The injured nervous system: a Darwinian perspective. Prog. In Neurobiol., 86, 48–59.

Weinshenker, B.G. *et al*., 1999. A randomized trial of plasma exchange in acute central nervous system inflammatory demyelinating disease. Annals of neurology., 46(6):878–886.

Weiss, N. *et al*., 2009. The blood-brain barrier in brain homeostasis and neurological diseases. Biochem. Biophys. Acta., 1788, 842-857.

Whitlock, J. R., *et al*., 2006. Learning induces long-term potentiation in the hippocampus. Sci., 313, 1093–7.

Williams, A. *et al*.,2007. Astrocytes-friends or foes in multiple sclerosis? Glia., 55(13),1300–1312.

Williams, K.C. *et al*., 1994. Immunology of multiple sclerosis. Clin. Neurosci., 2,229–245.

Wilson, K.C. *et al*., 2004. The effect of interleukin-16 and its precursor on T lymphocyte activation and growth. Growth Factors., 22, 97–104.

Wu, D.M. *et al*., 1999.Processing and release of IL-16 from $CD4^+$ but not $CD8^+$T cells is activation dependent, J. Immunol., 162(3), 1287-93.

Yan, H. & Rivkees, S. a, 2002. Hepatocyte growth factor stimulates the proliferation and migration of oligodendrocyte precursor cells. Journal of Neuroscience Research., 69(5):597–606.

Yednock, T.A. *et al*., 1992. Prevention of experimental autoimmune encephalomyelitis by antibodies against α4β1 integrin. Nature., 356, 63–66.

York, McGraw-Hill, 19 - 35.

Zamvil, S. *et al*., 1985 T-cell clones specific for myelin basic protein induce chronic relapsing paralysis and demyelination. Nature., 317, 355–358.

Zhang, H. *et al*., 2013.Regulation of AMPA receptor surface trafficking and synaptic plasticity by a cognitive enhancer and antidepressant molecule. Molec. Psychtry., 18, 471-484.

Zhang, Y., *et al*., 1998. Processing and activation of pro-interleukin-16 by caspase-3. J BiolChem., 273(2), 1144-9.

Zhao, C.B., *et al*., 2008. A new EAE model of brain demyelination induced by intra cerebro ventricular pertussis toxin, Biochem. Biophysicl Res.Communctn.,370, 16-21.

Ziv, Y. *et al*., 2006. Immune cells contribute to the maintenance of neurogenesis and spatial learning abilities in adulthood. Nat Neurosci., 9,268-75.

Zhou, X. *et al*., 2005. LPS activation of Toll-like receptor 4 signals CD11b/CD18 expression in neutrophils. Am J Physiol Lung Cell Mol Physiol., 288, L655–L662.

Zhu, J., Yamane, H. & Paul, W.E., 2010. Differentiation of effector CD4 T cell populations. Annual Review of Immunology., 28 : 445–89.

Zorumski, C. F., & Izumi, Y., 2012. NMDA receptors and metaplasticity: mechanisms and possible roles in neuropsychiatric disorders, Neurosci and BioBehav. Rev., 36, 989–1000.